EFFECT OF SUCTION ON DYNAMIC PROPERTIES OF UNSATURATED SOILS AT SMALL- TO MID-SHEAR STRAIN AMPLITUDES

by

ALEJANDRO HERNÁN PINO BRAVO

Presented to the Faculty of the Graduate School of

The University of Texas at Arlington in Partial Fulfillment

of the Requirements

for the Degree of

MASTER OF SCIENCE IN CIVIL ENGINEERING

THE UNIVERSITY OF TEXAS AT ARLINGTON

August 2013

Acknowledgements

First of all I express my thankfulness to the Lord in heaven for giving me the opportunity to come to this Country to study at UTA and for supporting me during all the time I have been living here. All what I got I owe to Him.

I would like to extend my honest gratitude to Dr. Laureano Hoyos for his guidance and support throughout my theoretical and experimental research study. It was a privilege to have worked with a professor with a vast knowledge as Dr. Hoyos has. I sincerely hope to meet his expectations in both the experimental procedures and the consequent research paper. All concepts he reviewed and taught me will always remain with me for my personal and professional development.

Sincere thanks are also extended to other members of my thesis committee: Dr. Anand Puppala and Dr. Xinbao Yu, for their valuable advice and for reviewing this document. I extend my gratitude to the whole civil engineering staff for their friendly help in various aspects during the course of my study at UTA.

I express my gratitude to my beloved wife Paola, for her patience and support in all aspects for successfully completing this masters program.

Finally I would like to thank to all of those who helped me in any way throughout my journey at UTA; they are so many that writing their names down in this document could make me overlook one of them. God bless all of you, God bless America.

July 22, 2013

Abstract

EFFECT OF SUCTION ON DYNAMIC PROPERTIES OF UNSATURATED SOILS AT MID- TO HIGH-SHEAR STRAIN AMPLITUDES

Alejandro Hernán Pino Bravo, M. S.

The University of Texas at Arlington, 2013

Supervising Professor: Laureano R. Hoyos

This paper presents the results from an experimental study that has been designed to assess the effect of the suction and net mean stress on the dynamic properties of poorly graded sand with silt subjected to small- to mid-shear strains. The practical implication of this study includes determining the effect on soil stiffness properties of increased matric suction (transpiration of water) at different net mean stresses (or depths) in the field. The engineering analysis of earth structures subjected to static and non-static loading under unsaturated conditions requires knowing the relevant parameters of the soil, such as shear wave velocity, shear modulus, and material damping. The traditional soil mechanics and geotechnical engineering have generally focused on soil extreme conditions, that is, completely dry or saturated state of soil; thus, these branches of soil mechanics present shortcomings to estimate the true soil strength and stiffness, and its behavior at small- to mid-shear strains, under partially saturated conditions. In the last years, additional efforts have been made to gain a better understanding of partially saturated soil behavior by using field and laboratory based measurements of soil suction. However, these efforts have not thoroughly covered the dynamic response of partially saturated soils at small- to mid-shear strain amplitudes. This work intends to study the dynamic response of unsaturated soils, particularly and the

effect of varying matric suction and net mean stress on shear modulus, material damping and threshold strain.

Table of Contents

List of Illustrations

List of Tables

Chapter 1

Introduction

1.1 Background

In engineering problems relating to the propagation of seismic waves through soil, two of the most important parameters required for dynamic analyses are the soil or rock stiffness and material damping. The shear modulus, G, and material damping ratio, D, are used to determine the amplitude and attenuation of stress waves as they travel through the geologic deposits. In seismic site response analyses, geology of a site is typically modeled as a series of horizontal layers with varying properties. Incoming seismic waves are amplified at certain frequencies as they travel between the bedrock and the surface due to soil deposits at the site, and the amplification of earthquake acceleration often governs the design of structures at the site. In building design in seismically active areas, the horizontal shear component of earthquake shaking is usually the most critical component. Therefore, an accurate determination of the shear modulus and material damping properties of the geotechnical materials are important for an accurate seismic response analysis.

The traditional soil mechanics idealizes geo-materials as being either in a dry or saturated state; however, a region immediately above the water table is in an unsaturated state. In most of the regions around the world the water table may seasonally fluctuate, thus often unsaturated soil conditions are generated. Therefore better explanations for soil behavioral patterns than conventional saturated soil mechanics are needed in order to improve the dynamic idealization of the seismic site response, according to the partially saturated ground conditions.

It is not possible to predict the behavior of partially saturated soils by using either Terzaghi's effective stress principle or any single stress variable combining pore-air

pressure (u_a), pore-water pressure (u_w), and total stress tensor (Bishop 1959, Atchison 1961, Jennings 1961). However, various attributes of the behavior of partially saturated soils have been modeled via suction-controlled oedometer, triaxial, and direct shear tests using the axis-translation technique (Fredlund and Morgenstern 1977, Alonso et al. 1987, Toll 1990, Alonso et al. 1990, Wheeler and Sivakumar 1992, Fredlund and Rahardjo 1993), by adopting matric suction, ($u_a - u_w$), and the excess of total stress over air pressure, ($\sigma - u_a$), as relevant stress state variables. Considering that the suction states of unsaturated soil heavily affect its static and dynamic responses, the lack of consideration of these suction effects in the strain dynamic characterization of unsaturated soils may lead to erroneous property measurements and, ultimately, faulty and/or excessively conservative designs of earth structures.

The small-strain behavior of soils cannot be detected by using conventional geotechnical testing methods; hence, seriously underestimate of the true soil stiffness is expected due to inaccuracies in small strain measurements. To overcome this disadvantage, the resonant column (RC) device is used to accurately assess the dynamic properties of soils at relatively small strains. In this test method a cylindrical specimen is torsionally excited in a special device and then swept at varying frequencies until its resonant frequency is found.

The shear modulus is determined as a function of the resonant frequency of the soil-driver system. This modulus representing the soil stiffness and also the damping are key parameters of unsaturated soils. The assessing of small strain behavior of unsaturated soils is important for engineering applications as it offers the possibility of taking into account the influence of these conditions on the mentioned key soil parameters, which affect the performance of geo-structures with regards to soil deformations (Vassallo 2006).

Generally, most of the geo-structures are composed by compacted unsaturated soil which is subjected to small strains; therefore, a thorough understanding of the dynamic response of the soil under these conditions is required. In the last years many efforts have been focused to obtain measurements of soil suction, assessments of soil-water retention properties, and analyses of swell-collapse behavior; however, the study of shear strain response of partially saturated soils has not been extensive enough. This research work, which uses the RC device, is partly motivated by these needs.

The intent of the current research work is to acquire a clearer understanding of the effect of the suction and net mean stress on the strain dynamic properties of unsaturated soils, such as shear modulus (G) and material damping (D). As previously was mentioned, these key sub-soil parameters are important for an appropriate design and/or analysis of partially saturated soils subjected to static and dynamic loading.

Also, it was outlined on the previous paragraphs that a rational procedure for engineering design related to unsaturated soil dynamic properties needs to be based on a complete understanding of the effects of suction and net mean stress states (i.e., seasonal variations that include wet-dry or freeze-thaw cycles at different depths in the ground). The present work is an attempt to contribute towards this goal.

1.2 Research Objectives

The main objective of this research work is to study the effect of matric suction and net mean stress states on the dynamic properties of unsaturated soils when subject to small- to mid-shear strain amplitudes. Specific tasks within the scope of this research work are described in the following:

To review the literature available on experimental work on partially saturated soils in order to measure dynamic properties via resonant column testing.

To conduct resonant column tests under different controlled suction and net mean stress states to evaluate the influence of these variables over the shear modulus and damping response of compacted poorly-graded sand with silt at different shear strain amplitudes.

To analyze the linear and non-linear behavior of compacted poorly-graded sand with silt from various shear-strain amplitude levels at different suction and net mean stress states.

To assess the normalized shear modulus, normalized damping and threshold strain as functions of shear strain, matric suction and net mean stress.

1.3 Thesis Organization

A brief summary of all the chapters included in this document is presented in the following:

Chapter 2 summaries the importance of soil dynamic properties for engineering analysis. A brief explanation of the existing laboratory methods to measure shear modulus and damping of geo-materials are also defined. The fundamentals of the resonant column test are described, moreover, the role of basic concepts of partially saturated soil mechanics in dynamic geotechnical engineering are also included. A concise literature review of previous works related to similar goals and findings is also incorporated.

Chapter 3 describes the functioning of the proximitor-based resonant column apparatus. Additionally, the basic soil properties evaluated during this research program are described in this section. The mechanisms for controlling and monitoring confining and pore-air pressures are also explained as the most important components of the proximitor-based resonant column device.

Chapter 4 is devoted to describe the Experimental Program and the testing procedures followed in this research work. The process employed for sample preparation as well as the basic properties of the test soil are mentioned. The experimental variables are listed in this section, as well as a description of the suction/net mean stresses states induced on the specimens prior to resonant column testing.

Chapter 5 presents a comparative analysis of all test results from Experimental Programs to assess the effect of suction/net mean stresses states on shear strain stiffness properties of unsaturated soils.

Chapter 6 contains the summary and conclusions from this research study, and also provides some recommendations for future research work.

Chapter 2

Literature Review

2.1 Introduction

This section reviews the fundamentals of soil behavior related to shear strain stiffness including trends under the influence of partially saturated conditions. A revision of different methods to calculate these properties in the laboratory is discussed as well.

The first part of this chapter explains the importance of some soil dynamic properties as the shear modulus, G, and the material damping ratio, D and also discusses various ways to obtain their values in the laboratory. Likewise, this chapter defines the basics of the Resonant Column (RC) test as a part of this research. Throughout this work elementary definitions and instrument principles will be offered. Basic information about partially saturated soil mechanics is covered in this chapter as well, this information includes the basic behavior of unsaturated soils and the current procedures intended to measure total suction and matric suction.

The laboratory Resonant Column test is widely used for assessing dynamic properties of soil at low to medium strains because of its reliability. During the test, the frequency spectrum is swept by vibrating a solid or hollow soil column at increasing frequency rates in order to determine its natural mode. This natural mode is defined as the resonant frequency at which the specimen undergoes the maximum shear strain amplitude as a result of torsional excitation. The shear modulus is then determined as a function of the resonant frequency.

A review of the last research works related to the subject is presented at the last part of this chapter. This works deal with the influence of suction levels on dynamic properties of soils. The findings of these works are briefly presented.

2.2 Importance of Dynamic Properties: Shear Modulus and Material Damping Ratio

The dynamic response of soil can be evaluated on base of two basic properties: one which relates shear stresses to shear strains known as shear modulus and denoted as G, and another which measures the energy dissipation during harmonic excitation, also known as material damping ratio, D. The relationship between shear stresses and shear strains is presented in Figure 2-1. At low strain levels, G is high as the curve is naturally linear.

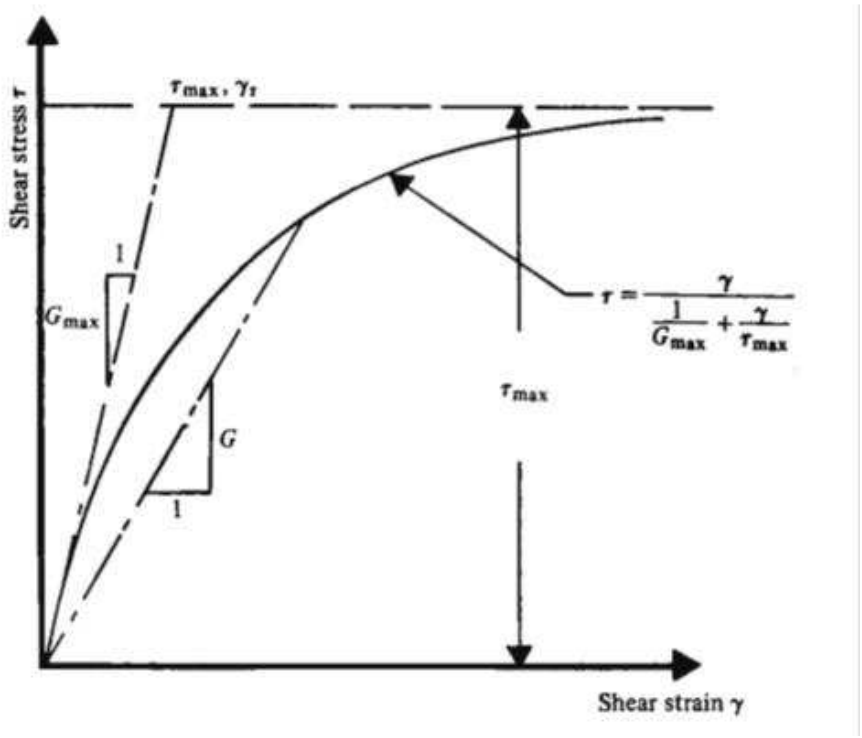

Figure 2-1 Shear stress as a function of shear strain (Hardin and Drnevich 1972)

This modulus is known as the low-strain shear modulus (G_{max}). With the continuing increase on strain, the curve shows up a non-linear trend, and the shear modulus associated to these strains is called the secant shear modulus (G_{sec}). Viggiani and Atkinson (1995) stated that the shear wave velocity of a particular soil can be related

to the shear modulus; thus by assessing the shear wave velocity of a geo-material, there will be the possibility to obtain the soil stiffness value.

Shear modulus is necessary to evaluate many types of geotechnical engineering problems affecting natural soil deposits, including stability of foundations for superstructures and deep foundation systems, dynamic soil structure interaction, protection of structures against earthquakes, deformations in embankments, and machine foundation design (Gazetas1982; Dyvik and Madshus 1985).

On the other hand, just after the seismic excitation has taken place, seismic waves are generated and travel through the soil mass. The initial amplitudes of the waves are reduced as waves propagate through the medium, generally, being this reduction due to energy looses inherent to mechanical materials. This reduction is called “attenuation” (Xia et al. 2002). Attenuation of seismic waves in geo-materials is complex since numerous mechanisms interact and then contribute to the energy dissipation phenomenon during dynamic excitation.

Different methods have been proposed for measuring energy dissipation in geological materials, many of these methods are dimensionless. In order to obtain repeatable results for energy dissipation, an idealization of the geo-materials behavior is needed, thus these materials are considered to be isotropic, perfectly elastic, and homogeneous, moreover, the soils are evaluated within a small range.

Geotechnical earthquake engineering and soil dynamics consider the material damping ratio, D as a usual factor to measure the energy dissipation. Damping can be defined as the correlation concerning the energy dissipated during one cycle, and the maximum strain energy stored during that cycle.

Any engineering analysis related to soil dynamics requires shear modulus and damping ratio values. However, ever since the beginning of soil mechanics research, the

major efforts were put on the area of static behavior. Classical elasto-plastic theories assumptions rule most of the constitutive models formulations. These theories sustain that part of deformation undergone by soil under load is due to elastic deformation of the soil particles. However, the total deformation is assumed to be the sum of the elastic and plastic deformations.

The elastic distortion is only a small part of the total deformation of the soil and is often masked by deformation resulting from slippage, rearrangement, and crushing of particles. Classical elasto-plasticity considers elastic and plastic deformations as separated components, also assumes that these deformations can be experimentally achieved by a loading-unloading process. The total strain magnitude is the sum of elastic and plastic strain, also, some of the total strain is assumed to be recoverable or elastic (Takkabutr 2006), but in geo-materials there is no possibility to separate the elastic strains by loading. Generally it is assumed that the recovery of strain in soils just before exceeding the yield stress is a result of stored elastic energy, although the recuperated strains are not always purely elastic. This strain recovery may be due to slippage at particle contacts points.

The behavior of soils exhibits a variation in the shear modulus with the cyclic shear strain amplitude. The shear modulus is inversely proportional to the cyclic shear strain. Figure 2-2 illustrates the stiffness variation of soil over a large range of strains, from very small to large, and distinguishes approximately between strain ranges. It can be seen that the shear modulus is nearly constant with strain, when strain values are very small. The shear modulus value at small strains is known as the limiting value G_0 or Gmax. For small strains, usually defined subjectively to be less than a maximum of about 1%, the tangent shear modulus G is a non-linear function of strain. In correspondence,

the zone where strain exceeds 1% is defined as that of large strains; there the shear stiffness is very small as the soil approaches failure.

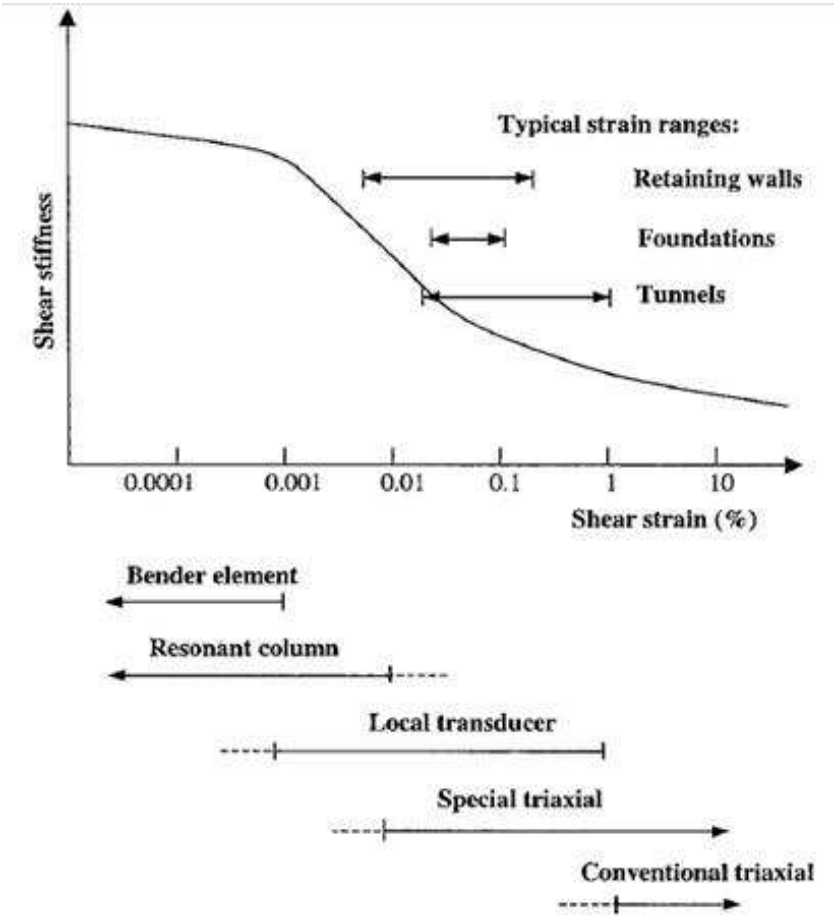

Figure 2-2 Shear stress decay as a function of shear strain (after Atkinson and Sallfors 1991; Mair 1993)

At small strains, the stiffness is typically reduced and continuously decreases as the state nears the critical state line. The stiffness decreases smoothly in the intermediate small strain range with increasing strain.

2.3 Linear and Non-Linear Dynamic Response of Soil

Typically behavior of most soils become progressively nonlinear, after a shear strain of 0.001% is exceeded. The selection of a method to calculate shear modulus and

material damping at large shear strain magnitudes must account for the level of cyclic strain variations; therefore, there is not a unique reliable method to determine these parameters.

Soil can be characterized by calculating shear modulus and damping ratio during vertically propagating shear waves generated by ground motions. Also, the waves must be coupled with small soil displacements in order to characterize the soil. The nonlinear portion of the stress-strain graph is typically expressed by the secant modulus and the damping correlated to the energy dissipation in one cycle of cyclic loading. Figure 2-3 depicts one cycle of loading where the secant modulus is defined as the ratio between maximum stress and maximum strain. The damping calculation considers the ratio between areas A_L (bounded by the hysteresis loop) and A_T, this parameter is related to the energy dissipated in one cycle of motion.

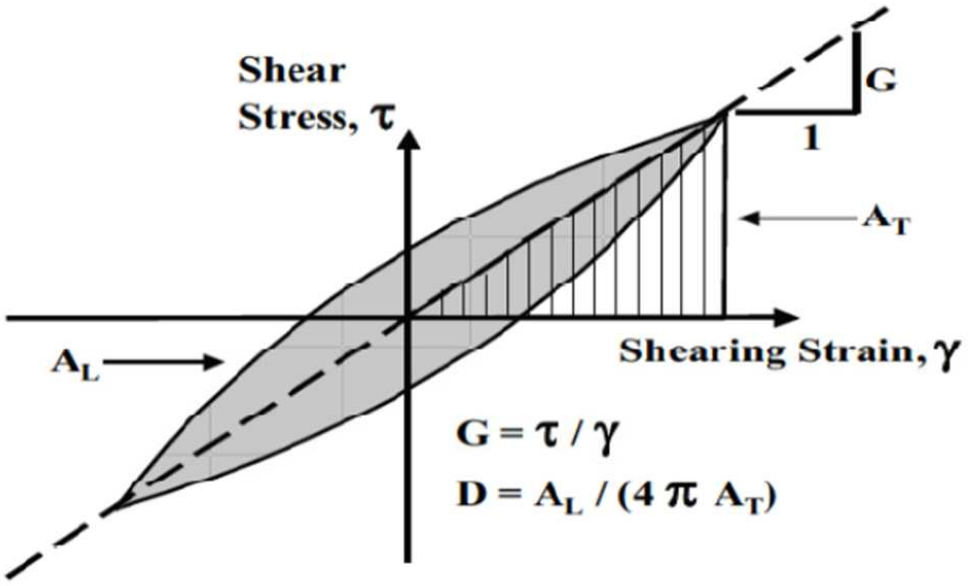

Figure 2-3 Hysteresis loop and calculation of the secant shear modulus and material damping ratio of the soil specimen (Darendeli 2001)

Models of this type which intend to describe the soils behavior can be idealized by elasto-plastic springs considered parallel among them, and then the response parameters will be obtained by fitting the measured data to a best fit curve.

2.4 Laboratory Techniques to Assess Soil Shear Modulus

Presently it is possible to perform different types of laboratory tests on soil samples in order to evaluate shear wave velocities, shear modulus, and the material damping ratio. Some of these techniques assess the shear modulus indirectly by calculating first the shear wave velocity of the soil while other tests evaluate the soil shear modulus directly. Also, the dynamic properties of soils can be estimated in the field by performing in-situ tests. The field testing methods can measure low strains (within the range of 10^{-3} thru 10^{-4} % and less), however, laboratory tests can manipulate the sample conditions to achieve the desired boundary conditions and precision required.

The experimental work developed during this research was based on laboratory techniques to determine the dynamic response of soils; therefore, the following paragraphs are dedicated to describe these methods for estimating the type of soil response.

2.4.1 Cyclic Triaxial Test

The Cyclic Triaxial apparatus is able to assess the dynamic properties of soils between the elastic and plastic range (strains levels of 0.001% and 2% respectively). To achieve the desired strain levels, the loading system of the device must apply cyclic sinusoidal loads ranging between 2 N (0.5 lbf) thru 225 N (50 lbf) coupled with deformations between 0.005 mm (0.0002 in.) and 2.5 mm (0.1 in.) respectively, at rates ranging between approximately 0.1 Hz and 1 Hz.

The rates applied throughout the Cyclic Triaxial test intend to represent forces associated with wave action and earthquake analysis, respectively. During the test

measurements of changes in axial load, deformation and pore water pressure are taken and recorded.

The maximum shear modulus is assessed by execution of three different stages of fluctuating sinusoidal cyclic loading at the recommended frequency, then five loading cycles are applied in every stage. In the initial step, the cyclic load of approximately ± 0.5 lbf (2 N) is applied. Then, the cyclic load applied has to be adjusted in the subsequent stages to achieve a uniform distribution of shear moduli data, G, versus shear strain amplitude, γ, up to a value of about $5x10^{-3}$ percent.

2.4.2 Resonant Column Test

In the beginning of this test, the resonant column (RC) apparatus was intended to determine the dynamic response of rocks. The RC device has been enhanced continuously to study the behavior of multiple types of geo-materials. In the 1970's a variety of the RC devices were designed by Dr. Stokoe and his colleagues. During the late 1970s, a new type of resonant column apparatus was developed by Professor Stokoe and his co-workers, this one was a free-fixed end type. The American Society for Testing and Materials standardized the Stokoe RC testing technique by issuing the ASTM D 4015-92. The shear modulus and damping ratio of soils can be obtained by using this test method with a high degree of reliability. In 1979, Isenhower implemented a torsional shear apparatus to the RC device, thus, the dynamic response of the soil is evaluated when a series of low frequency cycles are applied to the sample in the torsional shear test (Isenhower 1979).

The Stokoe RC test is known to have a fixed end as well as a free end at which torque is applied. The frequency spectrum is swept to find the frequency at which the sample undergoes the greatest strain; this frequency is known as the natural or resonant frequency. The shear modulus (G) and the shear wave velocity (V_s) of the soil can be

easily calculated once the resonant frequency (f_r) is obtained. The damping ratio can be assessed from the hysteresis loop or by free decay curve at very low strains.

The RC technique is very useful to assess the shear wave velocity, shear modulus and damping ratio of soil under different combination of variables as isotropic pressure, void ratios, and shear strain amplitude, and number of cycles.

2.5 Resonant Column Test Fundamentals

Resonant Column (RC) devices stared to be use since 1930's to evaluate dynamic response of soils and rocks. Several versions of the resonant column apparatus were developed by researches all over the world. Dr. Stokoe and his colleagues improved the resonant column device so it became a fixed-free cyclic reaction test. The idealization of the test is based on the theory of linear-elastic vibration by applying the one-dimensional wave propagation equation. The RC has strain amplitudes limits ranging from low to medium, however, the apparatus is capable of measuring larger strains such as up 0.4% (Stokoe et al. 1978).

The resonant column device is capable of testing solid cylindrical soil specimens or hollow cylindrical specimens under its fixed-free cyclic torsional condition. This condition means that the bottom of the sample tested is fixed to a roughly textured base on which it rests (the base of the resonant column apparatus contains 3-ceramic disks to allow water dissipation) while rotation is induced to the top by means of a motor (the top of the resonant column apparatus is part of the suction controlling device and has porous stones for air entry or dissipation). The device is depicted below in Figure 2-4.

The test is performed by applying torsional excitation to the top at constant amplitude and then increasing frequency until the frequency at resonance is found, this frequency is defined as the frequency at which the cylindrical specimen experiences the maximum shear strain for the given soil as is shown in Figure 2-5. This variable is also

known as resonant frequency, f_r. Stokoe and Huoo-Ni (1985) found that typical values of resonant frequency for soil samples may range from 6 to 150Hz.

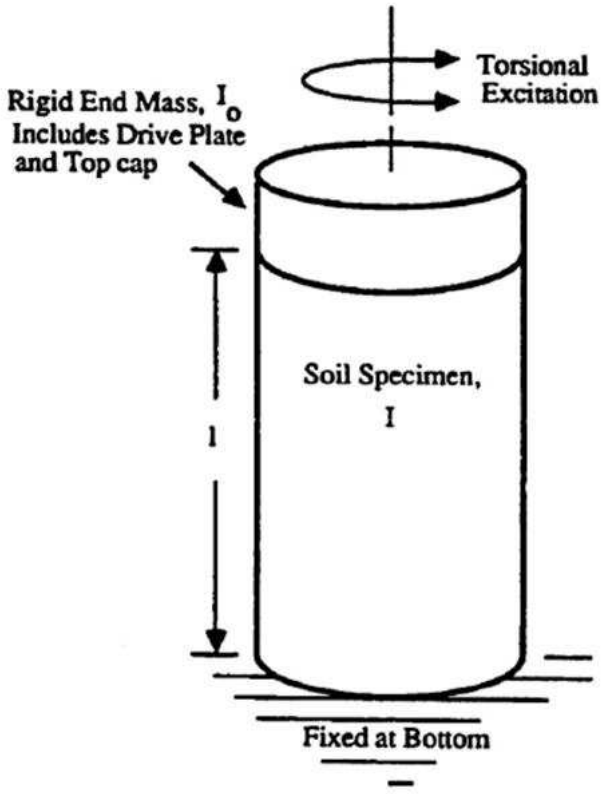

Figure 2-4 Idealization of fixed-free Resonant Column Apparatus (from Huoo-Ni 1987)

It is possible to determine the dynamic properties of the soil specimen after the resonant frequency has been obtained since these properties are a function of the frequency at resonance. However, dynamic response of the soil depends on several variables such as moisture content, density, weathering, voids ratio, in addition to external variables that impact its variation such as confinement pressure and suction levels.

The damping ratio, D, can be calculated by using Half-Power Bandwidth method, or Free-Vibration Decay method, as will be discussed. Throughout this research, these two methods will be used to obtain damping values.

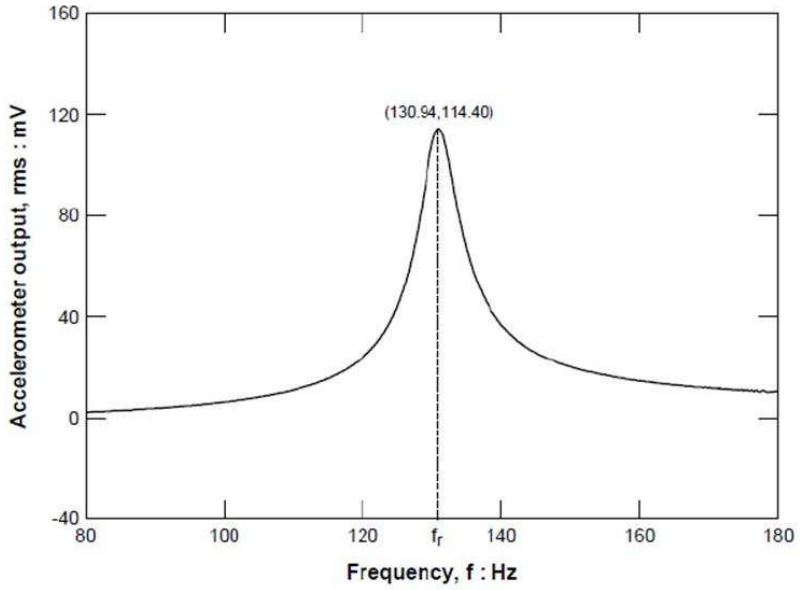

Figure 2-5 Frequency response curve obtained from RC test (Takkabutr 2006)

2.6 Dynamic Soil Properties Evaluation

2.6.1 Shear Modulus (G)

The conception of RC device is founded on the theory of elastic wave propagation, according to this theory, the material behaves under perfectly elastic conditions; thus, the dynamic properties of the soil are supposed to be constant and independent of any other variables as amplitude or frequency. The threshold limit is useful since it helps in the determination of the peak shear strain at which the specimen still remains within the elastic region or can be assumed to behave elastically. Any dynamic parameter of the soil in a region lower than this threshold limit is considered to be independent of strain.

The shear wave velocity of the soil behaving in the elastic region, Vs, can be obtained by applying the frequency equation defined by equation 2.1.

$$\frac{\sum I}{I_o} = \frac{w_r}{V_s}\tan\left(\frac{w_r\, L}{V_s}\right) \qquad (2.1)$$

Where, $\sum I = I_s + I_m + I_w + \cdots$

I_s = mass moment of inertia of soil specimen,

I_m = mass moment of membrane,

I_o = mass moment of inertia of top rigid mass (top cap + spider),

I_w = mass moment of central wire (only if sample is hollow)

w_r = soil natural frequency (rad/sec),

L = length of soil specimen.

According to the theory of elasticity, the shear modulus, G can be obtained as following:

$$G = \rho(V_s)^2 \qquad (2.2)$$

Where,

V_s = shear wave velocity,

ρ = total mass density of the soil (unit weight divided by gravitational acceleration)

Richard (1975) proposed an efficient method for estimating G from the resonant frequency value, f_r, and considering the geometric characteristics of the system I_o. The method considered that when the system reaches resonance, the equation 2.1 may be modified as,

$$\frac{I}{I_o} = \frac{w_r L}{V_s}\tan\frac{w_r L}{V_s} = \beta\tan\beta \qquad (2.3)$$

Where,

$$\beta = \frac{w_r L}{V_s} \qquad (2.4)$$

This result in,

$$V_s = \frac{w_r L}{\beta} = \frac{2\pi f_r L}{\beta} \qquad (2.5)$$

When equation 2.5 into equation 2.2

$$G = \rho(2\pi L)^2 \left[\frac{f_r}{\beta}\right]^2 \qquad (2.6)$$

In most cases,

$$\frac{I}{I_o} \ll 1$$

Because of treating small angles, $\beta = \tan\beta$, then from equation 2.3:

$$\beta^2 = \frac{I}{I_o}$$

Finally, equation 2.6 can be expressed as,

$$G = \rho(2\pi L)^2 \left[\frac{f_r}{\mathrm{F_r}}\right]^2 \qquad (2.7)$$

In equation 2.7, F_r is designated as dimensionless frequency factor. Also, Equation 2.7 was used in this research work to assess small-strain shear modulus, G.

2.6.2 Damping ratio (D)

The Half-power Bandwidth Method, and the Free Vibration-Decay method were used to determine the damping ratio of the material, D_{min}. The Half-power Bandwidth method determines damping based on the resonant frequency curve. According to this method, the frequencies corresponding to 0.707 both before, f_1 and after f_2 of the frequency at resonance have to be obtained, as depicted in Figure 2-6.

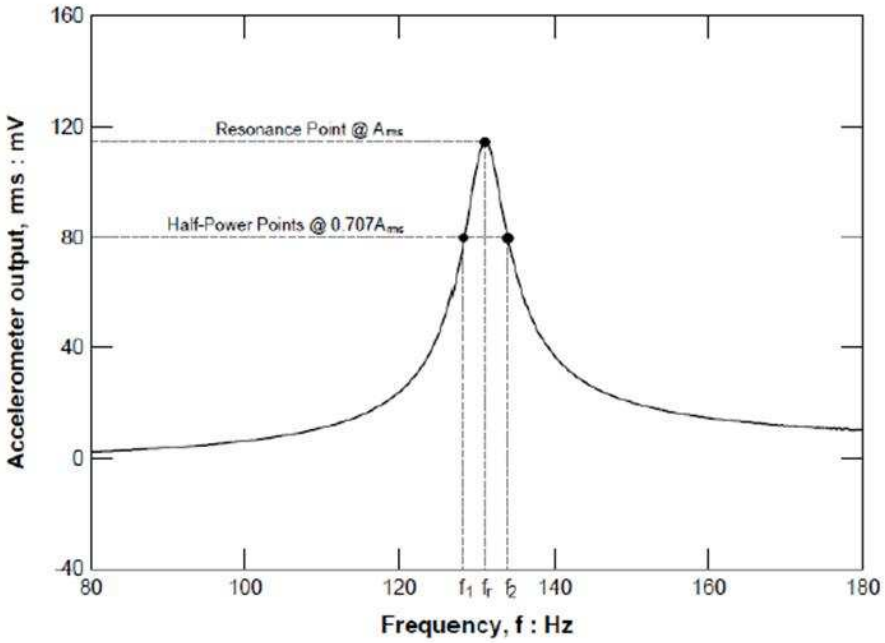

Figure 2-6 Soil damping ratio (D) calculation based on Half-power Bandwidth Method.

From this curve and following this step, the soil damping ratio (D) can be estimated as shown by equation 2.8:

$$\mathrm{D} = \frac{1}{2}\frac{\mathrm{f_2} - \mathrm{f_1}}{\mathrm{f_r}} \qquad (2.8)$$

Where, f_r is known as the frequency at resonance of the system.

The material damping ratio can also be computed from the data obtained after the soil specimen is allowed to freely vibrate. The vibrations decay rate is useful to do so. Huoo-Ni (1987) and Craig (1981) described that soil free vibration response in the resonant column test normally presents under-damped behavior, thus the general solution to this case is presented by equation 2.9:

$$\theta\,(\mathrm{x},\mathrm{t}) = \mathrm{C}e^{-\mathrm{D}w_n t}\sin(w_d t + \phi)\sin\left(\frac{w_n L}{V_s}\right) \qquad (2.9)$$

Where,

C = constant

D = $cw_n/2G$

Wd = $\sqrt{1 - D^2}$ (2.10)

ϕ = phase shift between excitation and response of the system (radians).

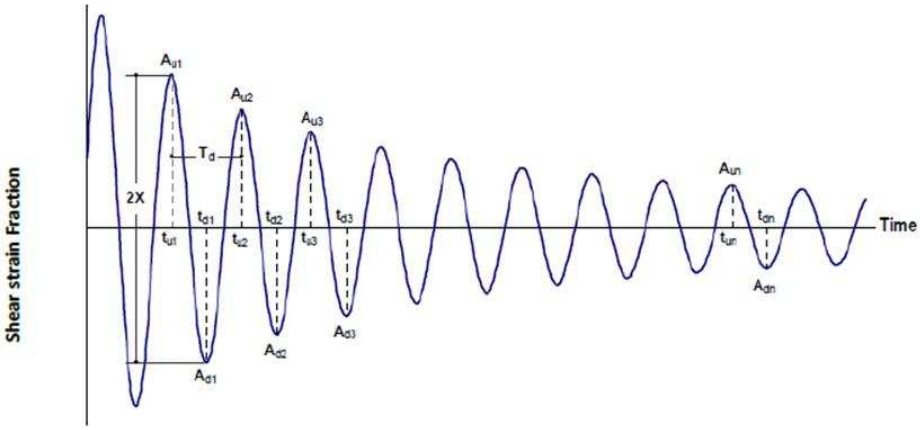

Figure 2-7 Free Vibration Decay curve used to obtain damping ratio

The relationship between two different peaks, as shown in Figure 2-7, is given by Equation 2.12:

$$\frac{x_n}{x_{n+1}} = e^{-w_n D(t_n - t_{n+1})} = e^{\frac{2\pi D}{\sqrt{1-D^2}}} \quad (2.11)$$

Where,

$t_n+1 = t_n + 2\pi/w_d$ (logarithmic decrement),

δ, is found by taking the natural logarithm of equation 2.11.

$$\delta = \ln\frac{x_n}{x_{n+1}} = \frac{2\pi D}{\sqrt{1 - D^2}} \quad (2.12)$$

Thus, it is possible to calculate the damping ratio as:

$$D = \sqrt{\frac{\delta^2}{4\pi\delta^2 + \delta^2}} \qquad (2.13)$$

During this work, the material damping ratio, D was calculated by using equations 2.8 and 2.13.

2.6.3 Shear Strain (γ)

The amount of shear strain undergone by a solid cylindrical specimen when it is torsionally excited in the resonant column device is a function of several variables among others: the angle of deformation, the distance from the axis, and of the height from the fixed base. The shear strain exhibits zero value at the center of the longitudinal axis and a maximum value at its outside face as shown in Figure 2-8.

The shear strain, γ is determined as follows:

$$\gamma(r) = \frac{r\,\theta_{max}}{h} \qquad (2.14)$$

where, r = radial distance from the soil specimen axis

θ_{max} = maximum angle of rotation, and

h = height of the soil sample.

Since the shearing strain is not constant throughout the specimen, the average shear strain undergone by the sample has to be represented by an equivalent shear strain, γ_{eq}.

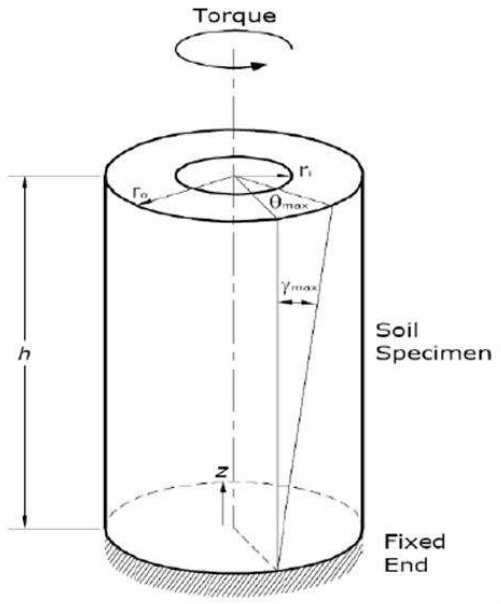

Figure 2-8 Idealization of shear strain occurrence during Resonant Column test, γ (GCTS RC manual, 2009)

2.7 Unsaturated Soil Mechanics Fundamentals

Conventional soil mechanics considers that the soil behavior may be assumed under either totally dry or totally saturated conditions. These traditional idealizations assume positive pore water pressures for those soils beneath the water table, on the other hand, this approach accepts fully dry conditions for those soils above ground water table. Terzaghi's effective stress theory is widely accepted to evaluate the shear strength of saturated soils. However, soils being under partially saturated conditions experience variations in soil strength and volume change, due to the inherent suction generated in the unsaturated soils. This particular behavior must be taken into account since a high percentage of soils all over the world are subjected to partially saturated conditions. Thus, this chapter presents an overview of the soil suction properties and describes the principles of the soil water characteristic curves.

In the last years, unsaturated soil mechanics has been recently developed and refined on its modeling and understanding. Many of these developments have been based on a detailed analysis of the unsaturated soil zone or vadose zone, located just above the ground water table (Fredlund and Rahardjo 1993). However, the increasing on the understanding of this engineering branch has been slow when compared to the gained understanding of the behavior of saturated soil mechanics.

The concepts needed to establish a clear understanding of partially saturated soil behavior have been slowly expanded (Bishop 1959).

The first efforts were focused on the capillary flow (Black and Croney 1957; Williams 1957; Bishop et al. 1960; and Atchison 1967). The researches previously mentioned yielded models which equations take into account the effective stress for soils under partially saturated conditions.

In mid 1970's, two independent normal stress variables were defined for unsaturated soils by a work developed by Fredlung a Morgenstern (1970). The variables are net normal stress ($\sigma_{net} = \sigma - u_a$) and matric suction ($\psi = u_a - u_w$).

In unsaturated soils, the water content of the soil is a function of its suction. The soil-water characteristic curve (SWCC) is a very important feature of partially saturated soils since it relates the volumetric water content of the soil and the suction in it.

These characteristics of unsaturated soils can be used to get a better understanding of changes in void and saturation levels in highly expansive soils, which may undergo extreme modifications in moisture content due to seasonal variations.

Thus, an advanced understanding of this particular behavior would help to obtain an enhanced explanation of the swelling and shrinking mechanisms acting on expansive soils.

The main properties of unsaturated soils will be presented in the following sections. Suction measurement techniques and fundamentals of soil-water characteristic curve will be described as well.

2.7.1 Partially Saturated Soil Profile

Three subzones can be easily identified in the unsaturated region: the capillary fringe, the intermediate zone (or vadose zone), and the soil water zone as shown in Figure 2-9. The type of soil encountered in the field will rule the final conditions of the unsaturated zone. If the soil is coarse grained it is supposed to be completely saturated when located below the ground water table. On the other hand, in fine grained soils, the saturated zone can reach higher levels than the ground water table due to capillary forces (Bear 1979). The extension of the capillary zone will depend on such parameters as the grain size distribution, the soil density, and the soil stratigraphy.

The unsaturated or vadose zone is located above the saturated part of the capillary zone (Bear 1979).

2.7.2 Matric Suction

The matric suction is known as the difference between the pore-air pressure, represented as u_a, and the pore-water pressure, u_w (Fredlund and Rahardjo 1993). The suction, denoted as (u_a-u_w) is related to tension in the capillary menisci of the pore water, and water absorption forces generated in the soil particles. These forces are associated to the geometric composition of the soil (Department of the Army USA 1983; Lu and Likos 2004). The matric suction may change reliant on variations of the surrounding ecological and oscillations in weather. Therefore, changes in the suction profile are created due to alternate occurrence of dry and wet seasons, these changes are more evident in the zones close to the surface (Fredlund and Rahardjo 1993). Moreover, several field factors play a significant role on the variation of suction into the soil profile,

some of these factors are permeability of soil, water table, ground surface conditions, environmental conditions and vegetation.

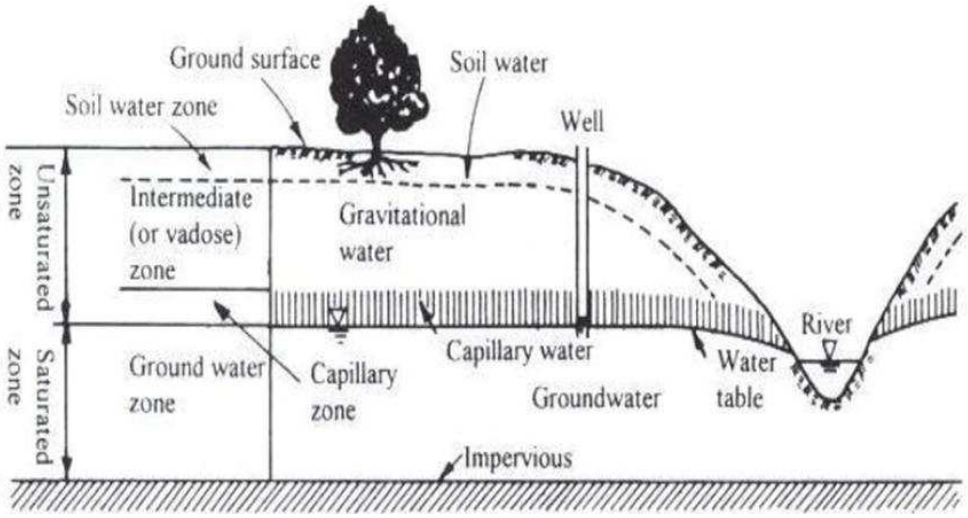

Figure 2-9 Typical profile for partially saturated soils (Bear 1979)

Soil permeability: The capacity of soils to drain and conduct water is weighed by the hydraulic permeability concept. This concept indicates the capacity of the soil to generate variations on matric suction as the environment changes (Fredlund and Rahardjo 1993).

Ground water table: The depth of this variable affects the magnitude of the matric suction. If the water table is deep, the matric suction is possibility higher (Fredlund and Rahardjo 1993).

Ground surface condition: The ground water table as well as the suction may change due to dry and wet seasons, particularly in the ground zone near to surface. Ground surface coverage affects the variations on suction; hence, suction may fluctuate with time in uncovered areas more than it does in covered areas (Fredlund and Rahardjo 1993).

Vegetation: The evapotranspiration process produced by the existence of vegetation on the ground surface may develop tension in the soil pore-water as much as 1 to 2 MPa. An increase in the matric suction can be expected in the soil close to surface since evapotranspiration process removes water from this zone. Factors as of climate, the type of vegetation, and the depth of the root zone can affect the rate of evapotranspiration (Fredlund and Rahardjo 1993).

2.8 Previous works

The dynamic response of soils has been modeled by several studies (e.g., Richart et al. 1970; Seed and Idriss 1970; Hardin and Drnevich 1972b; Iwasaki et al. 1978; Lee and Finn 1978; Zen et al. 1978; Kokusho et al. 1982; Seed et al.1986; Ni 1987; Sun et al. 1988; Vucetic and Dobry 1991; Ishibashiand Zhang 1993; Rollins et al. 1998; Vucetic et al. 1998; Stokoe et al. 1999, 2001). This research concluded that the main factors affecting G/G_{max} behavior include mean effective confining stress (σ'), soil type, shear strain magnitude γ, and plasticity index (PI). Other recognizable elements contributing to variations in G/Gmax include: degree of saturation, frequency of loading, overconsolidation ratio, void ratio, grain characteristics, and number of loading cycles (Darendeli 2001).

Great part of the research performed up to date has been developed to acquire a richer understanding of the influence of degree of saturation and capillarity on the small-strain stiffness properties of partially saturated soils.

Recently, a suction-controlled resonant column/torsional shear apparatus was developed at the University of Napoli, Italy. Mancuso et al. (2002) and Vasallo et al. (2007) used the device to perform a series of tests on unsaturated silty soil.

The axis-translation technique was used to induce the matric suction in the sample, at the same time as the torsional torque was gradually increased to study soil stiffness response at small, mid, and high-shear strain amplitude levels.

The literature review will focus on four papers which meet the most the objectives of the current research. These papers include: “Small Strain behavior of a Silty Sand in Controlled-Suction Resonant Column – Torsional Shear Tests (Mancuso et al. 2002); “Dynamic Properties of Chemically Stabilized Sulfate Rich Clay” (Hoyos et al. 2004); “Development of a Suction-Controlled Resonant Column Apparatus with Self-Contained Bender Elements (Suescun 2010)” and Effect of Stress and Suction Histories on Dynamic Properties of Statically Compacted Silty Sand” (Douglas 2012).

Mancuso et al. (2002) conducted a research looking forward to model the effect of moisture content on a sample subjected various suctions. Shear stiffness measurements were also taken during constant-suction tests.

Suescun (2010) worked to obtain a richer understanding of the effect of variable suction levels on compacted silty sand. During his work a suction controlled proximitor resonant column apparatus with bender elements was introduced. In Suescun’s work, the dynamic properties found from the proximitor RC test were matched with results in a traditional accelerometer based resonant column device. In his work a comparison between the results from the bender elements found on the proximitor RC device was also made.

Suescun calibrated the proximitor RC apparatus previous to initiating the series of tests on this new device. In the present research project this same equipment was employed; therefore, it is considered that the resonant column device did not require additional calibration. This equipment operates a pressure control panel for implementation of the axis translation technique since this panel allows individual

application of both pore-water and pore-air pressure and at the same time taking measurements of this variable parameters. This apparatus includes a set of self-contained bender elements to test simultaneously small-strain stiffness properties under both techniques. However, the present research project did not utilize this feature.

Empirical correlations between small-strain stiffness properties of compacted silty sandy soil, such as shear modulus and damping ratio, and important environmental factors, such as matric suction state and net mean stress, have been formulated based on Suescun's work.

Douglas (2012) worked aiming to ASSESS the effects of the stress/suction history of the soil on the G/G_{max} and D/D_{min}. His work intended to reproduce in situ stress states and loading paths at pre- and post-construction stages in shallow foundation and subgrade systems that remain under partially saturated conditions throughout any given year. To do so during his work, Douglas selected the adequate experimental variables and completed an extensive experimental program.

On the next chapter, a description of the functioning of the proximitor-based resonant column apparatus will be presented. Additionally, the basic soil properties evaluated during this research program are described in next chapter. The mechanisms for controlling and monitoring confining and pore-air pressures are also explained as the most important components of the proximitor-based resonant column device.

Chapter 3

Test Soil and Resonant Column Apparatus

3.1 Introduction

This chapter presents the characteristics of the soil used to perform the present research. The soil was analyzed and classified as white fine grained poorly graded sand with silty. The main properties of the soil are presented, including the general engineering properties of the soil, as well as the soil water characteristic curve. This chapter covers a detailed description of functioning and parts of the proximitor based-resonant column device. The main components such as driver system, measurement digital sensors, and software capabilities are presented. Each device characteristic is methodically described and categorized. Finally in this chapter, the procedure for sample preparation will be presented. As previously mentioned, this device had previously been calibrated and therefore did not necessitate further adjustment.

3.2 Properties of test Soil

3.2.1 Basic Engineering Properties

The test soil used in this research was classified as poorly graded fine-grained sand with silt which has a white color. The soil classifies as SP-SM according to the USCS.

The sieve analysis determined particle sizes varying between 0.9 mm and 0.012 mm, which indicates that the soil has the behavior of a granular soil. The fine percentages ranged between 6% and 8%, whereas the percentage of sand varied from 94% to 92%. The initial water content ranged from between 9% and 10%, with an average of 9.54% and the dry unit weight was 18.34 KN/m3. These values were obtained from the Standard Proctor test. The total unit weight was 20.09 kN/m^3. It was not possible to perform the plastic limit test on the soil; therefore, it was not possible to obtain a value

of liquid limit (LL) due to the obvious non-plastic nature of the material. The specific gravity value was estimated to be around 2.68, and the void ratio was estimated within a range of 0.29 and 0.34 for the soil at this density. A summary of the soil characteristics is listed in Table 3-1. Also, the soil gradation curve is presented in Figure 3-1.

Table 3-1 General Soil Properties and Classification

Property	Result
Color	White
Moisture content (%)	9.0 - 10.0
Passing No.200 sieve (%)	6.0 - 8.0
Specific gravity (Gs)	2.68
Plastic limit, PL (%)	NP
Liquid limit, LL (%)	NA
Plastic Index, PI (%)	NA
Dry unit weight, γ (kN/m^3)	18.34
Total unit weight, γ (kN/m^3)	20.09
Void ratio	0.32
USCS classification	SP-SM

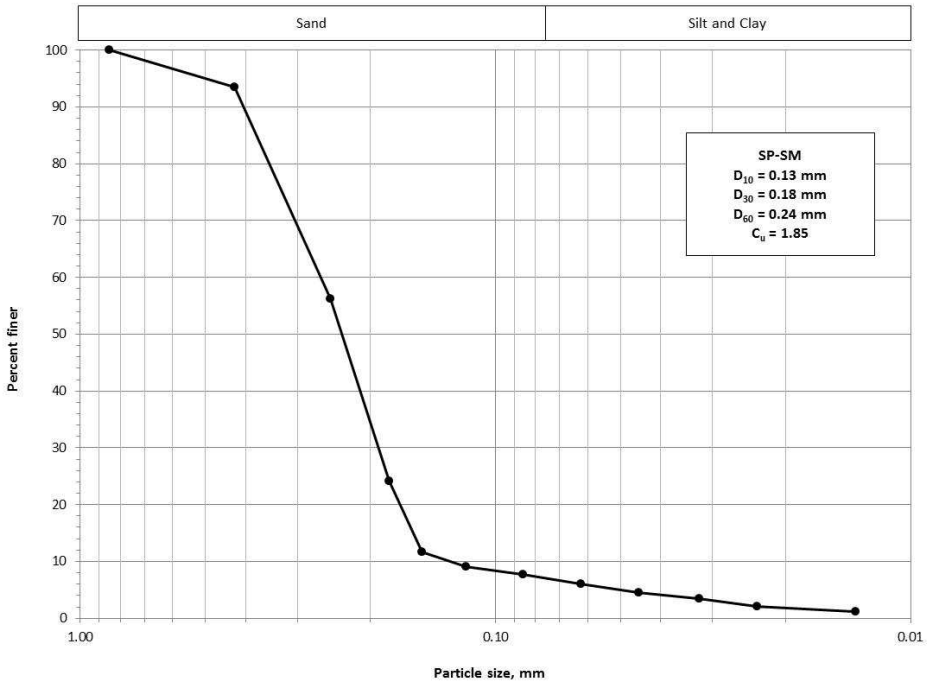

Figure 3-1 Particle-size distribution curve for SP-SM soil

3.2.2 Soil Water Characteristic Curve

The moisture content of the unsaturated soil is associated to the matric suction in it through the soil water characteristic curve (Fredlund and Rahardjo 1993). Ayalew (2013) worked on the acquisition of the graph and was used in this research in which precisely the same soil was used.

Ayalew obtained the SWCC for the soil via Tempe cell device by applying axis translation technique and conventional filter paper tests. Fifteen (15) samples were used to define the trend of this curve which is shown in Figure 3-2. In this figure it can be seen that the soil air entry value is approximately 40 kPa.

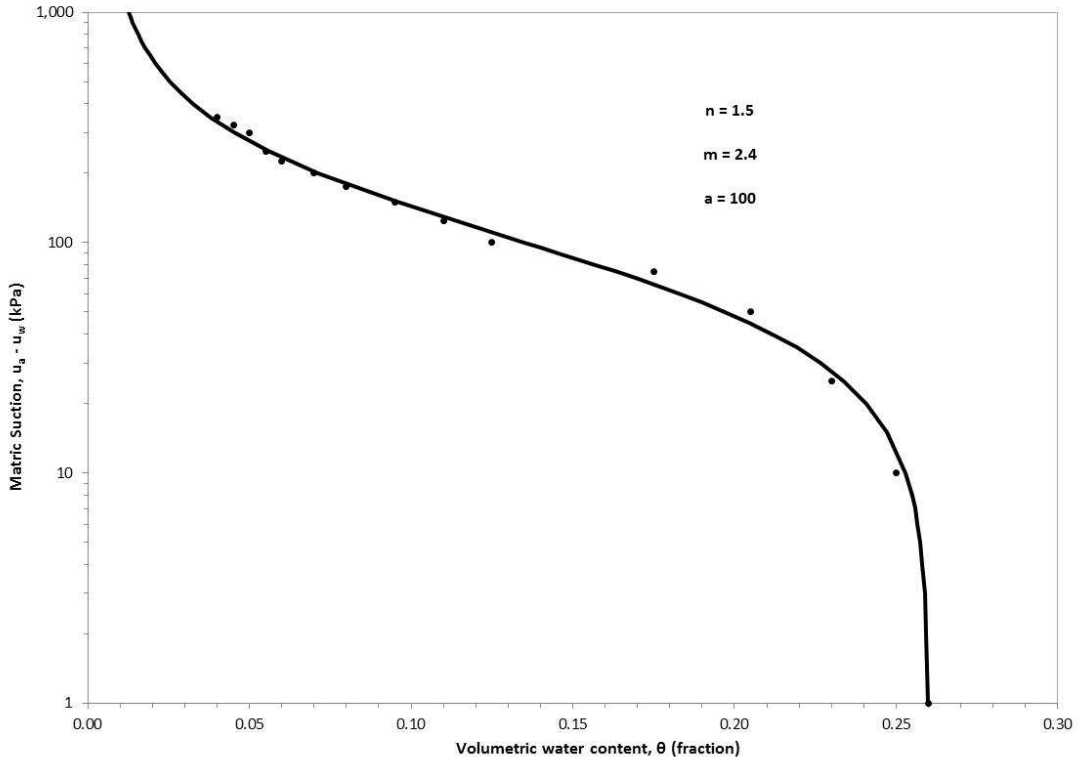

Figure 3-2 SWCC for SP-SM soil (Fredlund and Xing)

3.3 Proximitor-Based Resonant Column Apparatus Components

The refinements made up to date on The Proximitor-based Resonant Column device used for the present permit fully automated testing. Highly sensitive and advanced sensors and digitized electronics and computer software programs make testing an automated process.

The device applies a cyclic torque to the free (superior) end of the cylindrical specimen by means of a torsional motor which is controlled by a computer software. The applied load is a harmonic torque with constant amplitude. This load is applied at varying frequencies while the response of the sample is measured. The shear wave velocity is a function of the resonance frequency, This frequency causes the greatest shear strain in the sample. Likewise, shear modulus is achieved from the shear wave velocity and the soil density. As outlined in chapter 2, there are two different methods to obtain the material damping ratio: the first is the logarithmic decay curve method, which calculates the energy attenuation once the torque is no longer applied; the second is the Half-Power bandwidth method. There is another option to evaluate material damping: the Hysteresis loop method, however, it is recommended to utilize this method only when the sample is subject to very small-strains.

This RC device is capable of measuring the shear modulus ranging from very low strains to high strains. Figure 3-3 illustrates the Proximitor-based RC owned by UTA and used to complete the present work. The main components of the Proximitor-based RC testing system are as follows: (a) main cell, (b) servo controller and acquisition system, (c) resonant column software, (d) gauge deformation sensor, and (e) computer unit.

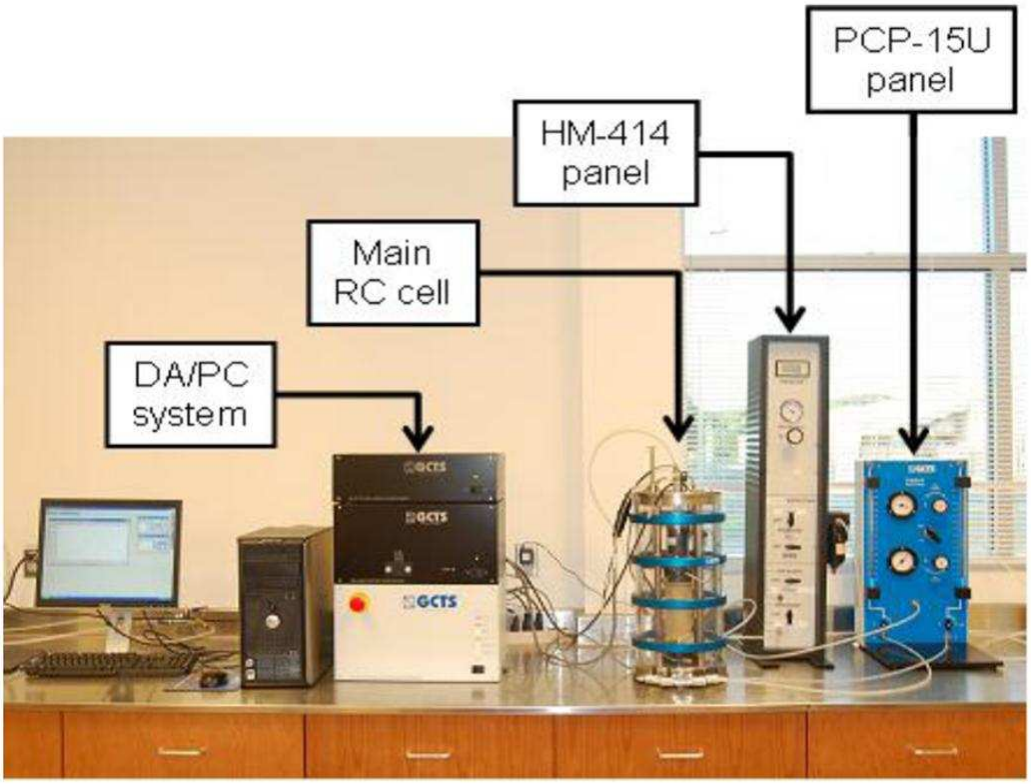

Figure 3-3 General arrangement of the proximitor-based RC system

3.3.1 Main Cell of the Resonant Column Apparatus

Four stainless steel columns sustain the basic assembly for the main cell, two of the columns are used as the support shaft for the gauge displacement sensor and motorized drive system. A transparent reinforced acrylic plastic with a thickness of a ¾ inch forms the cell; its wall withstands an isotropic confining pressure up to 1 MPa as the maximum capacity. The application of torque and the data acquisition are fulfilled by means of several connections that link the specimen to the computer. The drainage system of the main cell is located at both, the top and bottom of the main cell. This system will be further explained ahead in this chapter. All these connections were set to permit a regulated flow of water out of the sample, to allow the application of isotropic

pressure to the specimen, and to allow for direct air pressure into the sample. The main cell assembly is shown in Figure 3-5.

Figure 3-4 RC Main cell of the Proximitor-based RC

The function of the proximitor is to measure the internal angular displacement undergone by the sample due to harmonic torsional excitation. The Proximitor was set by means of a stainless steel guide fixed to the top cap of the main cell. The circular “target” was attached to the free end of the sample top cap and undergoes gentle rotation back and forth along with the cyclic torsional excitation.

3.3.2 Proximitor mount

The digital servo-controlled and acquisition system receives the signal acquired by the proximitor and processes this signal which is basically angular changes in order to calculate the shear strain. The proximitor is a fiber optics deformation sensor identified with the designation SR-DF-FO-250, it has dual range output +/- 0.1 mm low range and

+/-6.0 mm high range with 0-15 kHz flat frequency response. The Proximitor is shown in detail in Figure 3-5.

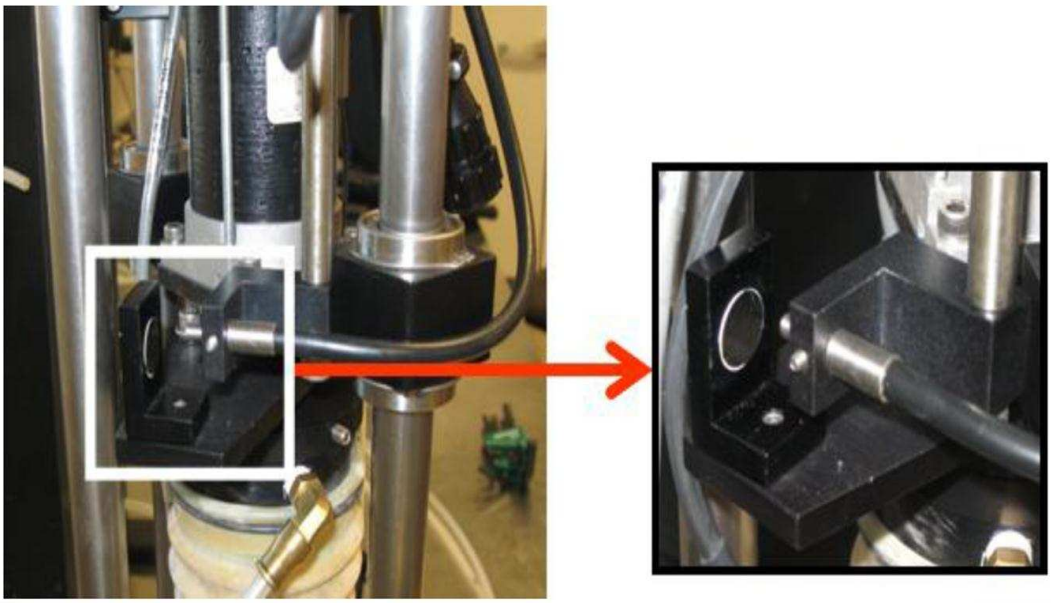

Figure 3-5 Proximitor mounting details (transducer for measuring internal angular displacement)

3.3.3 Digital Servo Controller and Acquisition System

GCTS SCON-1500 Digital System Controller is the designation given to the digital servo-controlled and acquisition system. The system consists of numerous digital electronics. The software operates the settings and configurations. Angular and vertical displacement data are controlled, activated and stored by the system.

The SCON-1500 model DA/PC comprises a microprocessor based digital servo controller, data acquisition, function generator, and a digital I/O unit. The performance of the resonant column tests can be monitored by software which also registers and stores the data obtained by the test execution. Based on this data, calculations on shear strain, shear modulus, and damping ratio can be made for shear strains ranging from 10% to

10-4%. The signal conditioning mother board accepts up to eight universal signal conditioning module slots.

3.3.4 Resonant Column Software

One of the main features of the Proximitor-based RC software is its compatibility with several resonant column apparatus. The software is designed to determine the dynamic response of soil samples tested in the RC by way of graphic evaluation of the resonant frequency and by assessment of data given from the free vibration decay to determine damping. The system designation is CATS-RC.

The following variables were obtained by using CATS-RC.

a) Resonant frequency (Hz)

b) Shear wave velocity (m/s)

c) Shear modulus (MPa)

d) Maximum shear strain (fraction)

e) Damping ratio-Free vibration decay (%)

f) Predominant frequency from Free vibration data FFT Analysis

g) Damping ratio-Half power bandwidth (%)

h) Natural frequency –from resonant frequency and free vibration decay (Hz)

i) Natural frequency –from resonant frequency and phase shift (Hz)

j) Natural frequency –from FFT frequency and free vibration decay (Hz)

Figure 3-6 below illustrates a representative software application in Windows environment.

The software requires some input data such as soil and specimen properties as well as starting frequency, stop frequency and cycles until steady state is reached. These input data are required for the software in order to perform automatic calculation of the parameters previously outlined. Once the testing is completed, for each test the user can

import and save the CATS-RC data which includes the calculated parameters and other substantial data, including the forced vibration data, as well as the free vibration data of the specimen, from which the damping was determined.

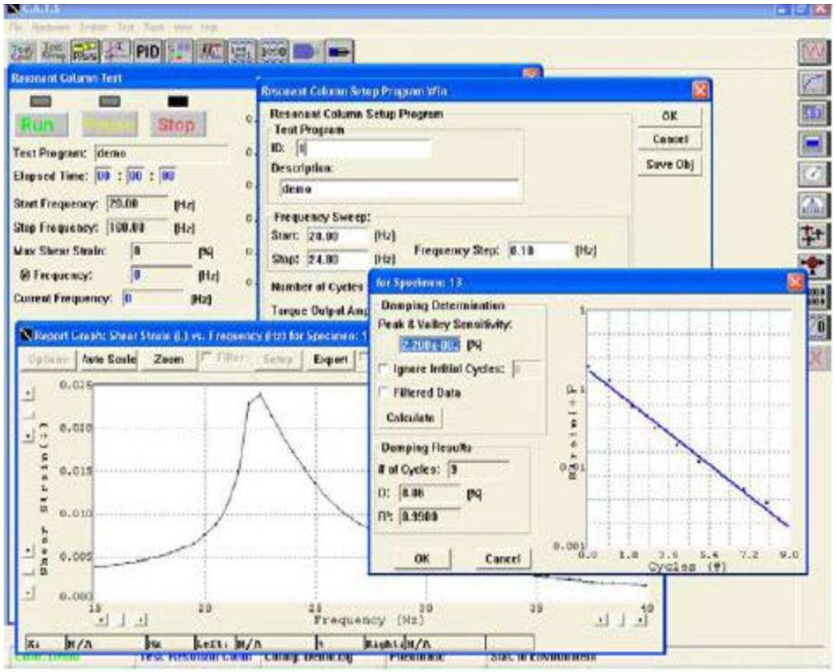

Figure 3-6 Display of CATS-RC software in Windows environment

3.4 Pressure control monitoring system

3.4.1 Pore-air Pressure Control

The HM-414 and the PCP-15U pressure panels regulate the external and pore-air pressure conditioning of the sample. The external confining pressure action on the specimen is controlled by the HM-414 model pressure panel; this is shown on the left side in Figure 3-7.

An inlet air-pressure port positioned on the cover plate of the main cell introduces the pressurized air. Previously it was mentioned the maximum air pressure that the acrylic cell can withstand is 1 MPa.

Pore-air pressure u_a application at the top of the soil specimen is controlled by the PCP-15U model pressure control panel as shown on the right side in Figure 3-7. The pore-air pressure application is performed by using dual pressure regulators and gauges in order to generate matric suction; $s = (u_a - u_w)$; $u_w = 0$.

The panel is equipped with a flushing mechanism which facilitates the air removal, the air diffuses into the compartment underneath the 5-bar HAVE ceramics located at the bottom pedestal.

Figure 3-7 Panels for pressure control

3.4.2 Pore-water Monitoring System

Three ceramic disks installed inside the rough surfaced bottom pedestal are used to dissipate the pore water pressure. The bottom pedestal is shown in part a, at the left side of Figure 3-8. Also, the top cap is supplied with three coarse porous stones (part b Figure 3-8), which are used to introduce air pressure into the sample. This procedure induces the target matric suction into the partially saturated soil specimen. To achieve

this goal, the air pressure is increased while the pore pressure is kept constant under atmospheric pressure conditions (assumed to be 0 as reference value). This technique is known as the axis translation technique.

The maximum value of matric suction anticipated to be applied during the RC test defines the air entry value for the HAE (High-Air-Entry) ceramic disk when testing unsaturated soils.

Throughout this research, the soil specimens were subjected to 200 kPa as maximum suction value; thus, 7.65mm height, 16.95 mm diameter, 5-bar HAVE ceramics, manufactured by GCTS were chosen as adequate for this work.

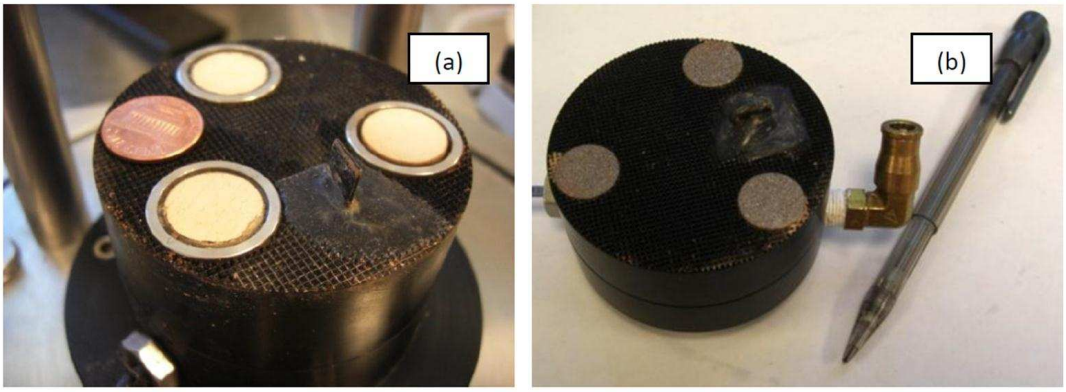

Figure 3-8 Bottom pedestal and top cap: (a) HAE ceramic disk at bottom pedestal, and (b) porous stones and tubing connector at top cap

3.5 Sample Preparation

Samples were statically compacted by applying on them a monotonic force delivered using a triaxial loading frame. The dimensions of the stainless steel split mold used to compact the specimens are 130-mm height, 70-mm diameter. The loading frame and the compacting mold can be seen in Figure 3-9. Samples were prepared by using five lifts and then applying constant compaction displacement rate of 1.0 mm/min (Venkatarama and Jagadih 1995).

A total mass of poorly graded silty sand of around 1100 g was placed in the compaction mold using five layers, and then the mold was placed on the triaxial loading base as shown in Figure 3-9. A steel cap has to be placed and leveled on top of the sample. Finally the load is applied to the specimen.

Figure 3-9 Triaxial loading frame used to compact cylindrical specimens

Once the degree of compaction for the sample was achieved, the loading mechanism was stopped letting the sample to sit for around one minute to reduce any rebound effect. Finally, the sample was taken out from the compaction mold and then placed on the base pedestal of the resonant column device to be tested.

Next chapter is devoted to describe the Experimental Program and the testing procedures followed in this research work. The process employed for sample preparation as well as the basic properties of the tested soil are also mentioned. The experimental

variables are also listed in next chapter, as well as a description of the suction/net mean stresses states induced on the specimens prior to resonant column testing.

Chapter 4

Experimental Program: Variables, Procedures and Results

4.1 Introduction

The accomplished series of testing sought to evaluate the dynamic response of compacted poorly-graded silty sand at different values of net mean stresses and matric suction. The application of various net mean stresses was aimed at reproducing different overburden pressure states in the field. Varying matric suction values aimed to represent the environmental and capillary effects on a soil subjected to moisture variations.

4.2 Experimental Variables

A goal of the present research work was to evaluate how the small-to-mid-shear-strain stiffness properties of the soil were affected by different combinations of confinement and matric suction. However, no multiple stress stage or stress history was considered for every sample; all of them were tested at “same” initial stress conditions and then applied prescribed values of cell and pore-air pressures at the specimen boundaries while waiting for the pore-air pressure to equalize. Thus, each specimen was subjected to a particular combination of experimental variables during this research. The combinations and ranges of the experimental variables are summarized in Figure 4-1 and Table 4-1.

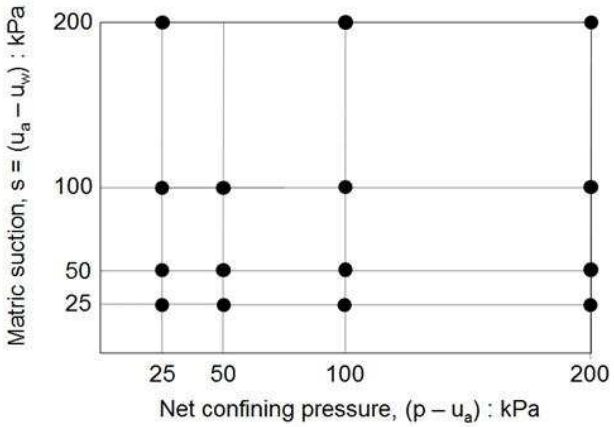

Figure 4-1 Combinations of stress variables applied on SP-SM soil samples

Table 4-1 Experimental Variables used for RC Testing during Experimental Program

Variable description	Number of variables
Confining pressure, p (kPa)	50 75 125 225 100 150 250 200 300 400
Net confining pressure, p-u_a (kPa)	25 50 100 200
Matric suction, u_a-u_w (kPa)	25 50 100 200

4.3 Test Procedure

The testing procedure used with the resonant column apparatus consists of two stages: compression and equalization and cyclic torsional excitation.

4.3.1 Compression and Equalization

The equalization stage is required to bring soil specimens to target values of net stress and matric suction. This is achieved by applying prescribed values of cell and pore-air pressures at the specimen boundaries and waiting for the pore-air pressure to equalize. During equalization both cell pressure (p, applied using the HM-414 panel) and pore-air pressure (u_a, increased using the PCP-15U panel) were gradually applied to the sample at a loading rate of 50 kPa/h, until reaching subsequent target values of net stress ($p - u_a$) and matric suction ($u_a - u_w$).

The end of the process was inferred by assuming a water content change rate limit of 0.2%/day (Sivakumar 1993). Equalization generally took about 5 to 6 days for samples subjected to suctions less than 100 kPa and almost 12 days for tests performed under suctions of 200 kPa, showing a final gradient of water content with time which was assumed to be negligible when compared with their initial gradient.

4.3.2 Cyclic Torsional Excitation

The linear and non-linear dynamic response of each soil sample was tested by using various torque amplitudes ranging from 0.5 pfs to 10 pfs (50 N·m to 1000 N·m), Thus, each test was started at 0.5-pfs and ended at 10-pfs. The frequency of the cyclic torque was swept from 1 Hz to 300 Hz. This was done to obtain the frequency response curve. These curves are presented as the change of the shear strain percentage (%) as a function of the frequency (Hz) with given constant torque amplitude.

At the end of the test, the cyclic torque is interrupted and the free torsional vibration of the specimen was plotted, this permitted to obtain the material damping from the logarithmic decay curve. The attenuation of shear strain was presented in terms of shear strain percentage (%) as a function of time (sec).

The same test procedure was repeated on different samples for several net confining pressures, pnet = ($p - u_w$) = 25, 50, 100, and 200 kPa, at constant matric suctions, s = (ua-uw) = 25, 50, 100, 150, and 200 kPa. The following section summarizes all the experimental results from the Experimental Program.

4.4 Test Results

4.4.1 Resonant Column Tests Performed under Constant Matric Suction, s = 25 kPa

This section presents all the frequency response curves, free-vibration decay curves and cyclic hysteretic loop curves from RC tests conducted at net confining pressures, ($p-u_a$) = 25, 50, 100, and 200 kPa, respectively, under a constant matric suction, s = 25 kPa.

It can be observed that there is an increment on the resonant frequency when the net mean stress or confinement pressure is increased. This fact reflects an increase on the shear modulus with any increment on the net mean stress, since, in shear modulus calculations, the frequency at resonance is directly proportional to shear modulus. This can be attributed to a direct increase in the total stress in the sample while the matric suction is kept constant, thereby causing closer contact between soil particles (higher packing) and stiffer material.

Also, it can be observed that the frequency at resonance undergoes decrement when the cyclic torque is increased. A well-defined curved tendency on the resonant frequency can be obtained with increasing input torque. This condition can be attributed to the initial yield locus being exceeded, which brings the soil sample into the elasto-plastic behavior.

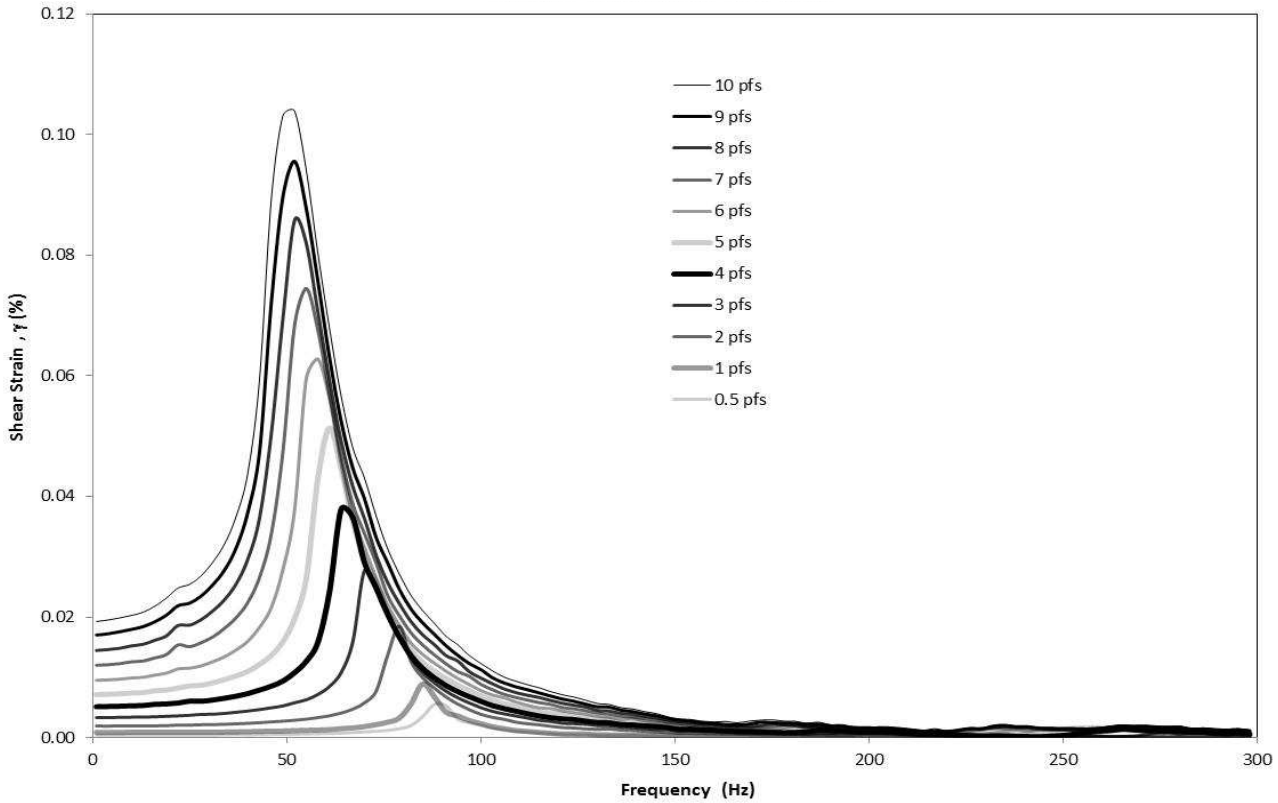

Figure 4-2 Frequency response curves, p - u_a = 25 kPa, u_a – u_w = 25 kPa, torque range = 0.5 pfs -10 pfs

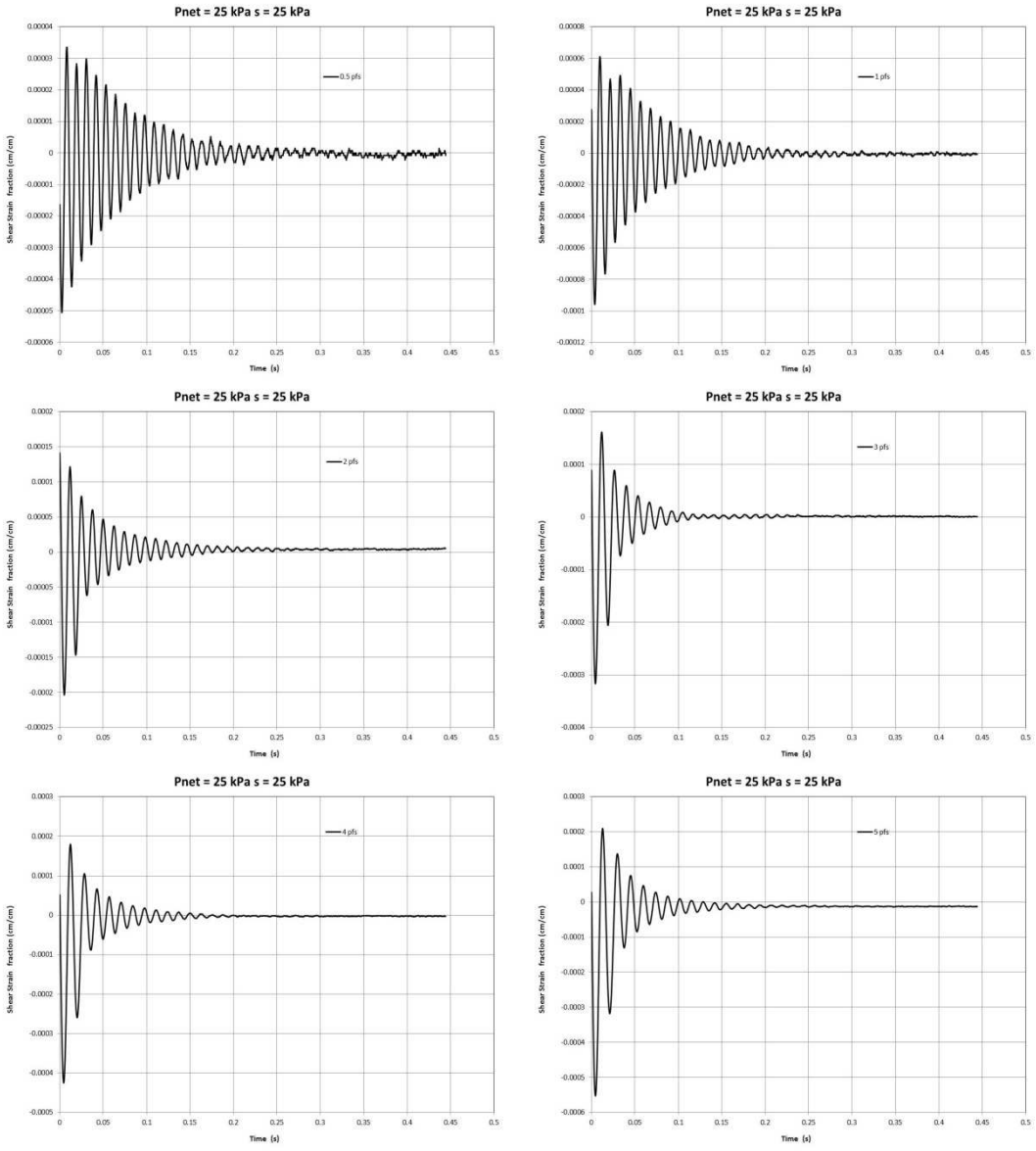

Figure 4-3 Free-vibration decay curves, p - u_a = 25 kPa, u_a – u_w = 25 kPa, torque range = 0.5 pfs - 5 pfs

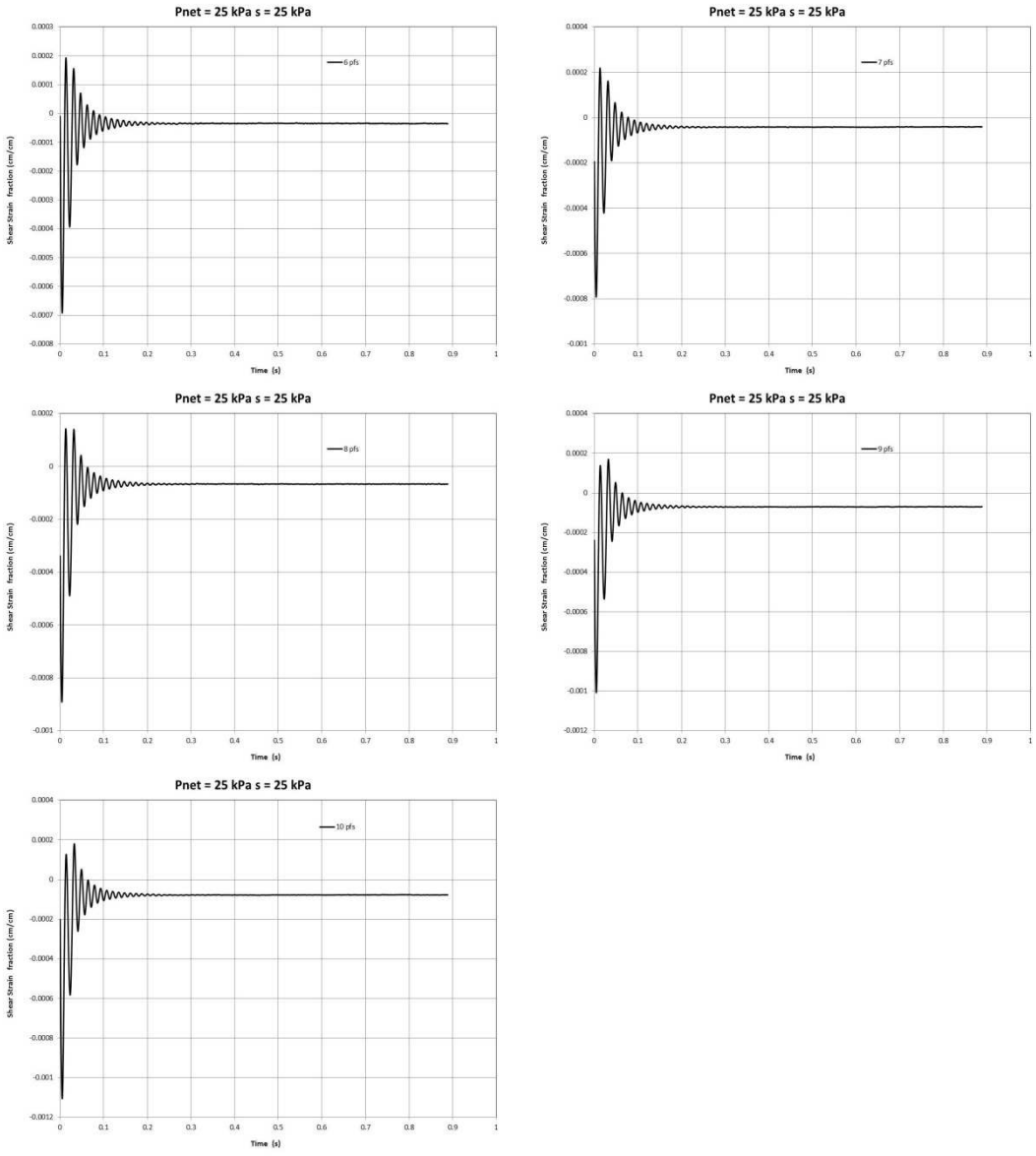

Figure 4-4 Free-vibration decay curves, p - u_a = 25 kPa, u_a – u_w = 25 kPa, torque range = 6 pfs - 10 pfs

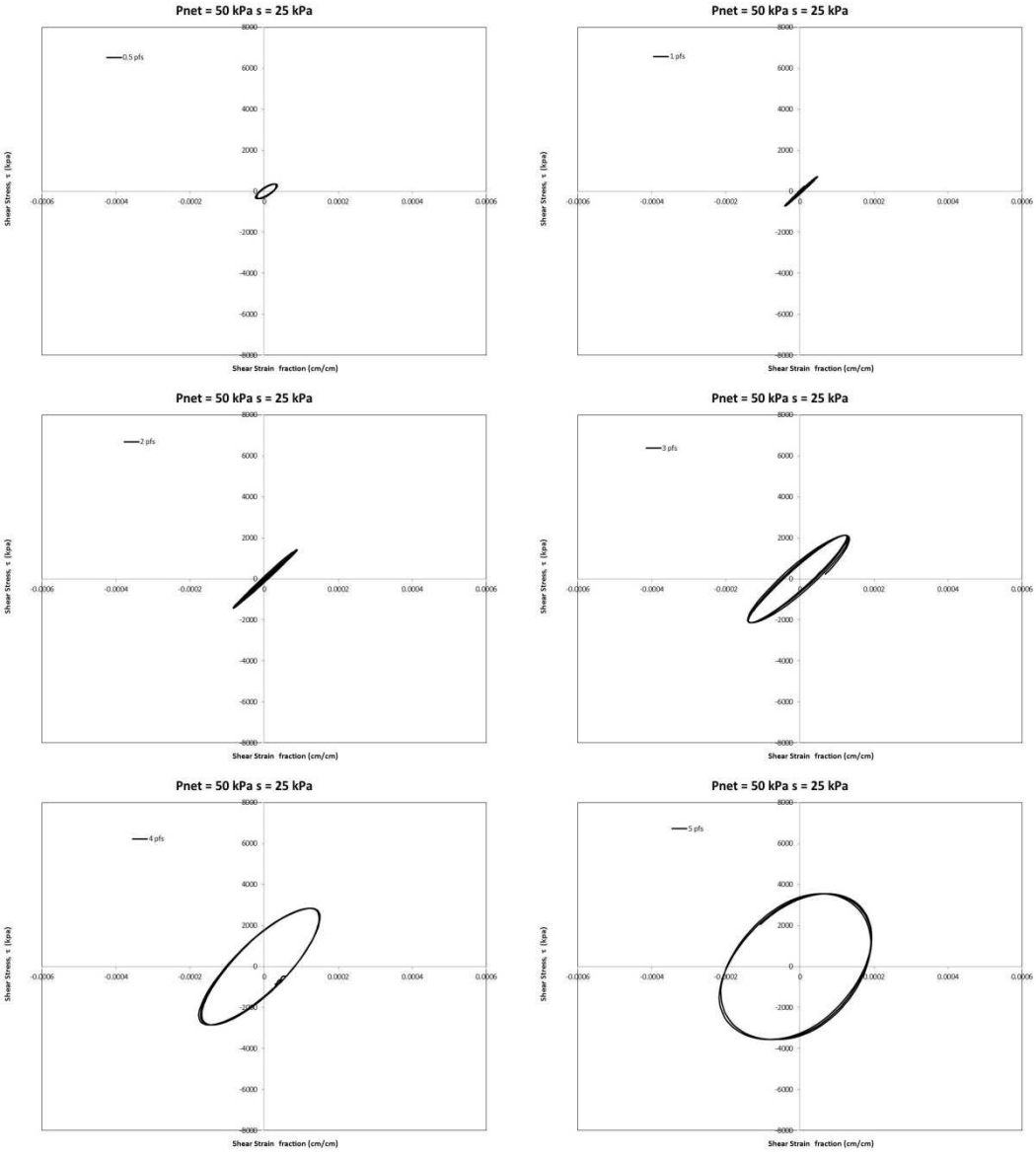

Figure 4-5 Hysteretic loop curves, p - u_a = 25 kPa, u_a – u_w = 25 kPa, torque range = 0.5 pfs - 5 pfs

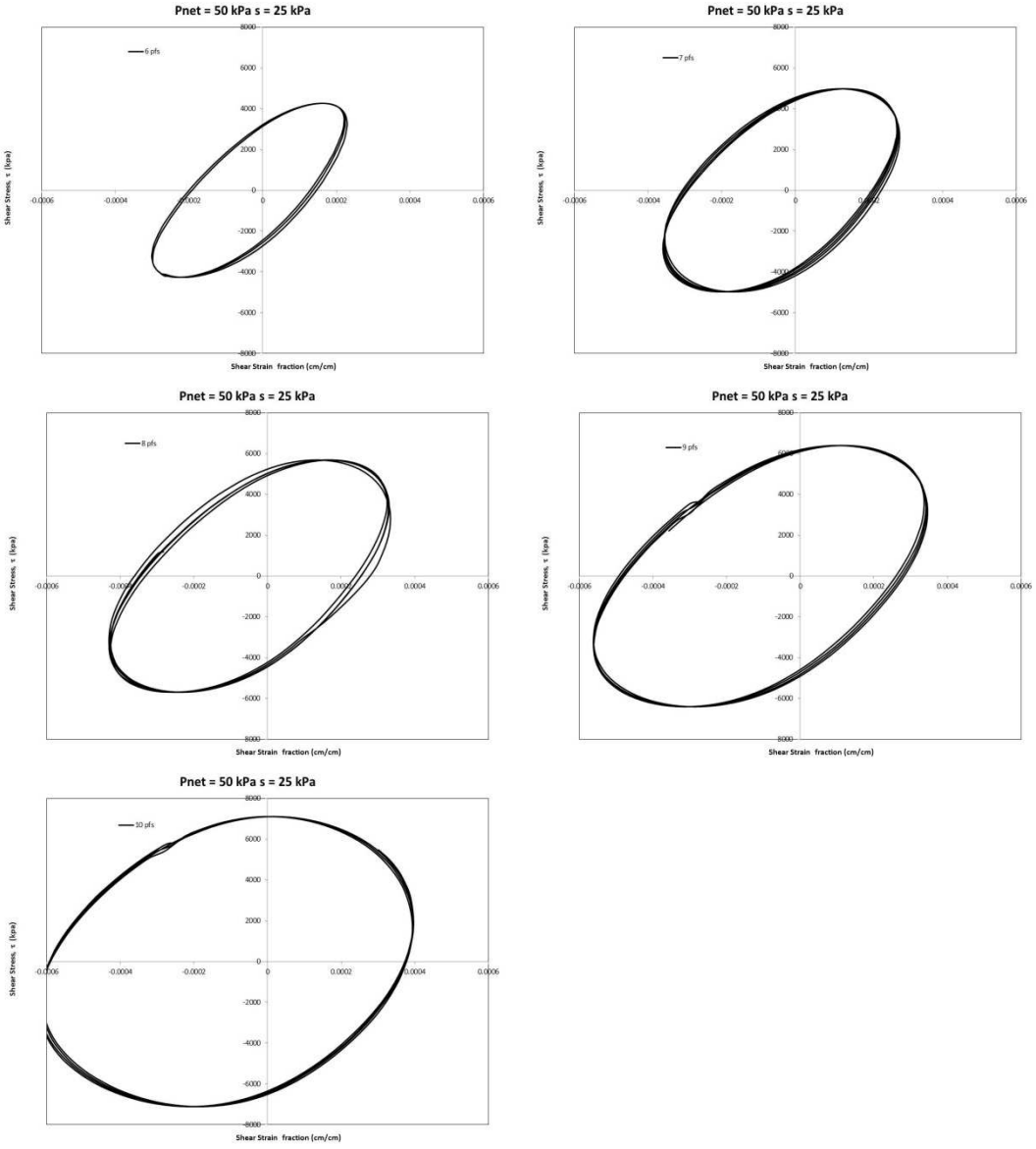

Figure 4-6 Hysteretic loop curves, p - u_a = 25 kPa, u_a – u_w = 25 kPa, torque range = 6 pfs - 10 pfs

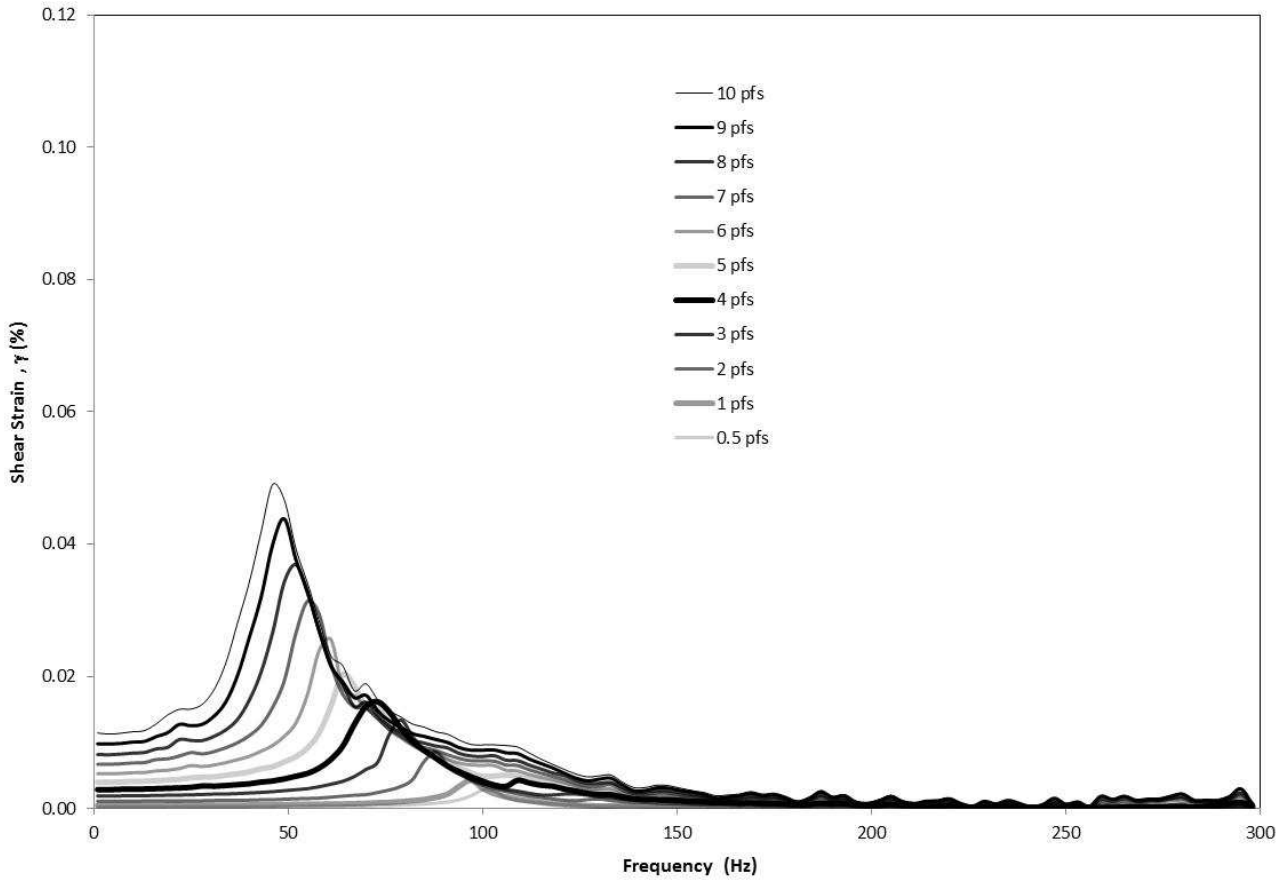

Figure 4-7 Frequency response curve, p - u_a = 50 kPa, u_a – u_w = 25 kPa, torque range = 0.5 pfs -10 pfs

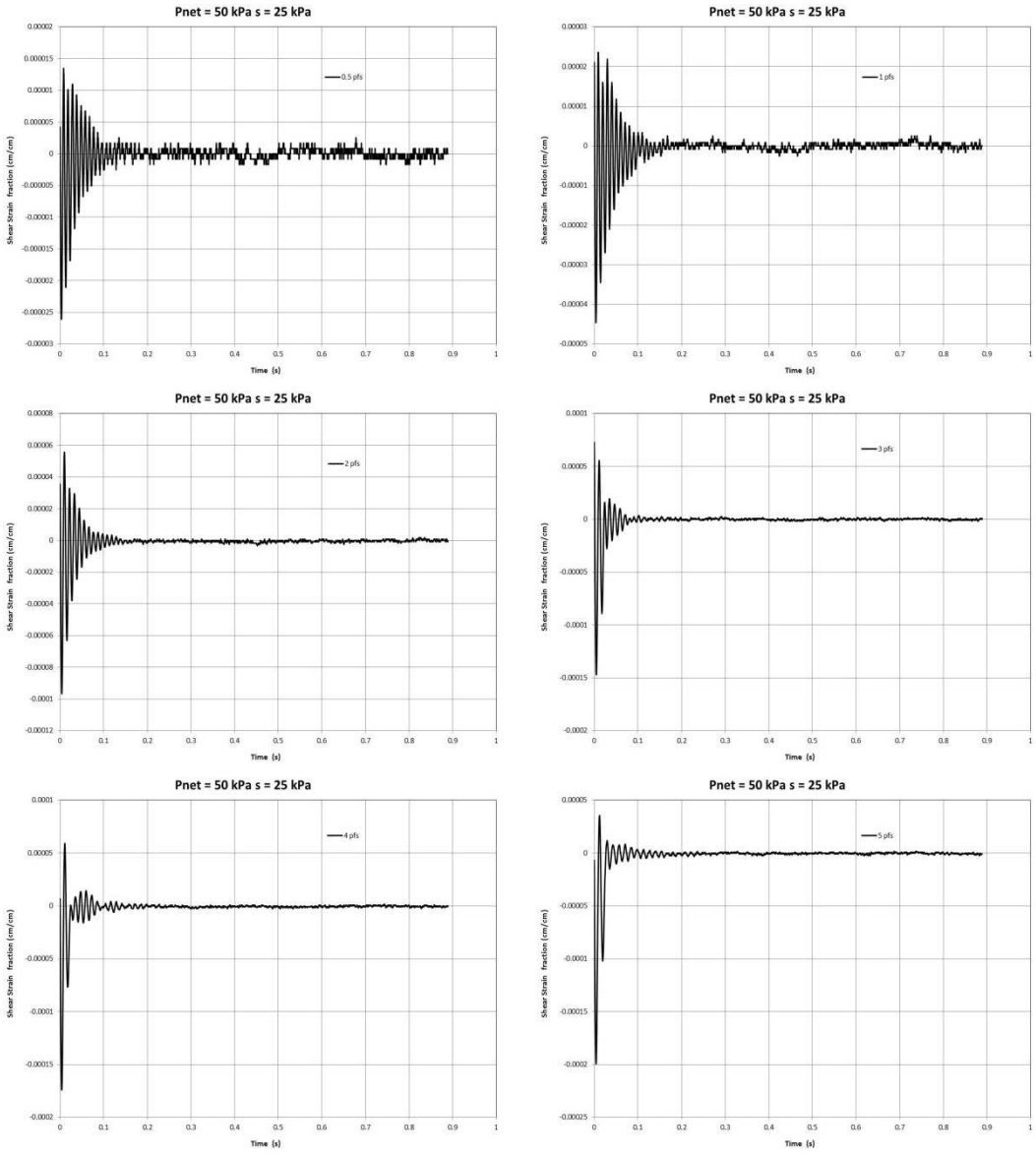

Figure 4-8 Free-vibration decay curves, p - u_a = 50 kPa, u_a – u_w = 25 kPa, torque range = 0.5 pfs - 5 pfs

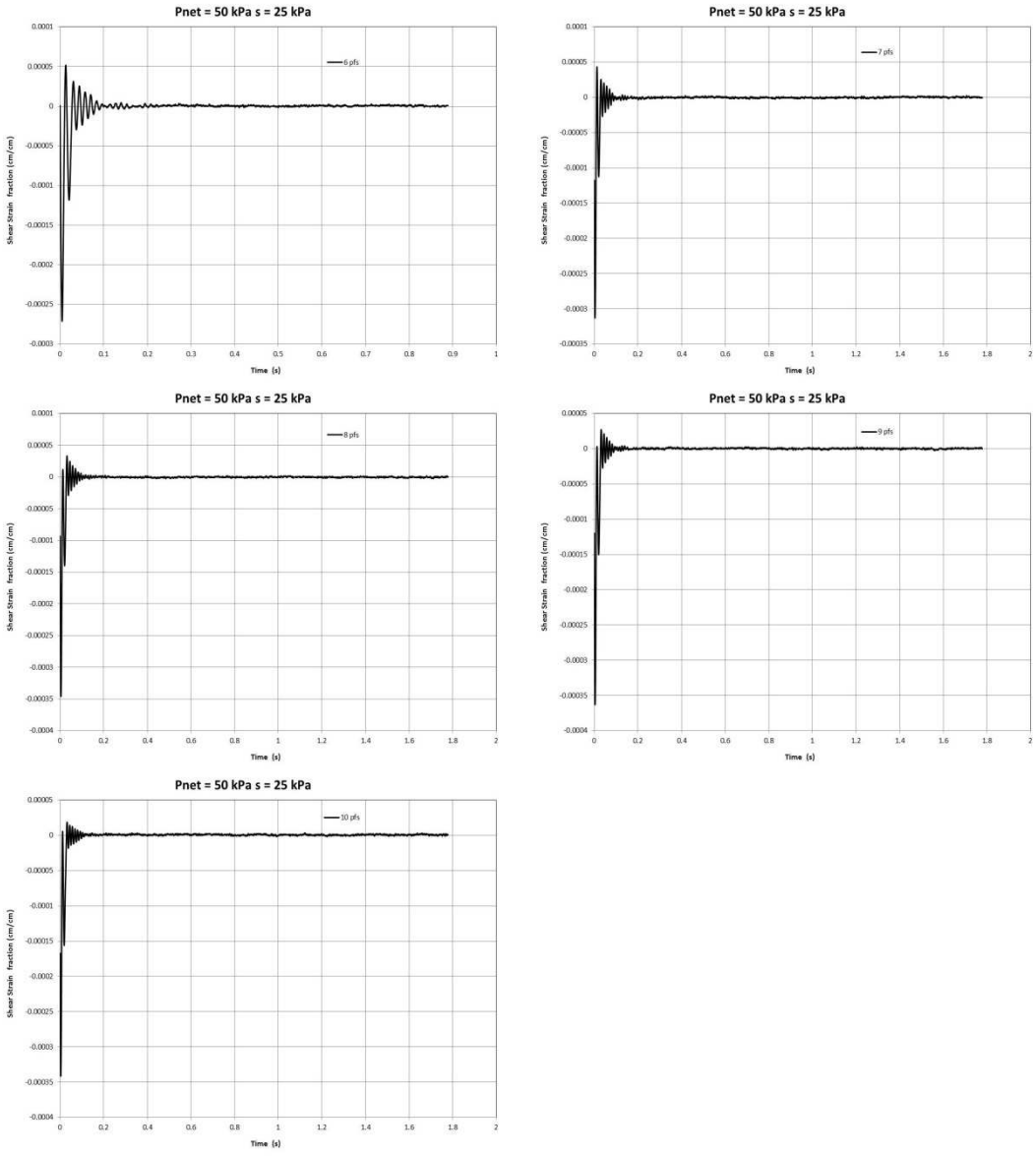

Figure 4-9 Free-vibration decay curves, p - u_a = 50 kPa, u_a – u_w = 25 kPa, torque range = 6 pfs - 10 pfs

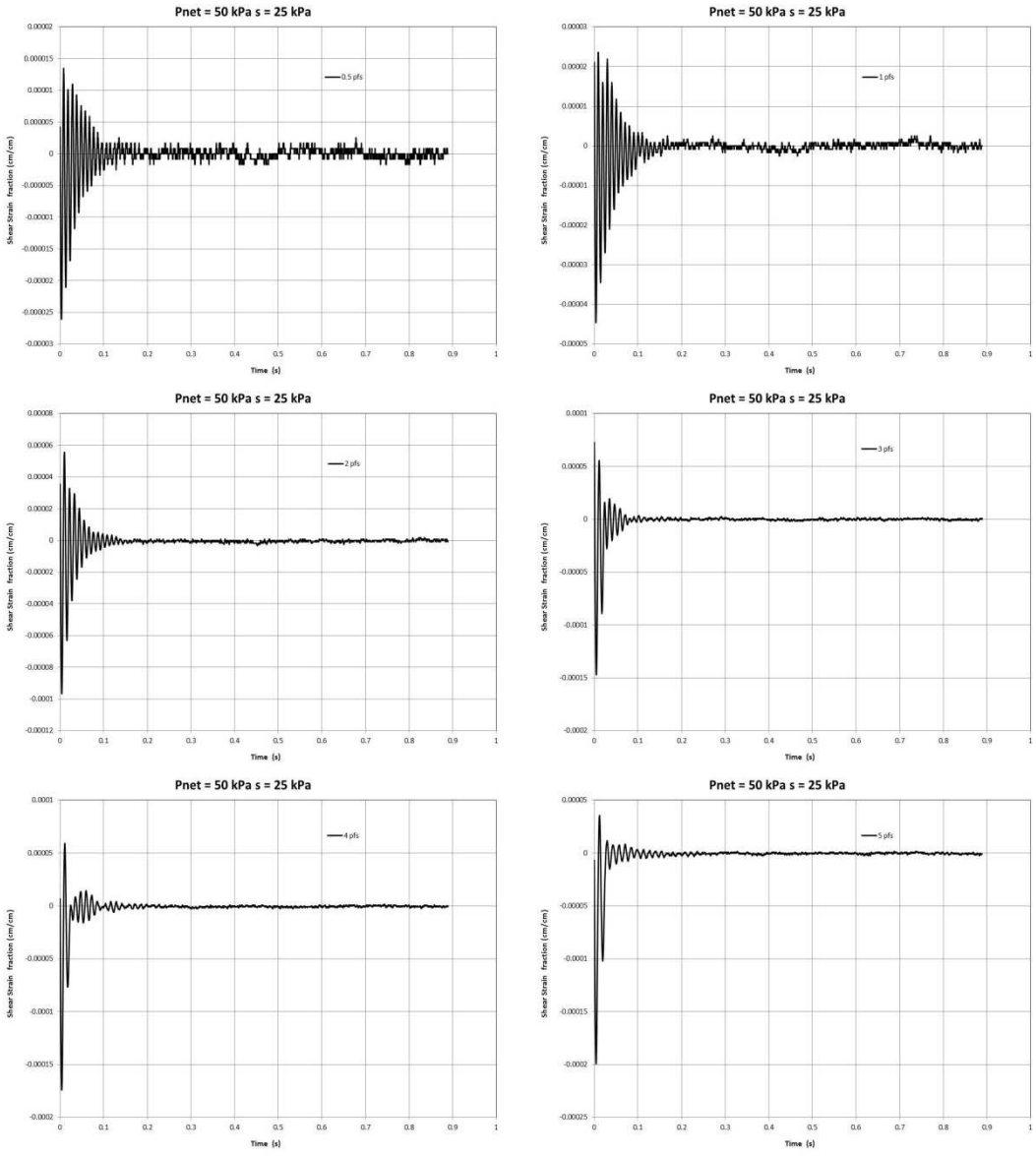

Figure 4-10 Hysteretic loop curves, p - u_a = 50 kPa, u_a – u_w = 25 kPa, torque range = 0.5 pfs - 5 pfs

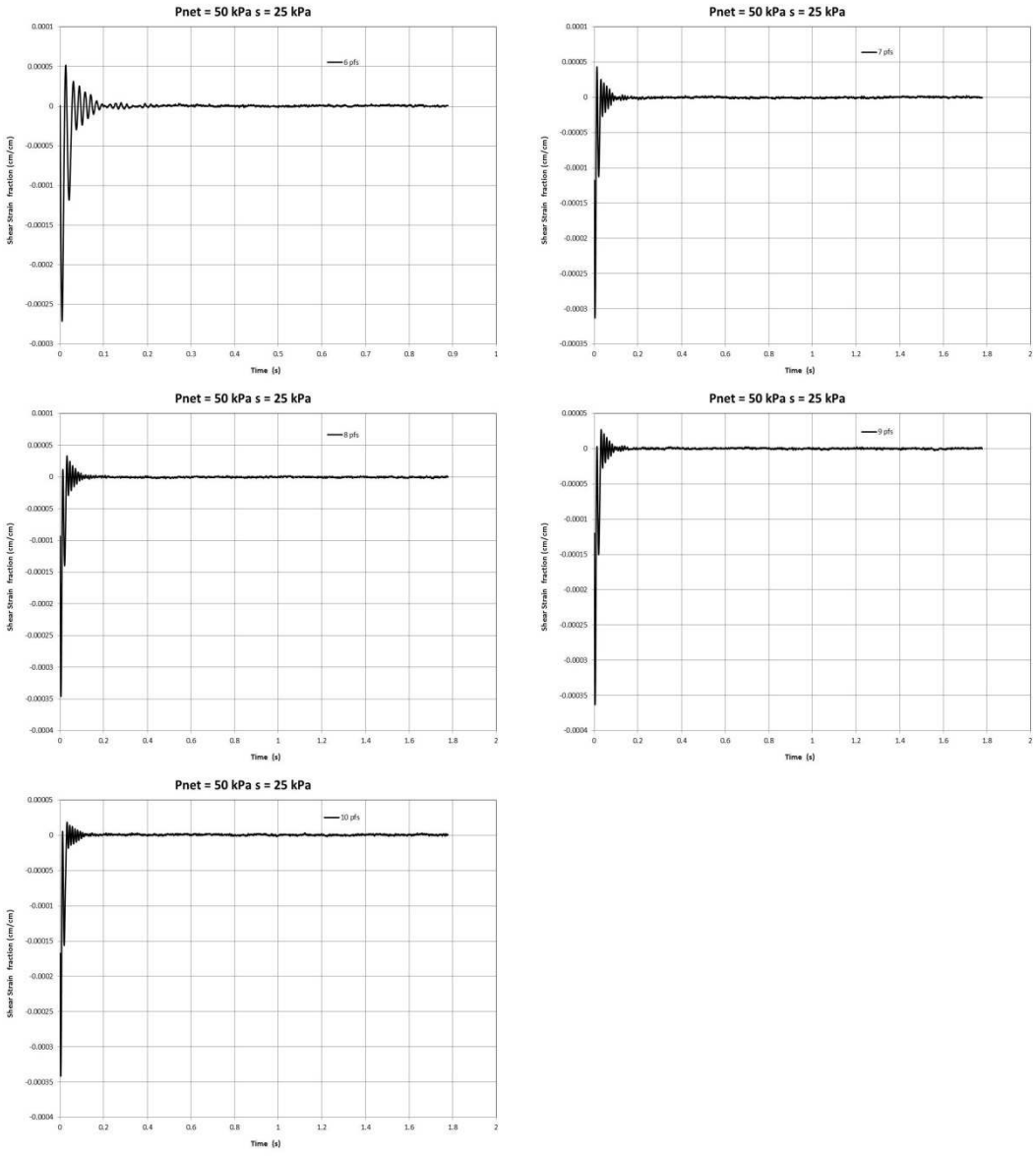

Figure 4-11 Hysteretic loop curves, p - u_a = 50 kPa, u_a – u_w = 25 kPa, torque range = 6 pfs - 10 pfs

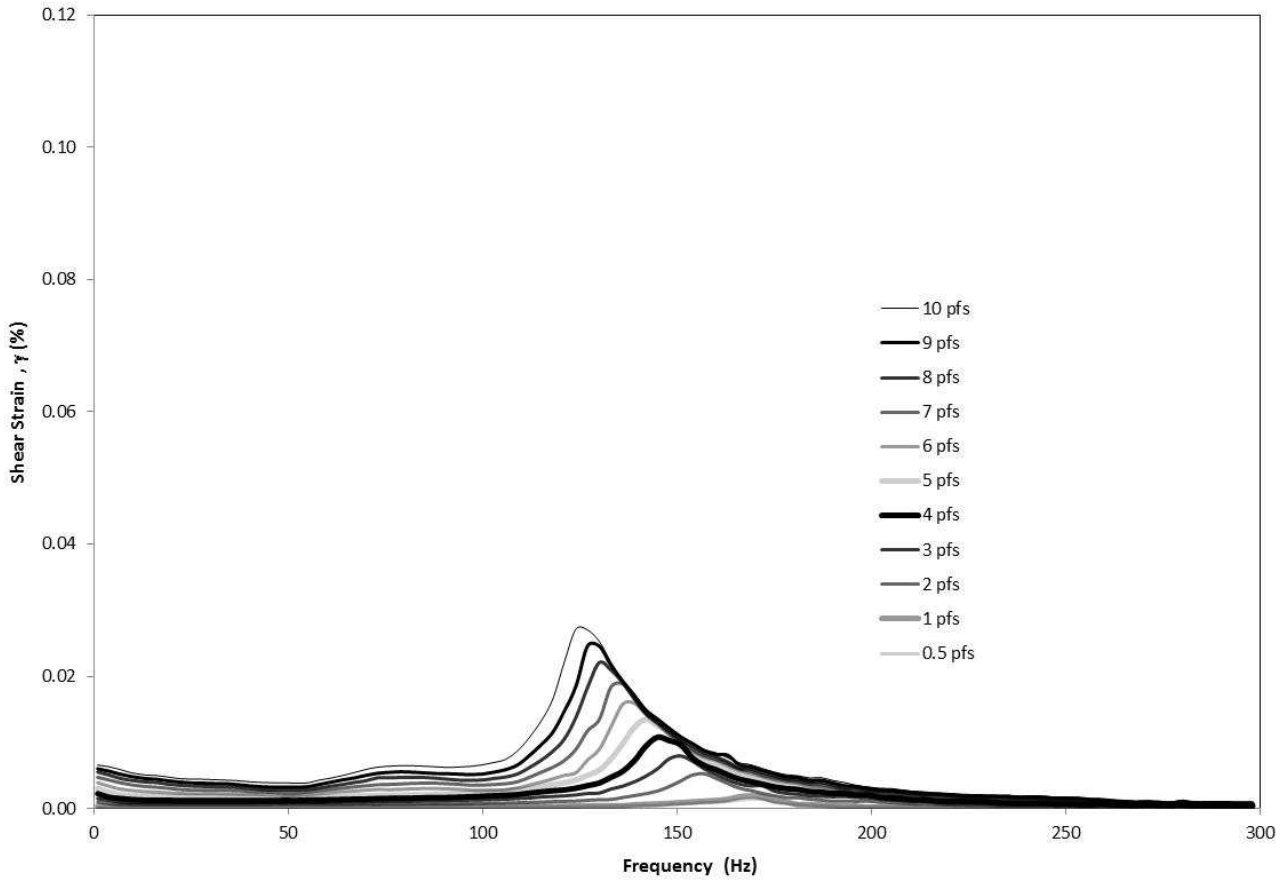

Figure 4-12 Frequency response curve, p - u_a = 100 kPa, u_a – u_w = 25 kPa, torque range = 0.5 pfs -10 pfs

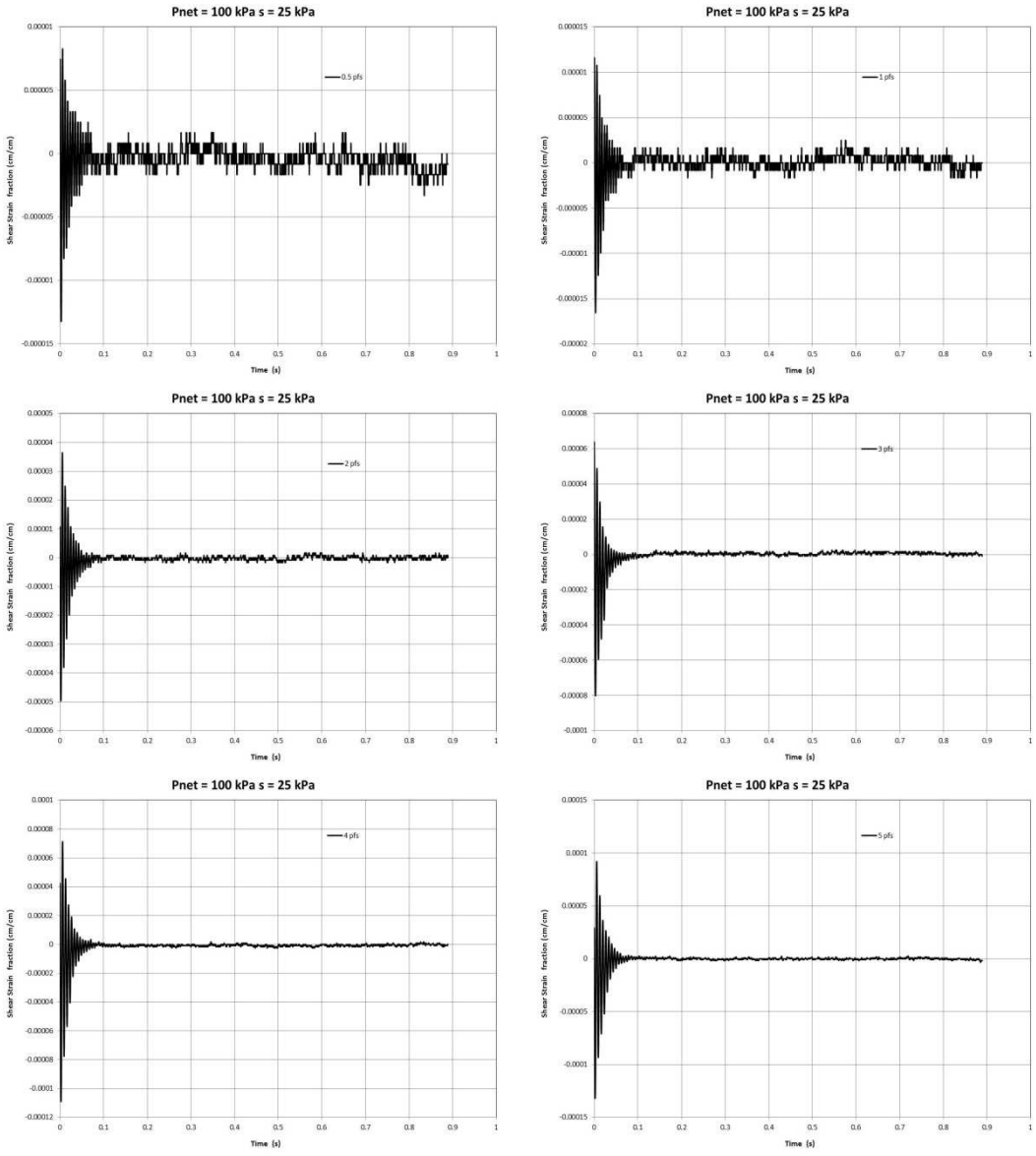

Figure 4-13 Free-vibration decay curves, p - u_a = 100 kPa, u_a – u_w = 25 kPa, torque range = 0.5 pfs - 5 pfs

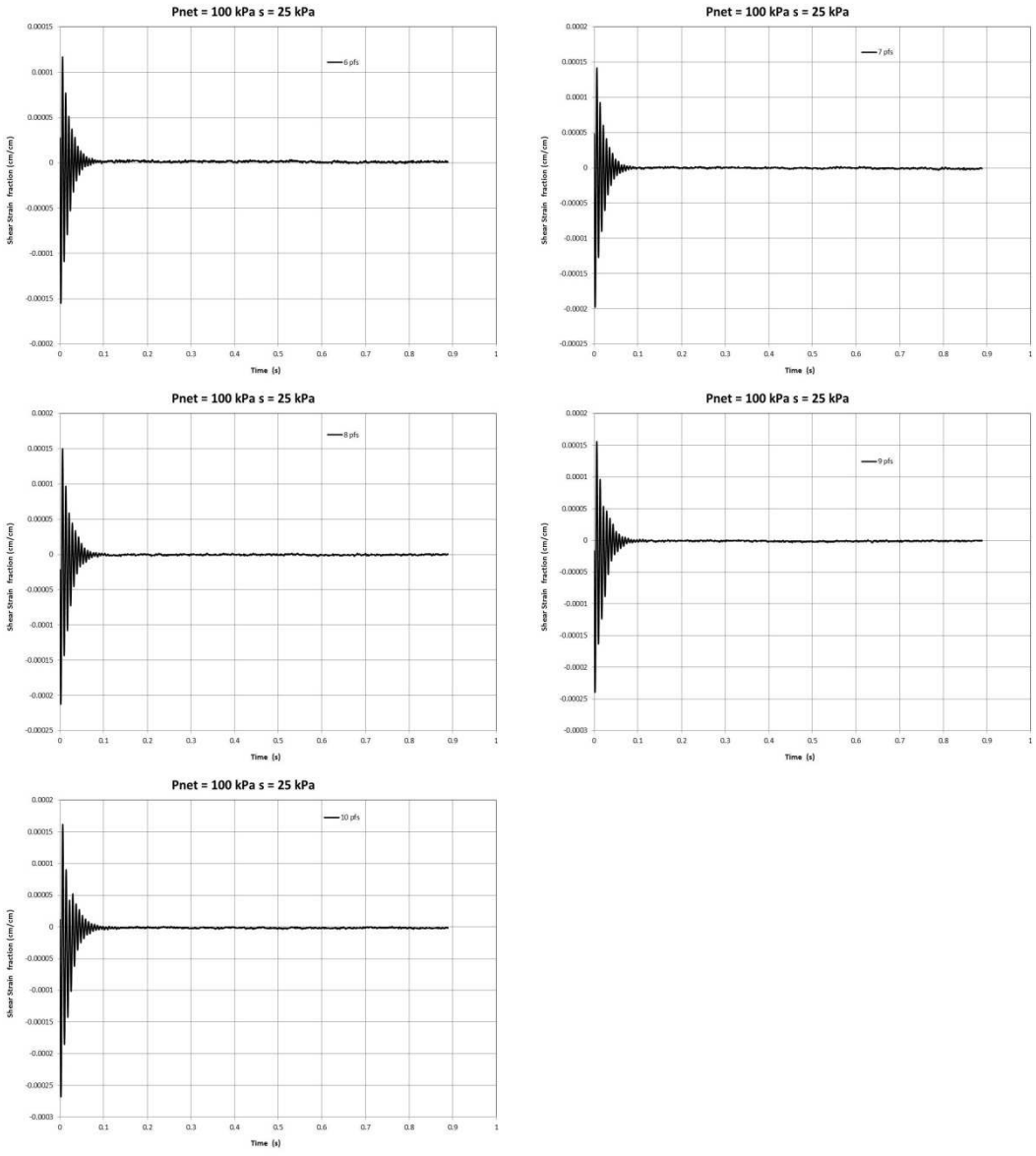

Figure 4-14 Free-vibration decay curves, p - u_a = 100 kPa, u_a – u_w = 25 kPa, torque range = 6 pfs - 10 pfs

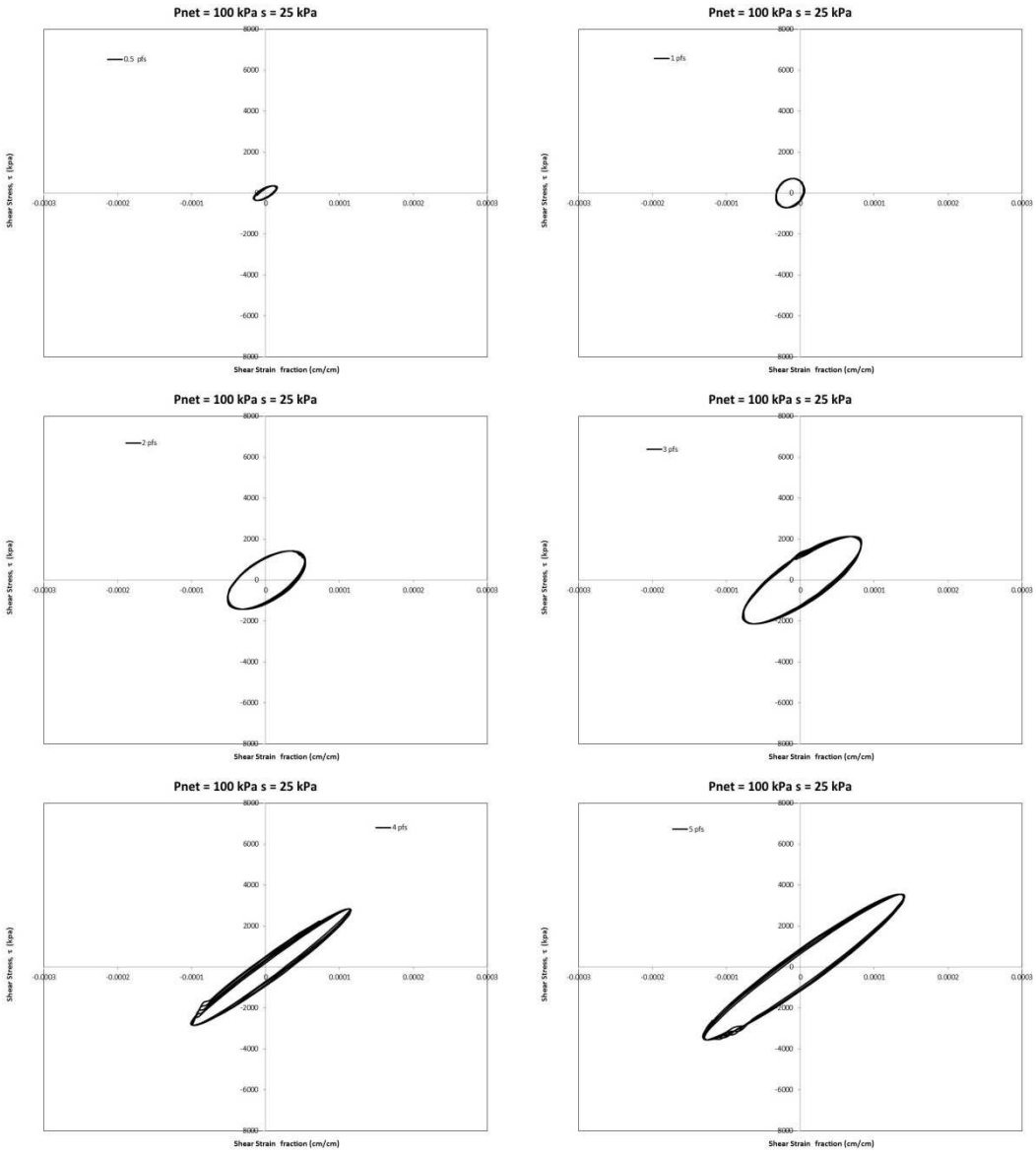

Figure 4-15 Hysteretic loop curves, p - u_a = 100 kPa, u_a – u_w = 25 kPa, torque range = 0.5 pfs - 5 pfs

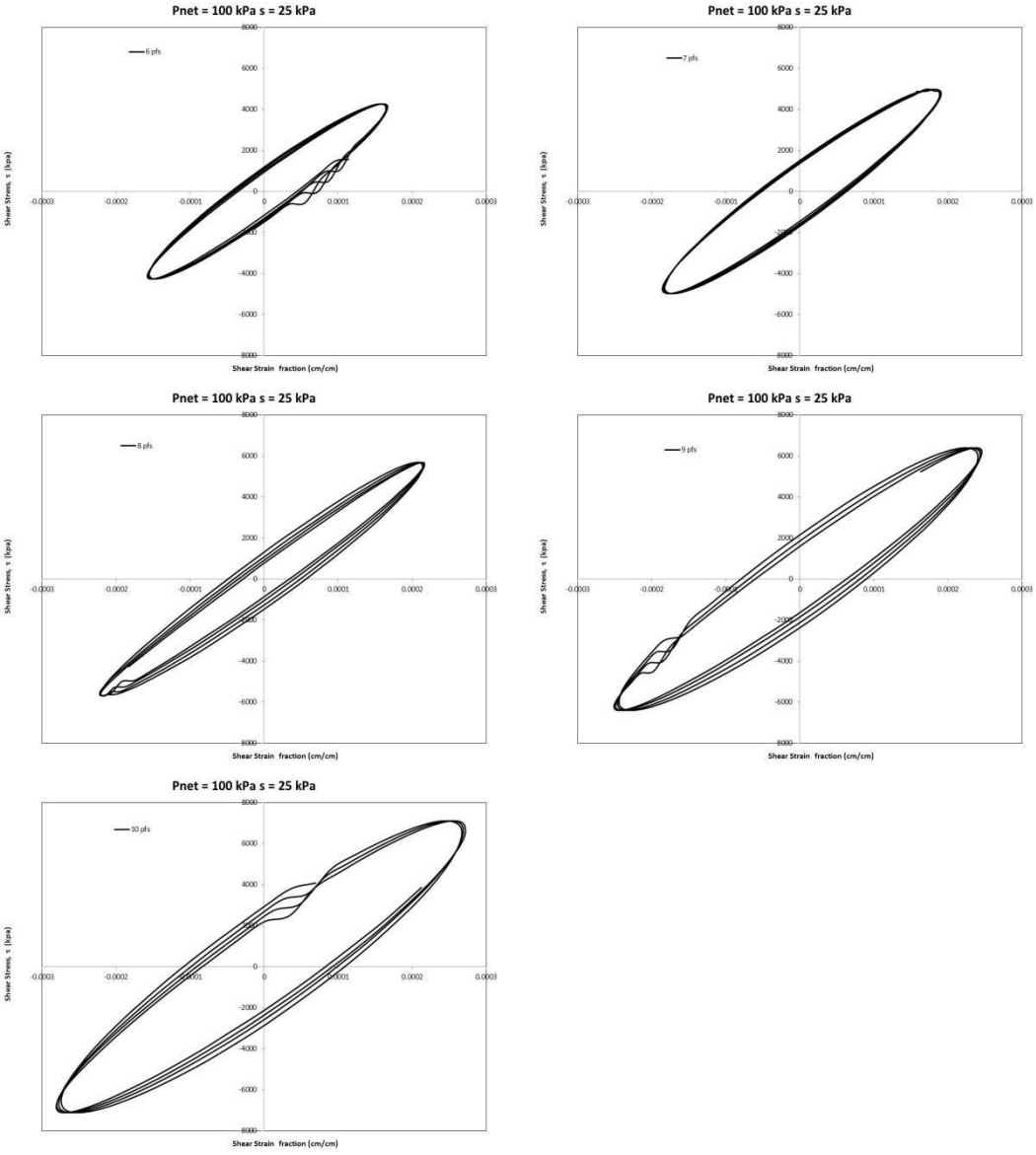

Figure 4-16 Hysteretic loop curves, p - u_a = 100 kPa, u_a – u_w = 25 kPa, torque range = 6 pfs - 10 pfs

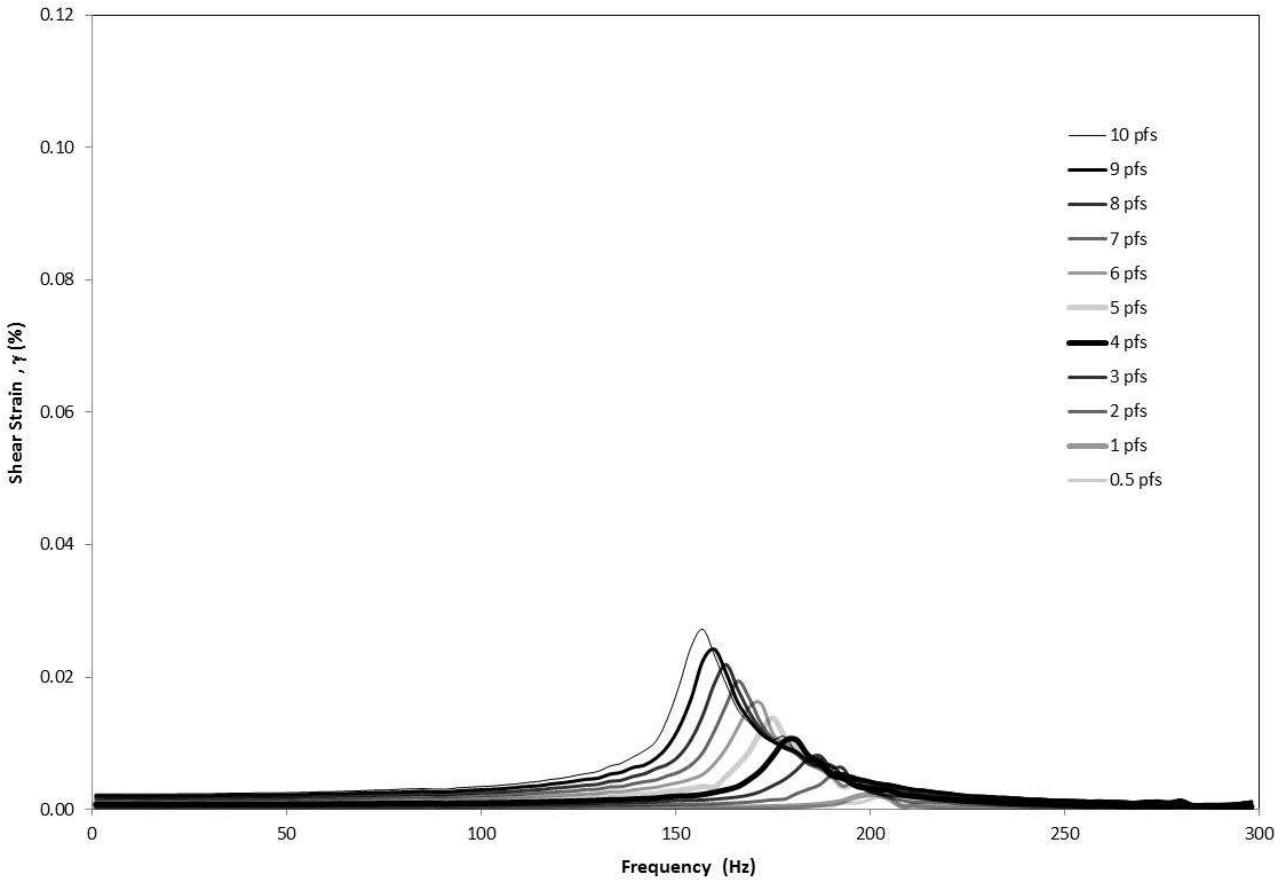

Figure 4-17 Frequency response curves, p - u_a = 200 kPa, u_a – u_w = 25 kPa, torque range = 0.5 pfs -10 pfs

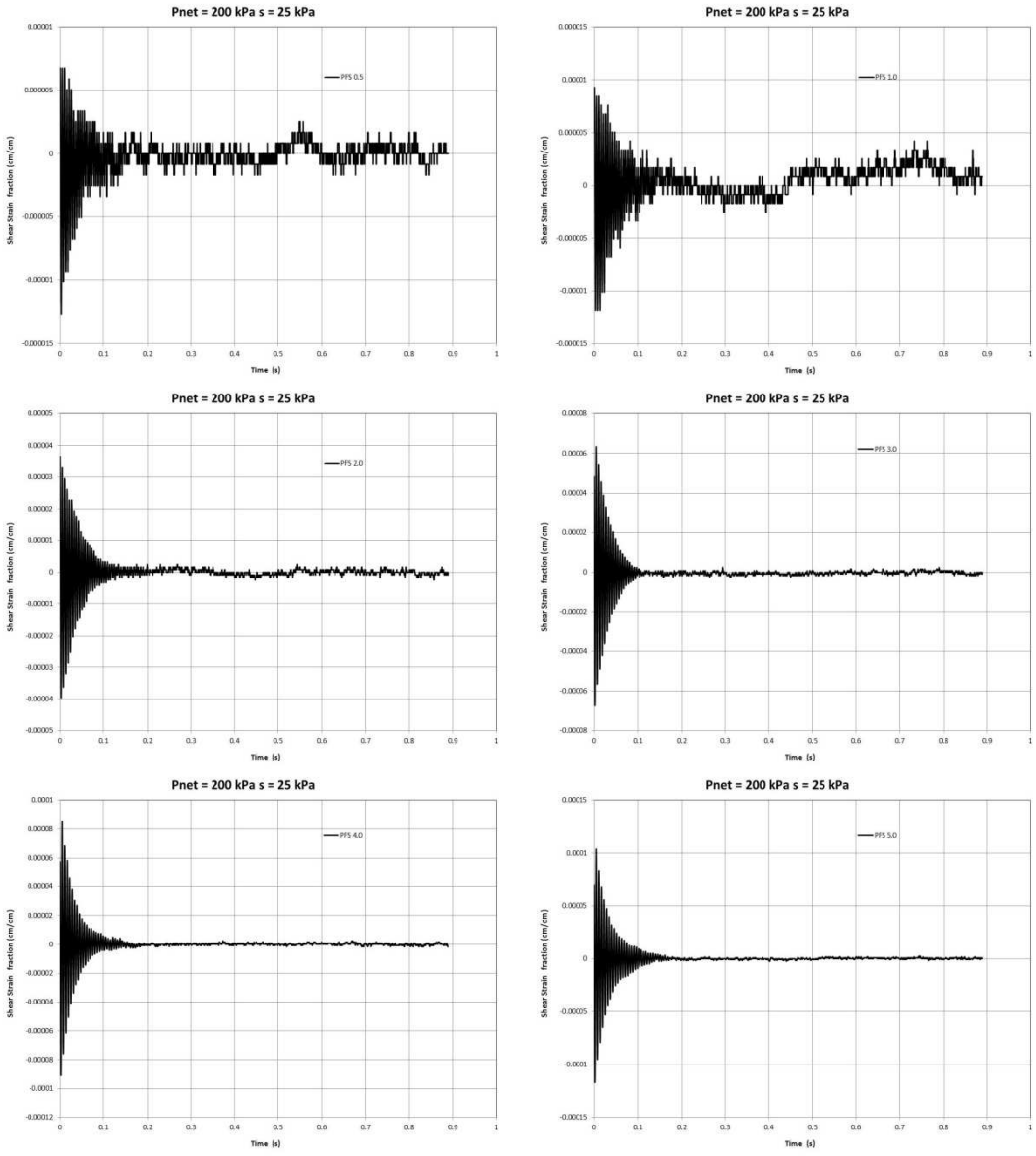

Figure 4-18 Free-vibration decay curves, p - u_a = 200 kPa, u_a – u_w = 25 kPa, torque range = 0.5 pfs - 5 pfs

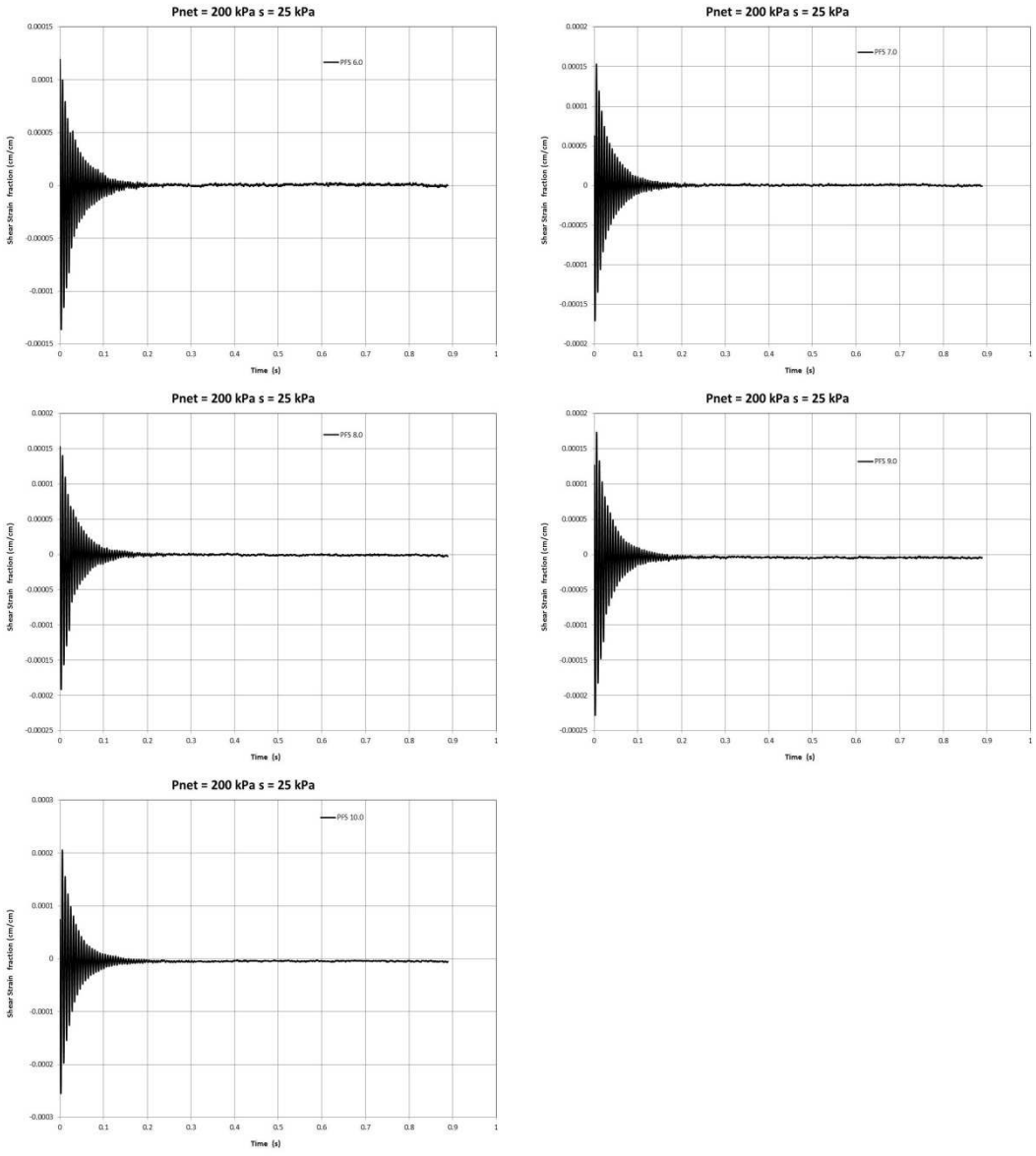

Figure 4-19 Free-vibration decay curves, p - u_a = 200 kPa, u_a – u_w = 25 kPa, torque range = 6 pfs - 10 pfs

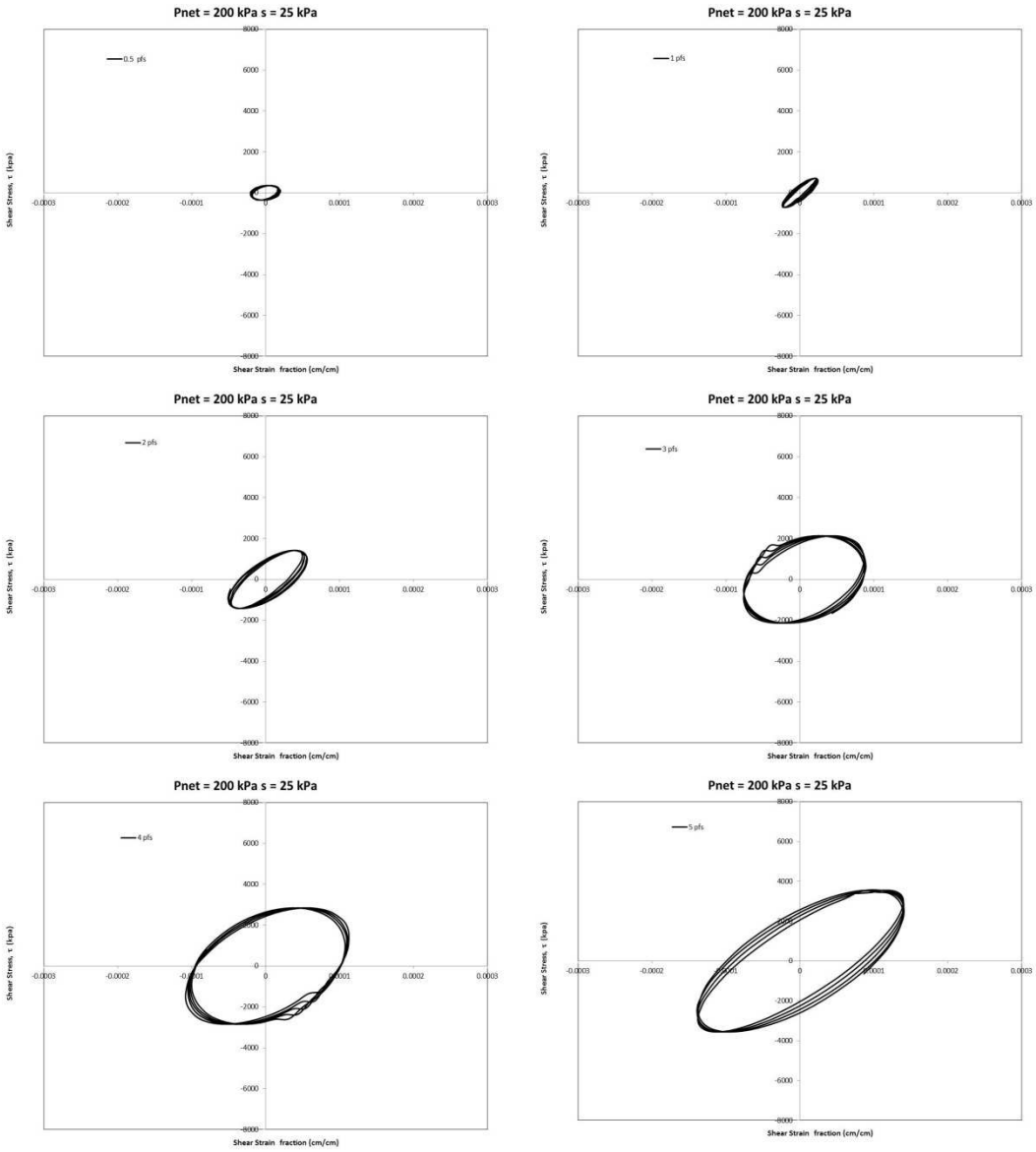

Figure 4-20 Hysteretic loop curves, p - u_a = 200 kPa, u_a – u_w = 25 kPa, torque range = 0.5 pfs - 5 pfs

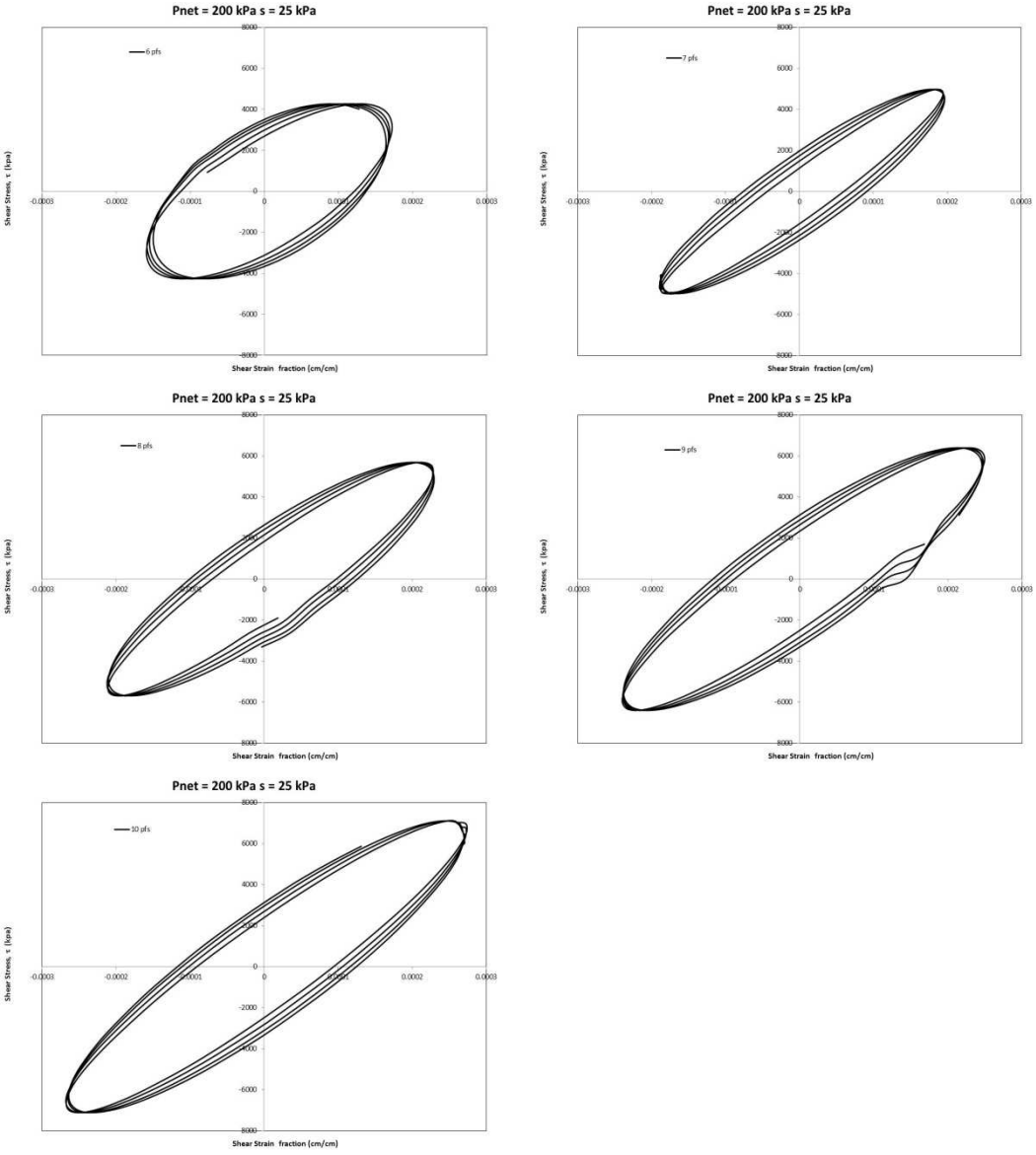

Figure 4-21 Hysteretic loop curves, p - u_a = 200 kPa, u_a – u_w = 25 kPa, torque range = 6 pfs - 10 pfs

4.4.2 Resonant Column Tests Performed under Constant Matric Suction, s = 50 kPa

This section presents all the frequency response curves, free-vibration decay curves and cyclic hysteretic loop curves from RC tests conducted at net confining pressures, $(p\text{-}u_a)$ = 25, 50, 100, and 200 kPa, respectively, under a constant matric suction, s = 50 kPa.

It can be observed that there is an increment on the resonant frequency when the net mean stress or confinement pressure is increased. This fact ensures an increase on the shear modulus with any increment on the net mean stress, since, in shear modulus calculations, the frequency at resonance is directly proportional to shear modulus. This can be attributed to a direct increase in the total stress in the sample while the matric suction is kept constant, thereby causing closer contact between soil particles (higher packing) and stiffer material.

Also, it can be observed that the frequency at resonance undergoes decrement when the cyclic torque is increased. A well-defined curved tendency on the resonant frequency can be obtained with increasing input torque. This condition can be attributed to the initial yield loci being exceeded, what brings the soil sample into the elasto-plastic behavior.

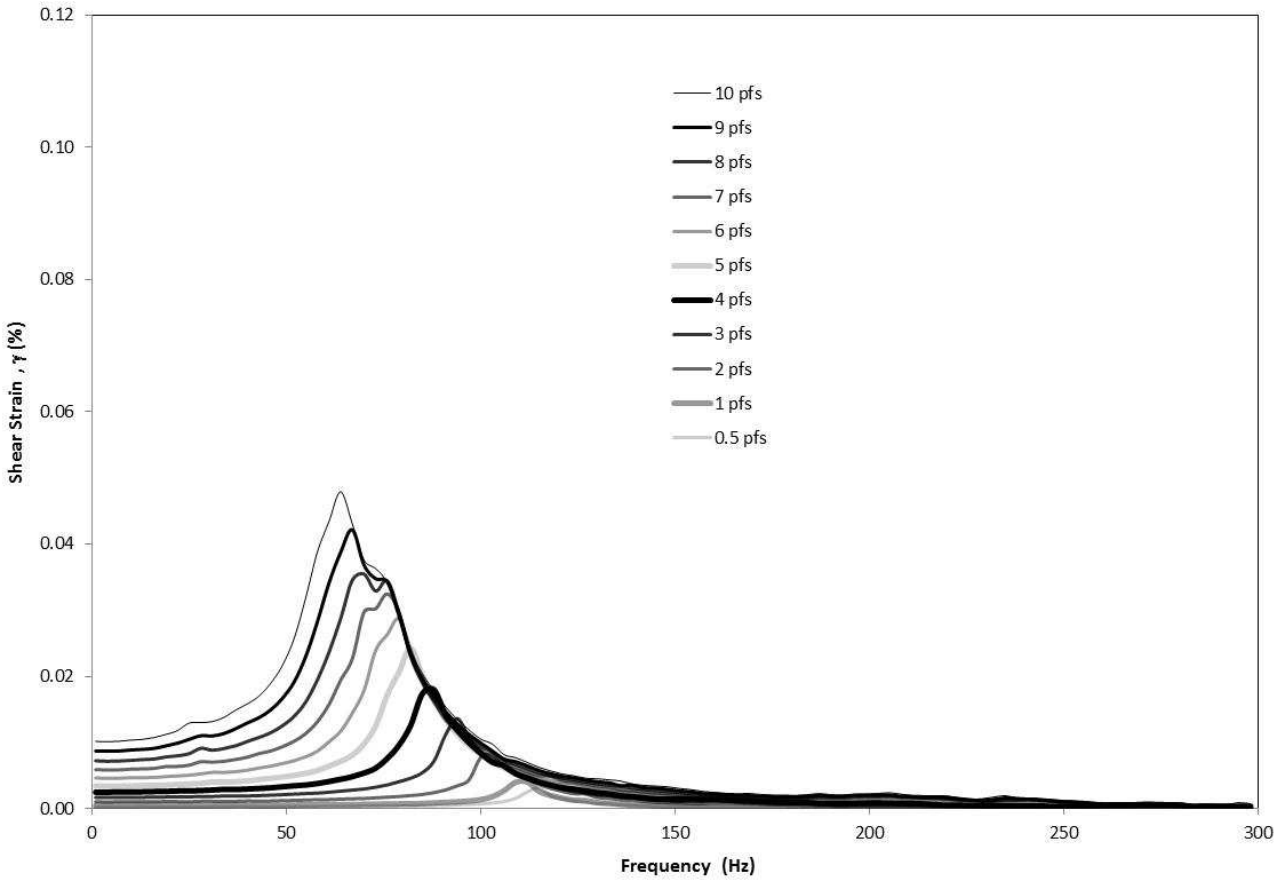

Figure 4-22 Frequency response curves, p - u_a = 25 kPa, u_a – u_w = 50 kPa, torque range = 0.5 pfs -10 pfs

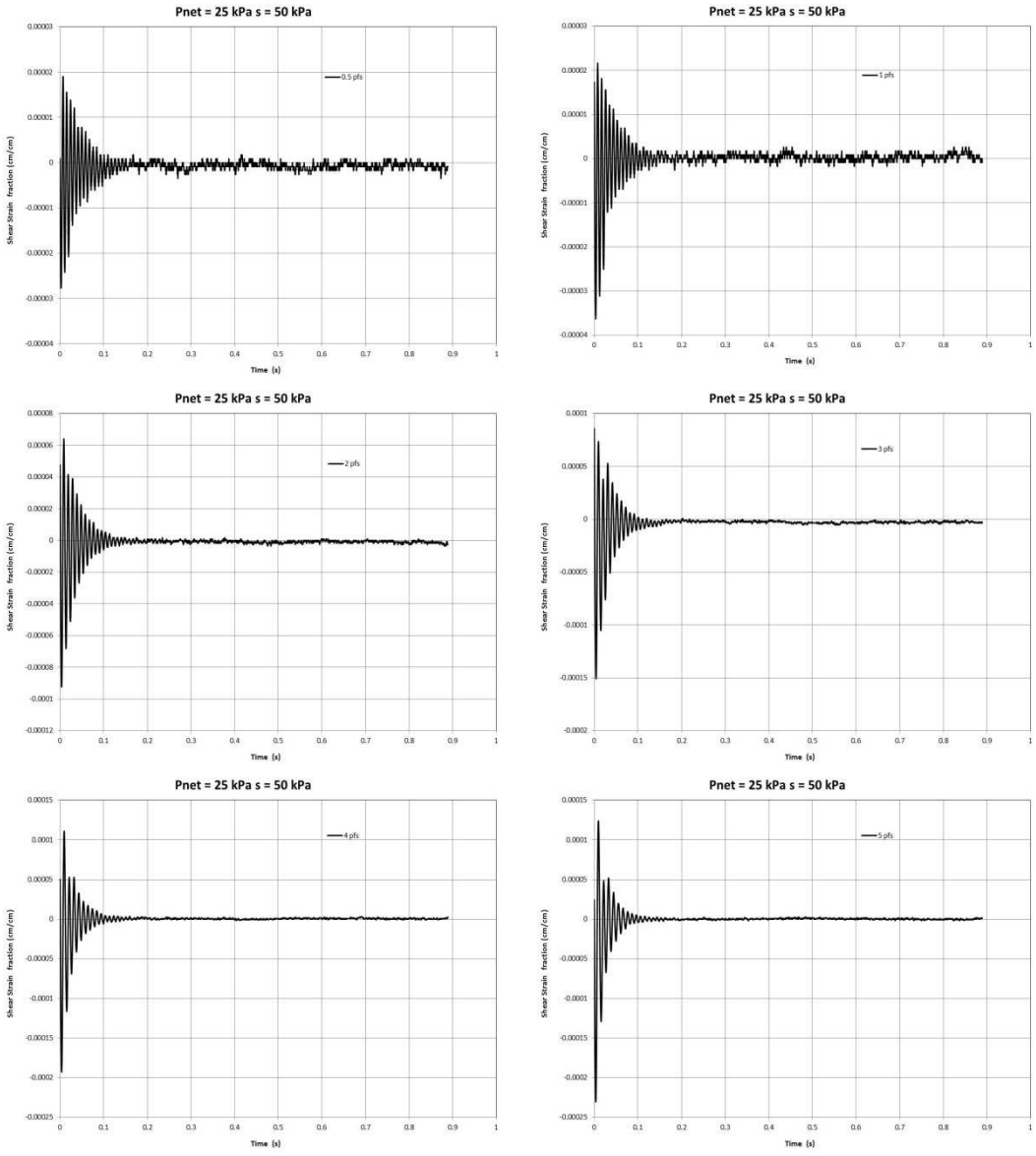

Figure 4-23 Free-vibration decay curves, p - u_a = 25 kPa, u_a – u_w = 50 kPa, torque range = 0.5 pfs - 5 pfs

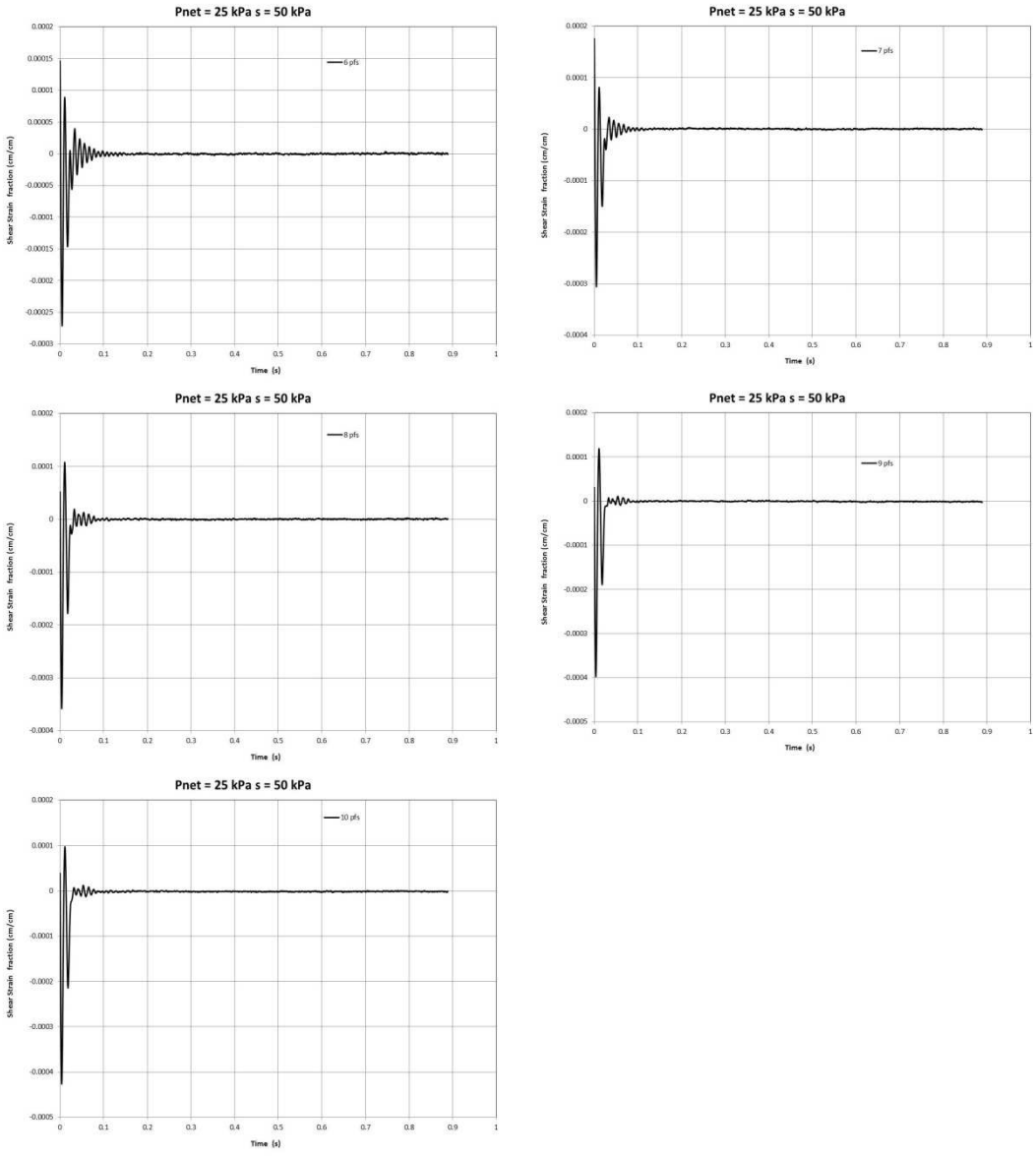

Figure 4-24 Free-vibration decay curves, p - u_a = 25 kPa, u_a – u_w = 50 kPa, torque range = 6 pfs - 10 pfs

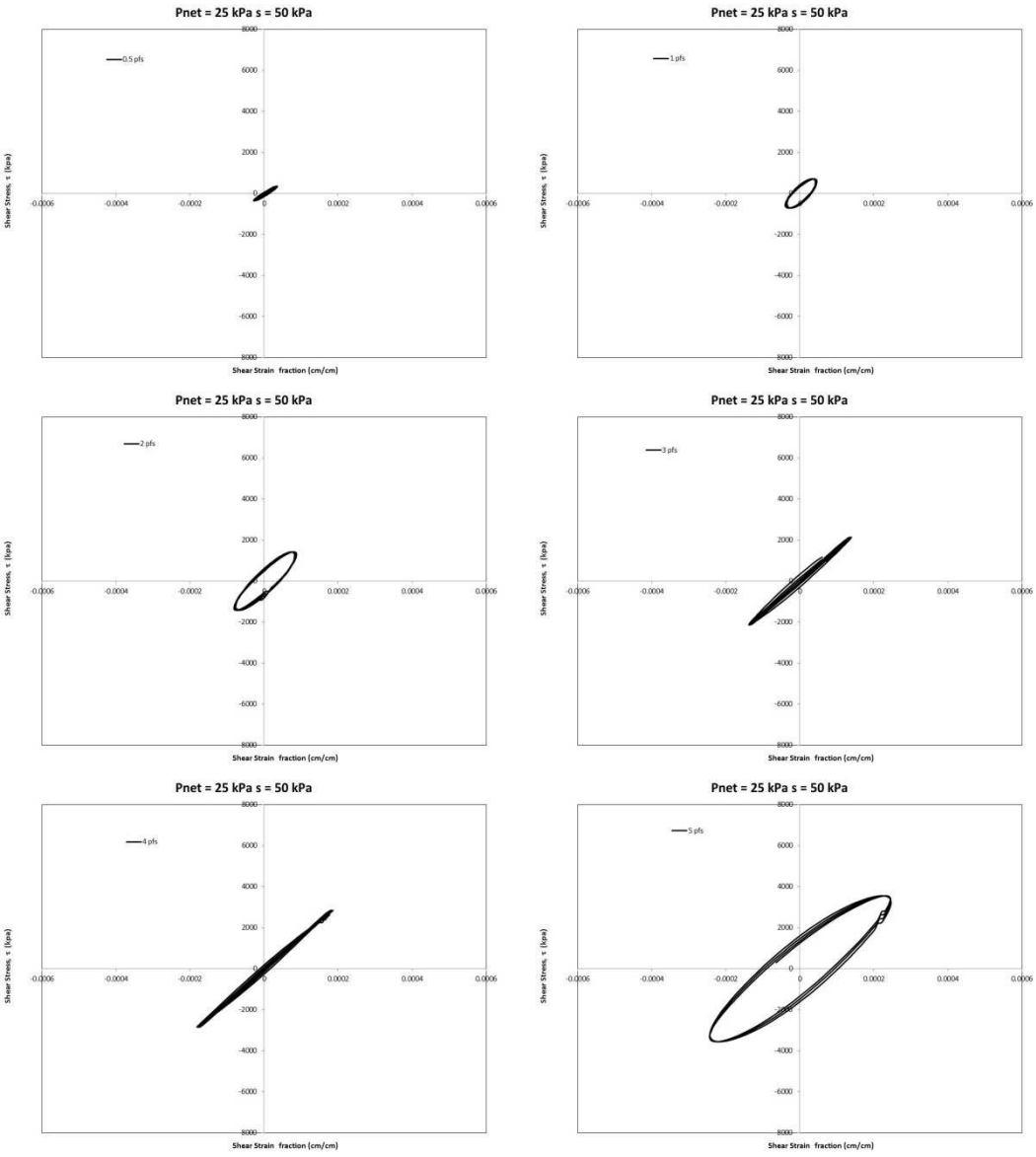

Figure 4-25 Hysteretic loop curves, p - u_a = 25 kPa, u_a – u_w = 50 kPa, torque range = 0.5 pfs - 5 pfs

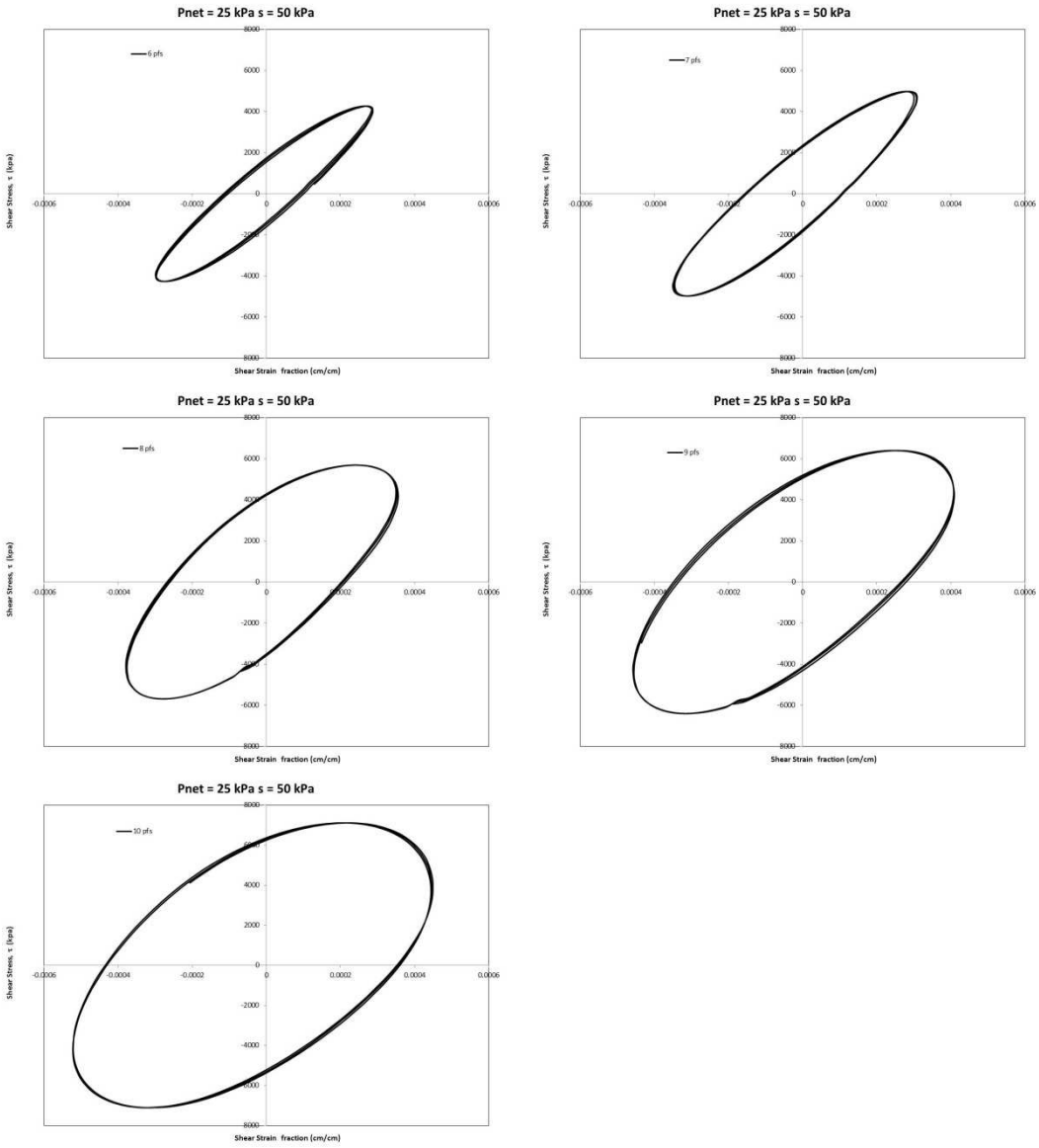

Figure 4-26 Hysteretic loop curves, p - u_a = 25 kPa, u_a – u_w = 50 kPa, torque range = 6 pfs - 10 pfs

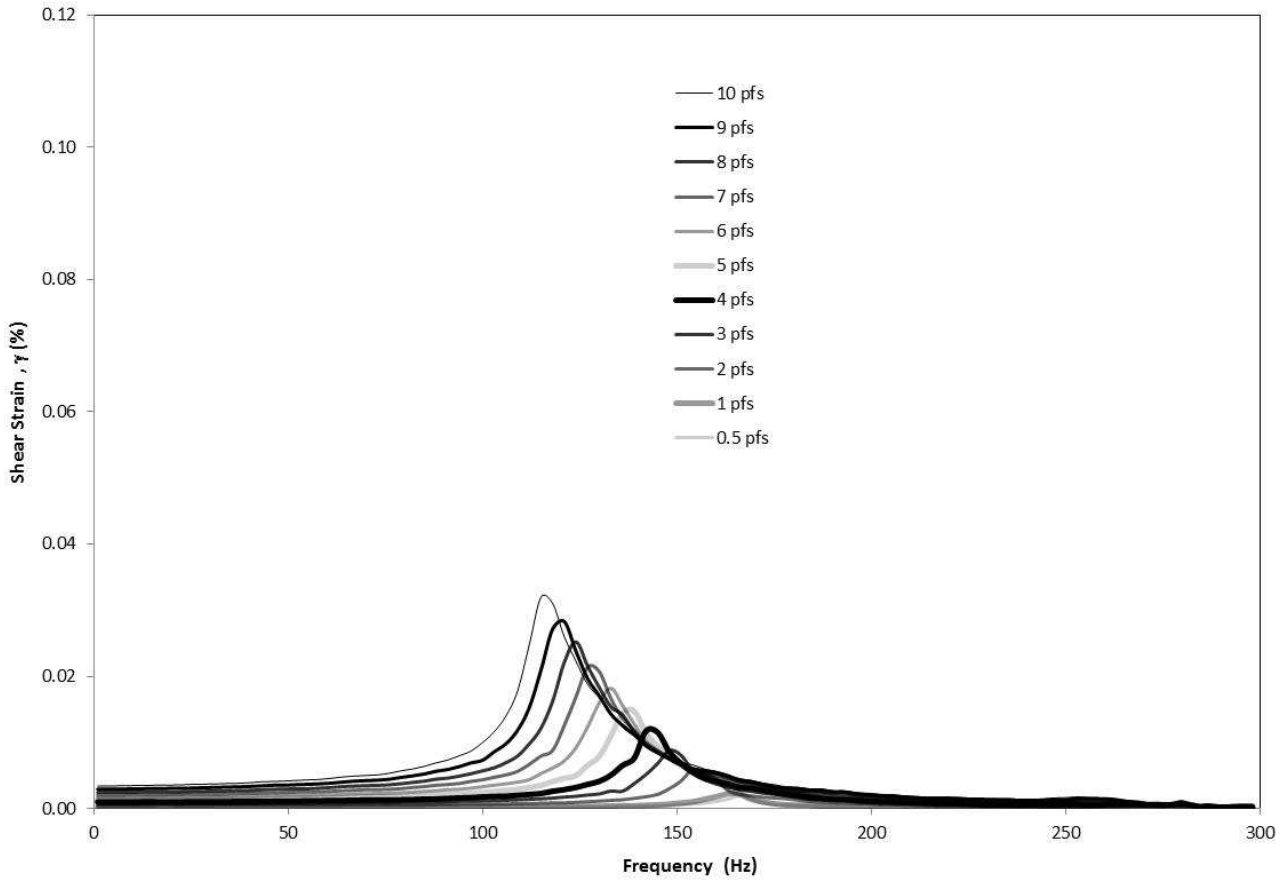

Figure 4-27 Frequency response curves, p - u_a = 50 kPa, u_a – u_w = 50 kPa, torque range = 0.5 pfs -10 pfs

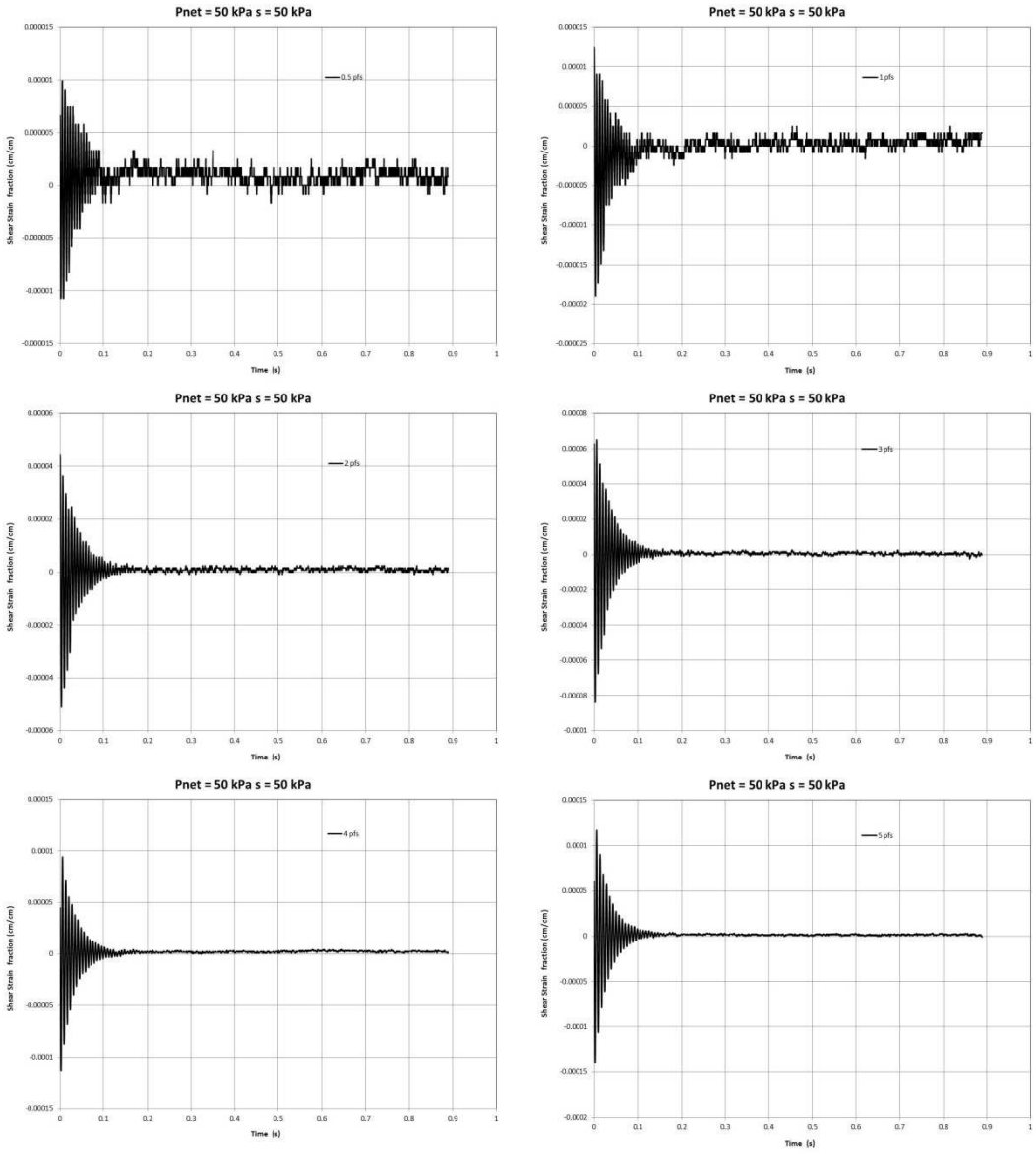

Figure 4-28 Free-vibration decay curves, p - u_a = 50 kPa, u_a – u_w = 50 kPa, torque range = 0.5 pfs - 5 pfs

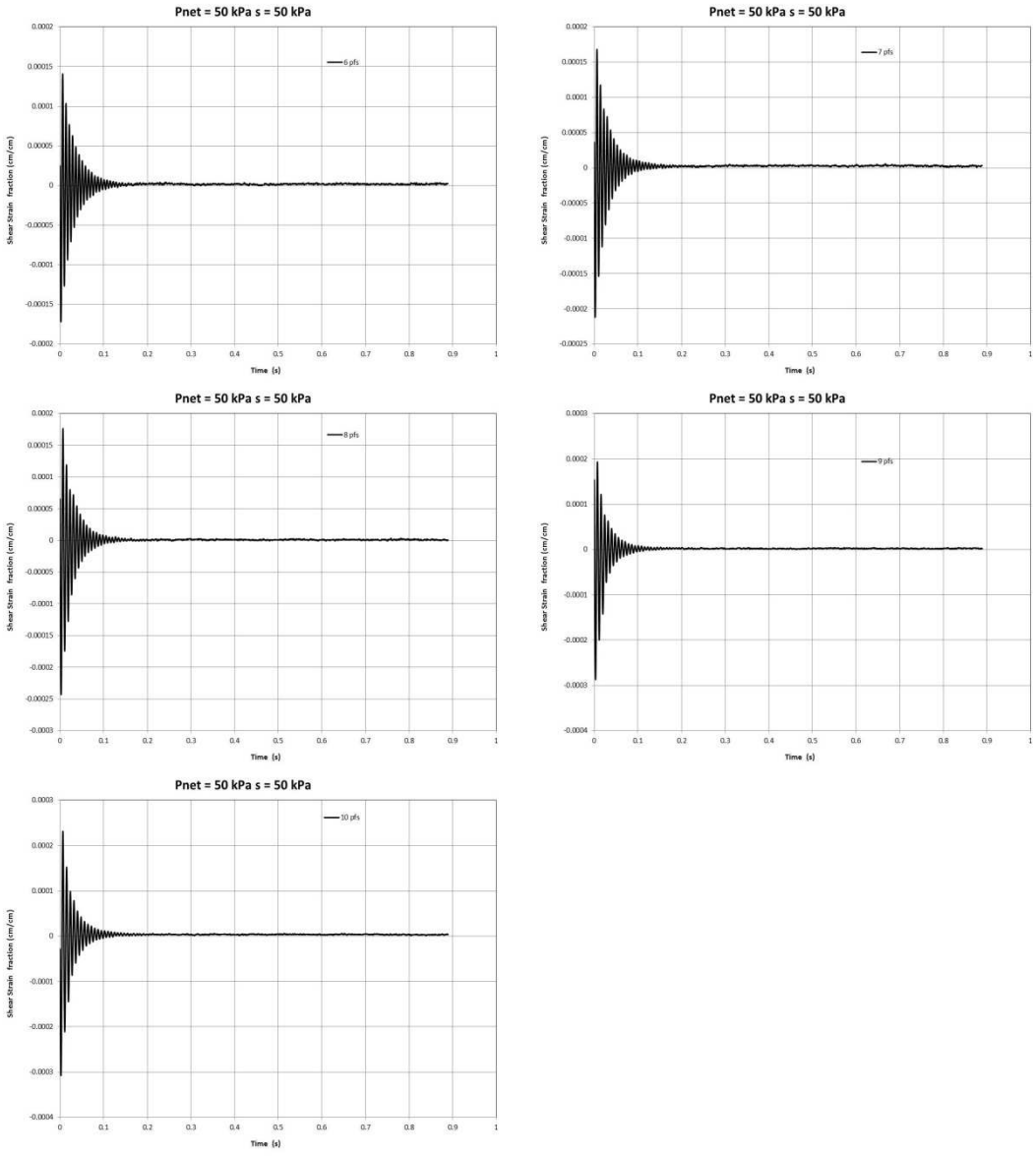

Figure 4-29 Free-vibration decay curves, p - u_a = 50 kPa, u_a – u_w = 50 kPa, torque range = 6 pfs - 10 pfs

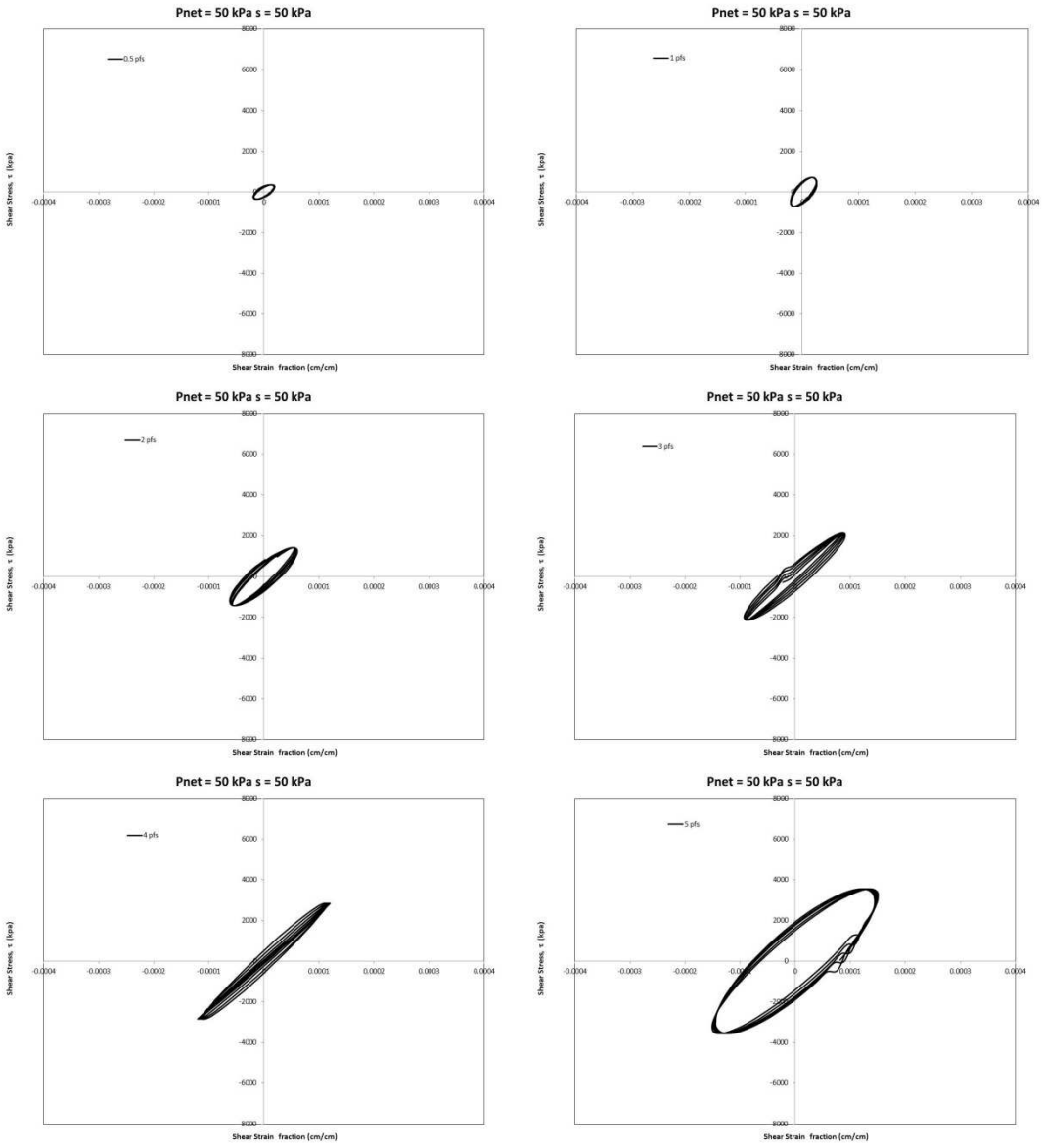

Figure 4-30 Hysteretic loop curves, p - u_a = 50 kPa, u_a – u_w = 50 kPa, torque range = 0.5 pfs - 5 pfs

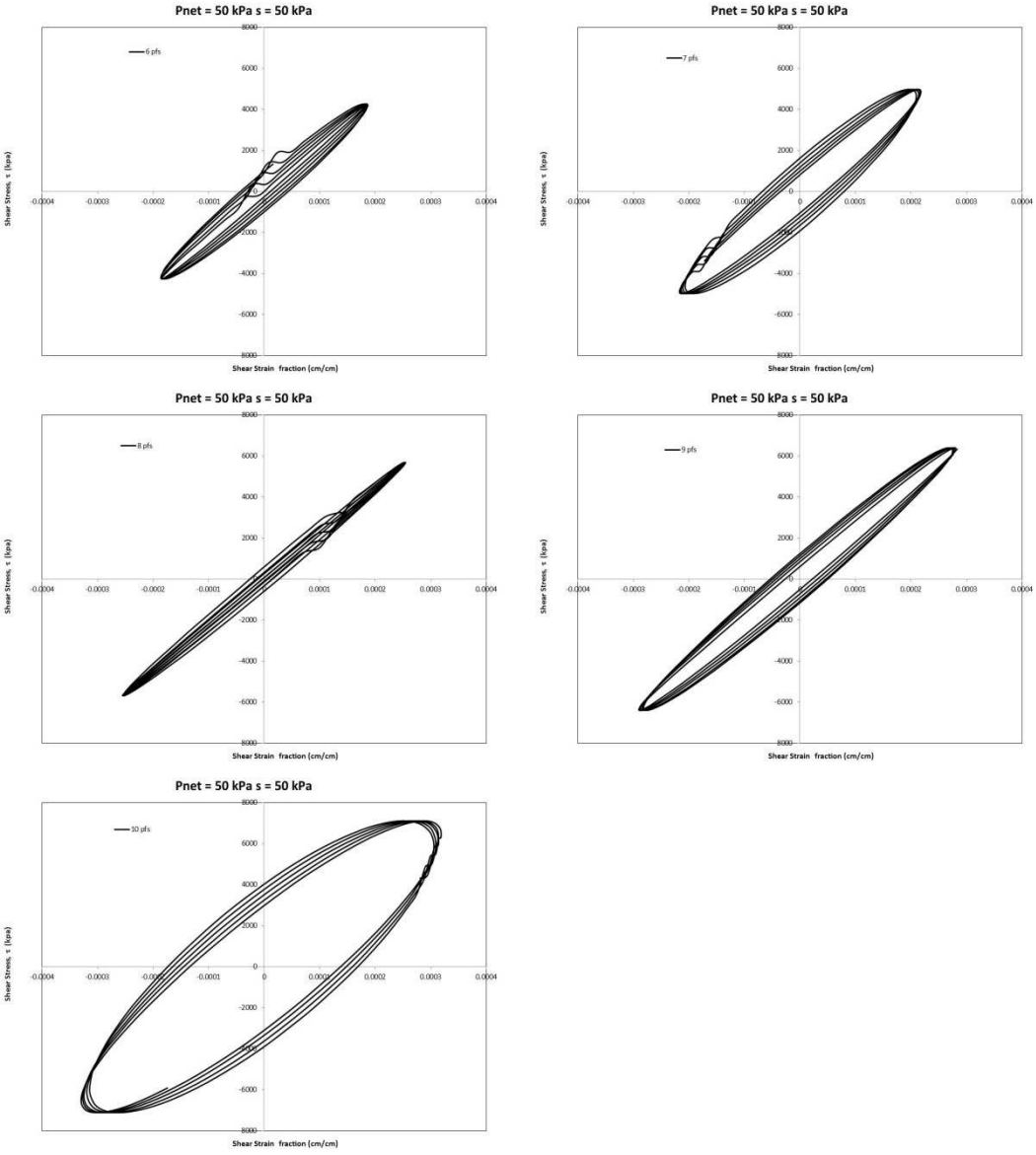

Figure 4-31 Hysteretic loop curves, p - u_a = 50 kPa, u_a – u_w = 50 kPa, torque range = 6 pfs - 10 pfs

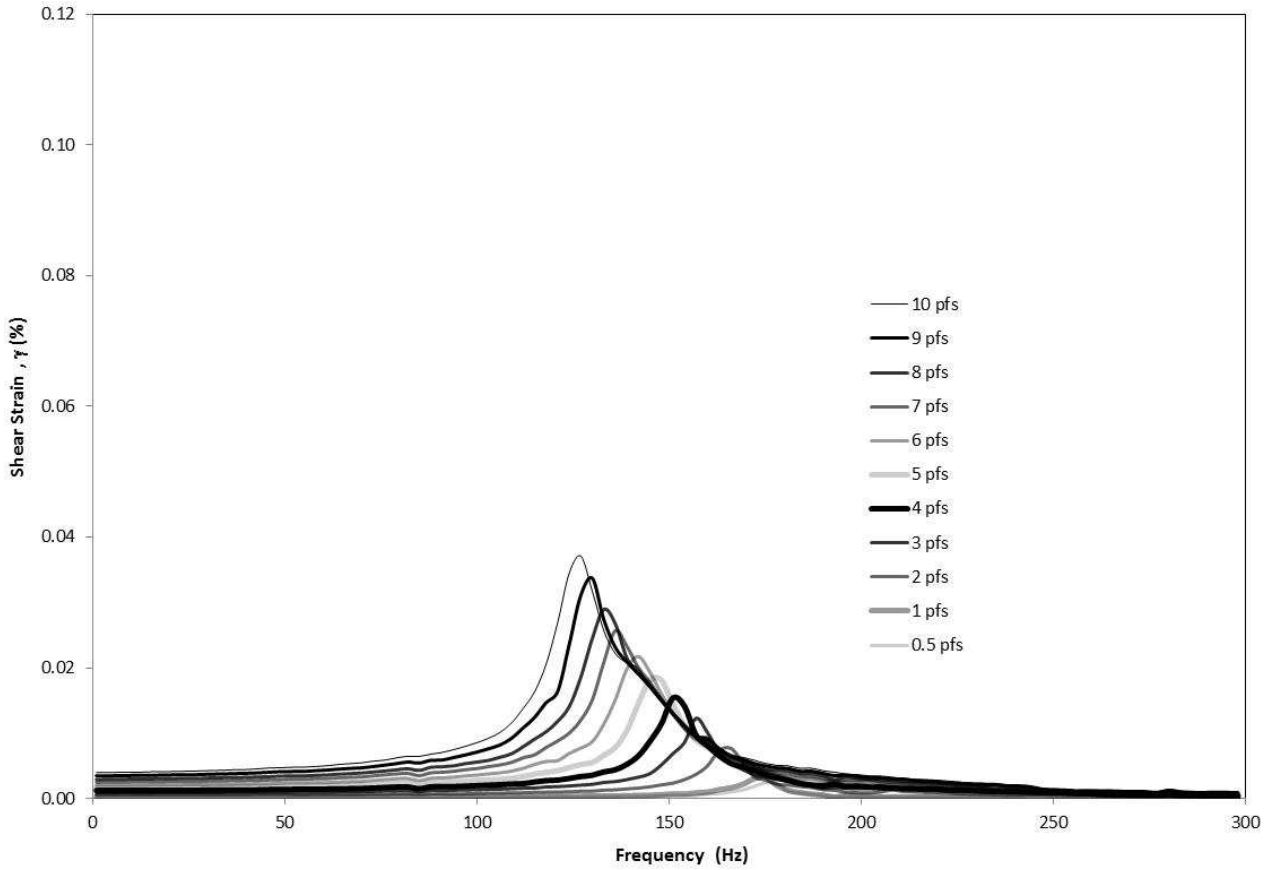

Figure 4-32 Frequency response curves, p - u_a = 100 kPa, u_a – u_w = 50 kPa, torque range = 0.5 pfs -10 pfs

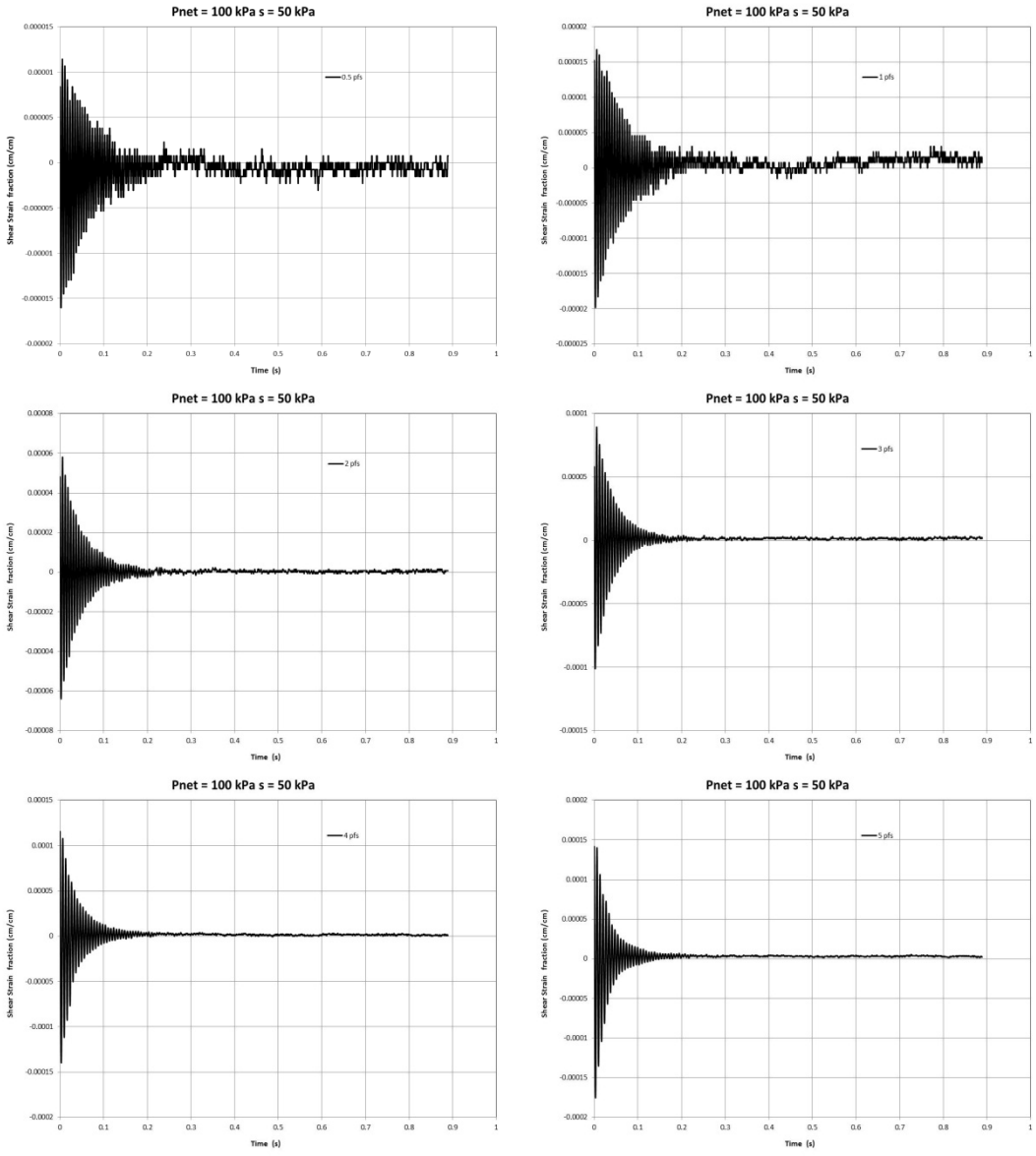

Figure 4-33 Free-vibration decay curves, p - u_a = 100 kPa, u_a – u_w = 50 kPa, torque range = 0.5 pfs - 5 pfs

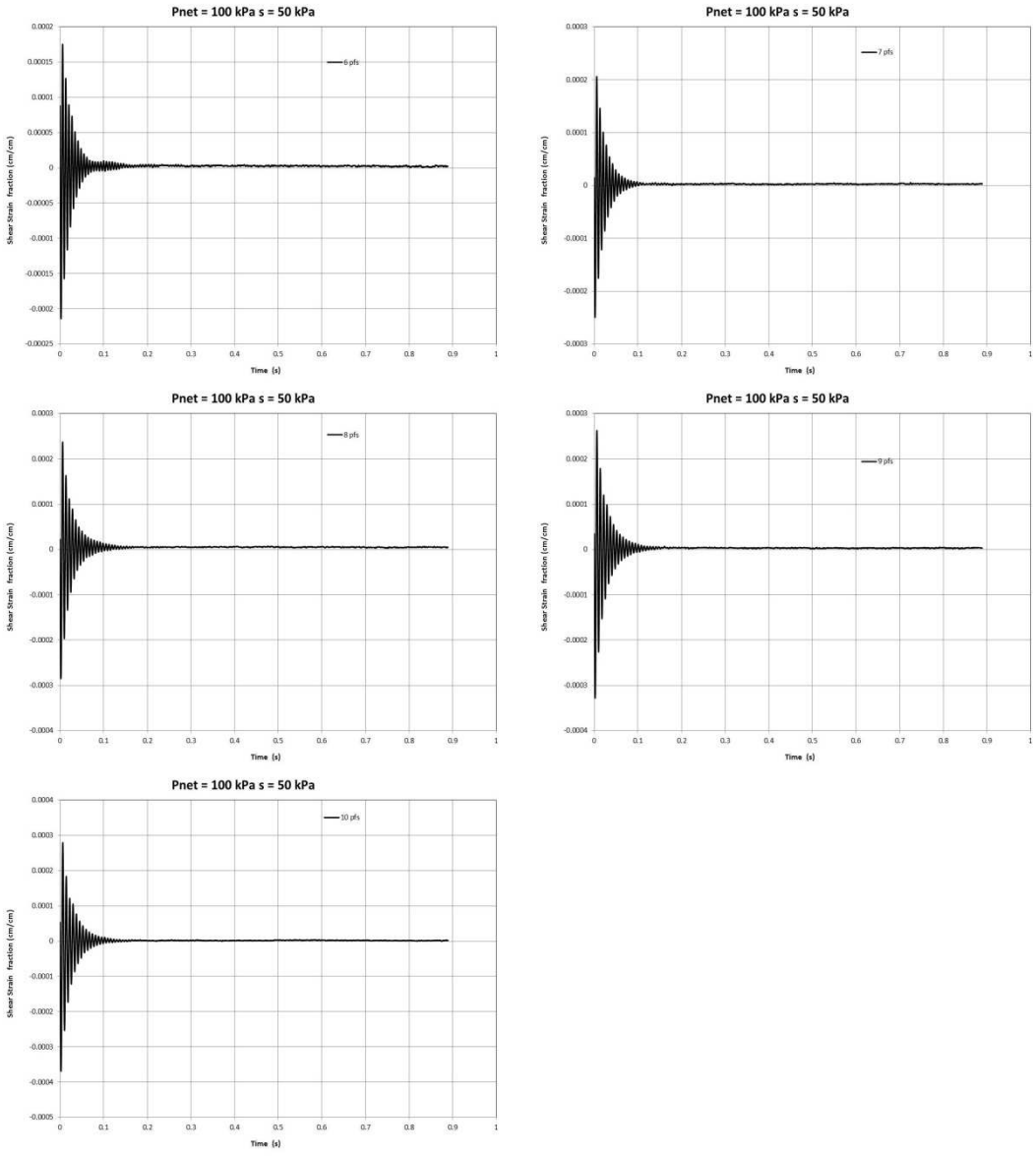

Figure 4-34 Free-vibration decay curves, p - u_a = 100 kPa, u_a – u_w = 50 kPa, torque range = 6 pfs - 10 pfs

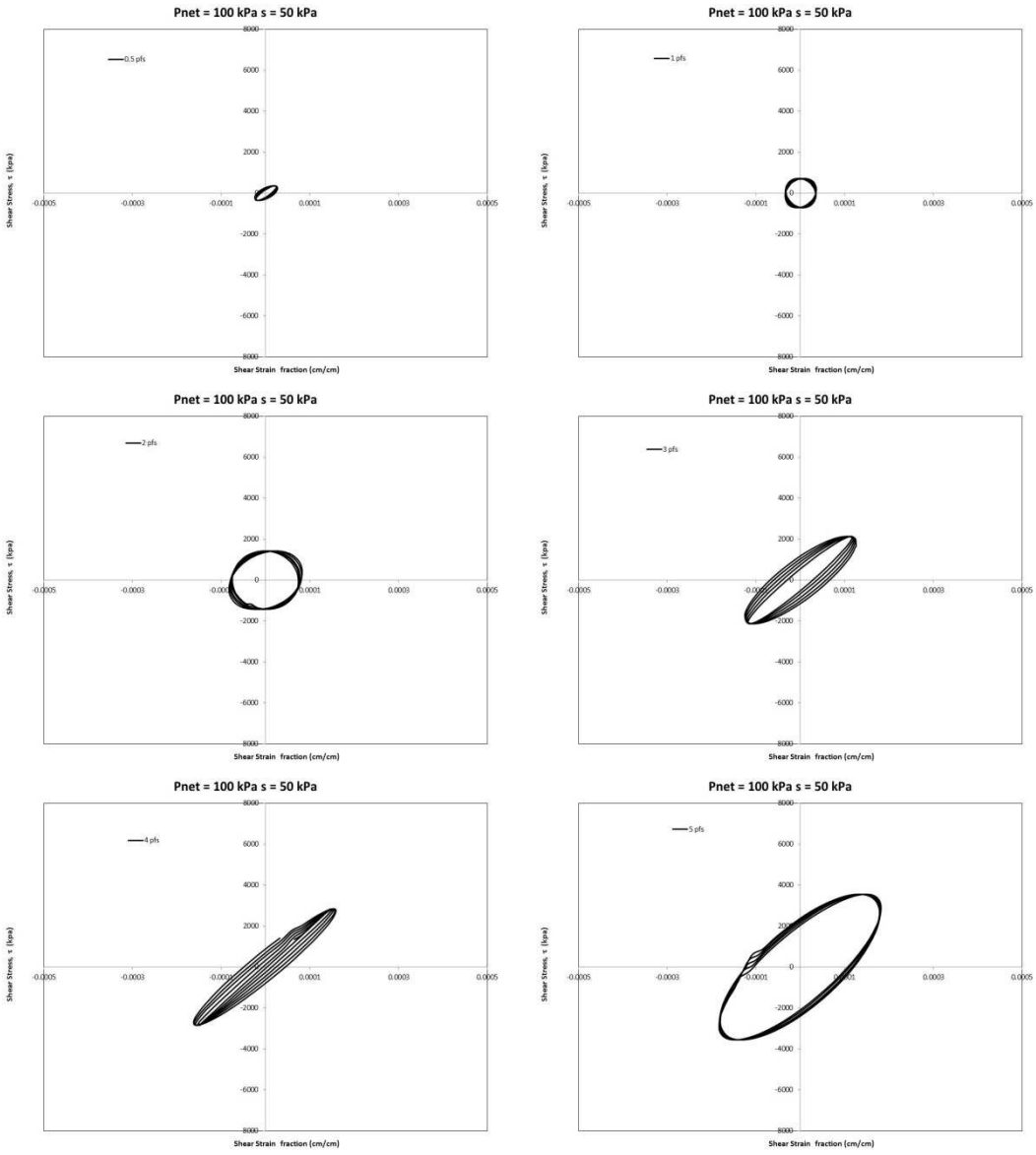

Figure 4-35 Hysteretic loop curves, p - u_a = 100 kPa, u_a – u_w = 50 kPa, torque range = 0.5 pfs - 5 pfs

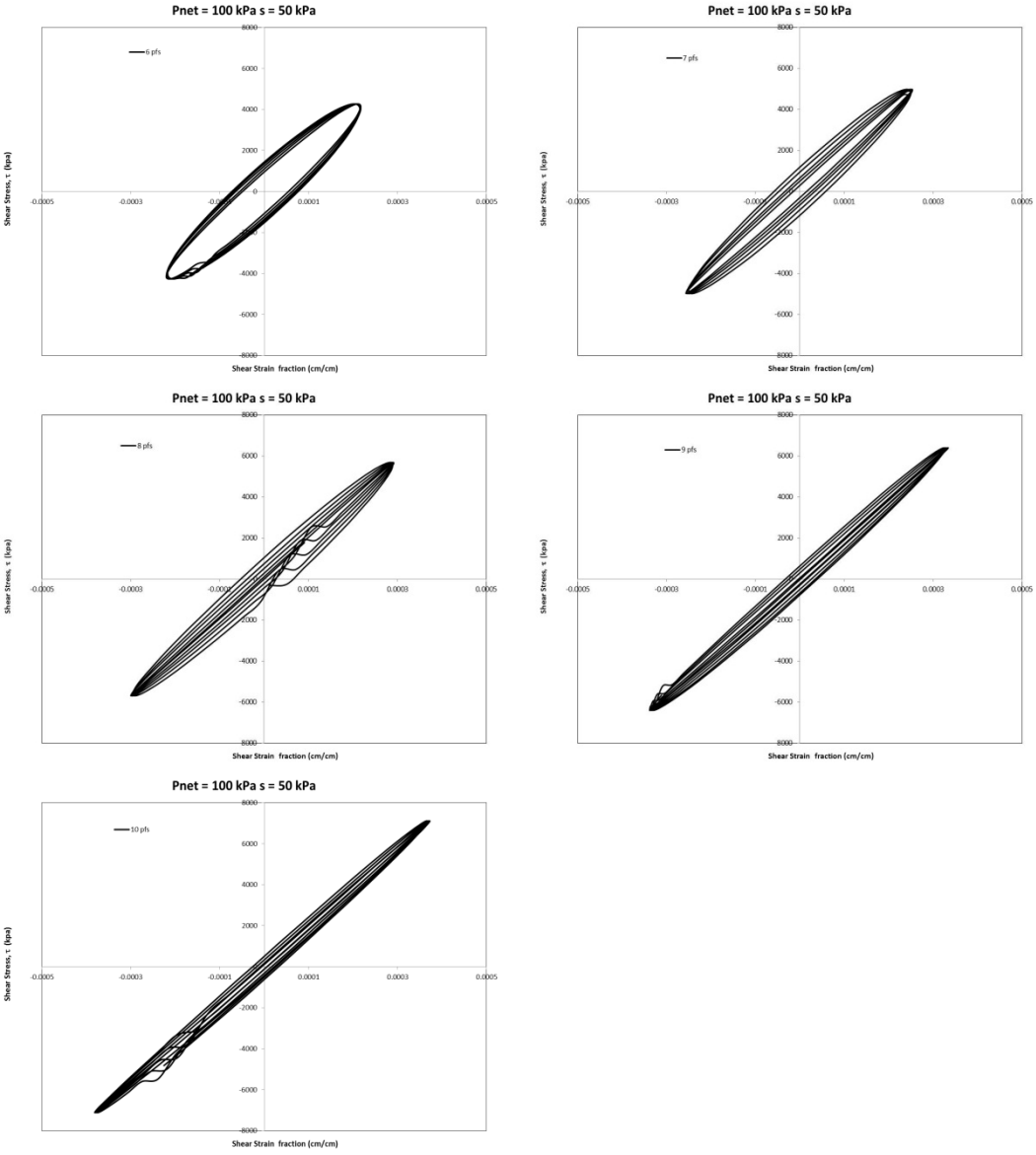

Figure 4-36 Hysteretic loop curves, p - u_a = 100 kPa, u_a – u_w = 50 kPa, torque range = 6 pfs - 10 pfs

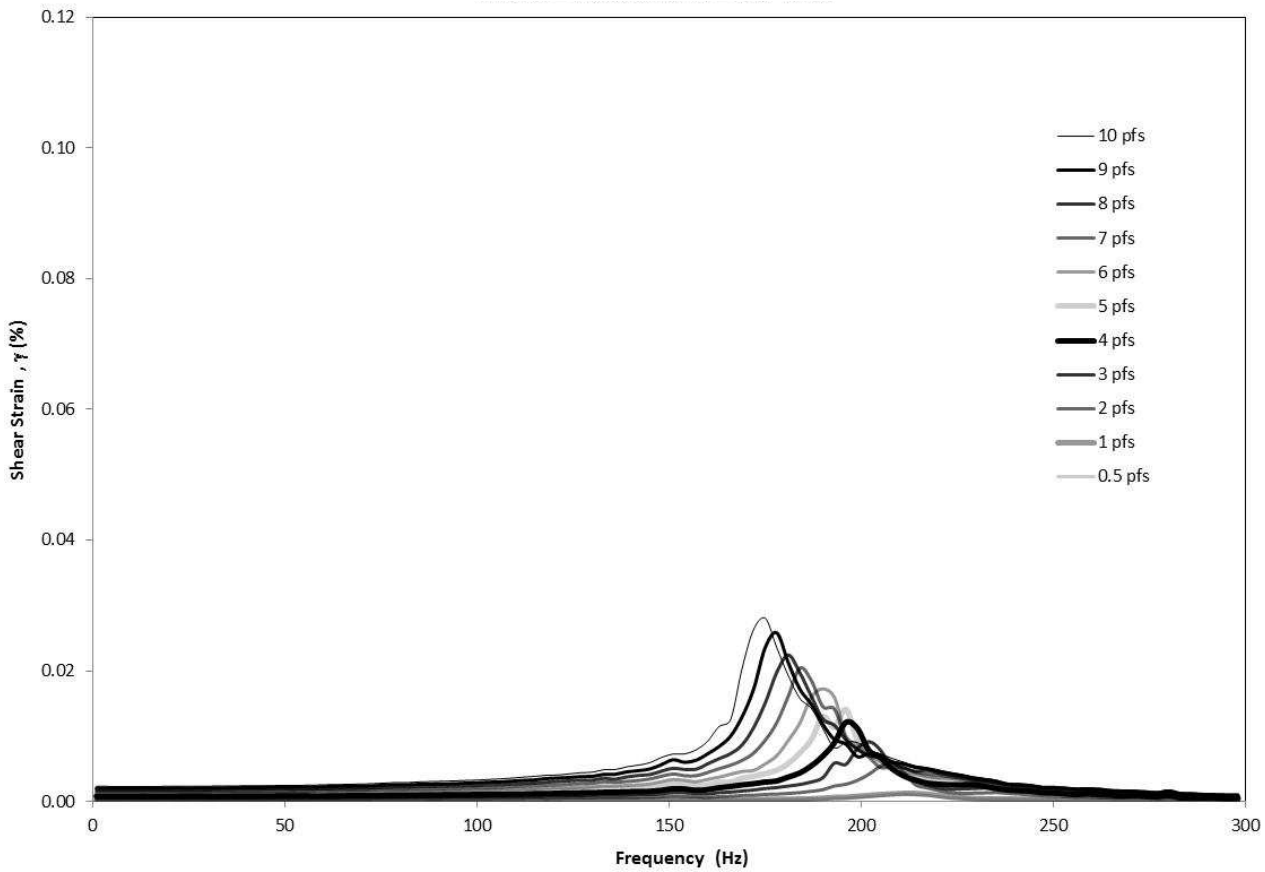

Figure 4-37 Frequency response curve, p - u_a = 200 kPa, u_a – u_w = 50 kPa, torque range = 0.5 pfs -10 pfs

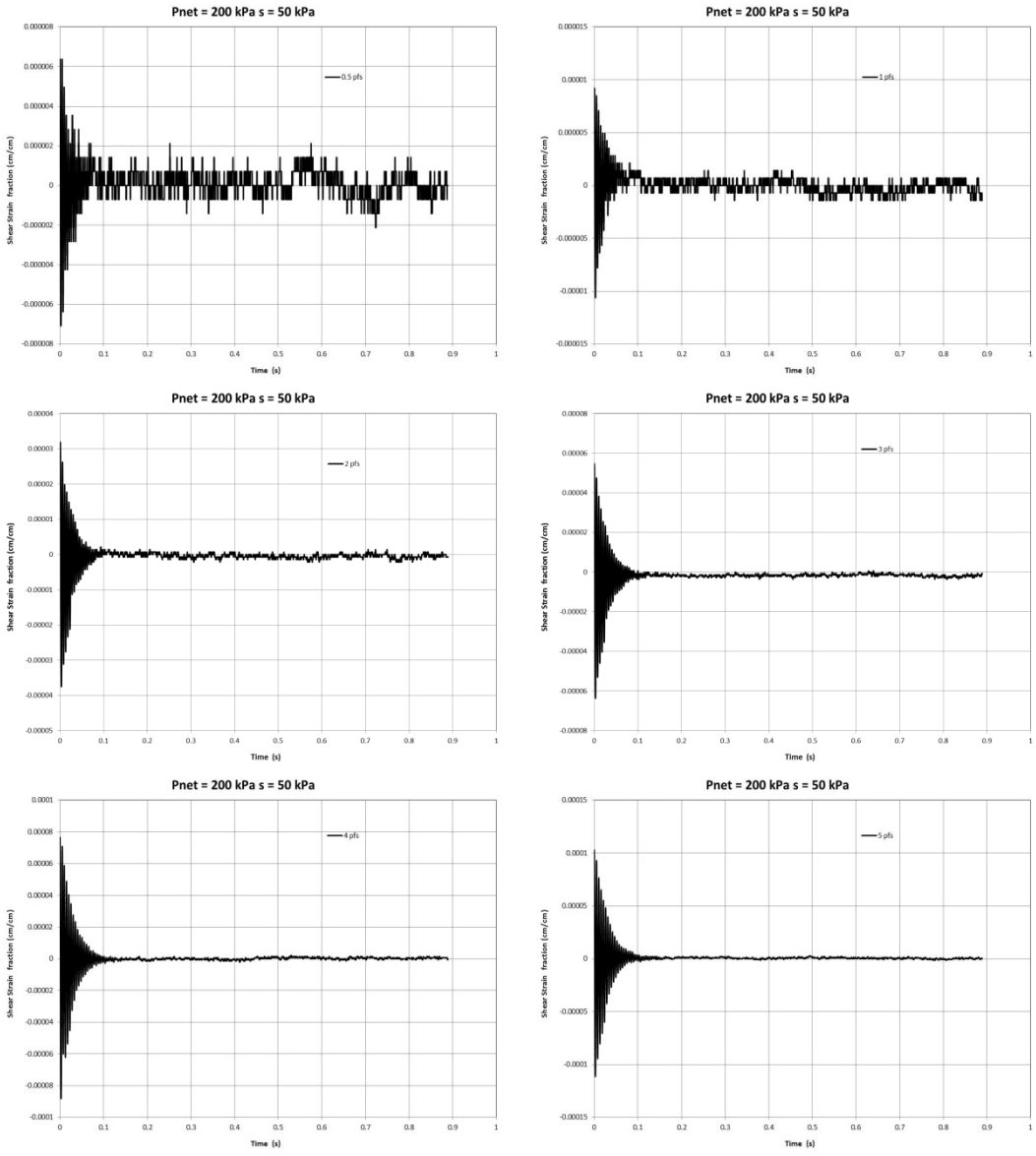

Figure 4-38 Free-vibration decay curves, p - u_a = 200 kPa, u_a – u_w = 50 kPa, torque range = 0.5 pfs - 5 pfs

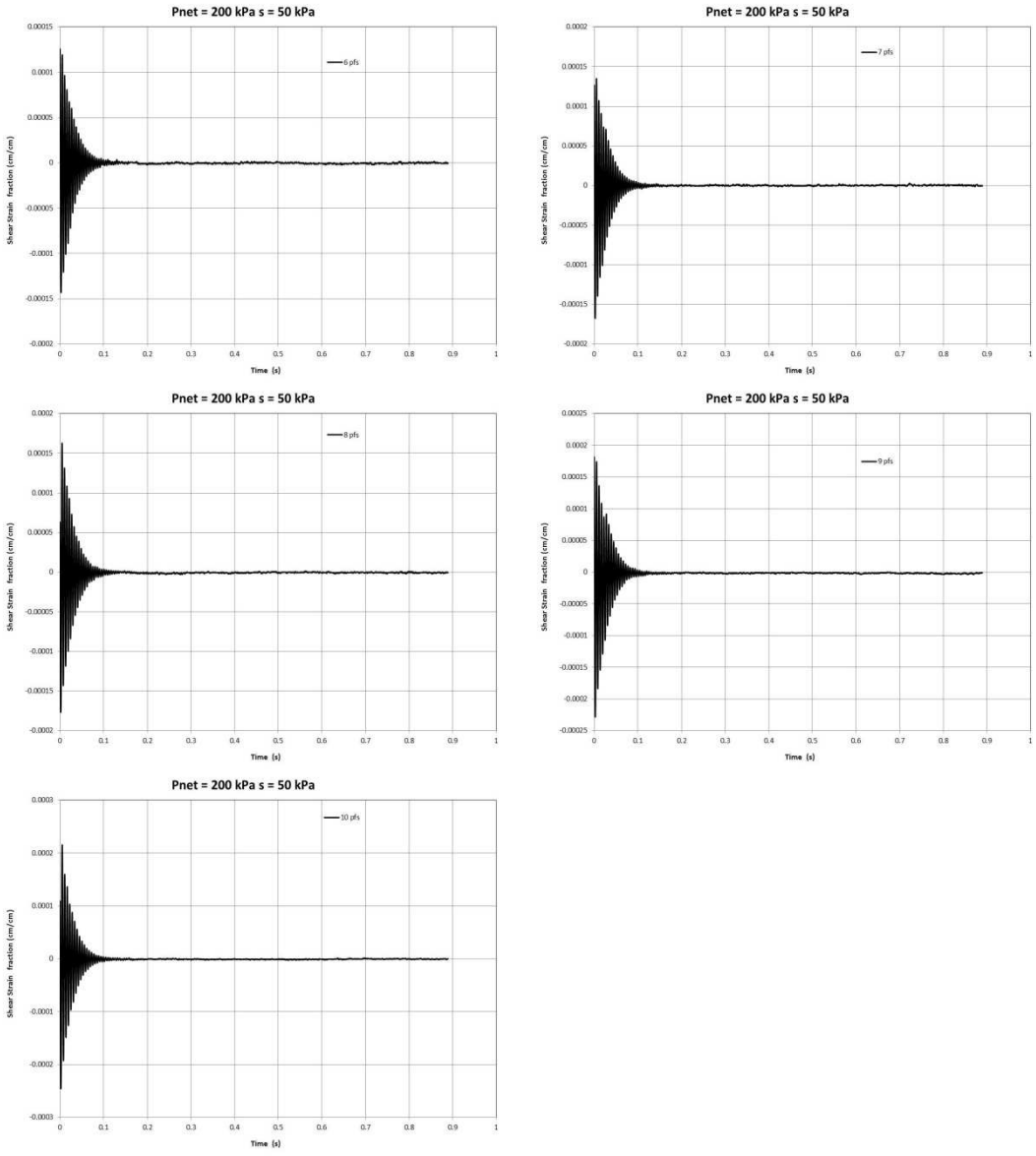

Figure 4-39 Free-vibration decay curves, p - u_a = 200 kPa, u_a – u_w = 50 kPa, torque range = 6 pfs - 10 pfs

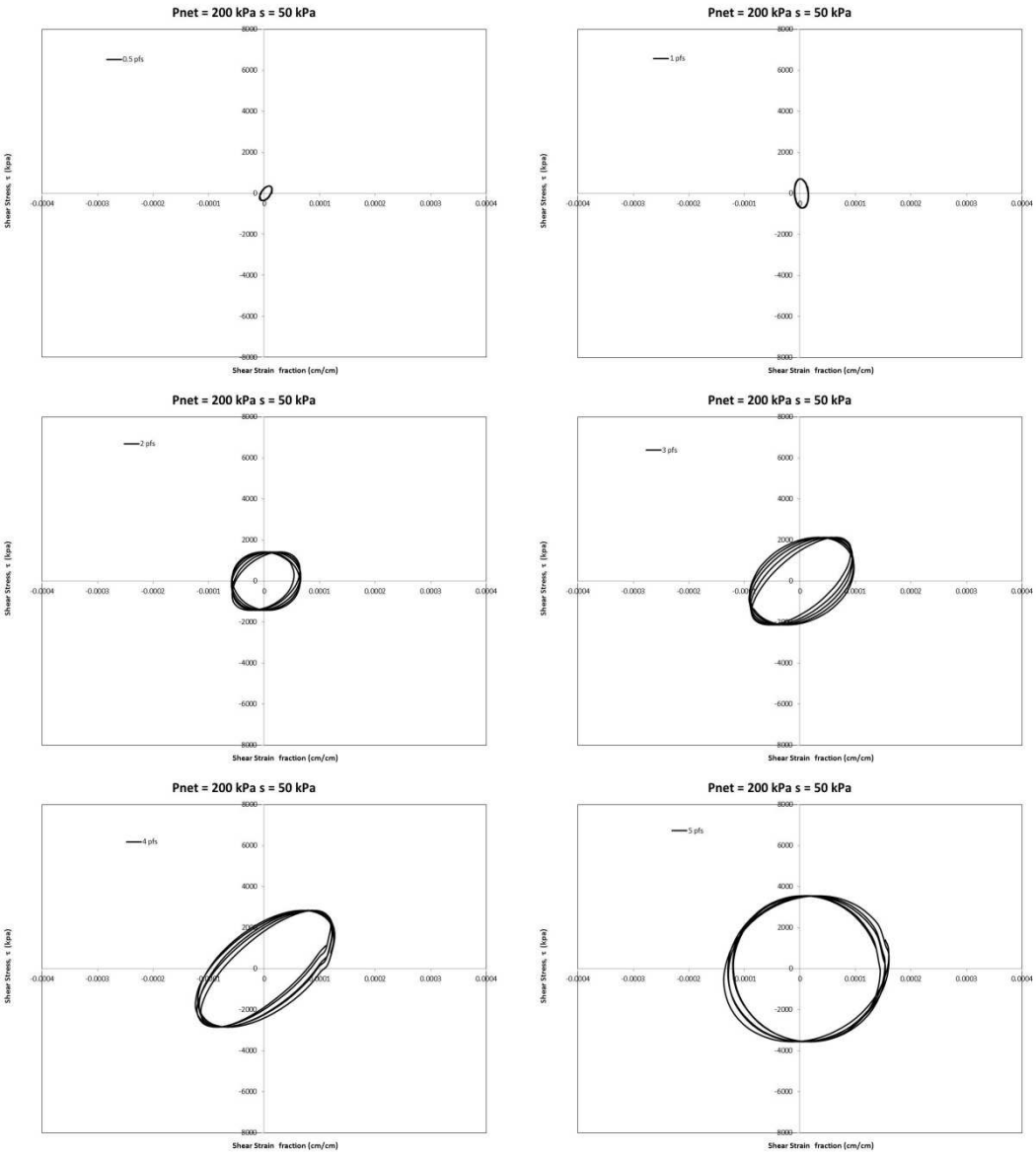

Figure 4-40 Hysteretic loop curves, p - u_a = 200 kPa, u_a – u_w = 50 kPa, torque range = 0.5 pfs - 5 pfs

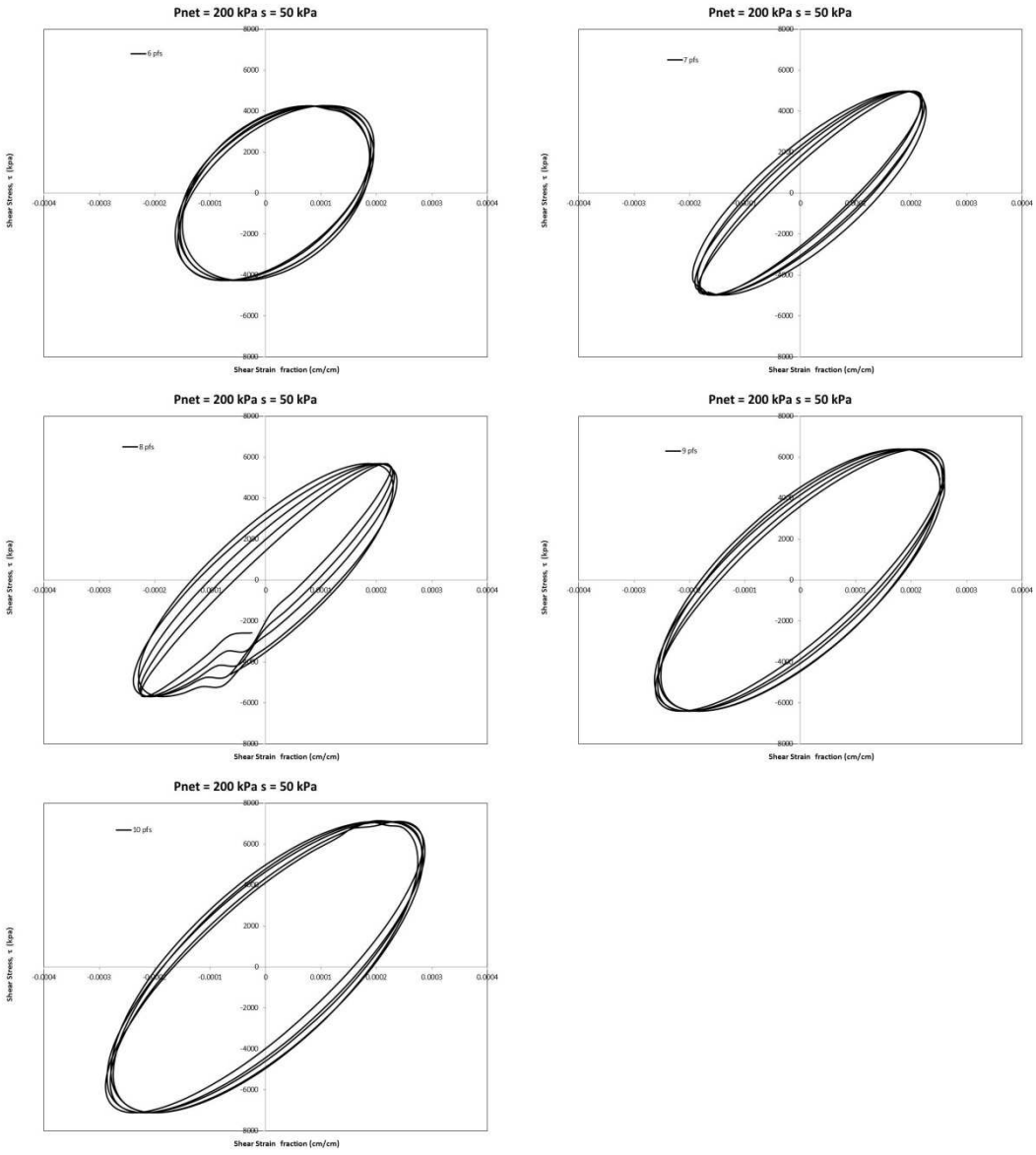

Figure 4-41 Hysteretic loop curves, p = 200 kPa, $u_a - u_w$ = 50 kPa, torque range = 6 pfs - 10 pfs

4.4.3 Resonant Column Tests Performed under Constant Matric Suction, s = 100 kPa

This section presents all the frequency response curves, free-vibration decay curves and cyclic hysteretic loop curves from RC tests conducted at net confining pressures, $(p\text{-}u_a)$ = 25, 50, 100, and 200 kPa, respectively, under a constant matric suction, s = 100 kPa.

It can be observed that there is an increment on the resonant frequency when the net mean stress or confinement pressure is increased. This fact ensures an increase on the shear modulus with any increment on the net mean stress, since, in shear modulus calculations, the frequency at resonance is directly proportional to shear modulus. This can be attributed to a direct increase in the total stress in the sample while the matric suction is kept constant, thereby causing closer contact between soil particles (higher packing) and stiffer material.

Also, it can be observed that the frequency at resonance undergoes decrement when the cyclic torque is increased. A well-defined curved tendency on the resonant frequency can be obtained with increasing input torque. This condition can be attributed to the initial yield loci being exceeded, what brings the soil sample into the elasto-plastic behavior.

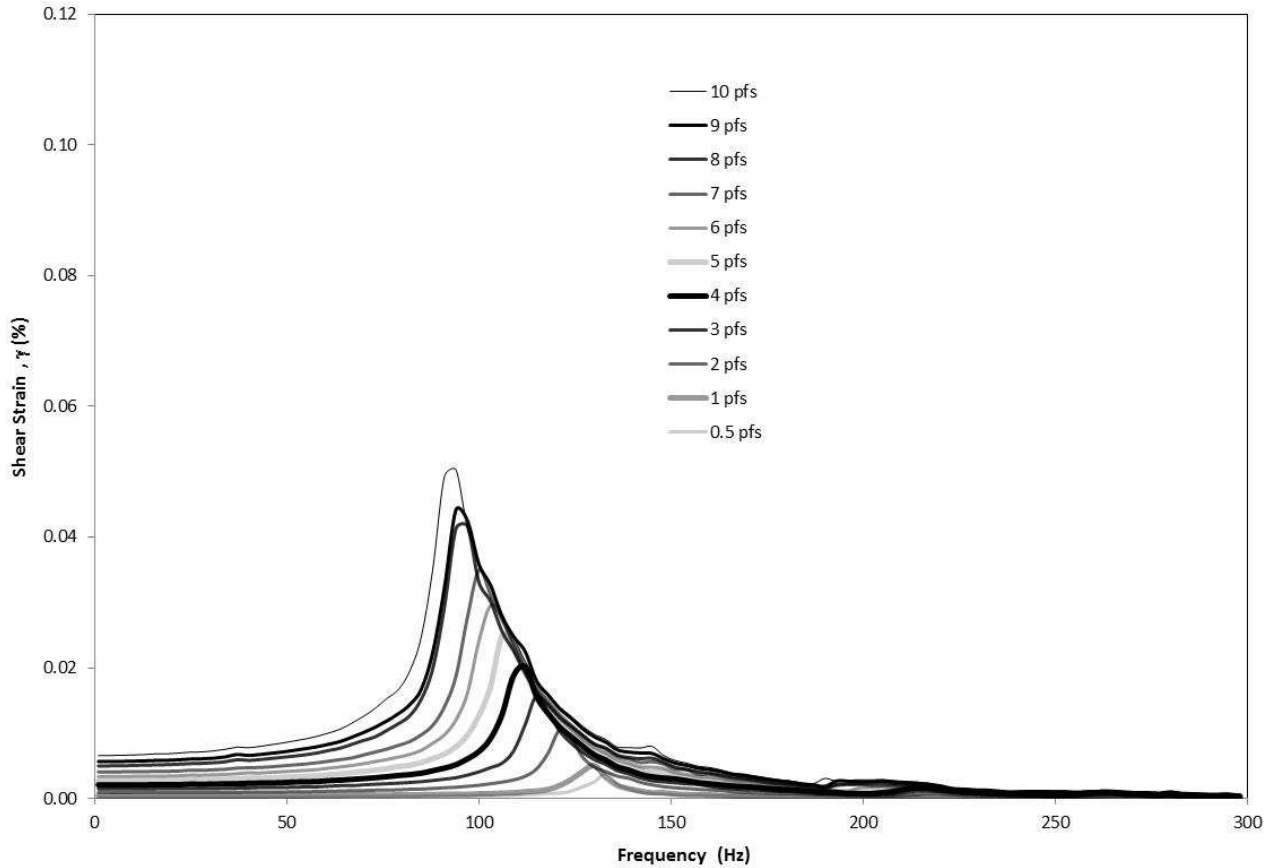

Figure 4-42 Frequency response curves, p - u_a = 25 kPa, u_a – u_w = 100 kPa, torque range = 0.5 pfs -10 pfs

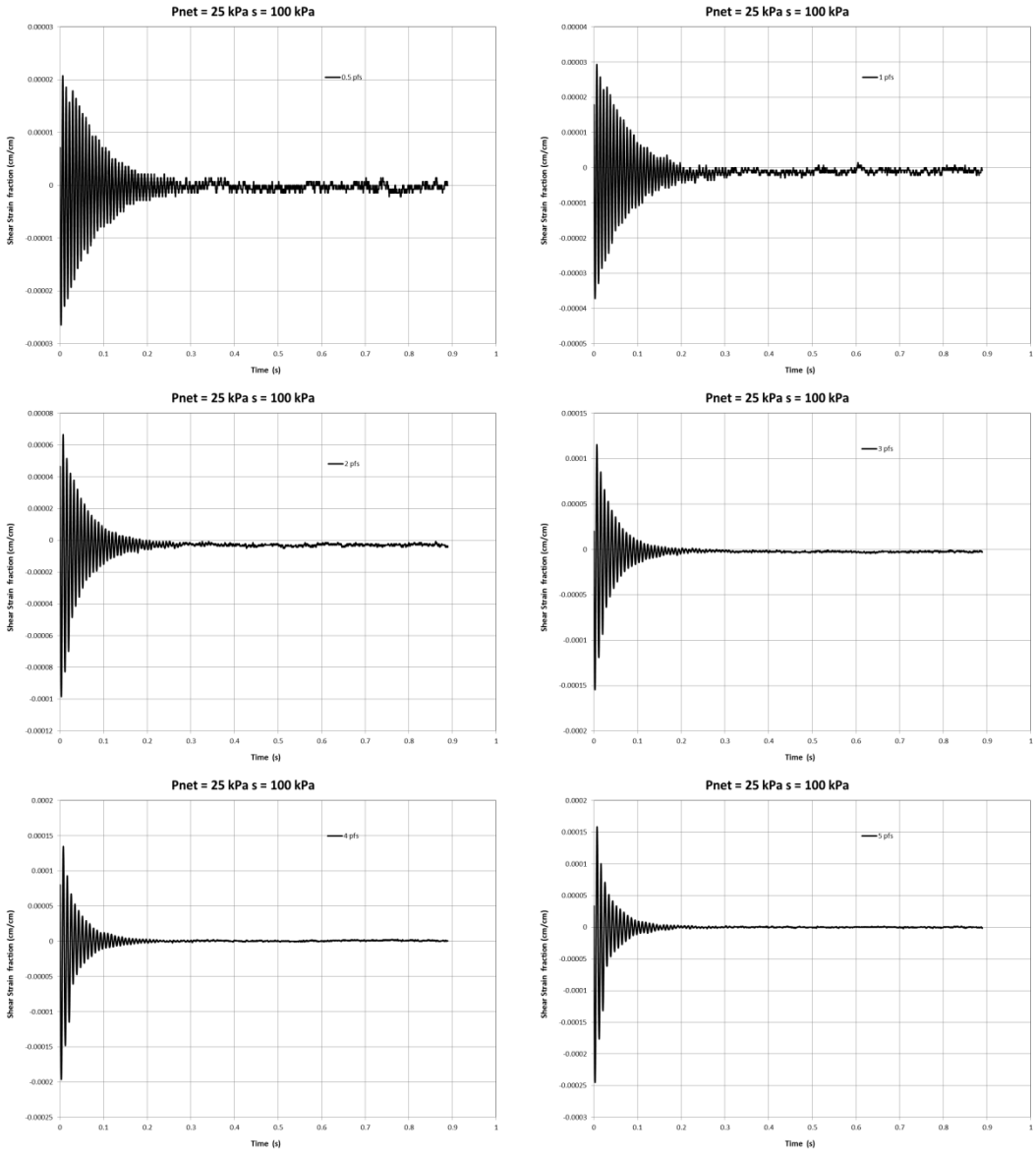

Figure 4-43 Free-vibration decay curves, p - u_a = 25 kPa, u_a – u_w = 100 kPa, torque range = 0.5 pfs - 5 pfs

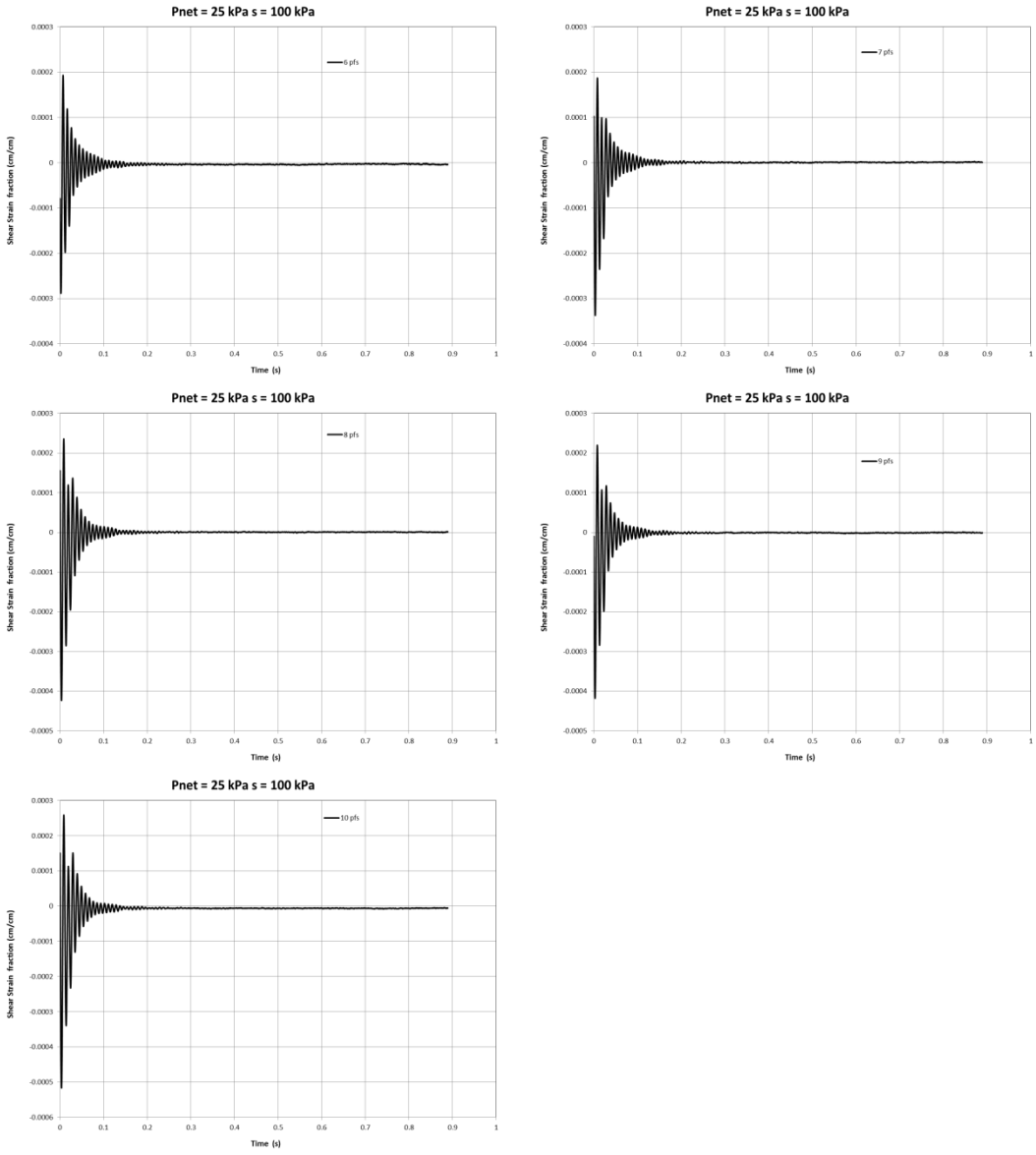

Figure 4-44 Free-vibration decay curves, p - u_a = 25 kPa, u_a – u_w = 100 kPa, torque range = 6 pfs - 10 pfs

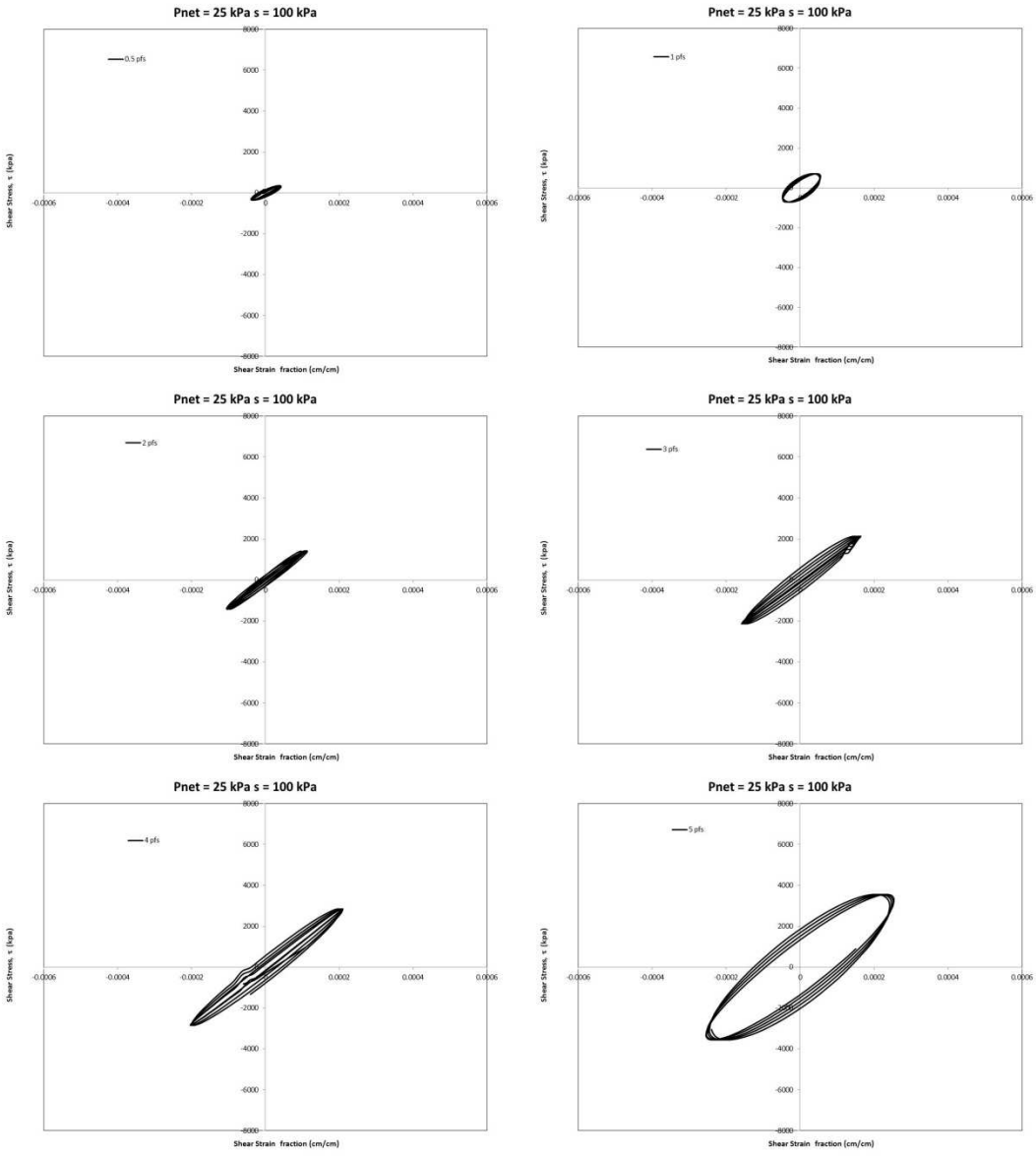

Figure 4-45 Hysteretic loop curves, p - u_a = 25 kPa, u_a – u_w = 100 kPa, torque range = 0.5 pfs - 5 pfs

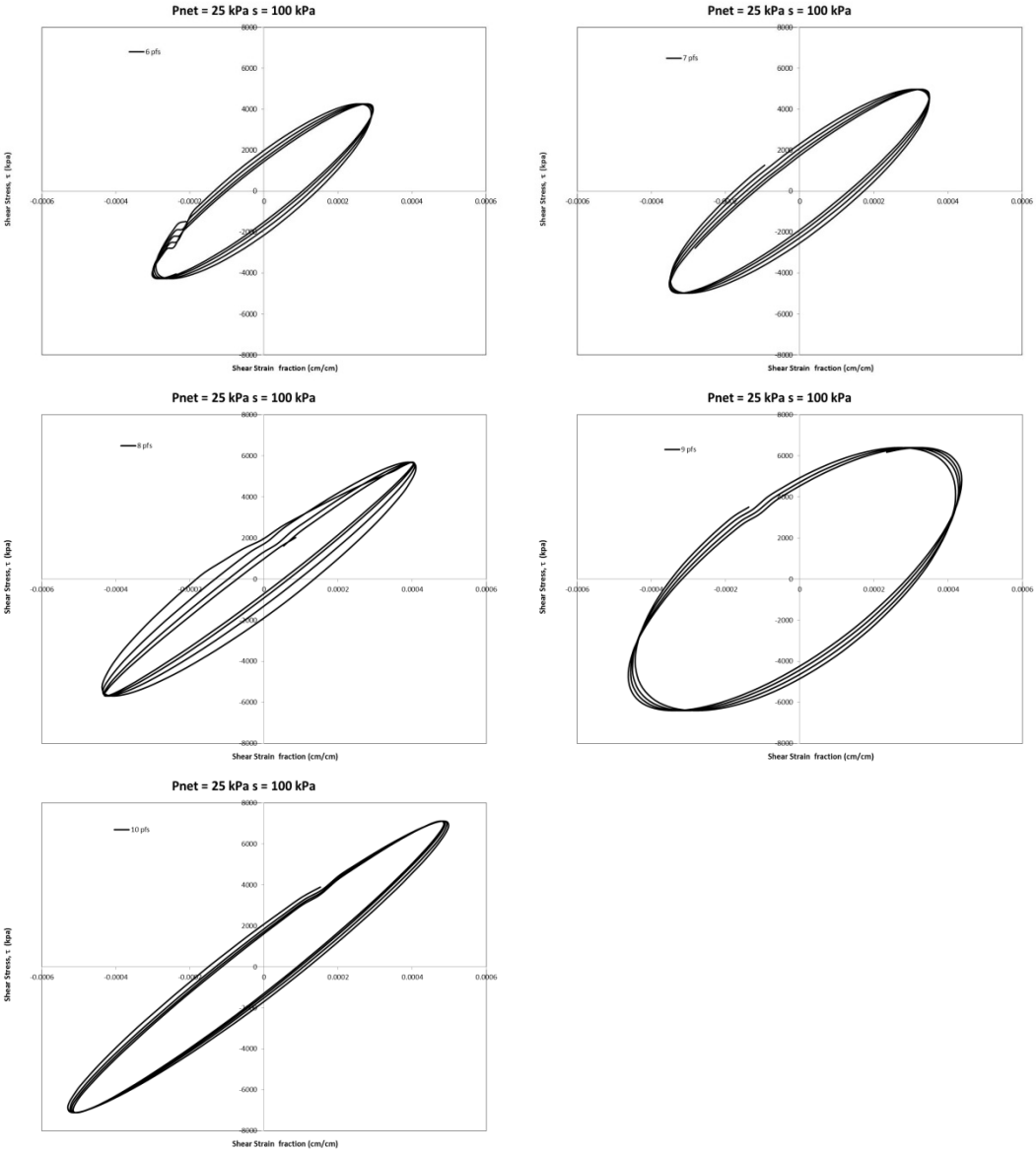

Figure 4-46 Hysteretic loop curves, p - u_a = 25 kPa, u_a – u_w = 100 kPa, torque range = 6 pfs - 10 pfs

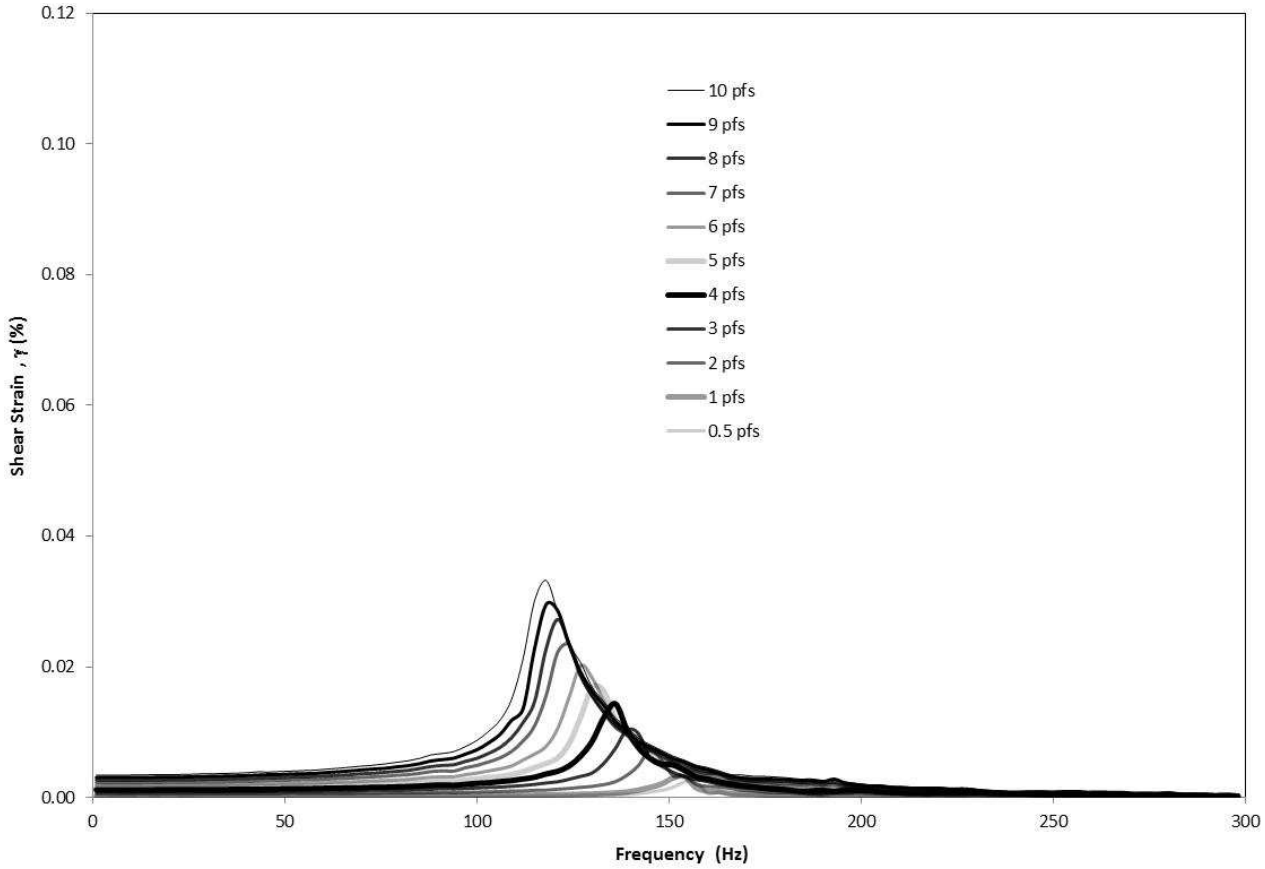

Figure 4-47 Frequency response curves, p - u_a = 50 kPa, u_a – u_w = 100 kPa, torque range = 0.5 pfs -10 pfs

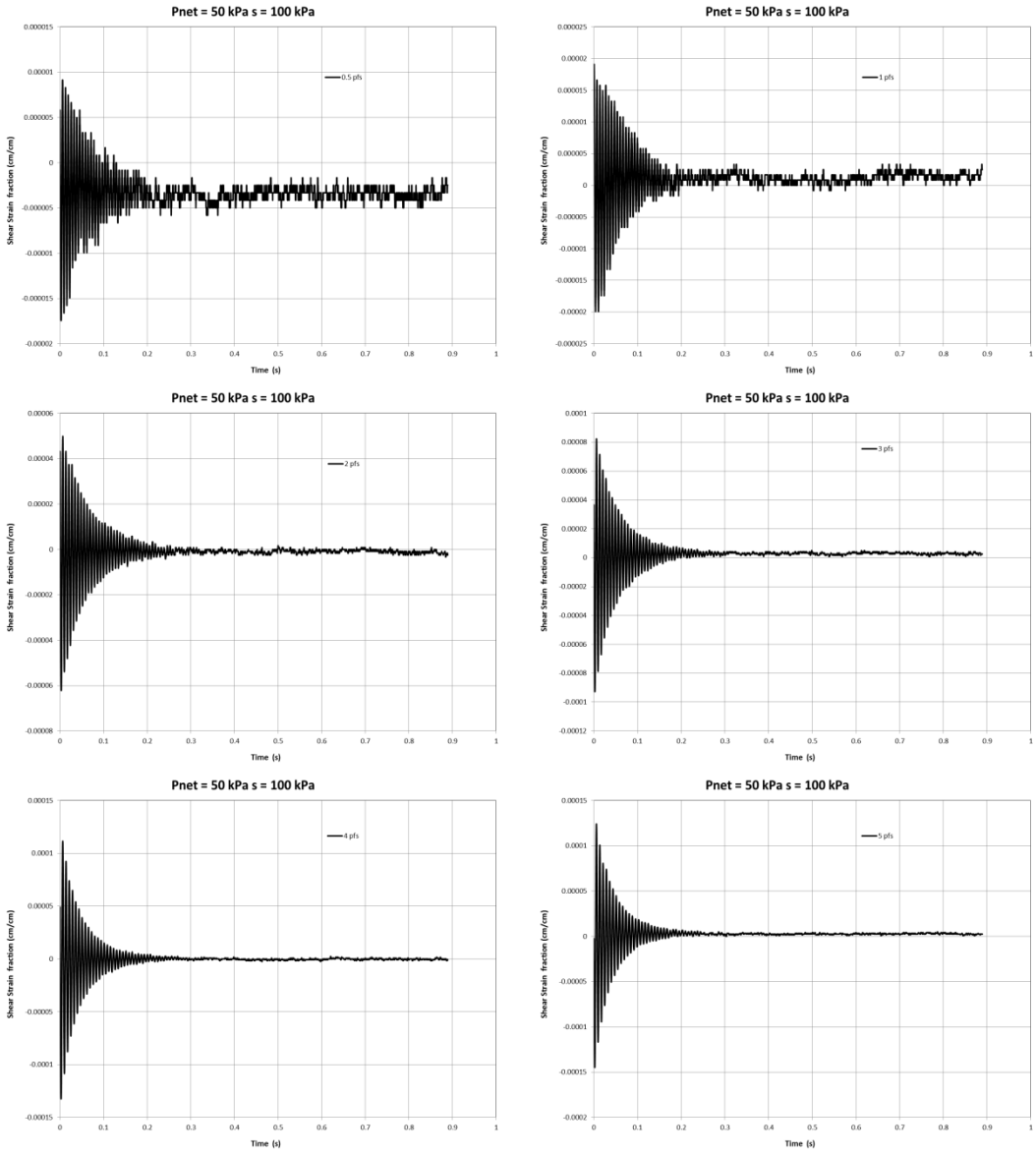

Figure 4-48 Free-vibration decay curves, p - u_a = 50 kPa, u_a – u_w = 100 kPa, torque range = 0.5 pfs - 5 pfs

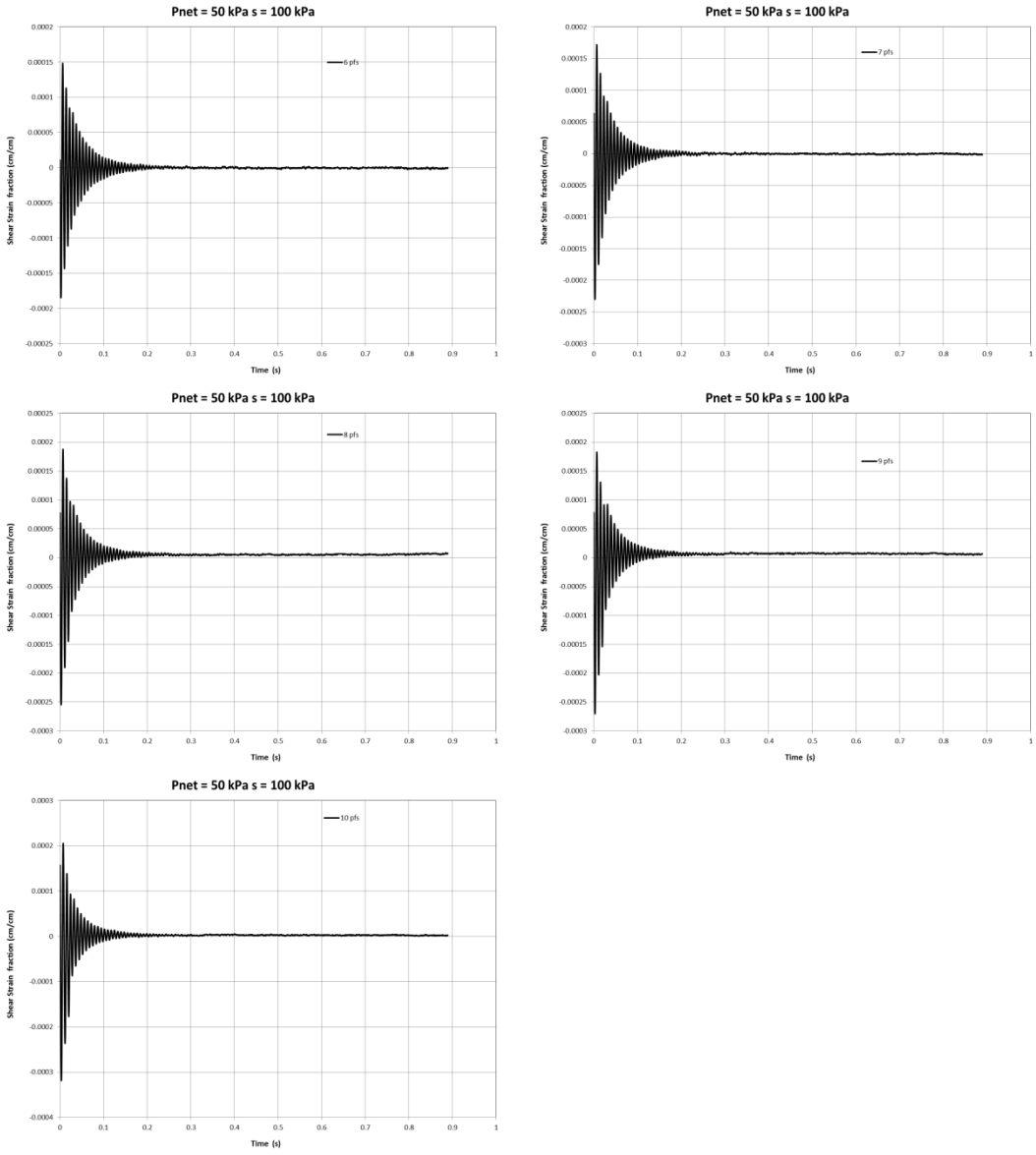

Figure 4-49 Free-vibration decay curves, p - u_a = 50 kPa, u_a – u_w = 100 kPa, torque range = 6 pfs - 10 pfs

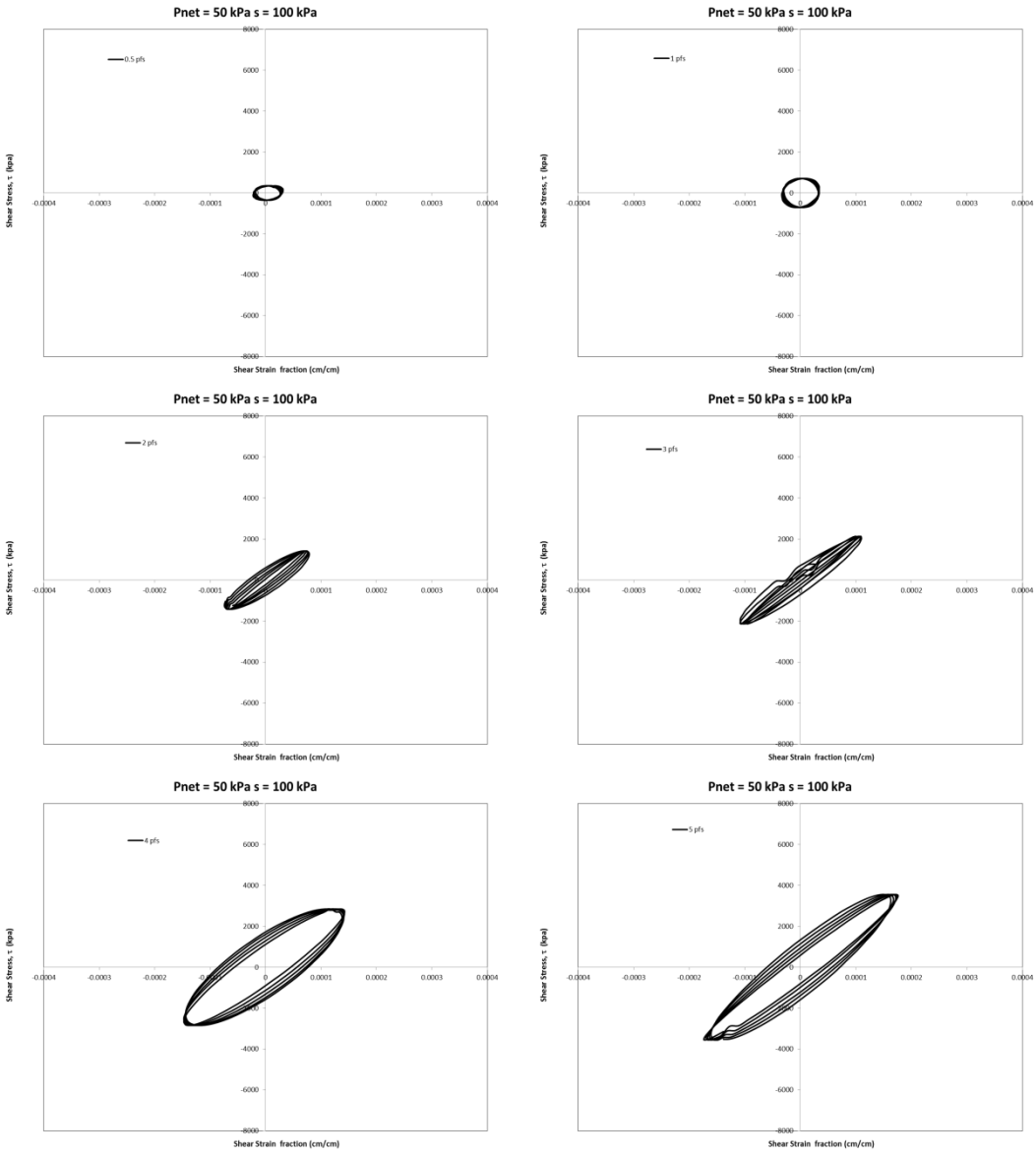

Figure 4-50 Hysteretic loop curves, p - u_a = 50 kPa, u_a – u_w = 100 kPa, torque range = 0.5 pfs - 5 pfs

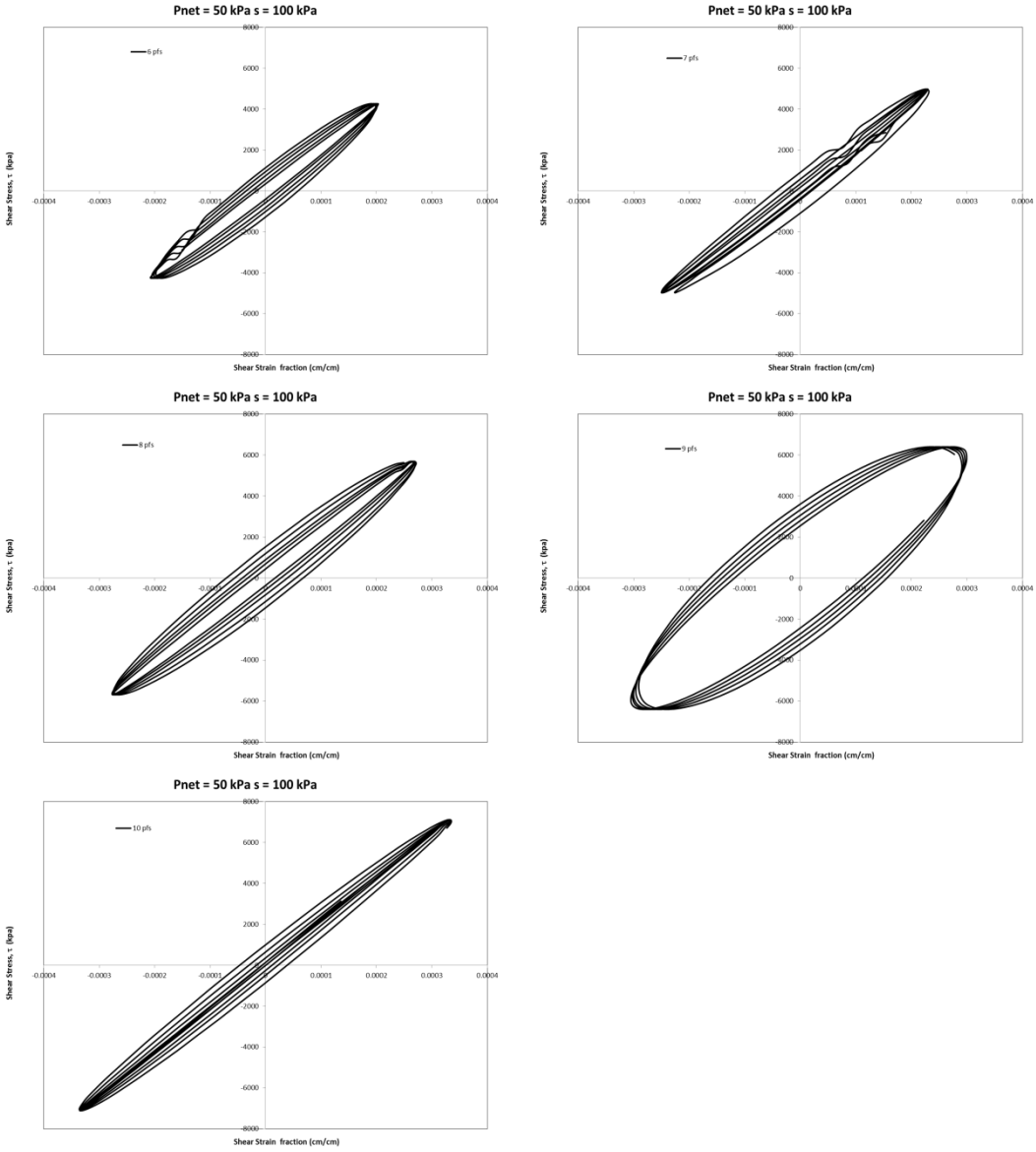

Figure 4-51 Hysteretic loop curves, p - u_a = 50 kPa, u_a – u_w = 100 kPa, torque range = 6 pfs - 10 pfs

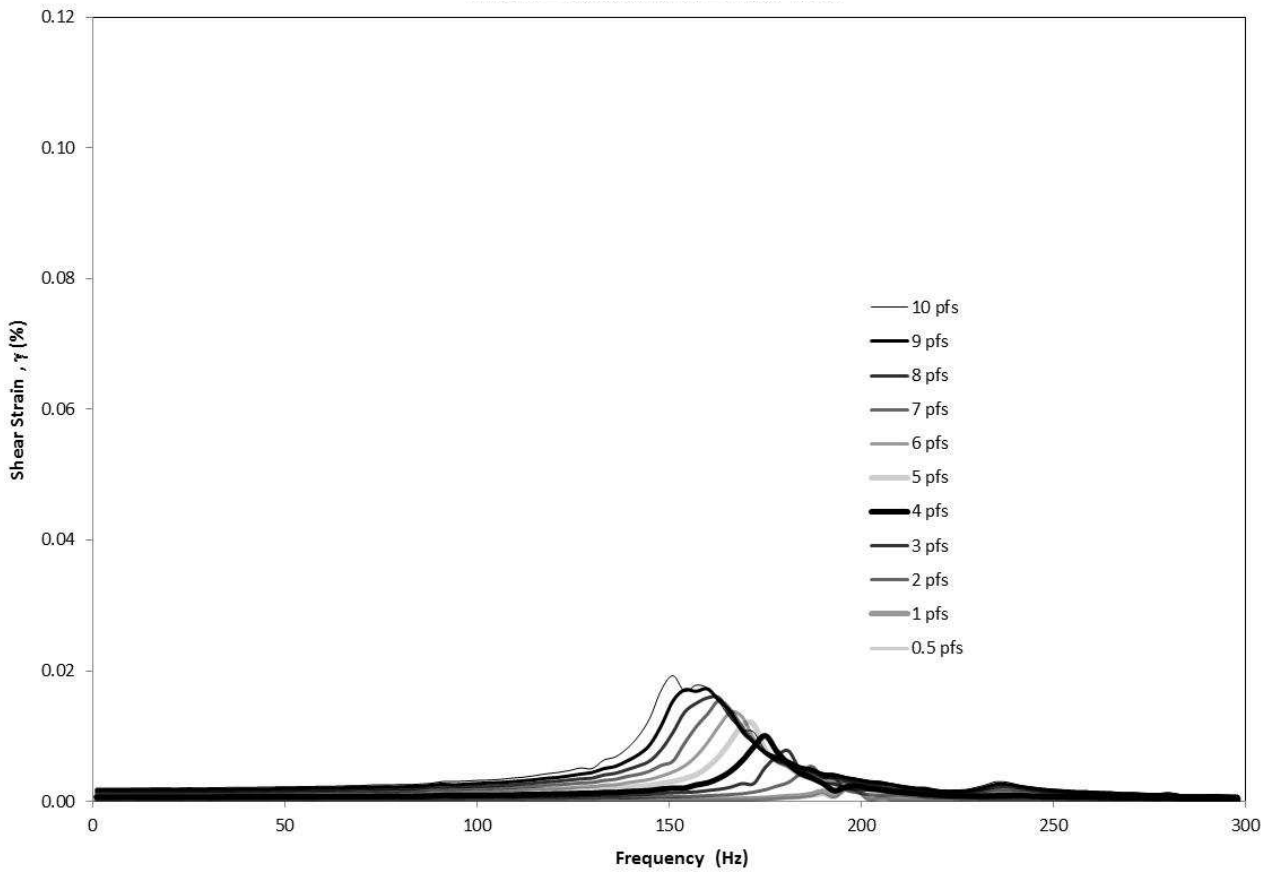

Figure 4-52 Frequency response curves, p - u_a = 100 kPa, u_a – u_w = 100 kPa, torque range = 0.5 pfs -10 pfs

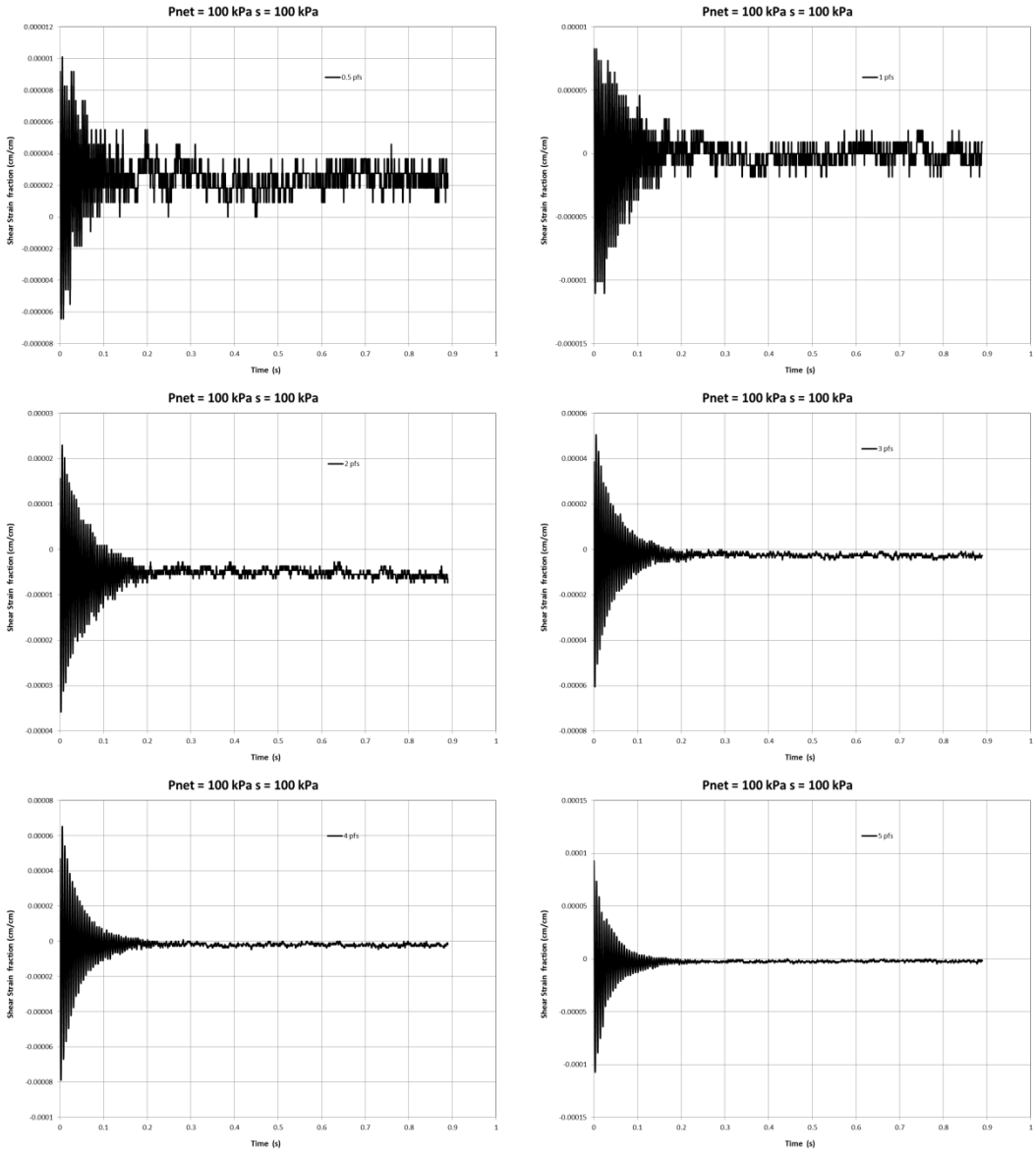

Figure 4-53 Free-vibration decay curves, p - u_a = 100 kPa, u_a – u_w = 100 kPa, torque range = 0.5 pfs - 5 pfs

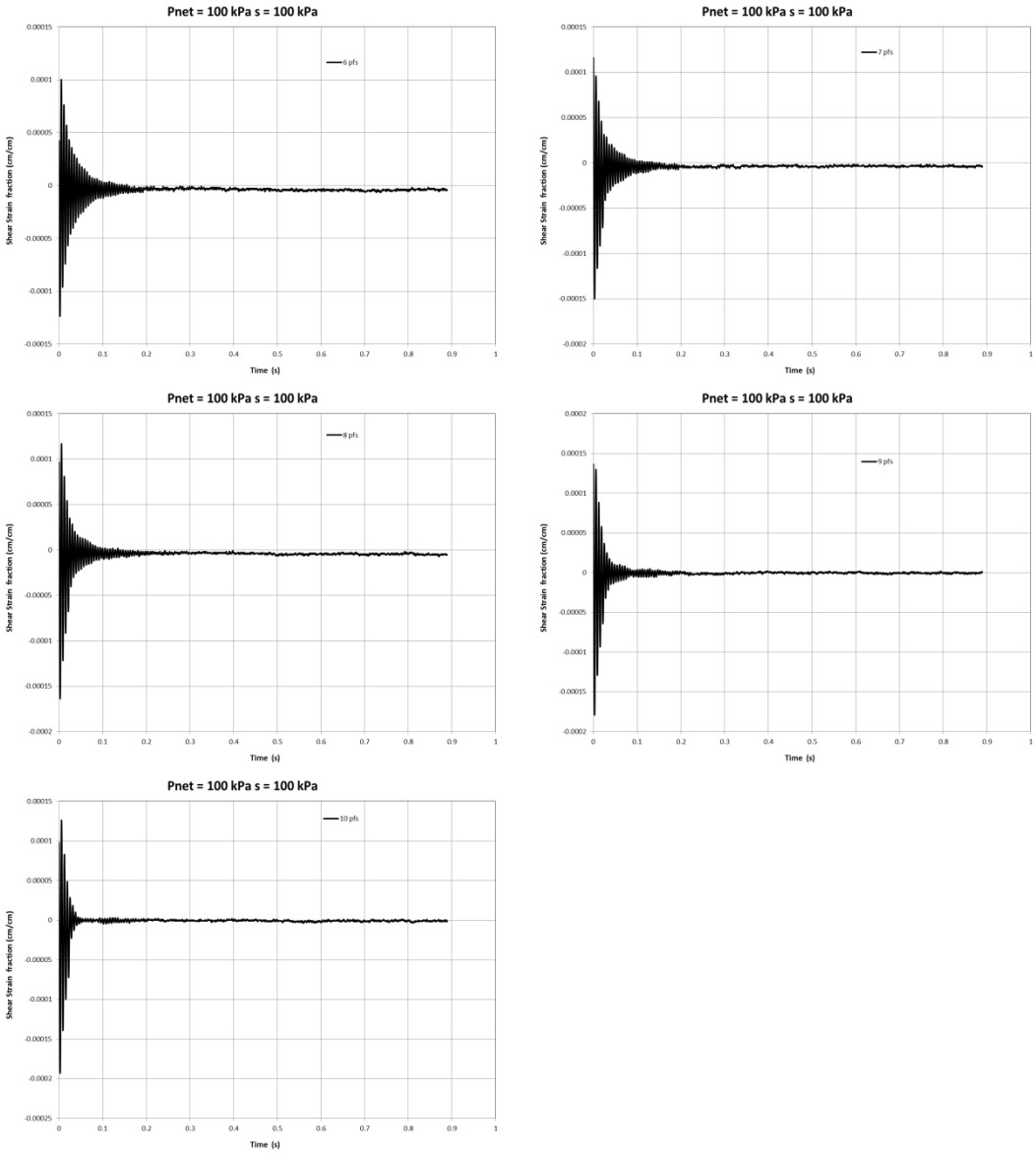

Figure 4-54 Free-vibration decay curves, p - u_a = 100 kPa, u_a – u_w = 100 kPa, torque range = 6 pfs - 10 pfs

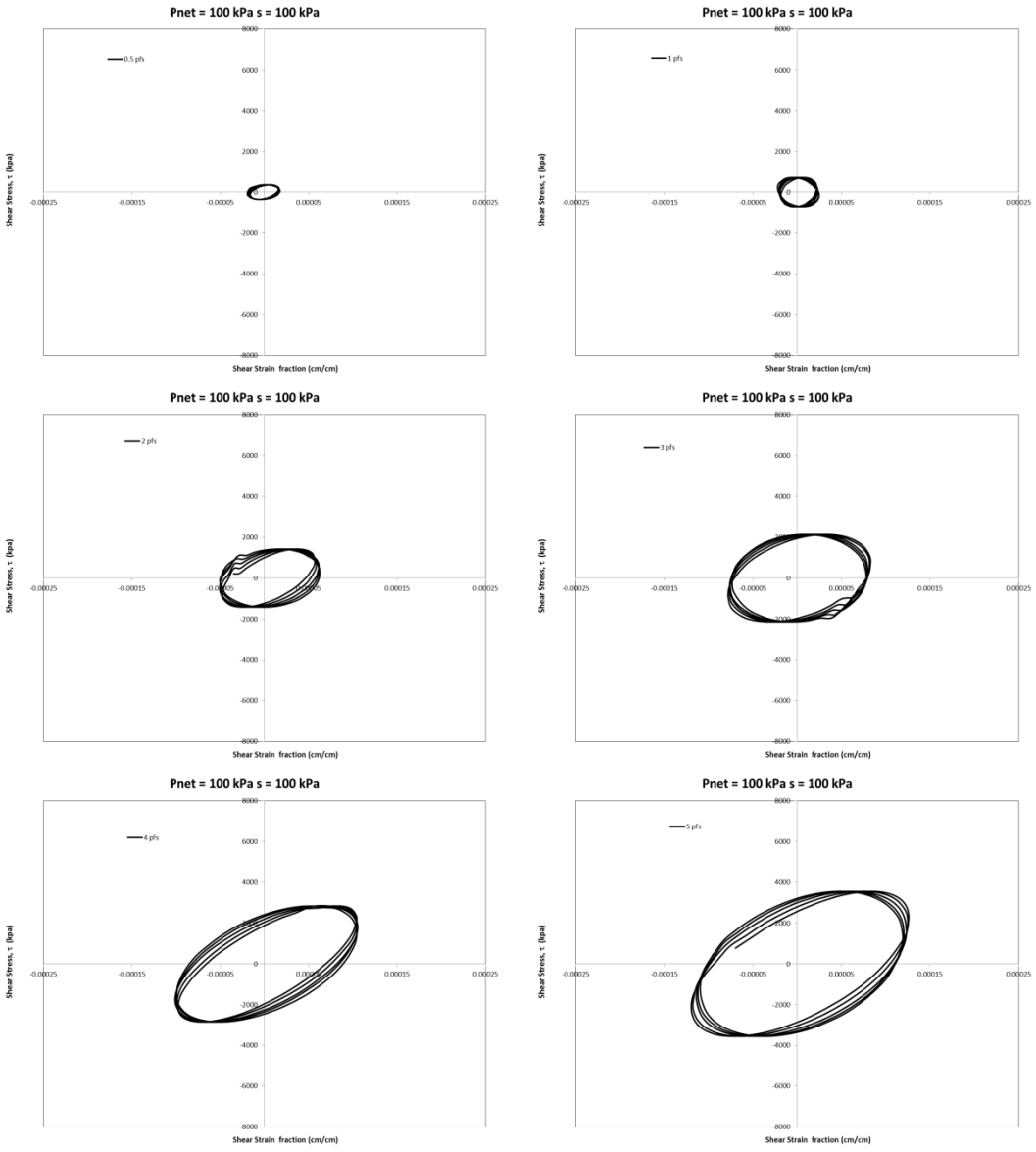

Figure 4-55 Hysteretic loop curves, p - u_a = 100 kPa, u_a – u_w = 100 kPa, torque range = 0.5 pfs - 5 pfs

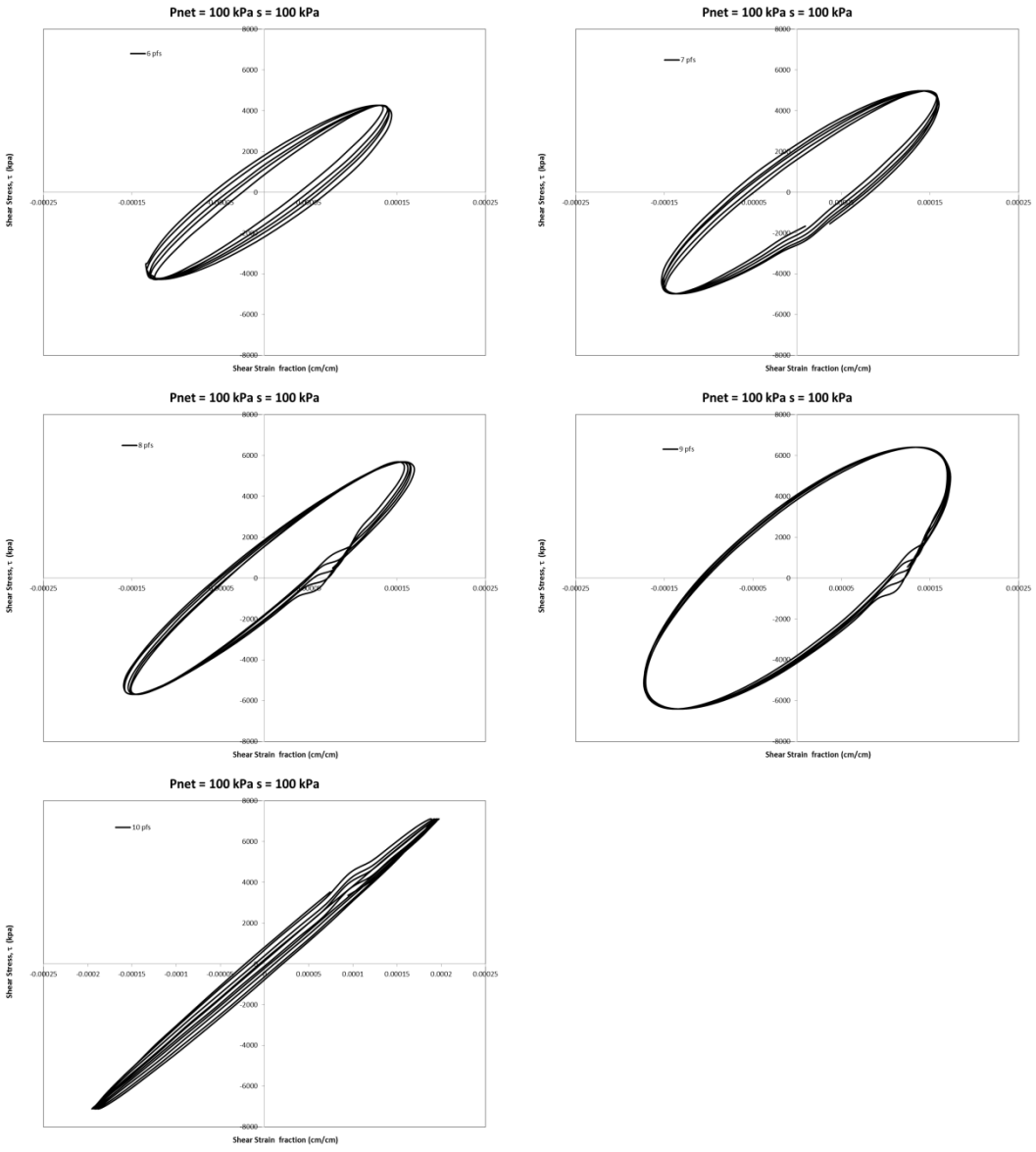

Figure 4-56 Hysteretic loop curves, p - u_a = 100 kPa, u_a – u_w = 100 kPa, torque range = 6 pfs - 10 pfs

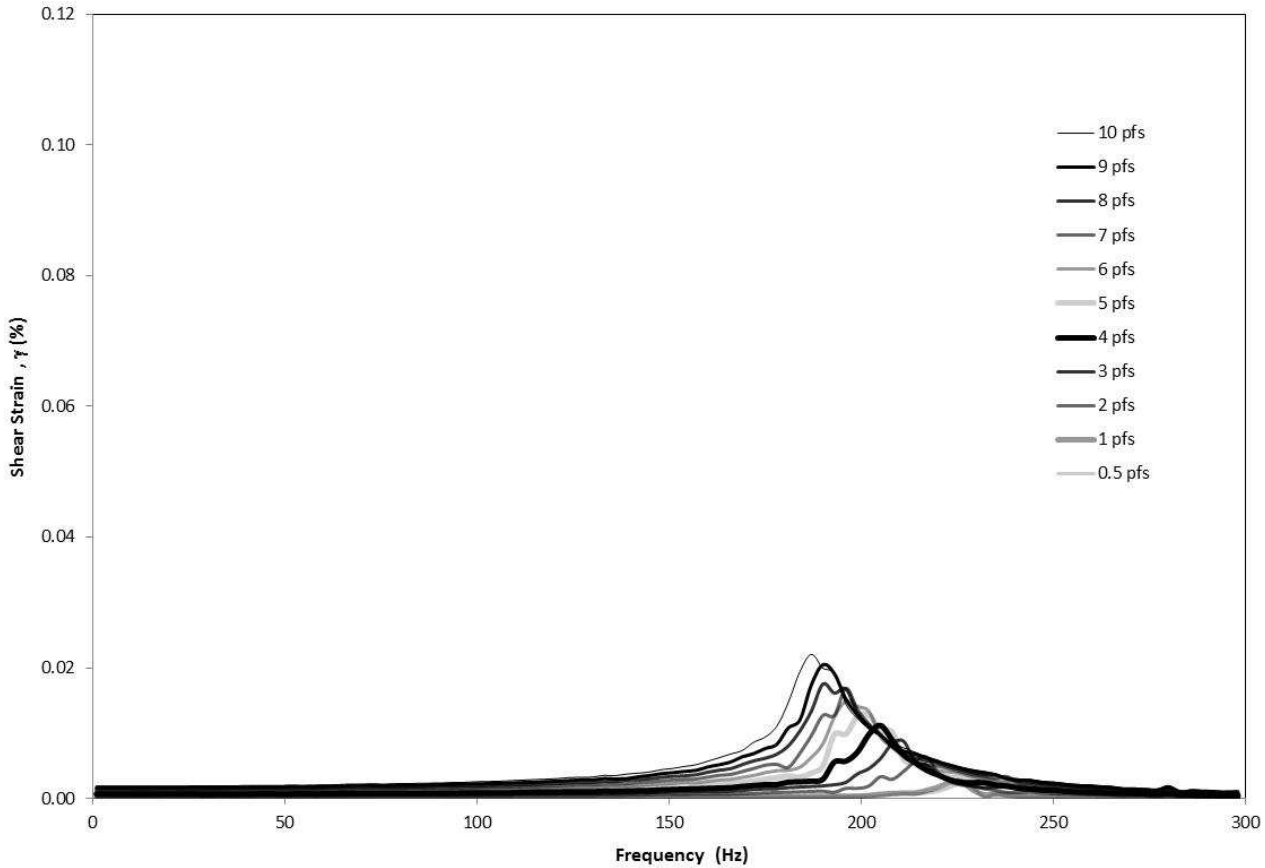

Figure 4-57 Frequency response curves, p - u_a = 200 kPa, u_a – u_w = 100 kPa, torque range = 0.5 pfs -10 pfs

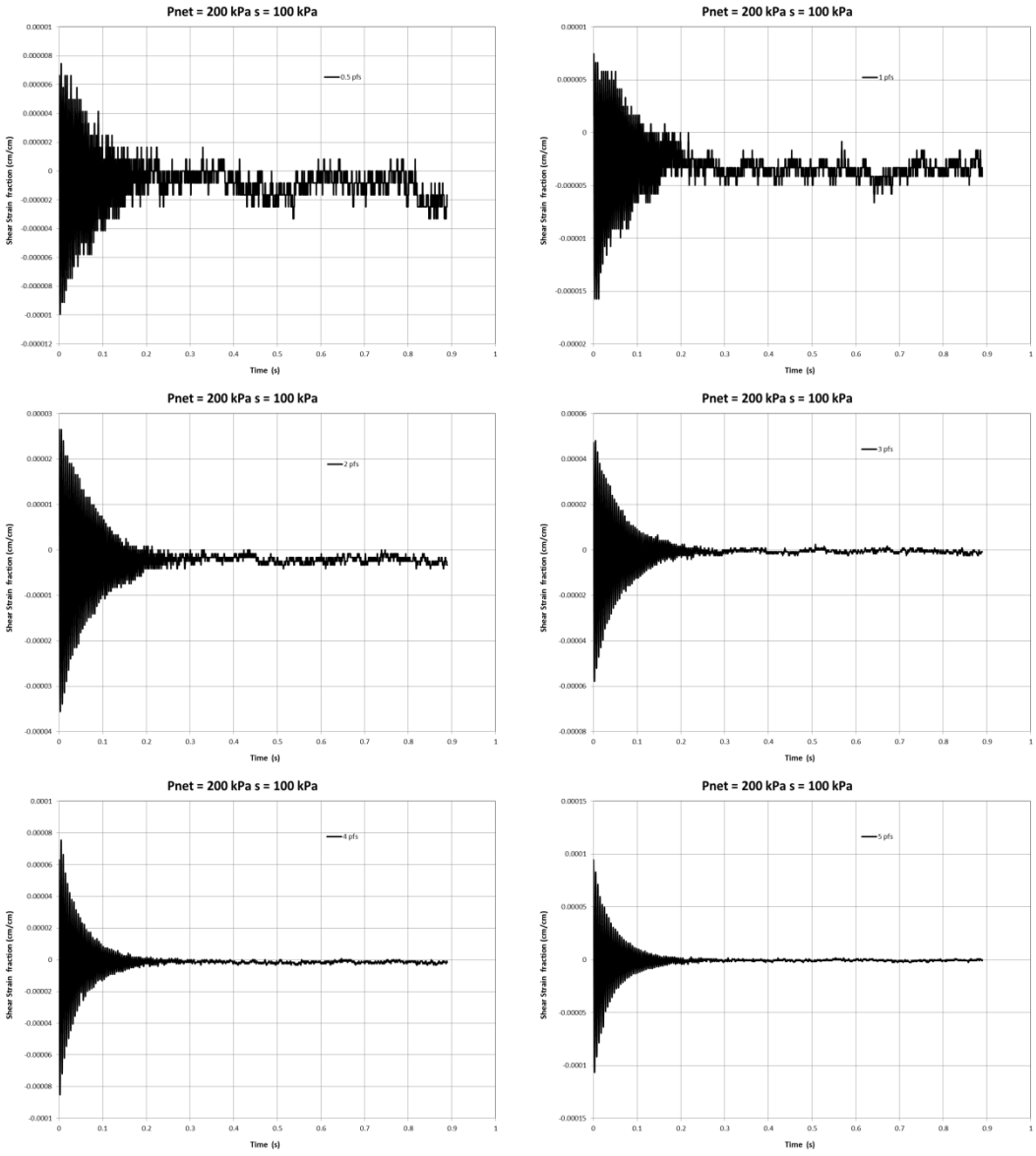

Figure 4-58 Free-vibration decay curves, p - u_a = 200 kPa, u_a – u_w = 100 kPa, torque range = 0.5 pfs - 5 pfs

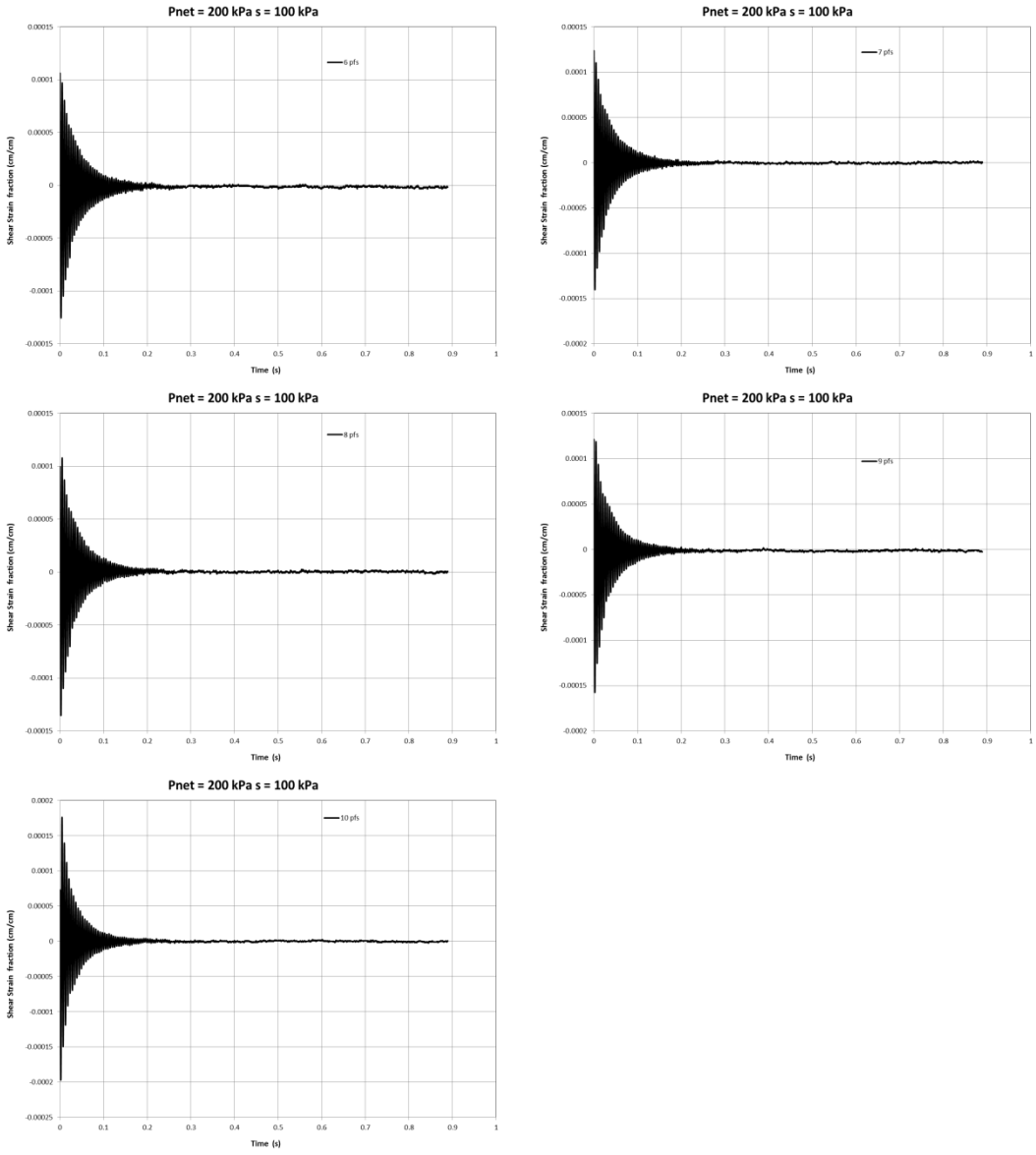

Figure 4-59 Free-vibration decay curves, p - u_a = 200 kPa, u_a – u_w = 100 kPa, torque range = 6 pfs - 10 pfs

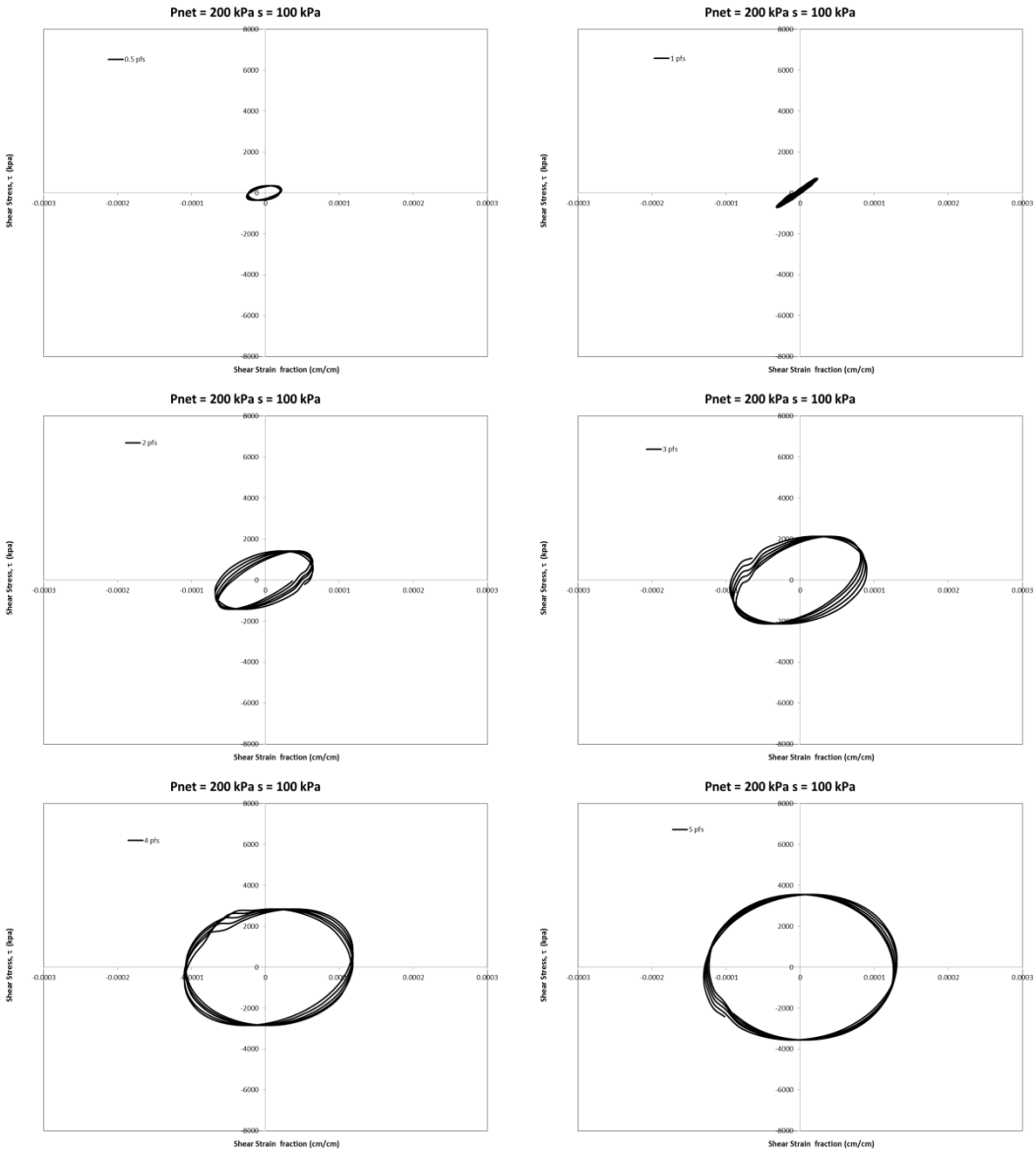

Figure 4-60 Hysteretic loop curves, p - u_a = 200 kPa, u_a – u_w = 100 kPa, torque range = 0.5 pfs - 5 pfs

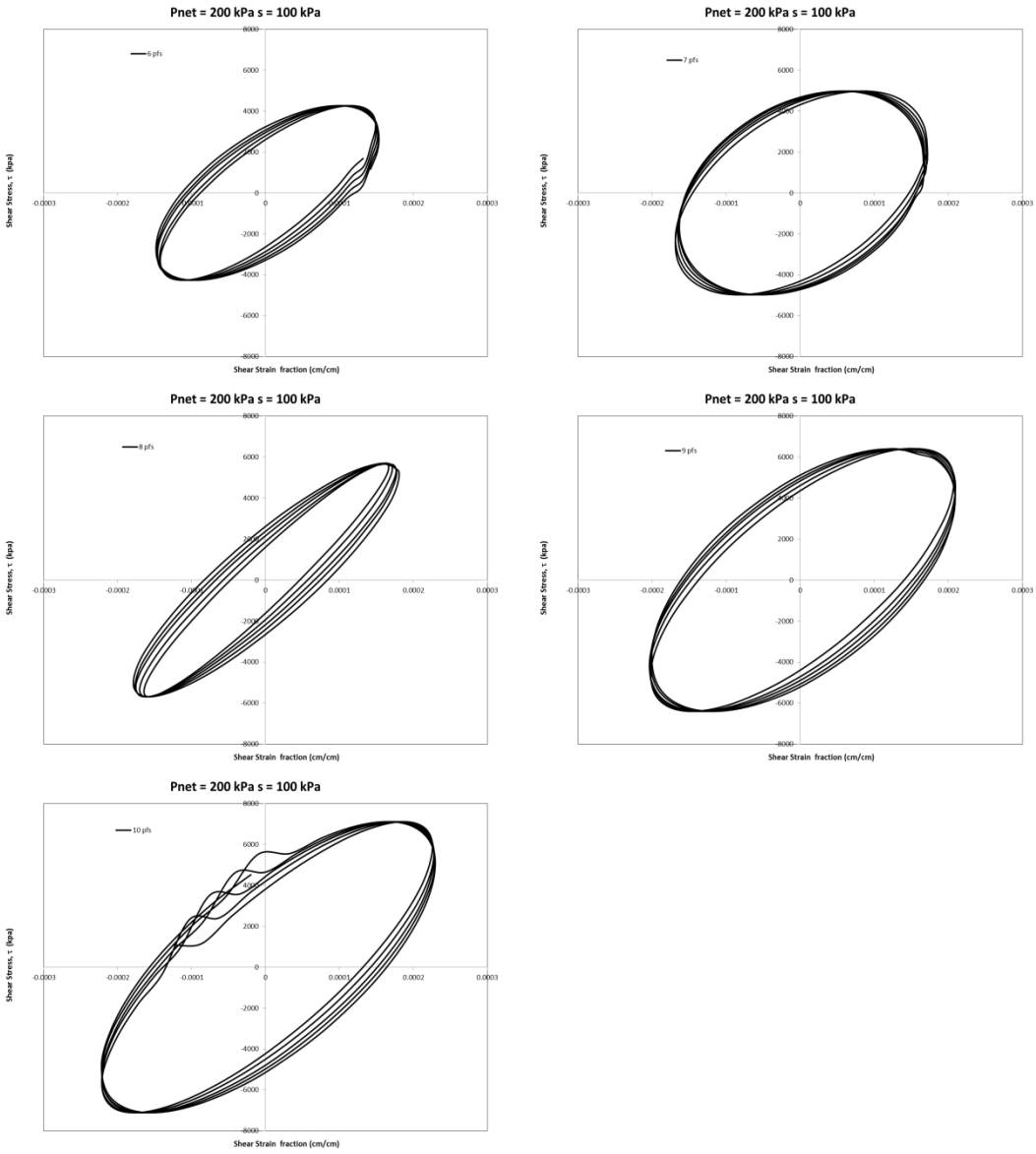

Figure 4-61 Hysteretic loop curves, p - u_a = 200 kPa, u_a – u_w = 100 kPa, torque range = 6 pfs - 10 pfs

.

4.4.4 Resonant Column Tests Performed under Constant Matric Suction, s = 200 kPa

This section presents all the frequency response curves, free-vibration decay curves and cyclic hysteretic loop curves from RC tests conducted at net confining pressures, $(p\text{-}u_a)$ = 25 and 200 kPa, respectively, under a constant matric suction, s = 200 kPa.

It can be observed that there is an increment on the resonant frequency when the net mean stress or confinement pressure is increased. This fact ensures an increase on the shear modulus with any increment on the net mean stress, since, in shear modulus calculations, the frequency at resonance is directly proportional to shear modulus. This can be attributed to a direct increase in the total stress in the sample while the matric suction is kept constant, thereby causing closer contact between soil particles (higher packing) and stiffer material.

Also, it can be observed that the frequency at resonance undergoes decrement when the cyclic torque is increased. A well-defined curved tendency on the resonant frequency can be obtained with increasing input torque. This condition can be attributed to the initial yield loci being exceeded, what brings the soil sample into the elasto-plastic behavior.

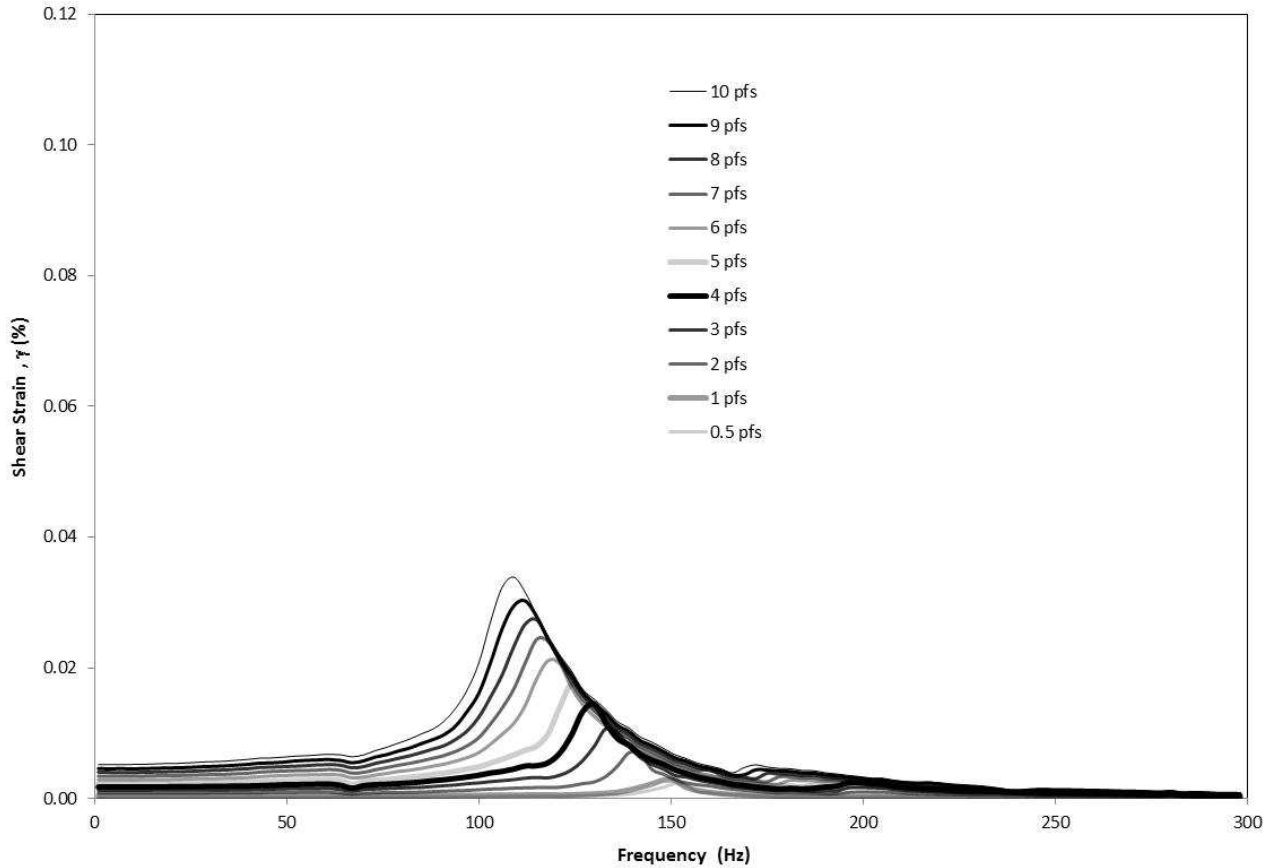

Figure 4-62 Frequency response curves, p - u_a = 25 kPa, u_a – u_w = 200 kPa, torque range = 0.5 pfs -10 pfs

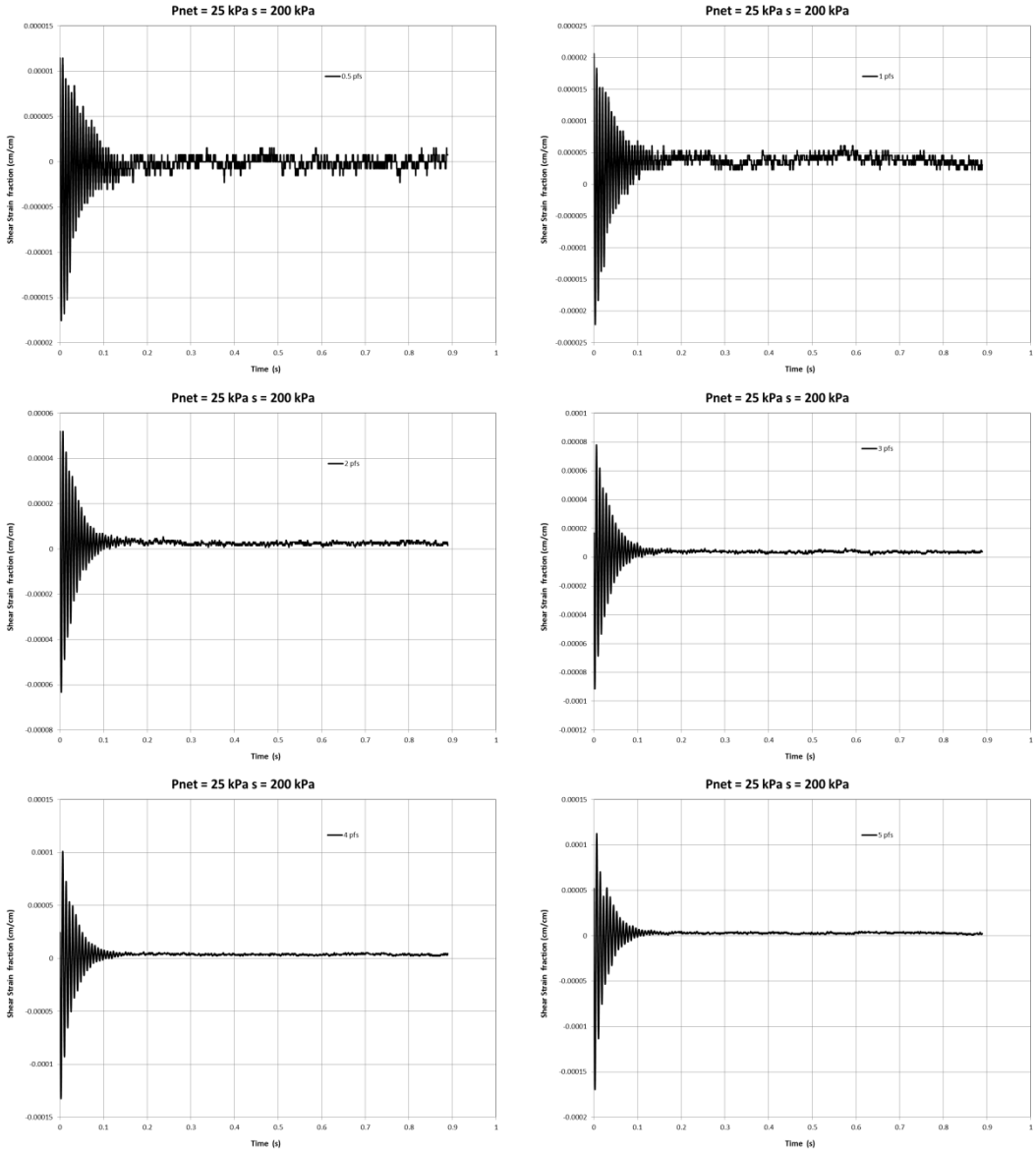

Figure 4-63 Free-vibration decay curves, p - u_a = 25 kPa, u_a – u_w = 200 kPa, torque range = 0.5 pfs - 5 pfs

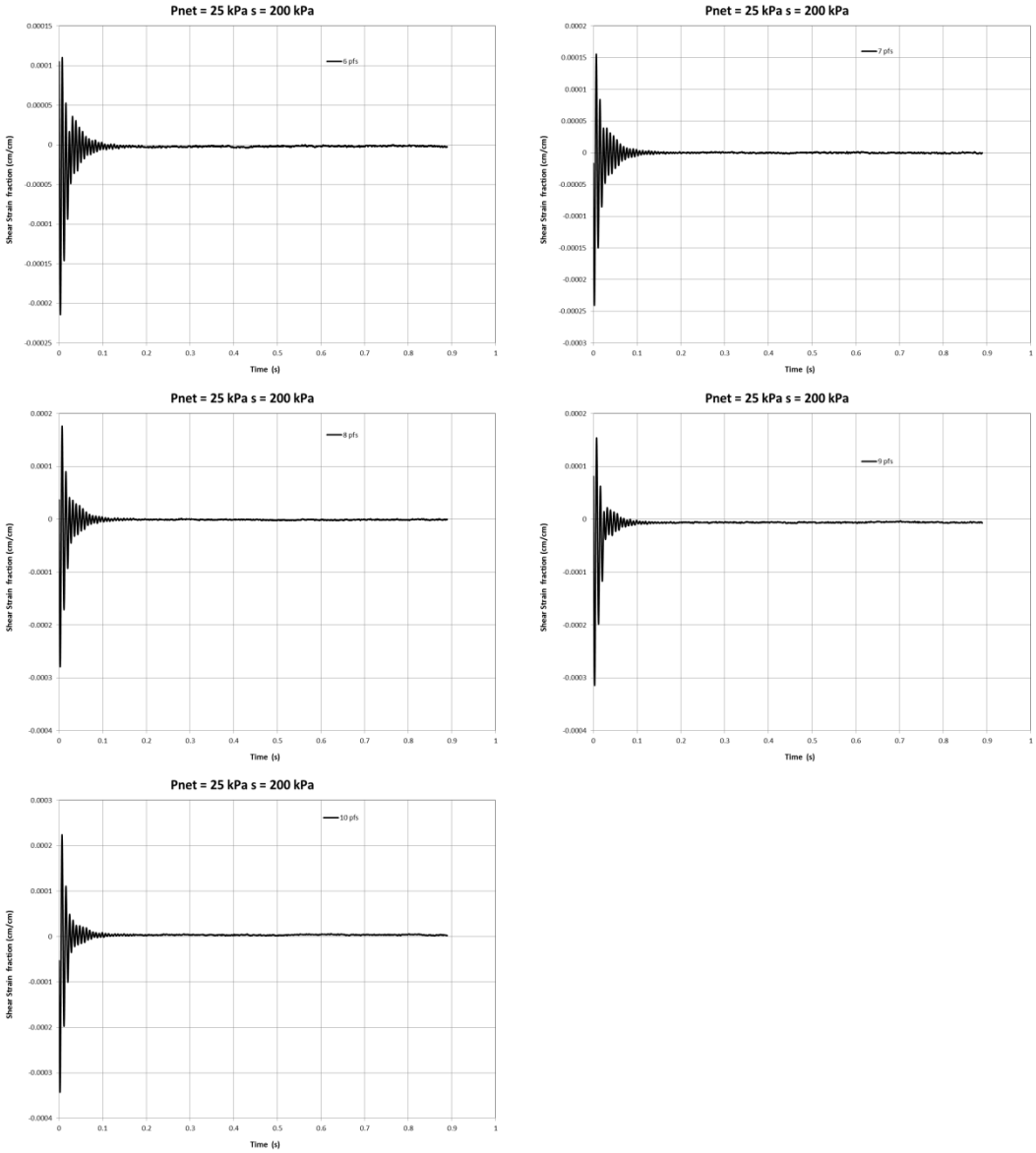

Figure 4-64 Free-vibration decay curves, p - u_a = 25 kPa, u_a – u_w = 200 kPa, torque range = 6 pfs - 10 pfs

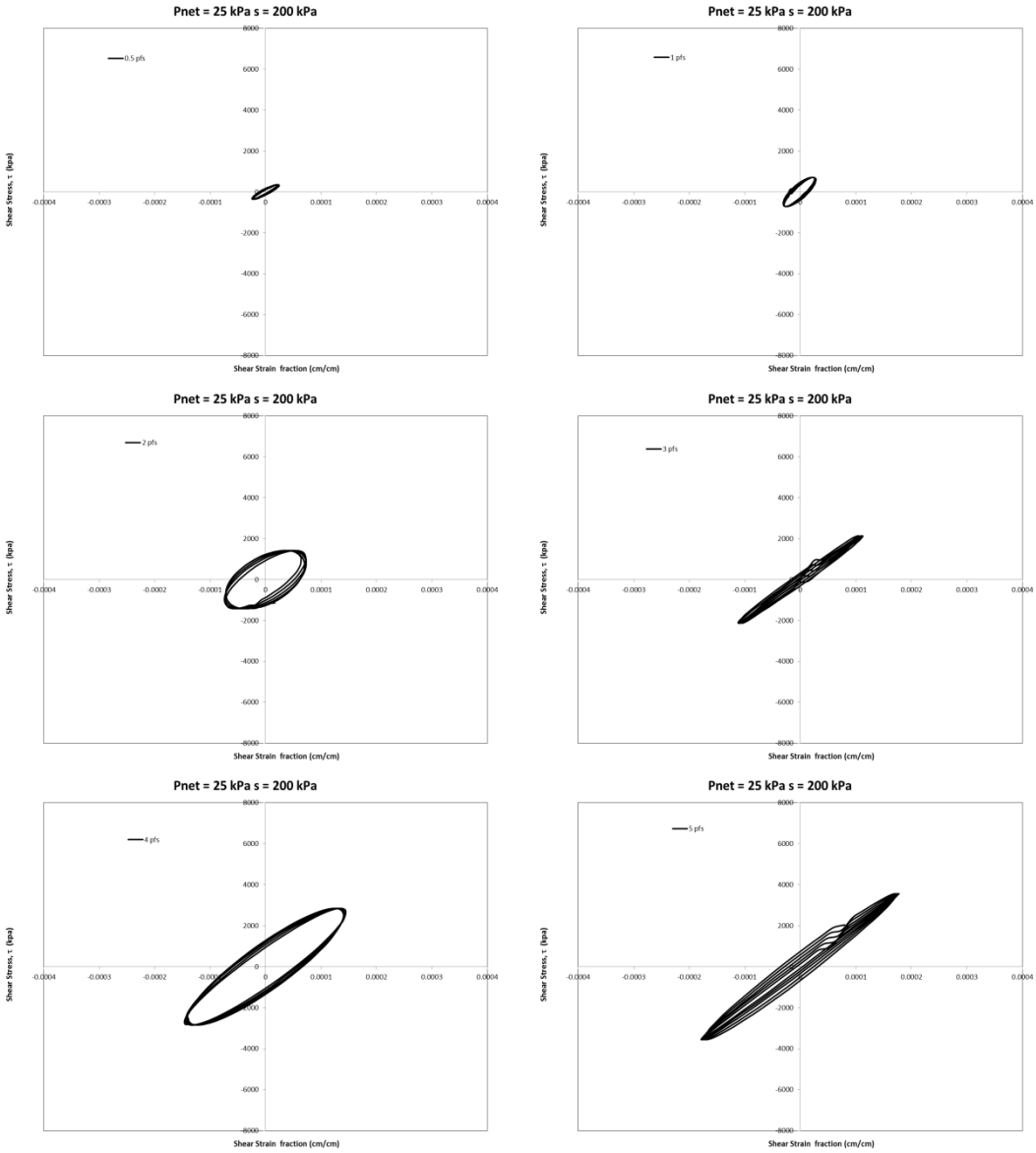

Figure 4-65 Hysteretic loop curves, p - u_a = 25 kPa, u_a – u_w = 200 kPa, torque range = 0.5 pfs - 5 pfs

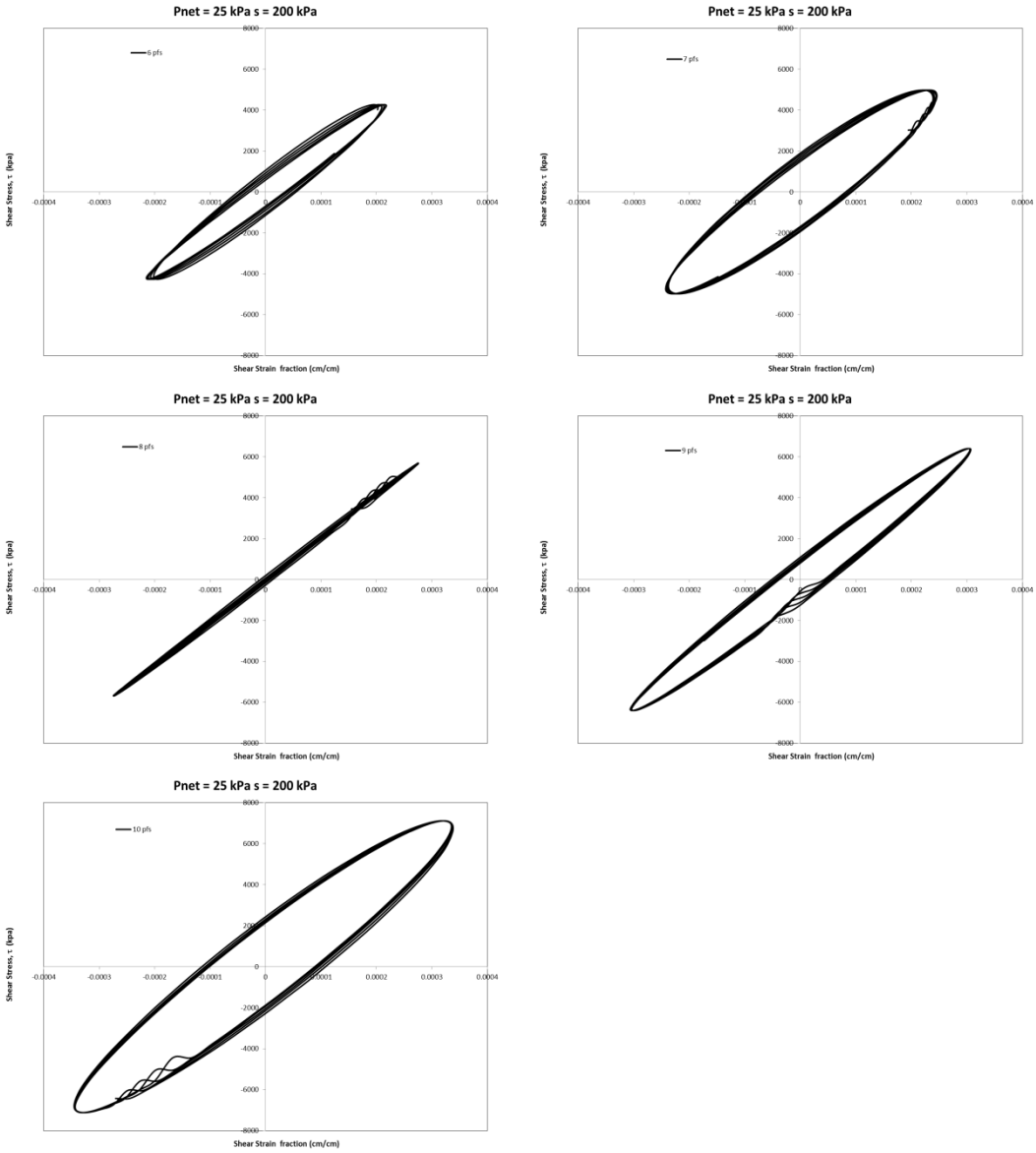

Figure 4-66 Hysteretic loop curves, p - u_a = 25 kPa, u_a – u_w = 200 kPa, torque range = 6 pfs - 10 pfs

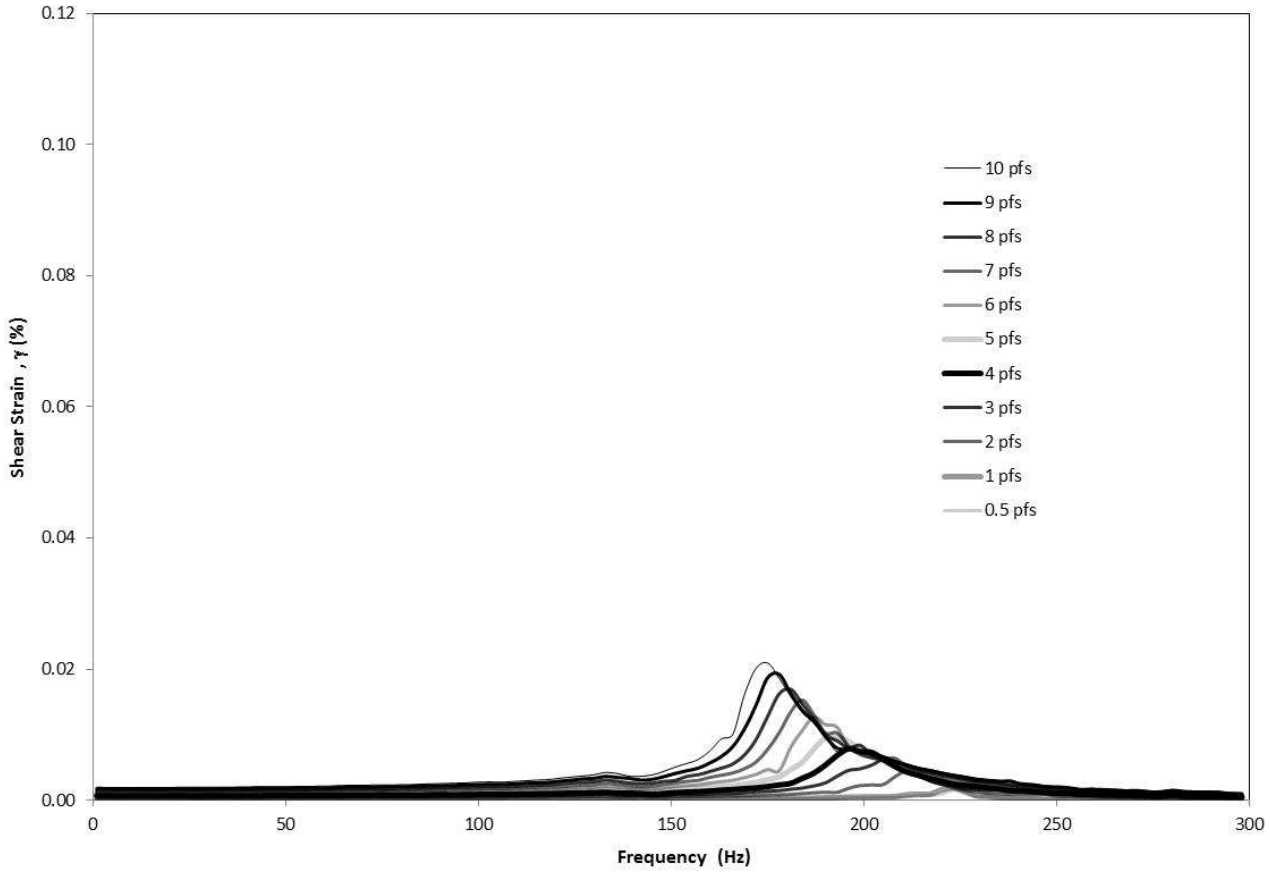

Figure 4-67 Frequency response curves, p - u_a = 100 kPa, u_a – u_w = 200 kPa, torque range = 0.5 pfs -10 pfs

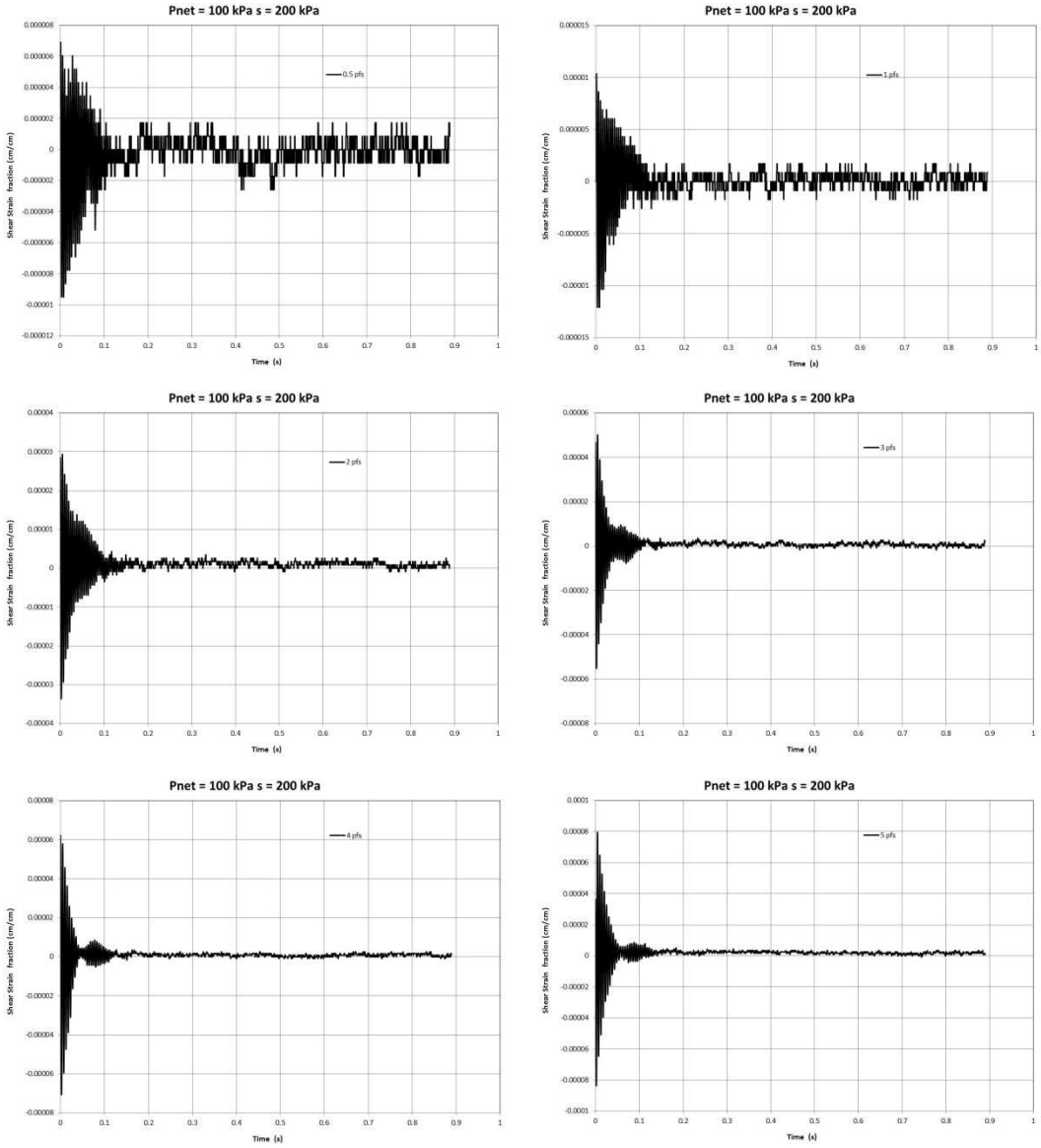

Figure 4-68 Free-vibration decay curves, p - u_a = 100 kPa, u_a – u_w = 200 kPa, torque range = 0.5 pfs - 5 pfs

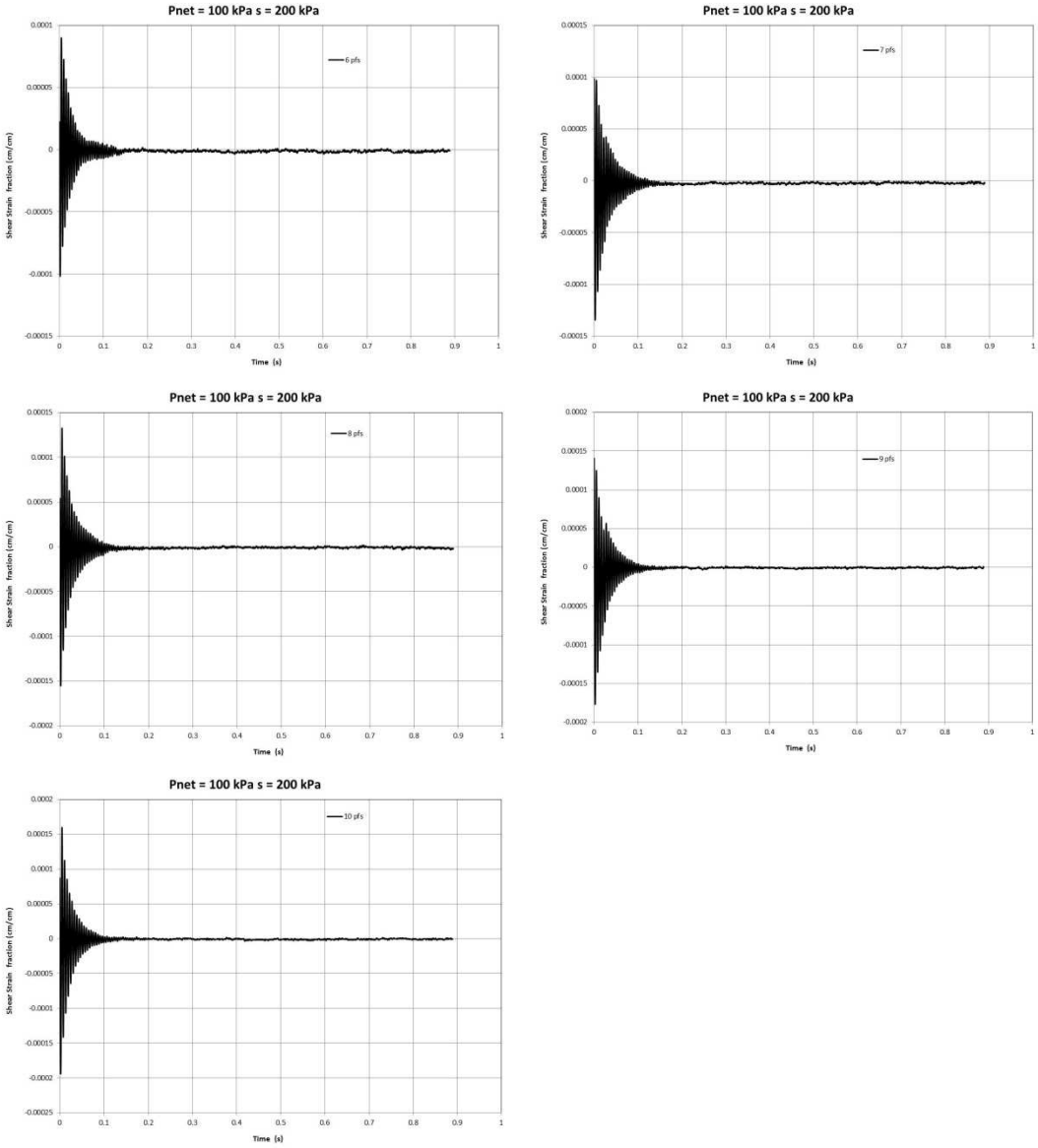

Figure 4-69 Free-vibration decay curves, p - u_a = 100 kPa, u_a – u_w = 200 kPa, torque range = 6 pfs - 10 pfs

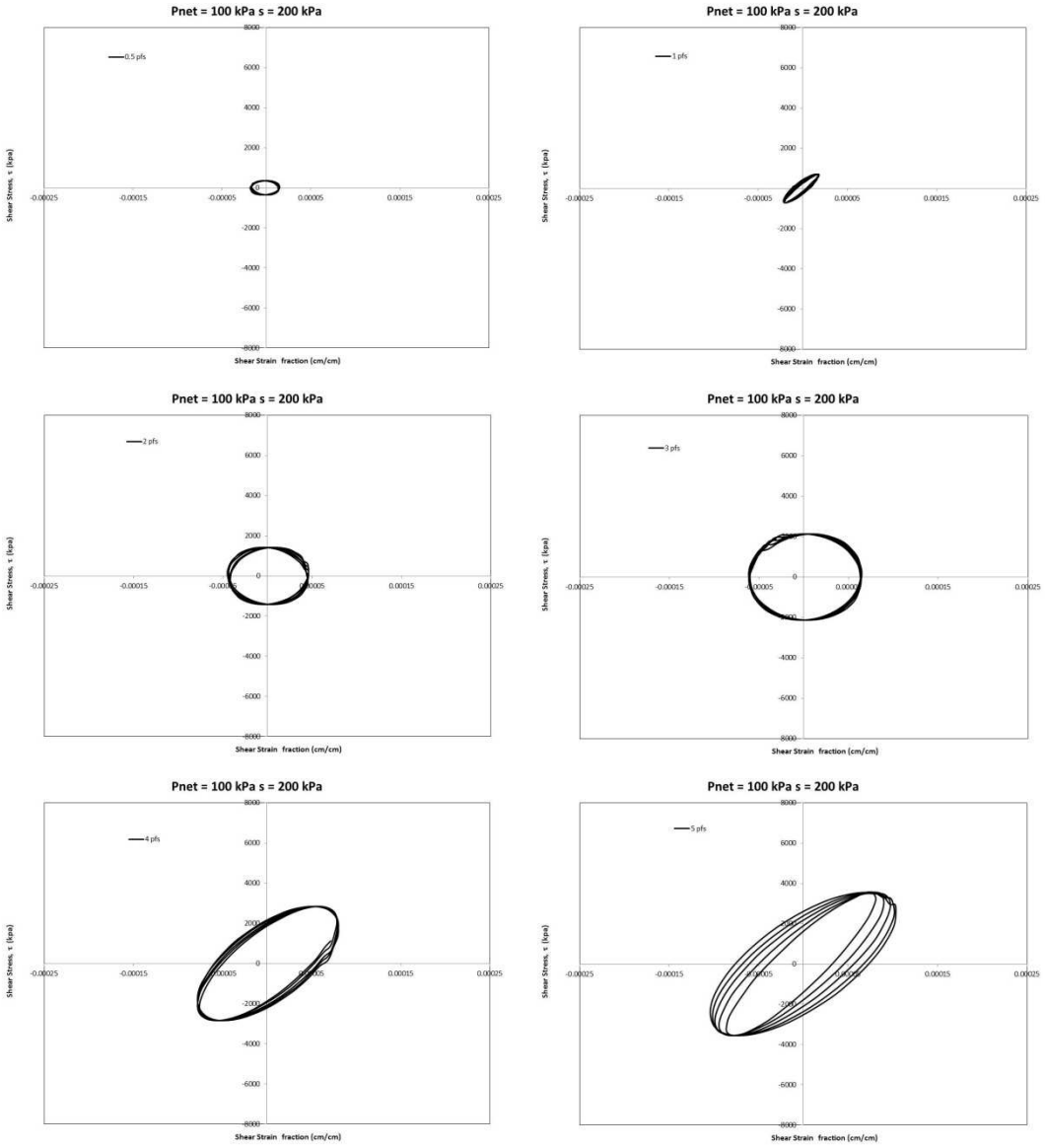

Figure 4-70 Hysteretic loop curves, p - u_a = 100 kPa, u_a – u_w = 200 kPa, torque range = 0.5 pfs - 5 pfs

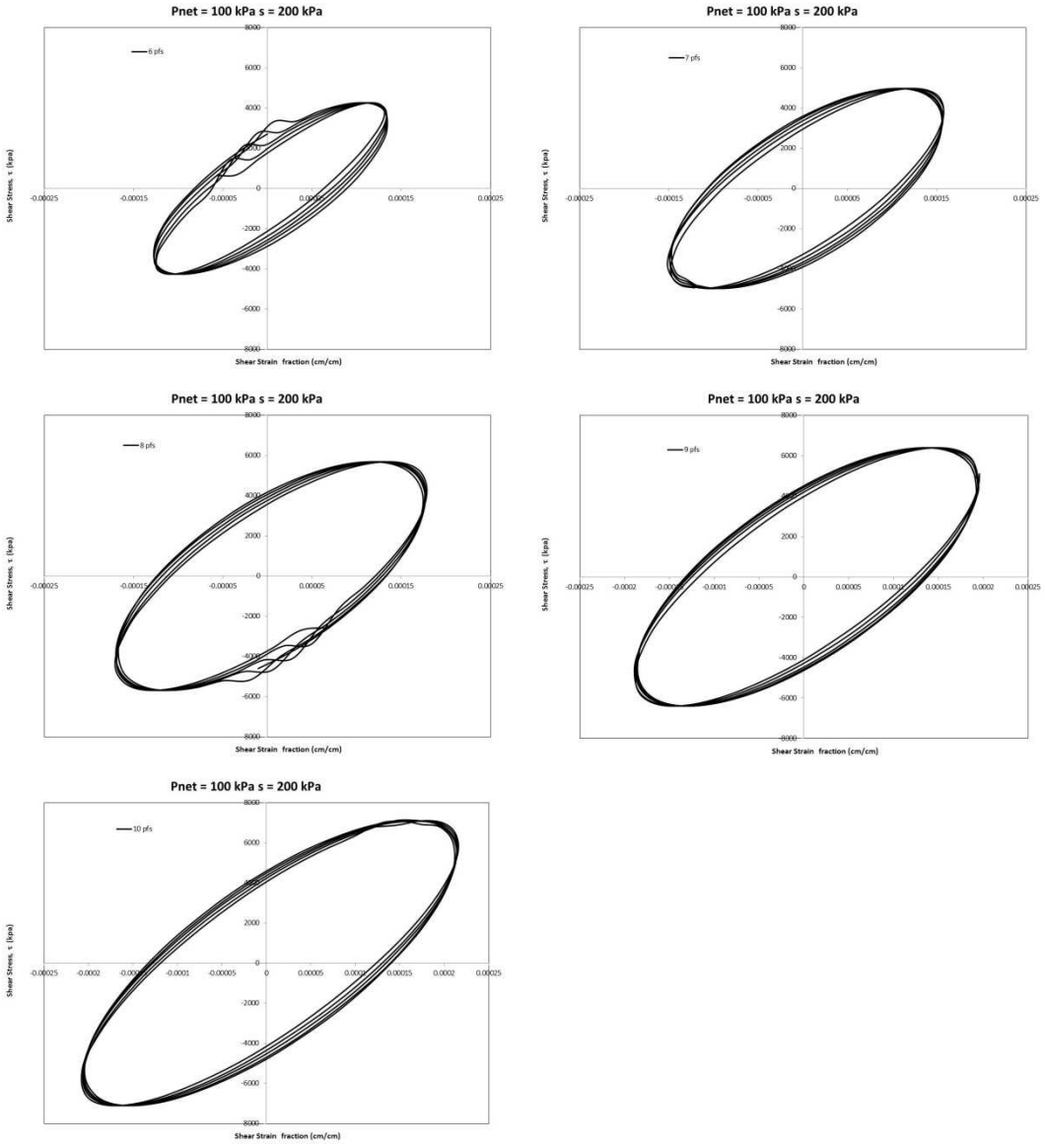

Figure 4-71 Hysteretic loop curves, p - u_a = 100 kPa, u_a – u_w = 200 kPa, torque range = 6 pfs - 10 pfs

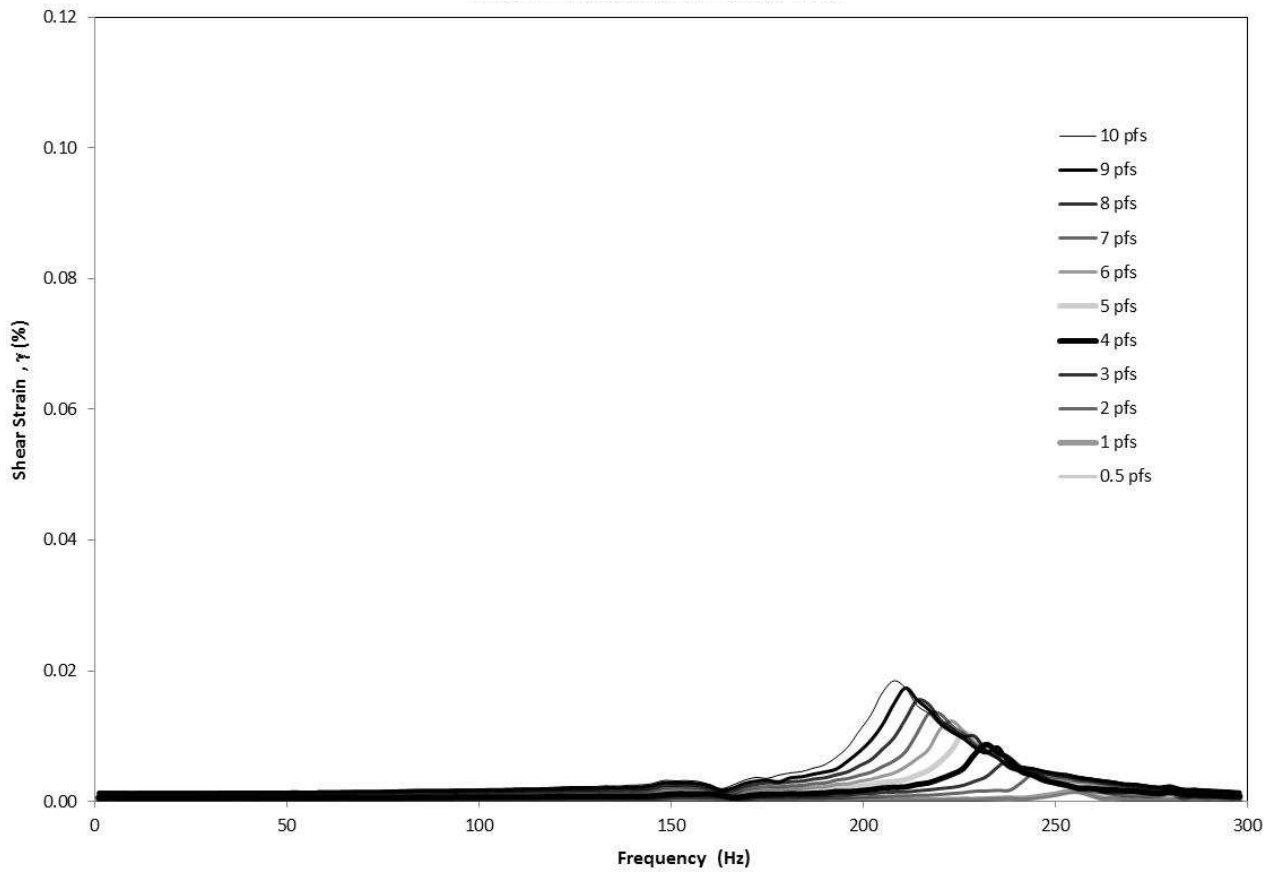

Figure 4-72 Frequency response curves, p - u_a = 200 kPa, u_a – u_w = 200 kPa, torque range = 0.5 pfs -10 pfs

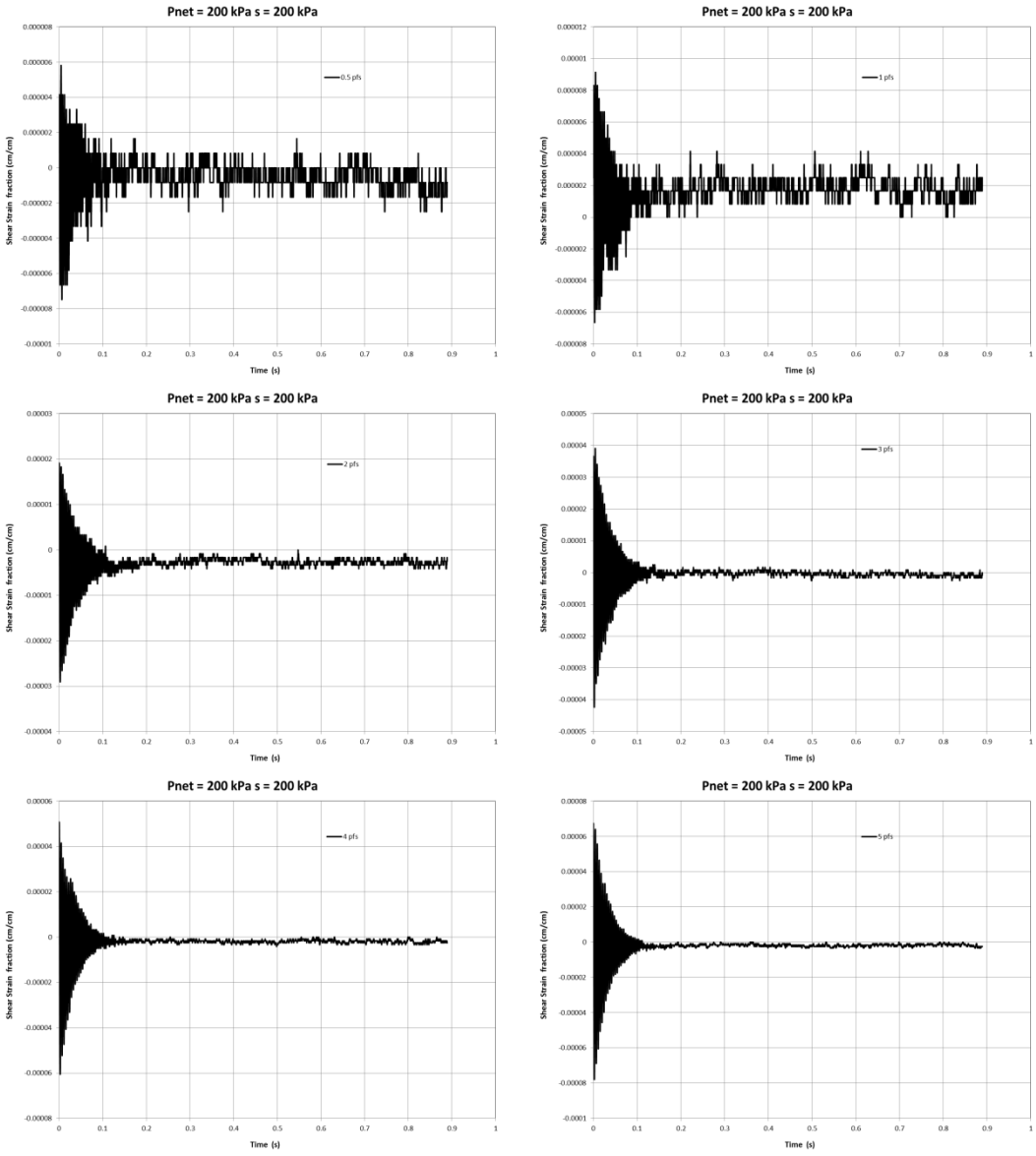

Figure 4-73 Free-vibration decay curves, p - u_a = 200 kPa, u_a – u_w = 200 kPa, torque range = 0.5 pfs - 5 pfs

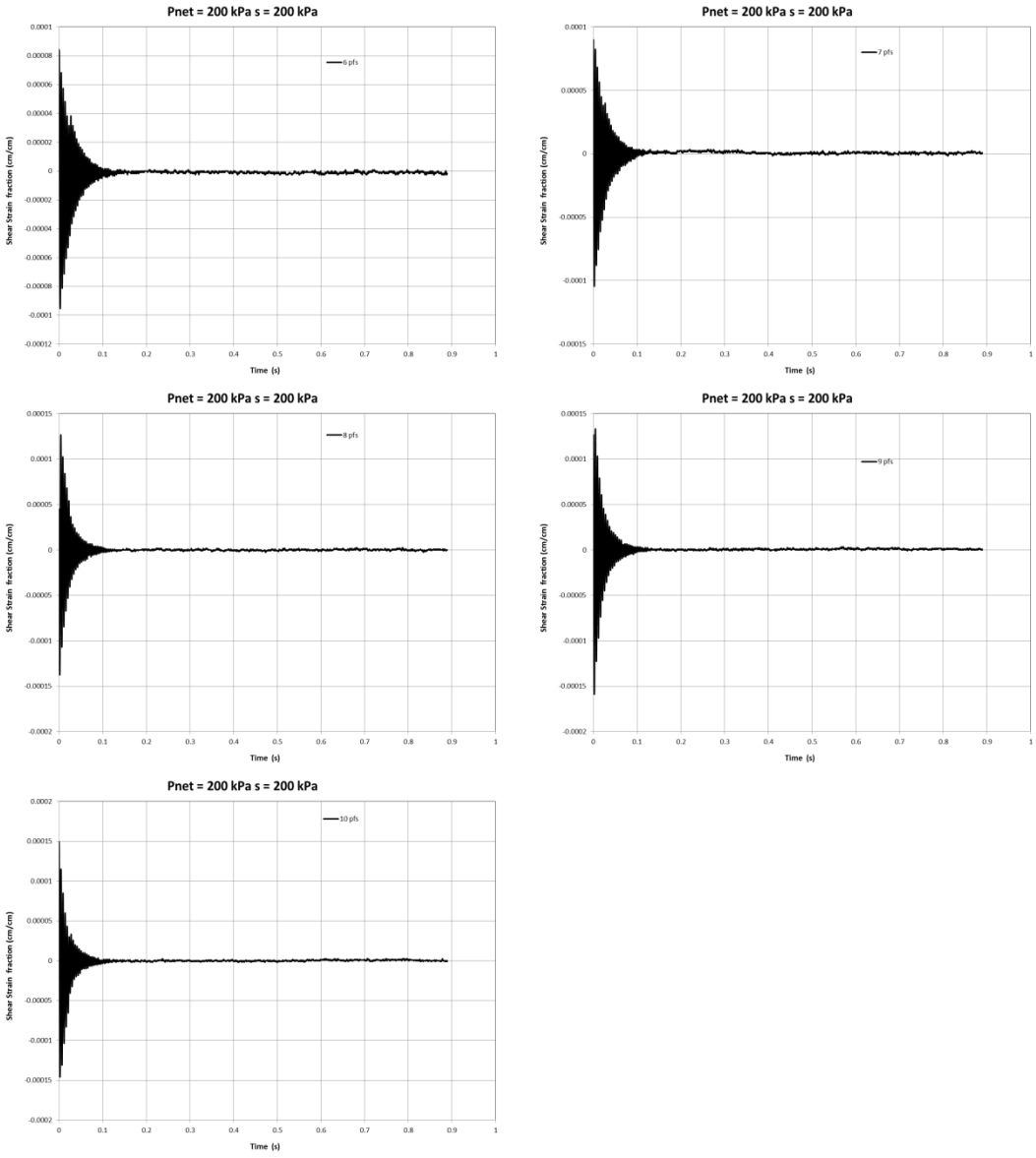

Figure 4-74 Free-vibration decay curves, p - u_a = 200 kPa, u_a – u_w = 200 kPa, torque range = 6 pfs - 10 pfs

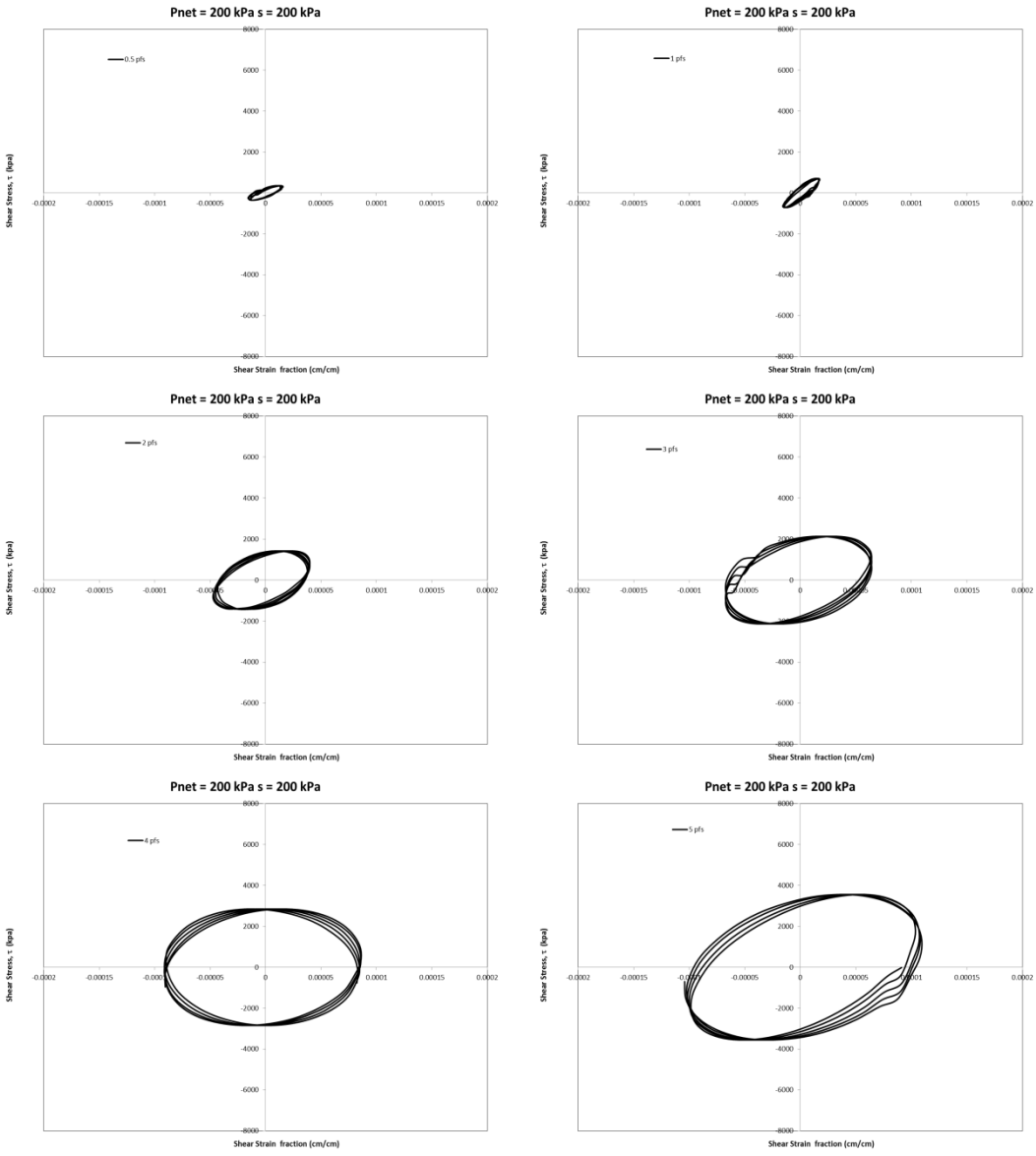

Figure 4-75 Hysteretic loop curves, p - u_a = 200 kPa, u_a – u_w = 200 kPa, torque range = 0.5 pfs - 5 pfs

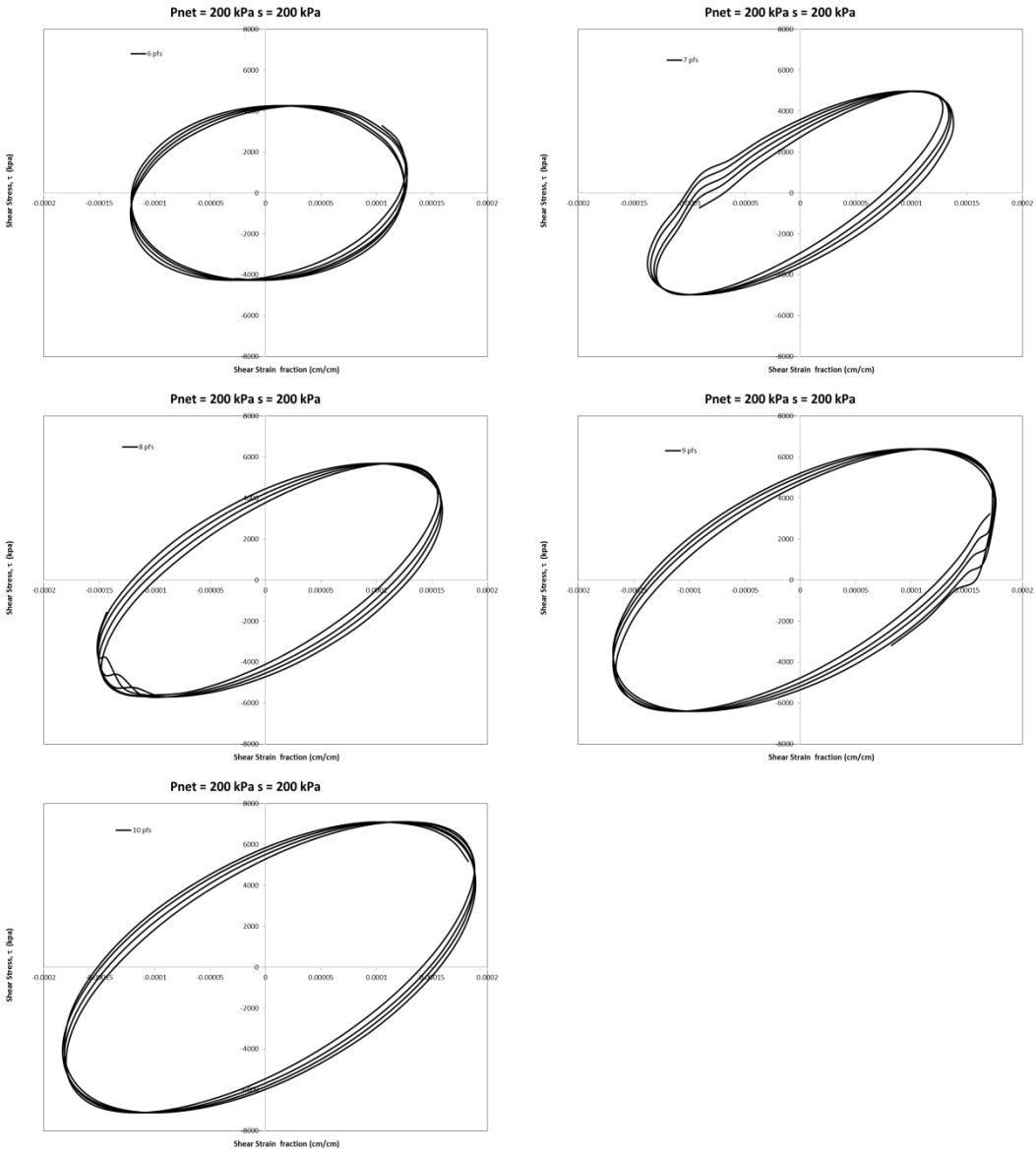

Figure 4-76 Hysteretic loop curves, p - u_a = 200 kPa, u_a – u_w = 200 kPa, torque range = 6 pfs - 10 pfs

Next chapter presents a comparative analysis of all test results from the Experimental Program in order to assess the effect of suction/net mean stress states on shear strain stiffness properties of unsaturated soils.

Chapter 5

Comparative Analysis of Test Results

In engineering problems relating to the propagation of seismic waves through soil, two of the most important parameters required for dynamic analyses are the soil or rock stiffness and material damping. The shear modulus, G, and material damping ratio, D, are used to determine the amplitude and attenuation of stress waves as they travel through the geologic formations. Also, most soils are not in a totally dry or saturated state since there is a region immediately above the water table that is in an unsaturated state mostly due to seasonally fluctuations on water table.

Therefore, if partially saturated ground conditions are considered, it is possible to obtain a more realistic idealization of the soil behavior when subjected to the horizontal shear component of earthquake shaking. This component is the most critical to be considered for building design in seismically active areas since it will induce shear strains in the soil due to mass distortion (Figure 5-1). The occurrence of cyclic distortion generates shear modulus degradation as well as soil damping increasing.

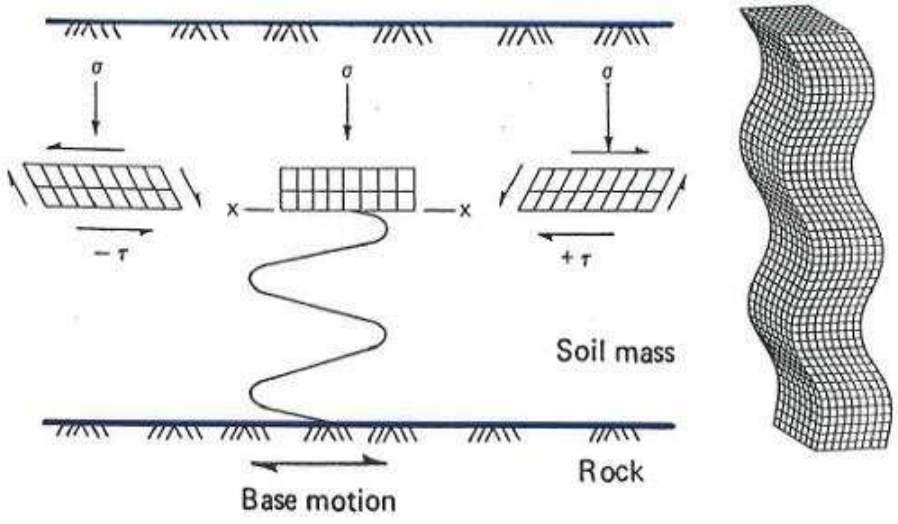

Figure 5-1 Cyclic distortion induced in the soil mass by shear waves

Furthermore, the geology of a site is generally modeled as a series of horizontal layers with varying properties. Thus, the stiffness and attenuation characteristics of any of the identified subsoil layers above water table must be considered in order to adopt a more precise and robust idealization of the dynamic response of a partially saturated soil (Figure 5-2).

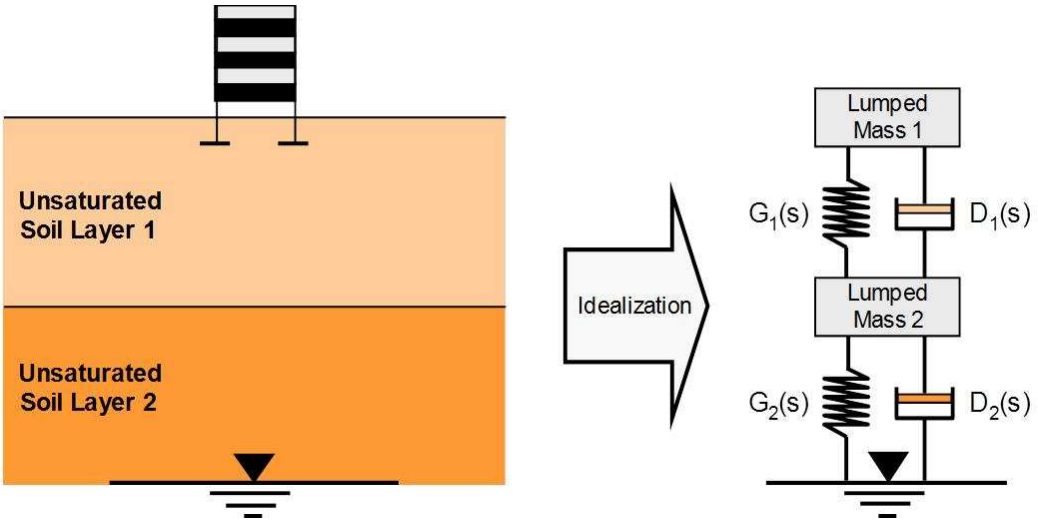

Figure 5-2 Idealization of multi-layered unsaturated soil was deposit for dynamic analysis.

The evaluation of the dynamic response of the SM-SP soil intended to be as broad as possible; hence it was based on a wide range of variables with particular focus on five key aspects: shear modulus, damping ratio, threshold strain, peak strain and modulus and damping degradation.

5.1 Shear Modulus Response

The influence of matric suction and net mean stress on the dynamic response of the tested sandy soil is clearly observed in Figure 5-3, where G_{max} has been plotted as function of net mean stress, on the basis of matric suction, for all specimens tested.

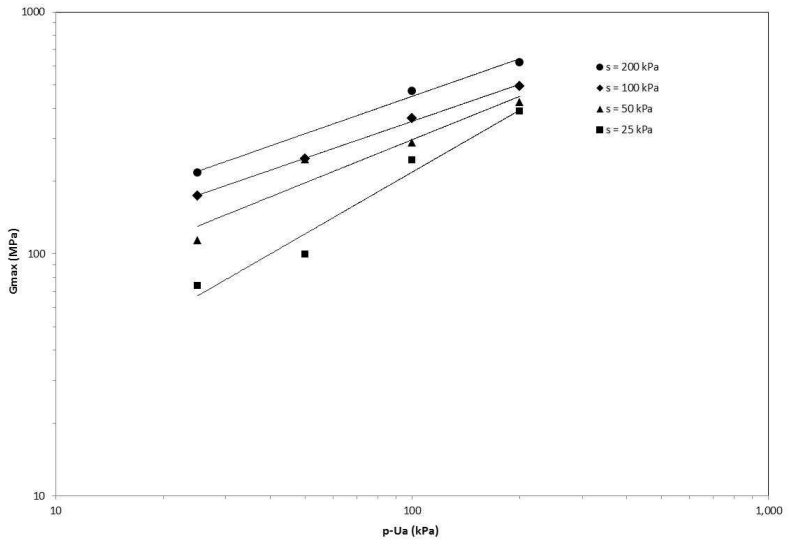

Figure 5-3 G_{max} variation as function of net mean stress

As expected, in all cases G_{max} increases with an increase in net mean stress and suction, with a linear tendency. Solid lines in Figure 5-3 represent best-fit, power regression functions of the form:

$$G_{max} = A(p - u_a)^B \qquad (5.1)$$

In Eq. 5.1 constant A represents G_{max} (MPa) at $p - u_a = 1$ kPa, and constant B is representative of the soil's susceptibility to changes in $p - u_a$. Power regression constants A and B from Eq. 5.1 used in Figure 5-3 are summarized in Table 5-1.

Table 5-1 Values of Best-Fit Power Regression for G_{max}

Suction (kPa)	A	B	r^2
25	41.927	0.5243	0.9935
50	34.158	0.5072	0.9978
100	19.271	0.5257	0.9210
200	4.3656	0.5421	0.9663

The shear modulus increment can be also noticed in the hysteretic loop curves obtained throughout this work and which were presented in the previous chapter. Some

of the most representative ones are shown in Figure 5-4 and Figure 5-5. (Refer to Figure 2-3 for related parameters).

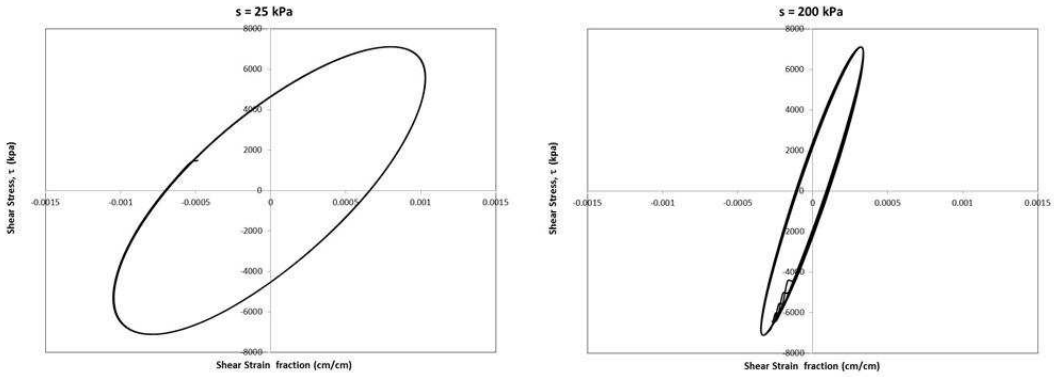

Figure 5-4 Hysteretic loop curves, p - u_a = 25 kPa, u_a – u_w = 25, 200 kPa, torque = 10 pfs

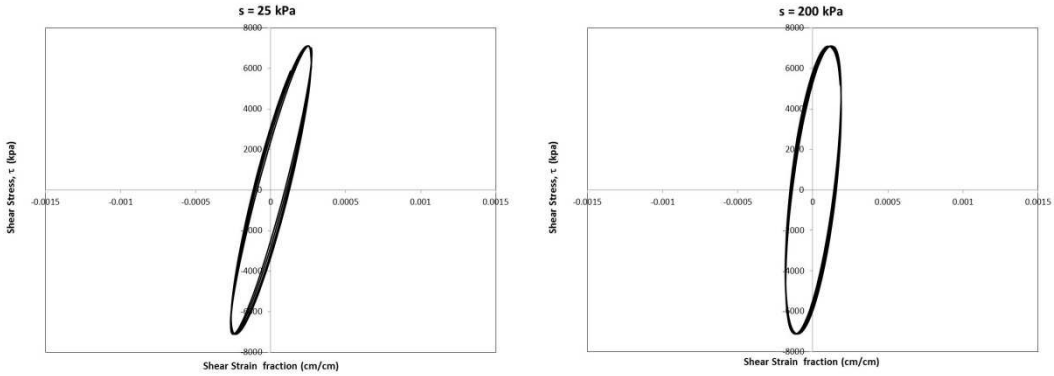

Figure 5-5 Hysteretic loop curves, p - u_a = 200 kPa, u_a – u_w = 25, 200 kPa, torque range = 10 pfs

5.2 Damping Response

The influence of matric suction and net mean stress on the dynamic response of the tested sandy soil is clearly observed in Figure 5-6, where D_{min} based on logarithmic

decay method has been plotted as function of net mean stress, on the basis of matric suction, for all specimens tested.

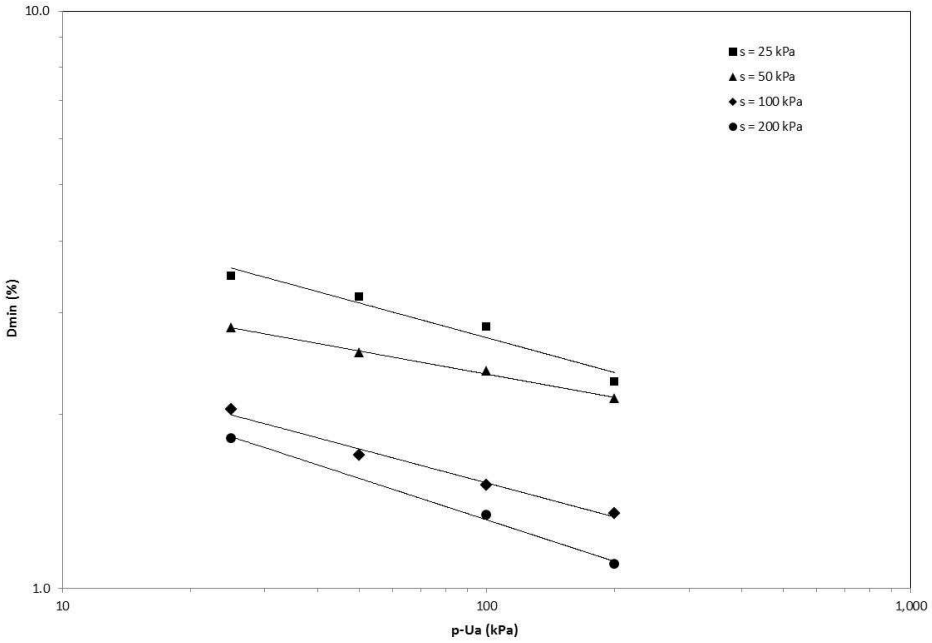

Figure 5-6 D_{min} variation as function of net mean stress

As expected, in all cases D_{min} decreases with an increase in net mean stress and suction, with a linear tendency.

Solid lines in Figure 5-6 represent best-fit, power regression functions of the form:

$$D_{min} = F(p - u_a)^E \qquad (5.2)$$

In Eq. 5.2 constant F represents D_{min} (%) at $p - u_a$ = 1 kPa, and constant E is representative of the soil's susceptibility to changes in $p - u_a$.

Power regression constants A and B from Eq. 5.2 used in Figure 5-6 are summarized in Table 5-2.

Table 5-2 Values of Best-Fit Power Regression for D_{min}

Suction (kPa)	F	E	r^2
25	6.9137	-0.331	0.8383
50	5.2281	-0.388	0.9324
100	4.0548	-0.448	0.9307
200	3.9543	-0.239	0.9956

5.3 Threshold Shear Strain

Dynamic properties measured at shear strain amplitude levels below a threshold limit γ_{th} are referred to as linear (low amplitude) shear modulus G_{max} and damping ratio D_{min}. If soils are strained to levels greater than γ_{th}, the soil does not exhibit linear elastic behavior as it undergoes strain softening or degradation (Seed and Idriss 1970; Isenhower 1979; Dobry et al. 1981, 1982; Huoo-Ni 1987).

In this work, there was no clear tendency on γ_{th}, however, the trends obtained by means of visual analyses of normalized G/G_{max} and D/D_{min}, are shown in Figure 5-7. To establish a threshold limit γ_{th} it is necessary to conduct small- to mid-shear strain amplitude RC testing, such that shearing strains γ surpass the linear range into a region where the soil's response becomes strongly strain dependent.

It can be seen that the threshold strain tendency tends to decrease when the suction and net mean stress states are increased.

The nonlinearity of the soil's response is manifested by the so-called backbone curve, as shown in chapter 4.

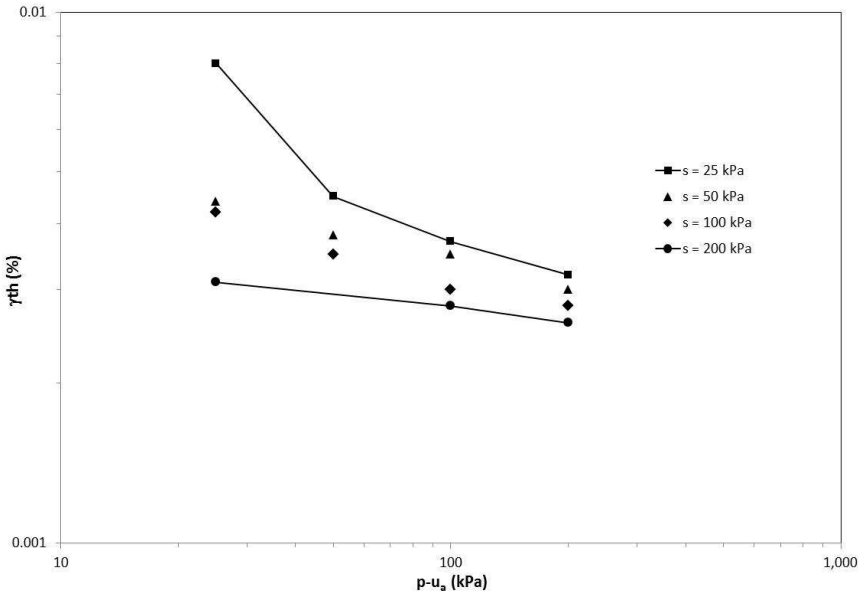

Figure 5-7 Threshold shear strain tendencies

5.4 Peak Shear Strain

The peak shear strain is the maximum shear strain that each one of the specimens underwent during the torsional excitation generated by the Resonant Column test (frequency response curves presented in Chapter 4).

This shear strain was experienced by the specimen when the RC device induced the resonant frequency to the sample. The trends obtained are shown in Figure 5-8.

It can be seen that the peak strain tendency tends to decrease when the suction and net mean stress states are increased.

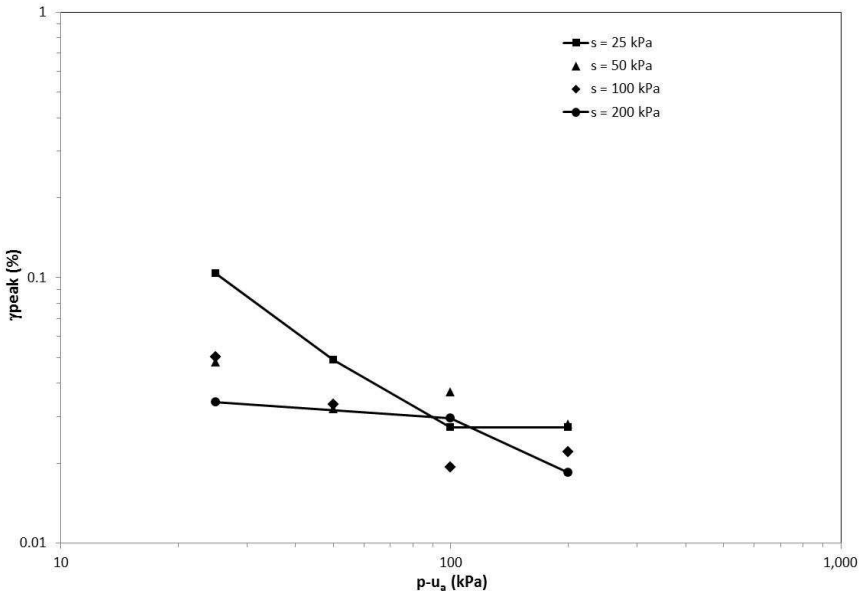

Figure 5-8 Peak shear strain tendencies

5.5 Modulus Degradation

The influence of matric suction and net mean stress on the variation of normalized shear modulus G/G_{max} with shear strain amplitude γ of the tested sandy soil is clearly observed in Figure 5-9 through Figure 5-22.

Solid lines in the mentioned figures represent best-fit, power regression functions of the form:

$$\frac{G}{G_{max}} = \frac{1}{\{1 + a(\gamma)^b\}^c} \qquad (5.3)$$

In Eq. 5.3 constants a, b, and c represent the decay rate of G/G_{max} with an increase in shear strain amplitude □ (Borden et al. 1996). Power regression constants a, b, and c from Eq. 5.3 used in the figures are summarized in Table 5-3.

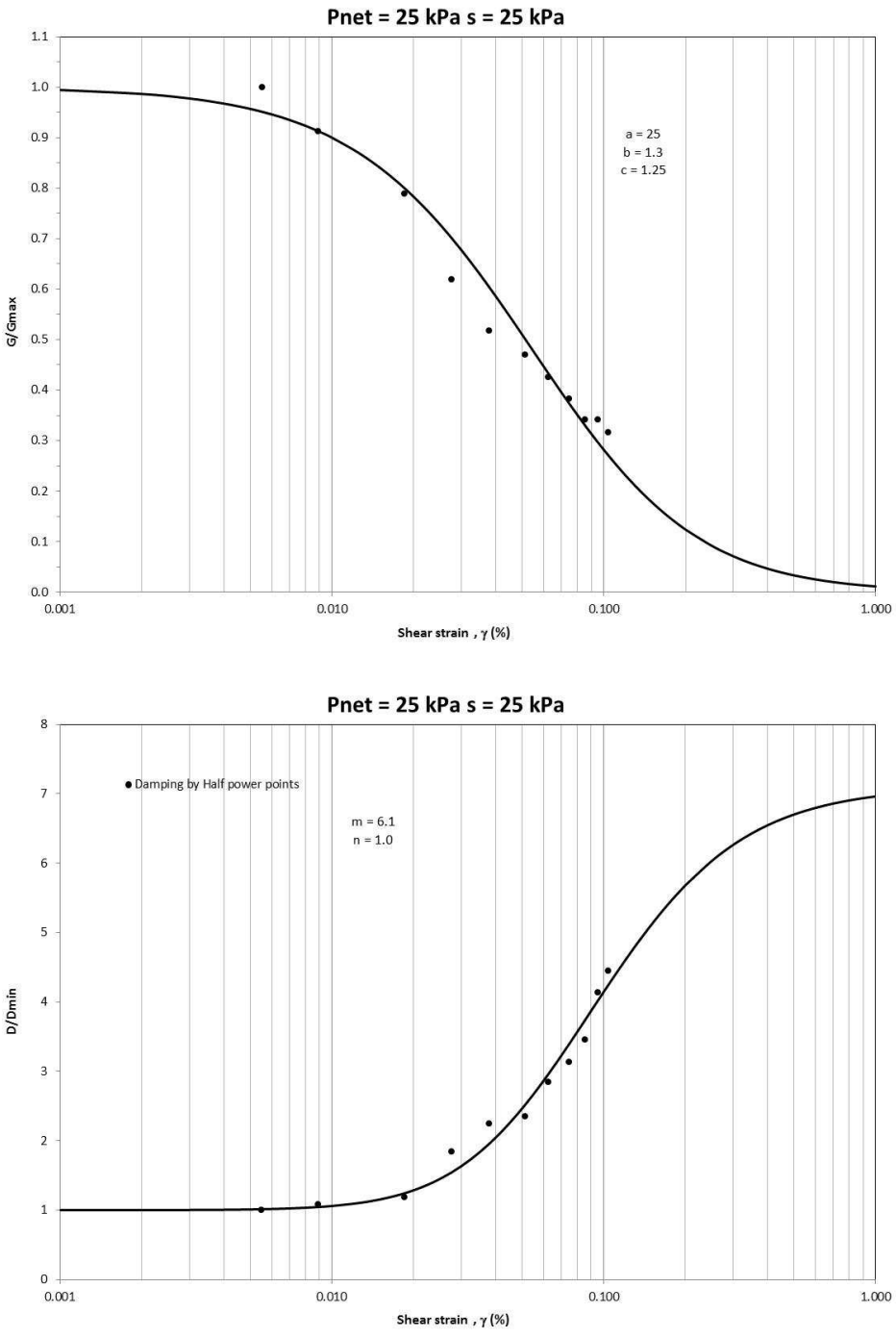

Figure 5-9 Variation of G/G_{max} and D/D_{min} with □, $p - u_a$ = 25 kPa, s = 25 kPa

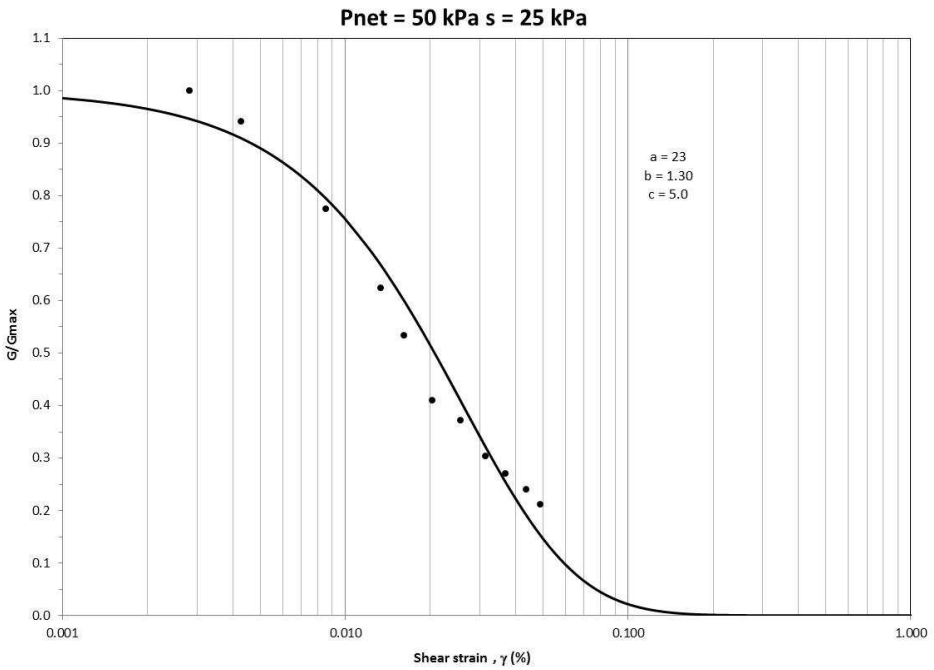

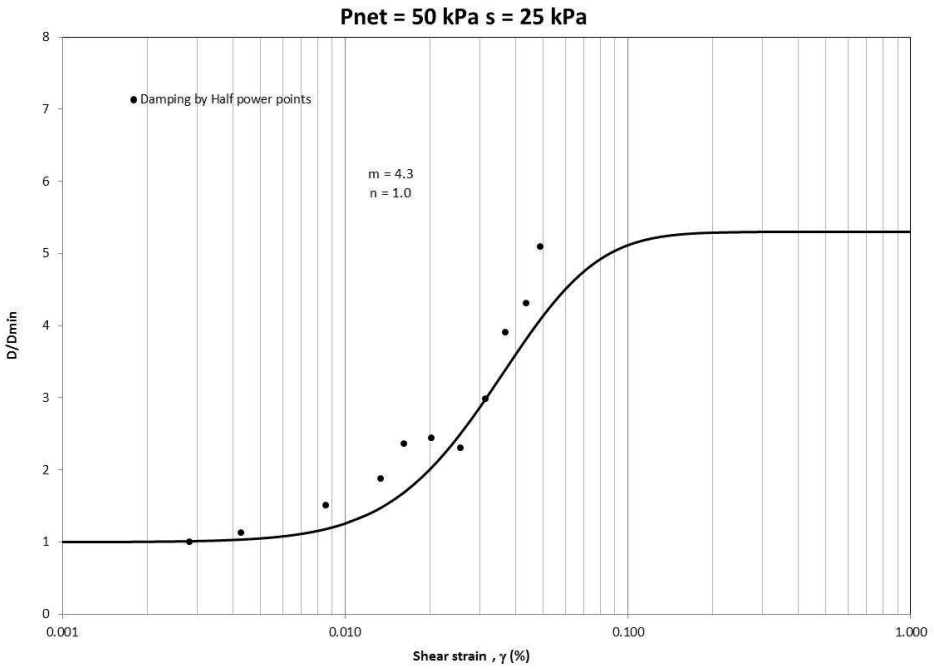

Figure 5-10 Variation of G/G_{max} and D/D_{min} with □, $p - u_a$ = 50 kPa, s = 25 kPa

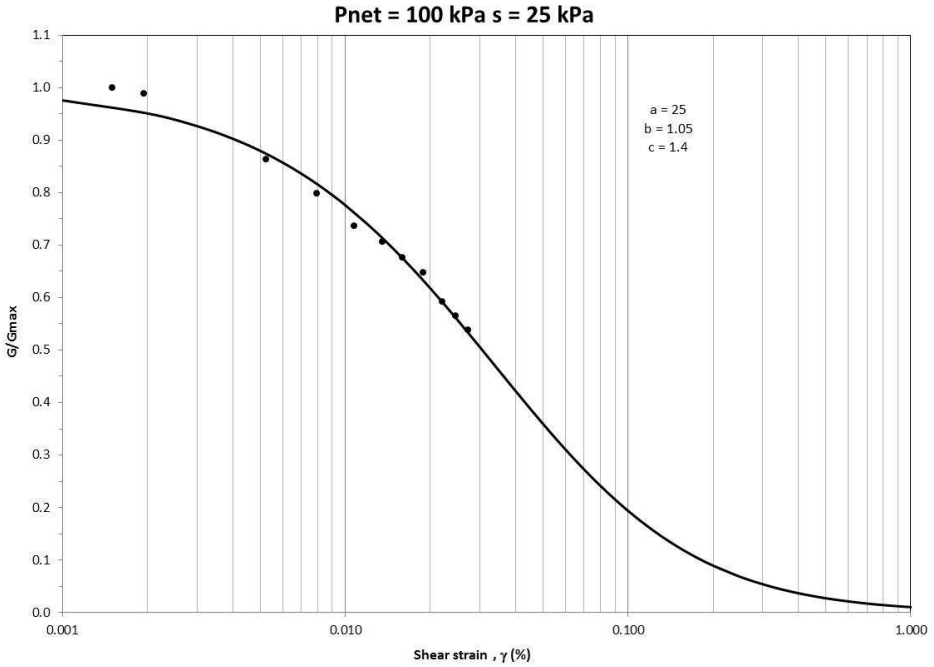

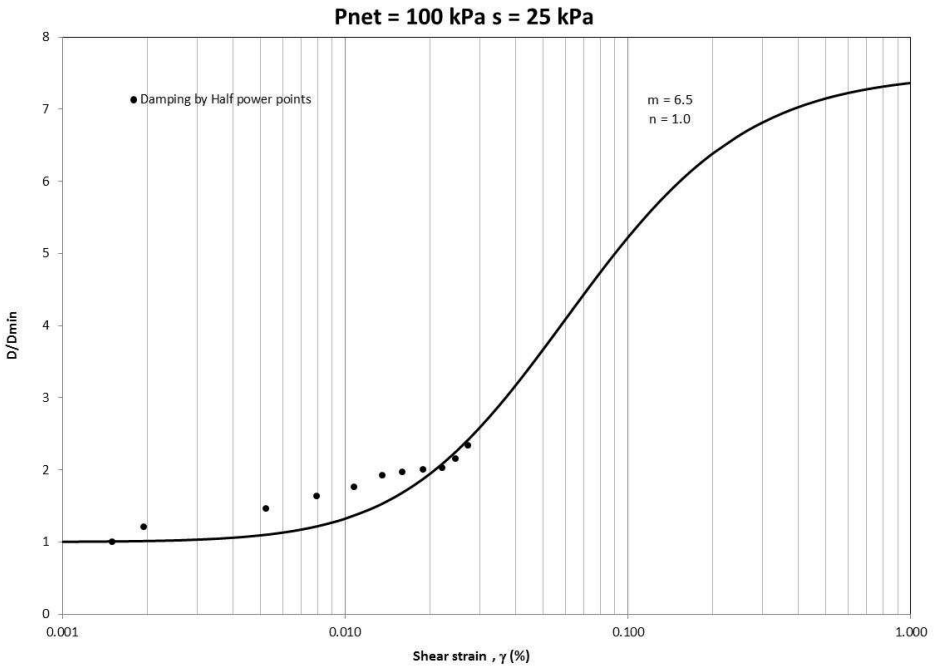

Figure 5-11 Variation of G/G_{max} and D/D_{min} with □, $p - u_a$ = 100 kPa, s = 25 kPa

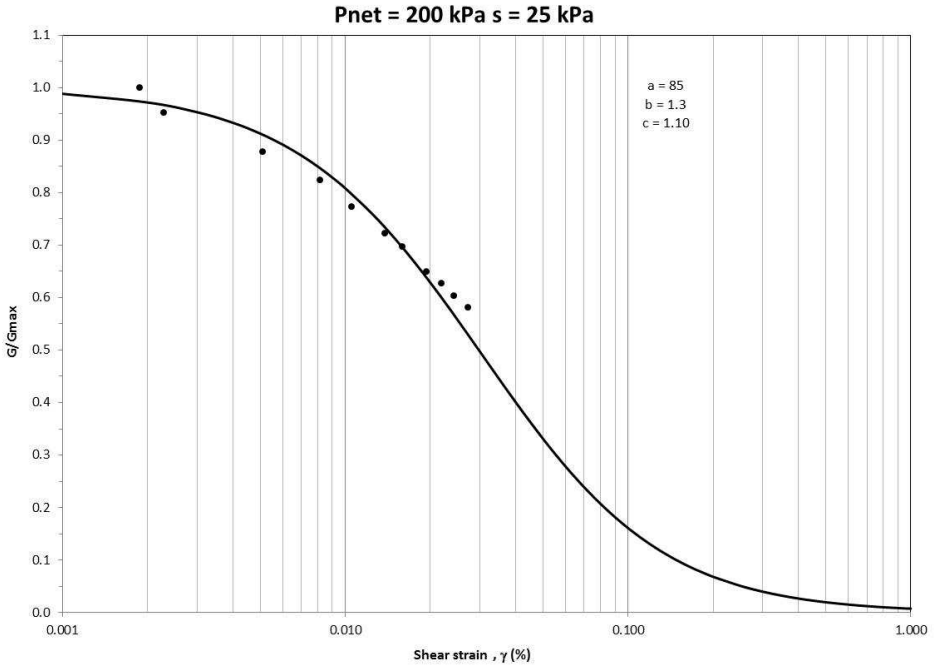

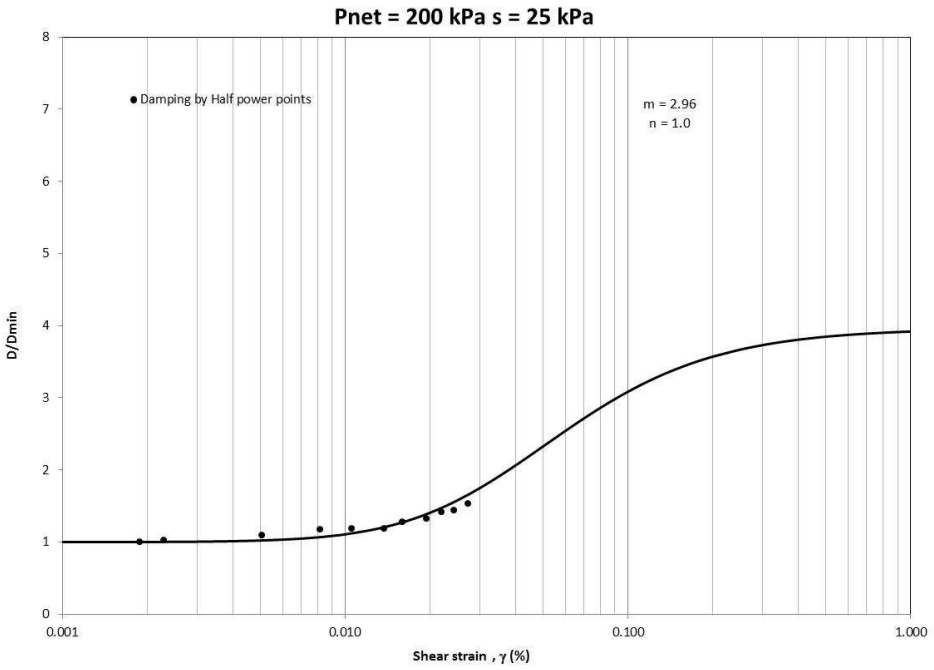

Figure 5-12 Variation of G/G_{max} and D/D_{min} with □, $p - u_a$ = 200 kPa, s = 25 kPa

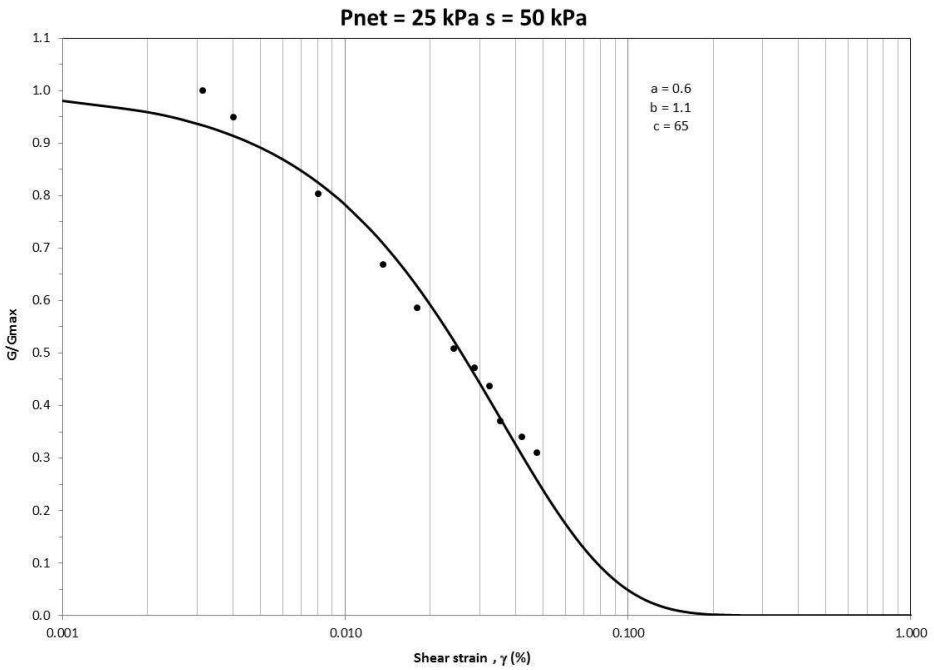

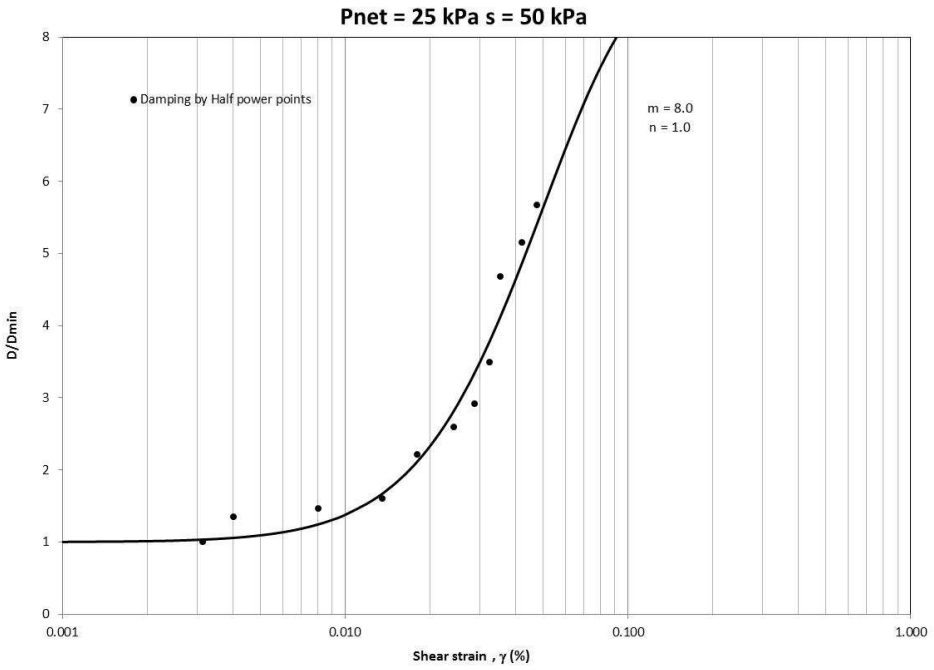

Figure 5-13 Variation of G/G_{max} and D/D_{min} with □, $p - u_a$ = 25 kPa, s = 50 kPa

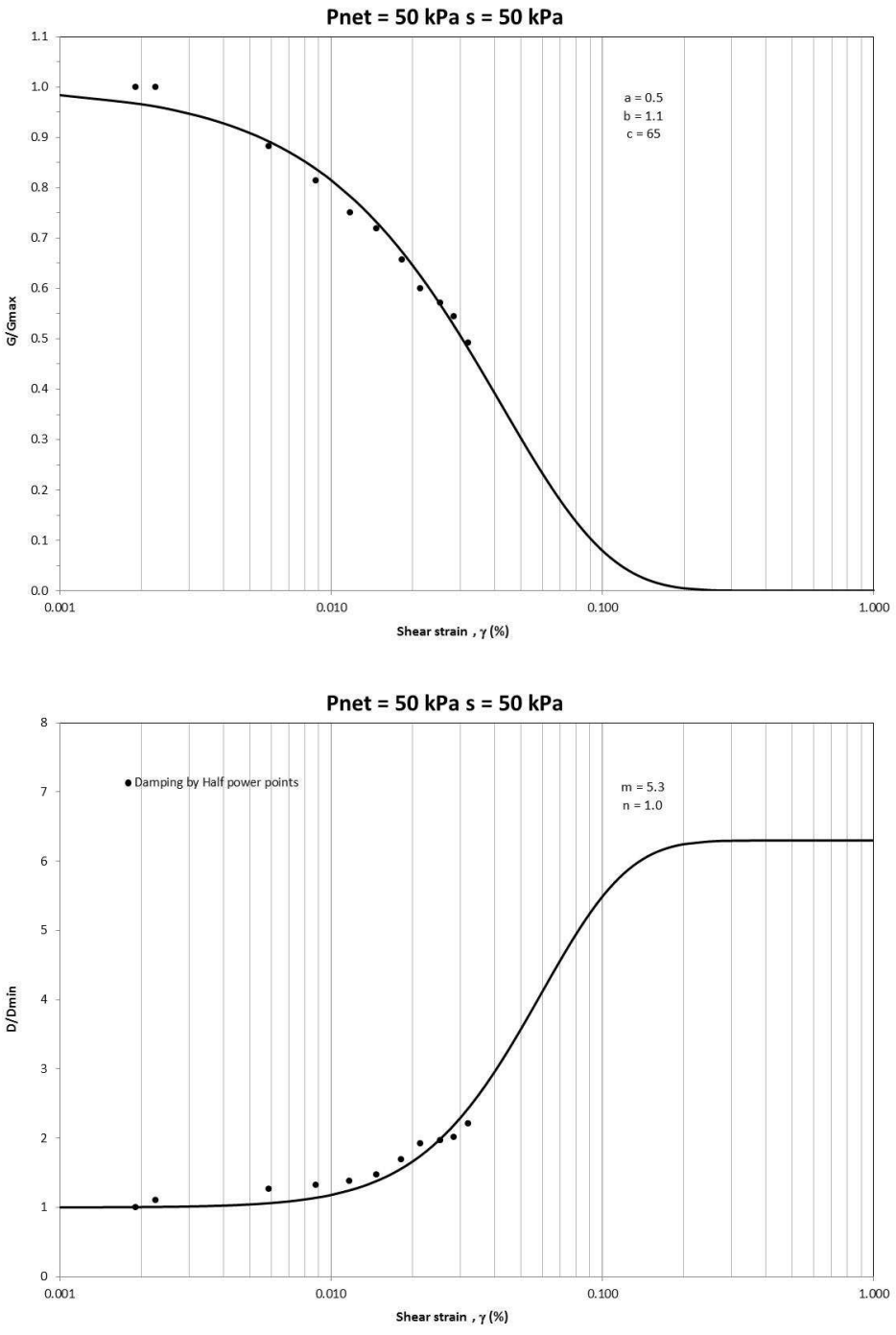

Figure 5-14 Variation of G/G_{max} and D/D_{min} with □, $p - u_a$ = 50 kPa, s = 50 kPa

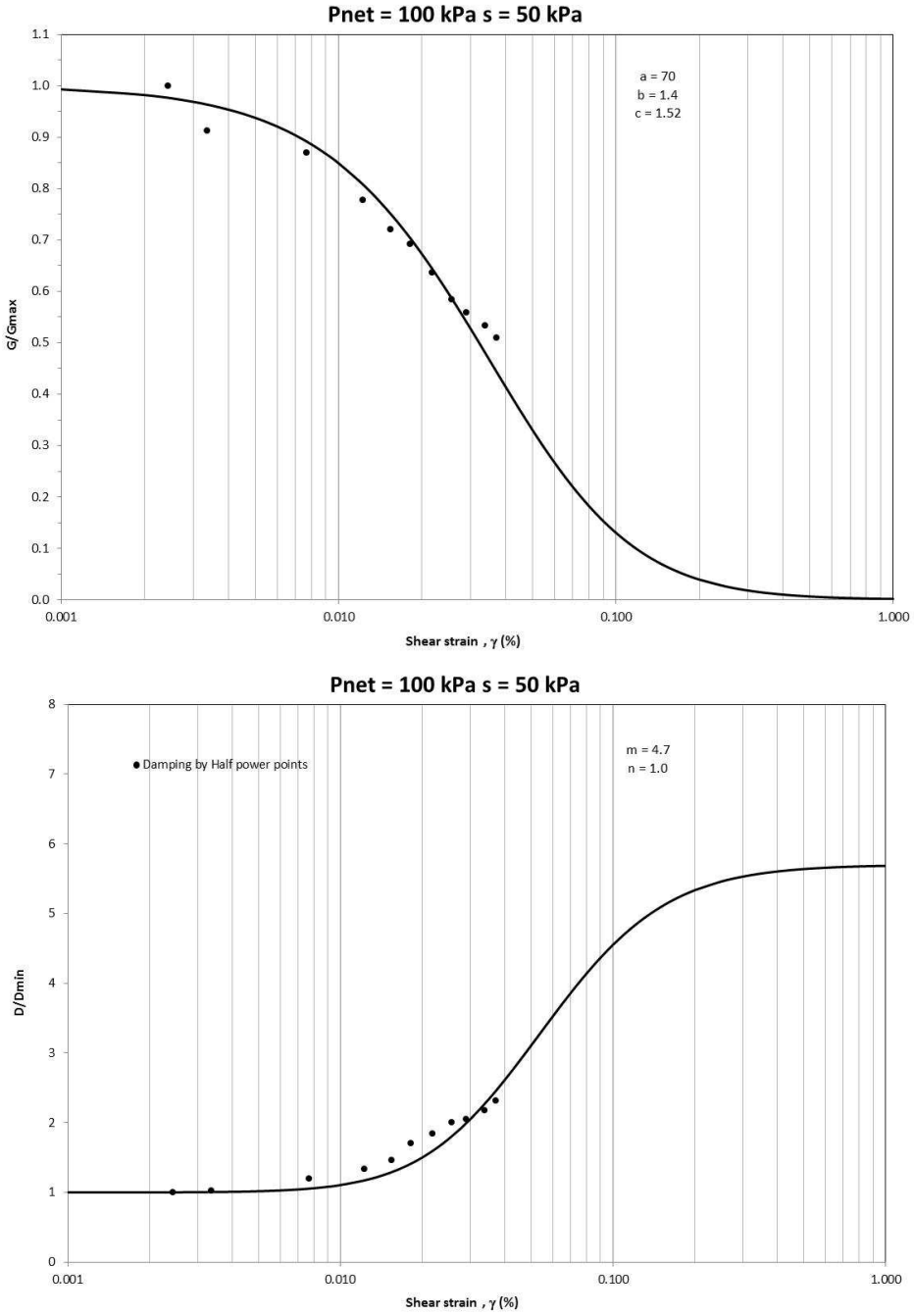

Figure 5-15 Variation of G/G_{max} and D/D_{min} with □, p – u_a = 100 kPa, s = 50 kPa

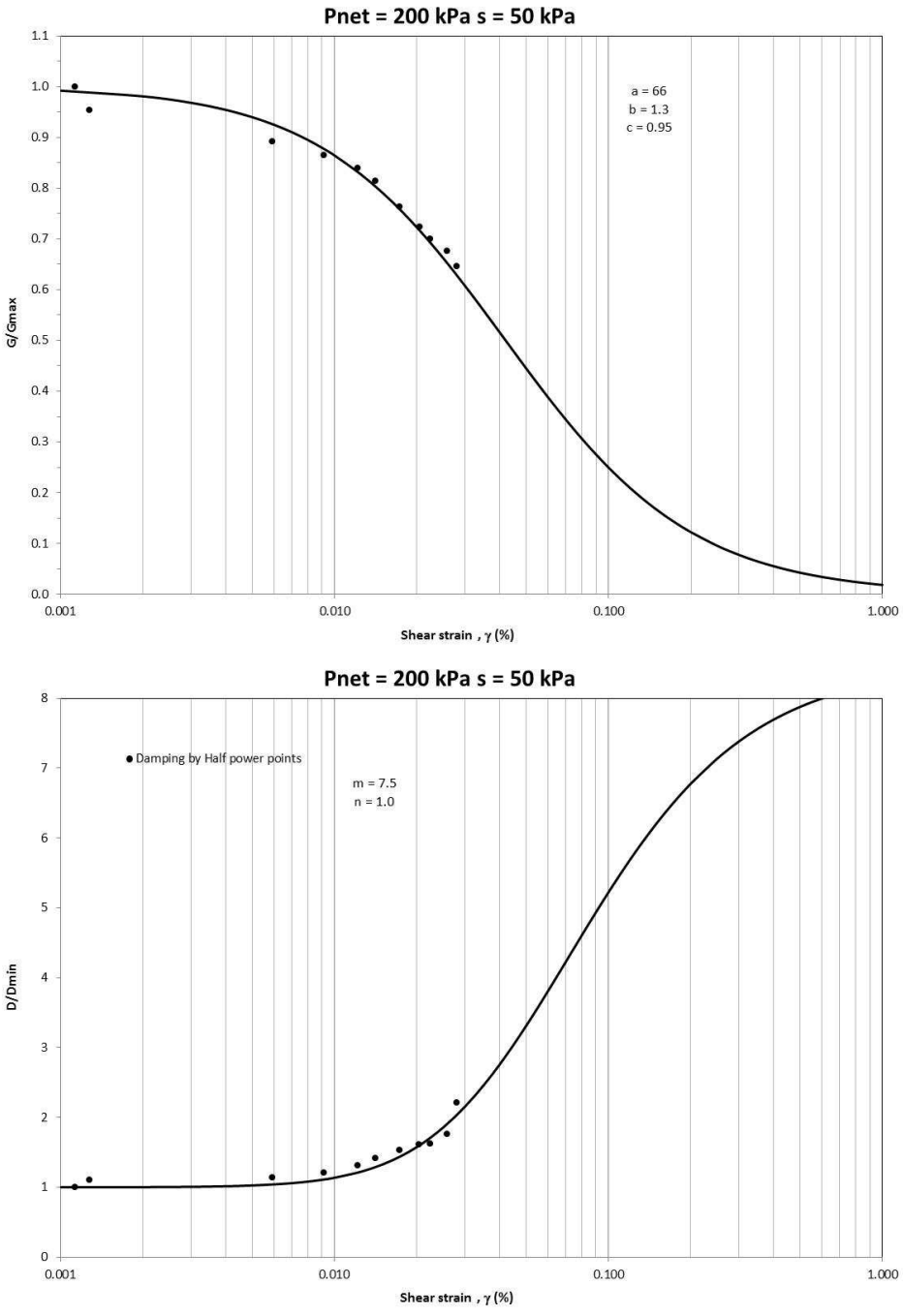

Figure 5-16 Variation of G/G_{max} and D/D_{min} with □, p – u_a = 200 kPa, s = 50 kPa

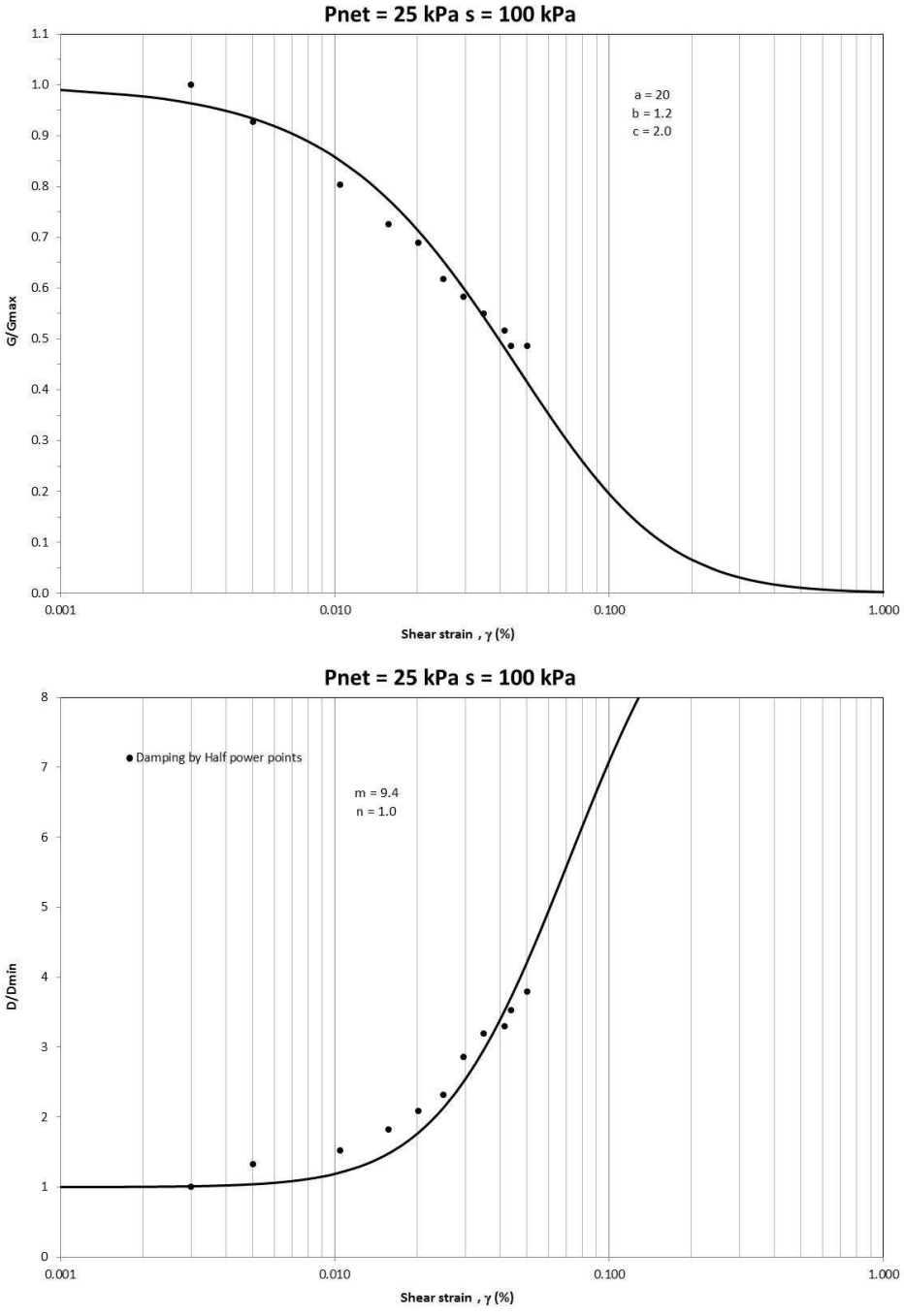

Figure 5-17 Variation of G/G_{max} and D/D_{min} with □, $p - u_a$ = 25 kPa, s = 100 kPa

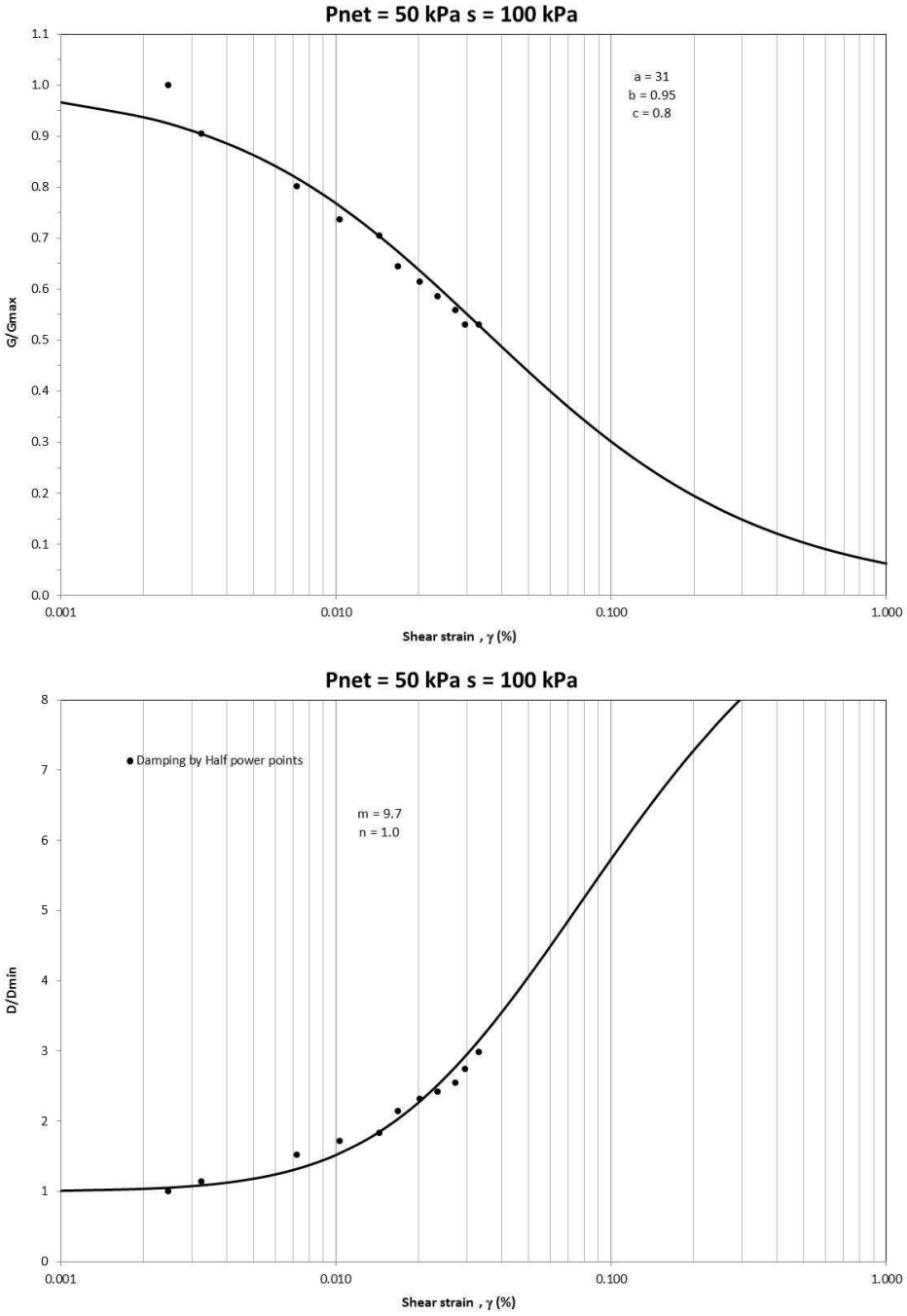

Figure 5-18 Variation of G/G_{max} and D/D_{min} with □, $p - u_a$ = 50 kPa, s = 100 kPa

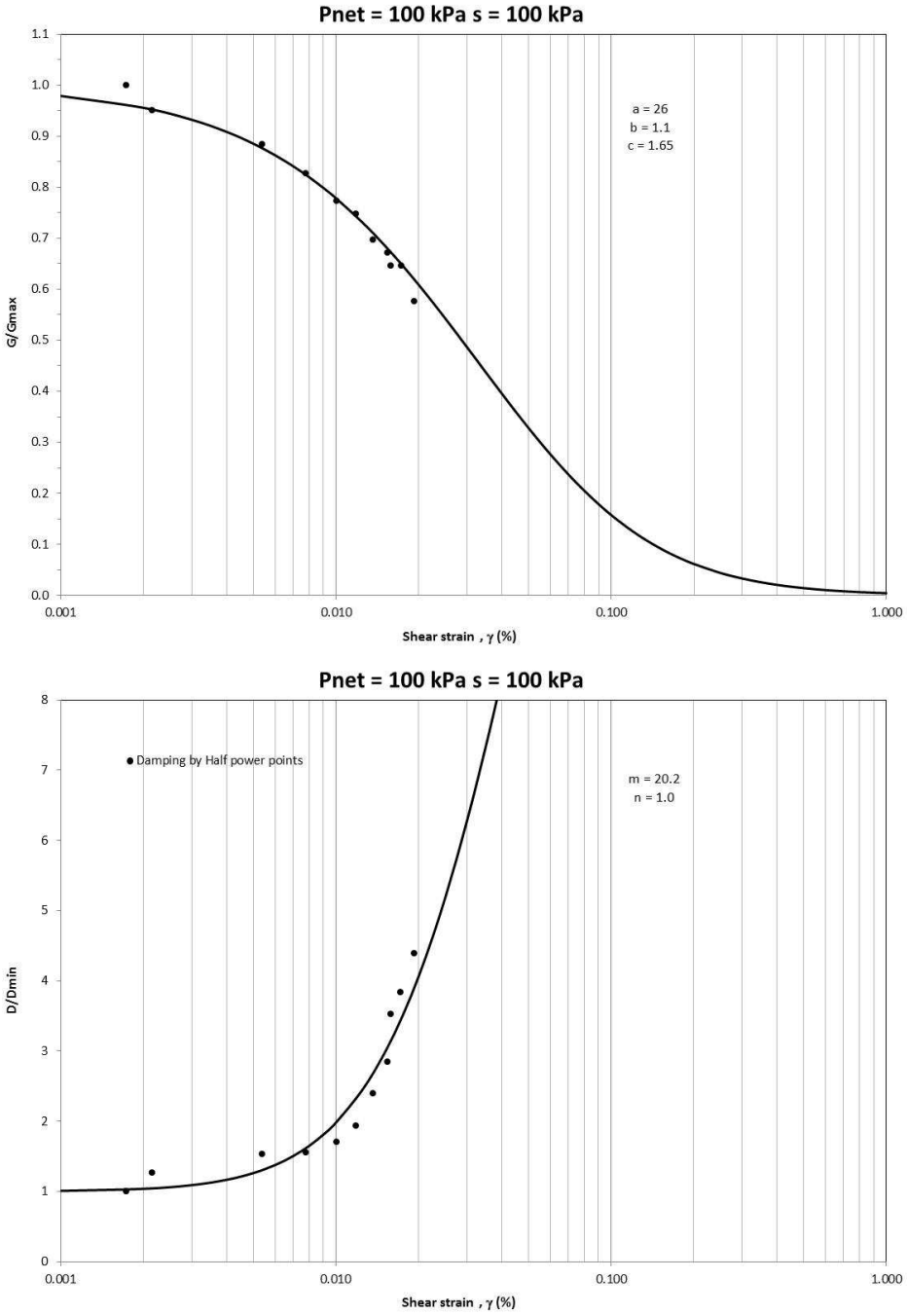

Figure 5-19 Variation of G/G_{max} and D/D_{min} with □, $p - u_a$ = 100 kPa, s = 100 kPa

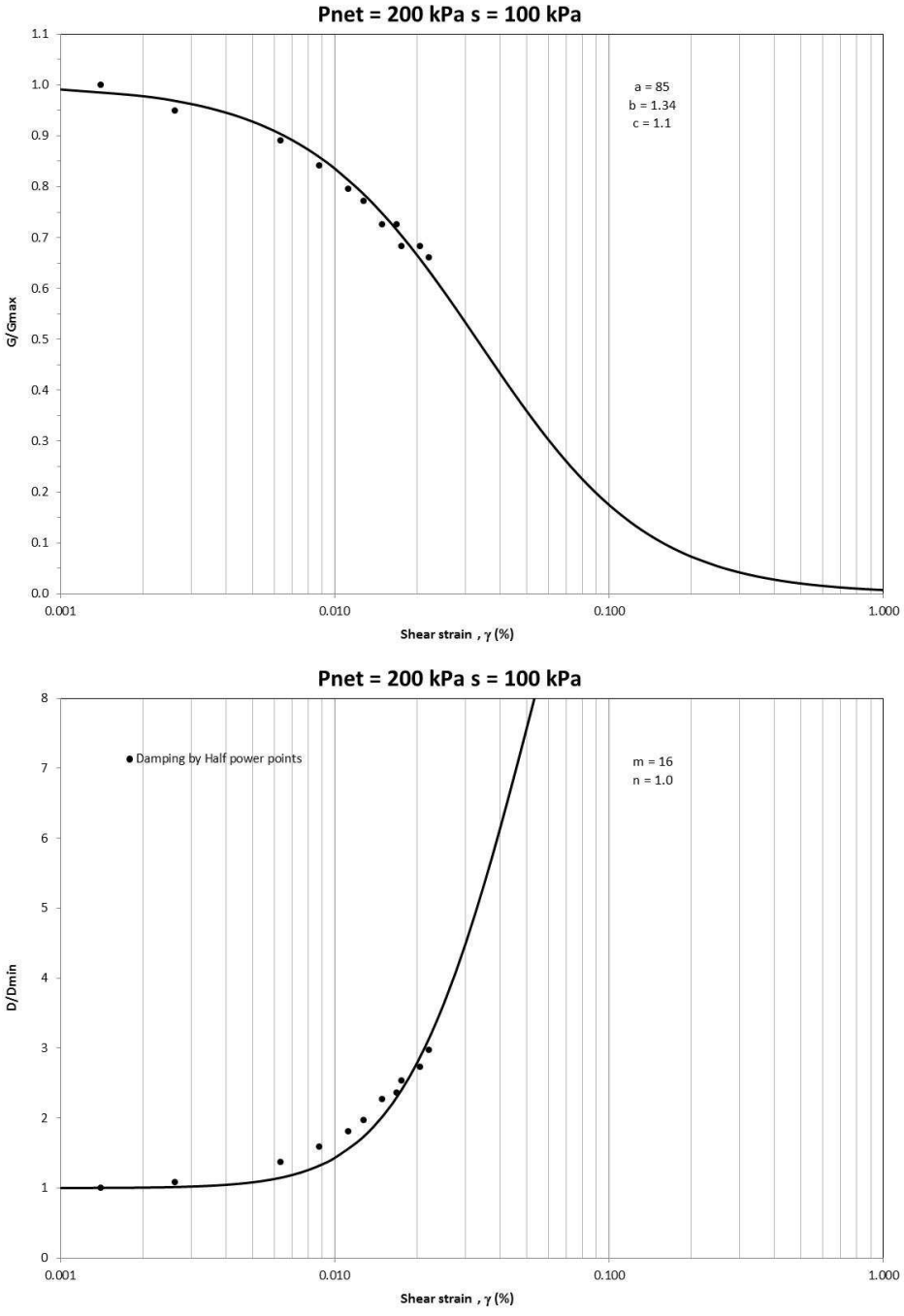

Figure 5-20 Variation of G/G_{max} and D/D_{min} with □, $p - u_a$ = 200 kPa, s = 100 kPa

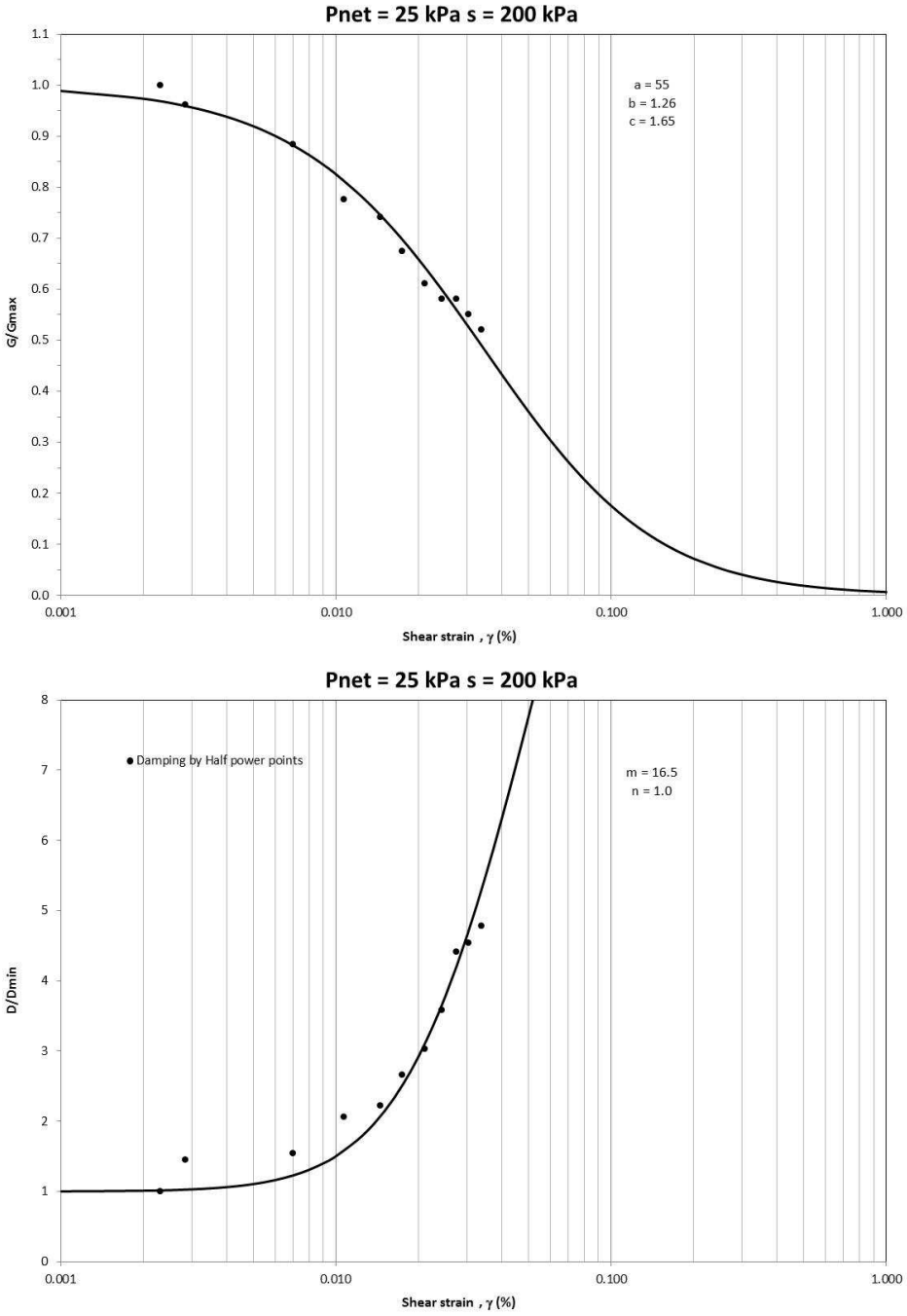

Figure 5-21 Variation of G/G_{max} and D/D_{min} with □, $p - u_a$ = 25 kPa, s = 200 kPa

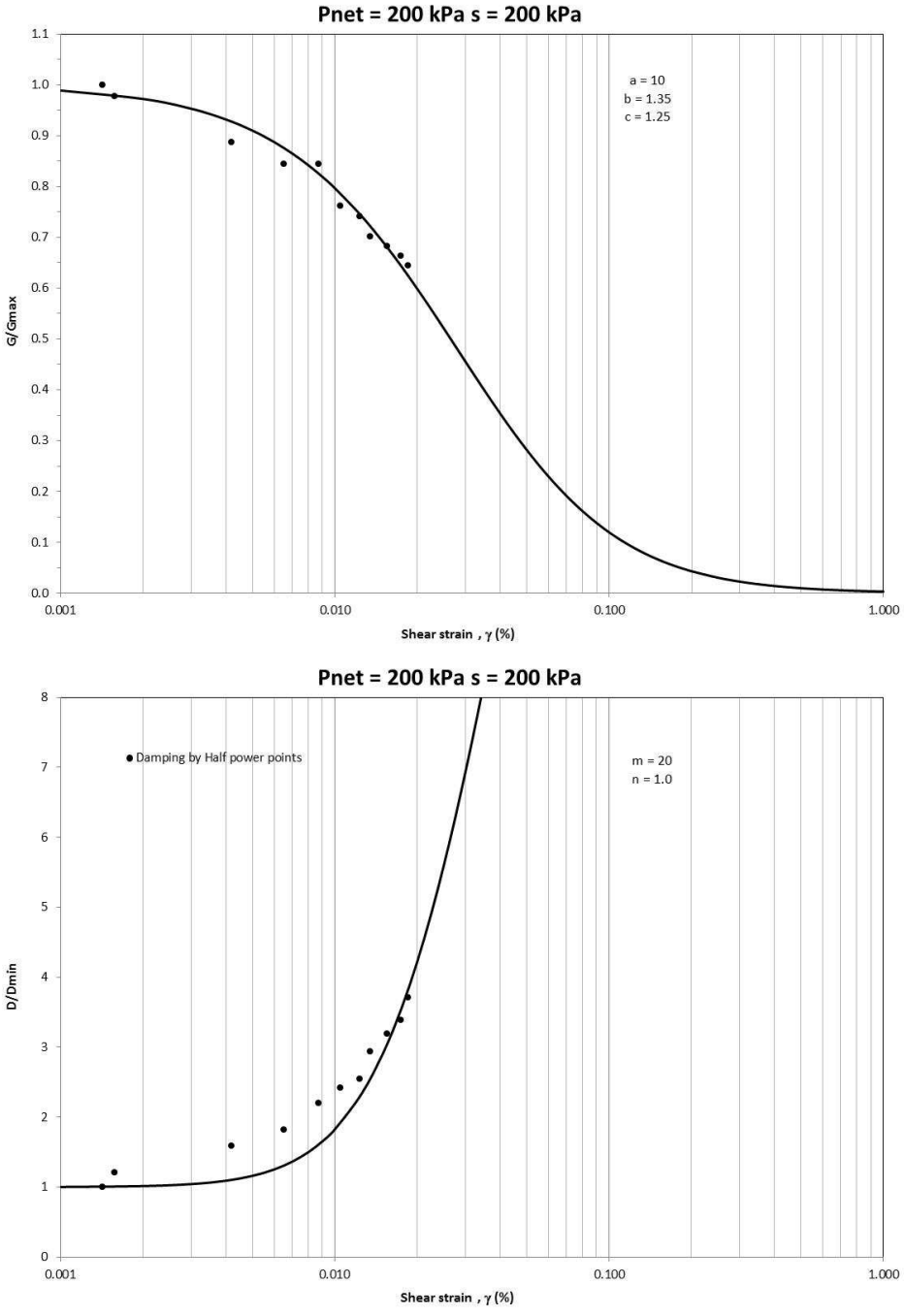

Figure 5-22 Variation of G/G_{max} and D/D_{min} with □, $p - u_a$ = 200 kPa, s = 200 kPa

Table 5-3 Values of Best-Fit Power Regression for G/G_{max}

Suction (kPa)	Net pressure (kPa)	a	b	c
25	25	3.5	1.3	1.25
	50	23	1.3	5.0
	100	25	1.05	1.4
	200	85	1.3	1.1
50	25	0.6	1.1	65
	50	0.5	1.1	65
	100	70	1.39	1.52
	200	66	1.3	0.95
100	25	20	1.2	2.0
	50	31	0.95	0.8
	100	26	1.1	1.65
	200	85	1.34	1.1
200	25	55	1.26	16.5
	200	100	1.35	1.25

One can realize that the normalized shear modulus G/Gmax decreases with increasing shear strain after a relatively well-defined “threshold” limit. This ratio, however, seems to undergo a significant decrease when the matric suction applied to the soil specimen is less than the soil air-entry value.

On the other hand, the normalized damping ratio D/Dmin increases with increasing shear strain after a relatively well-defined “threshold” limit. This ratio undergoes a significant decrease when the net mean stress applied to the soil specimen is increased; this decrement seems to be independent of the matric suction state applied to the specimen.

Moreover, useful D–G/G_{max} relationships can also be devised from the series of small- to mid-shear strain amplitude RC tests, as shown in Figure 5-23 through Figure 5-26. This figure shows the variation of damping ratio D with G/G_{max}, on the basis of matric suction, for all tested specimens.

Solid lines in the figures previously mentioned represent best-fit regression functions of the form:

$$D = x(\frac{G}{G_{max}} - 1)^2 + z \qquad (5.4)$$

In Eq. 5.4 constant x represents values of damping D (%) for G/G_{max} = 1 (i.e., D_{min}), and constant z is representative of the rate of increase in D as the material softens when sheared from small- to mid-shear strain amplitude levels (Borden et al. 1996; Hoyos and Macari 1999). Power regression constants m and n from Eq. 5.4 used in the mentioned figures are summarized in Table 5-4.

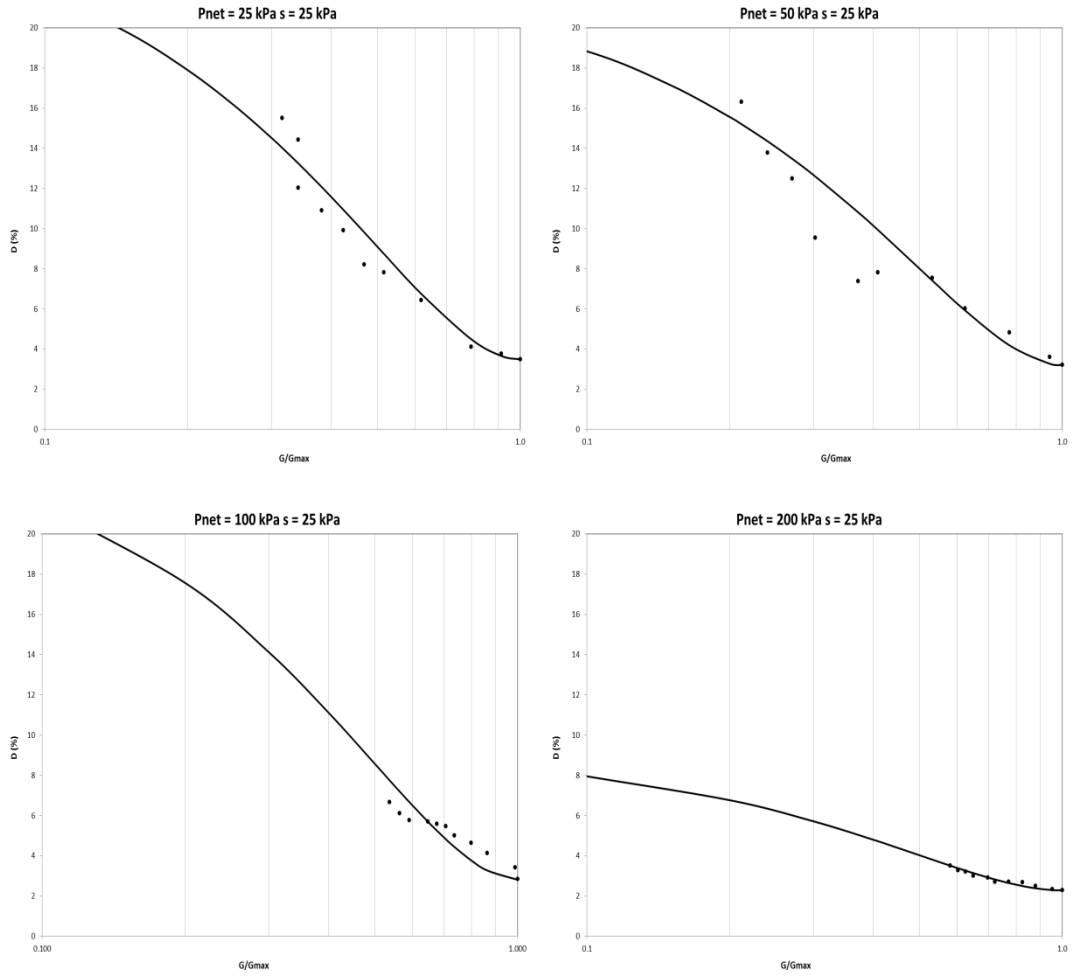

Figure 5-23 Variation of damping D with G/G_{max}, $p - u_a$ = 25, 50, 100, 200 kPa, s = 25 kPa

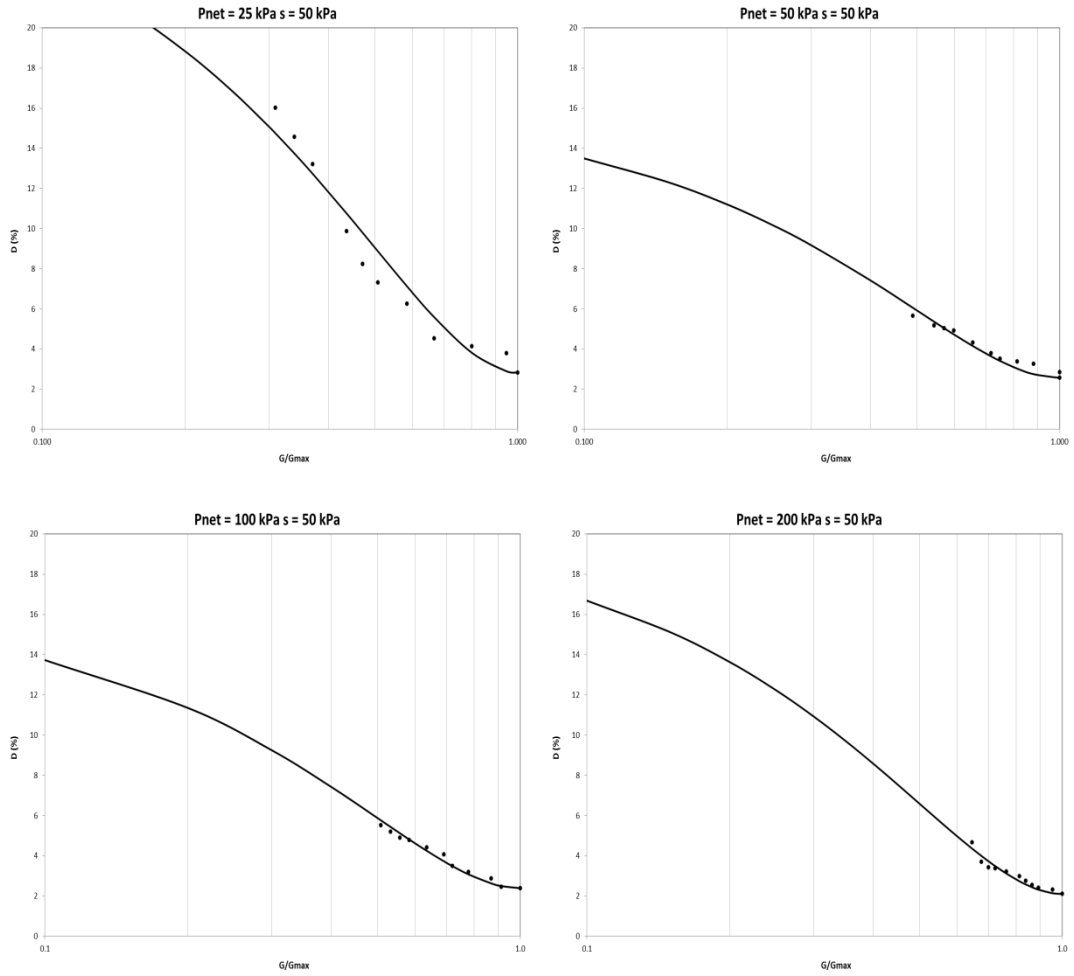

Figure 5-24 Variation of damping D with G/G_{max}, $p - u_a$ = 25, 50, 100, 200 kPa, s = 50 kPa

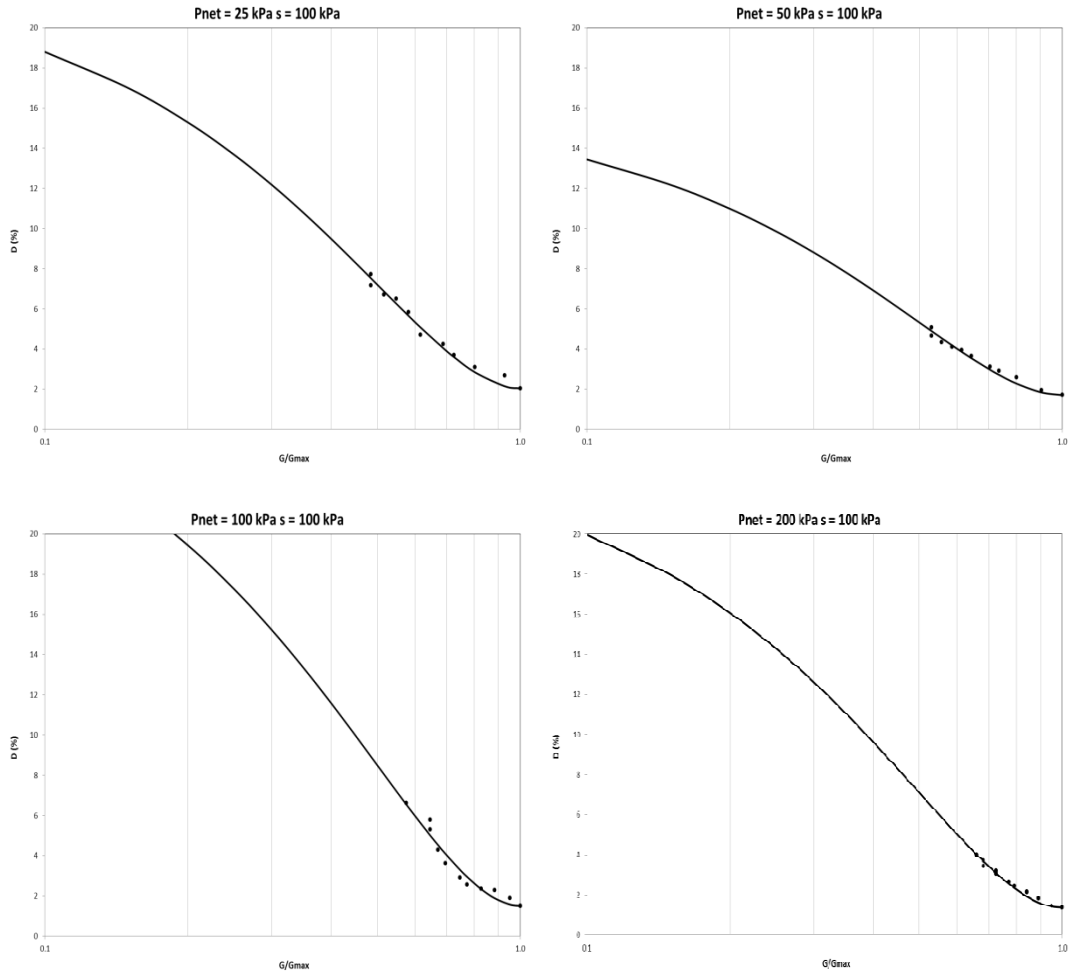

Figure 5-25 Variation of damping D with G/G_{max}, $p - u_a$ = 25, 50, 100, 200 kPa, s = 100 kPa

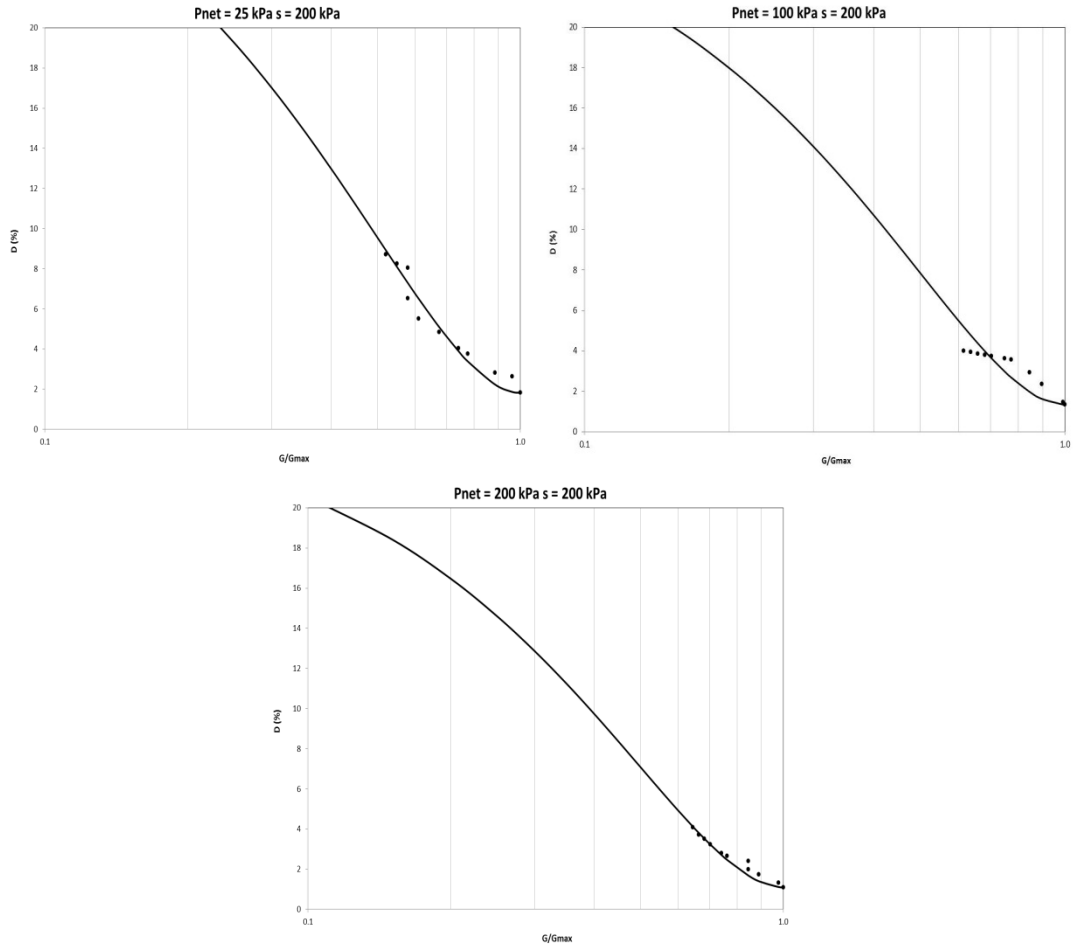

Figure 5-26 Variation of damping D with G/G_{max}, $p - u_a$ = 25, 200 kPa, s = 200 kPa

Table 5-4 Values of Best-Fit Power Regression for D–G/G_{max}

Suction (kPa)	Net pressure (kPa)	x	z
25	25	22.5	3.48
	50	19.3	3.20
	100	23.0	2.84
	200	7.0	2.28
50	25	25.0	2.83
	50	13.5	2.56
	100	14.0	2.39
	200	18.0	2.10
100	25	20.7	2.04
	50	14.5	1.40
	100	28.0	1.51
	200	23.0	1.35
200	25	31.0	1.82
	200	24.0	1.10

Finally, general tendencies obtained for variations of G/Gmax and D/Dmin, at extreme valves of matric suction (s=25kPa and s=200kPa), are presented in Figure 5-27 and Figure 5-28.

Based on this figures, it can be concluded that at high confinement pressures, it appears that the dynamic response of partially saturated soils is not significantly affected by changes in the matric suction.

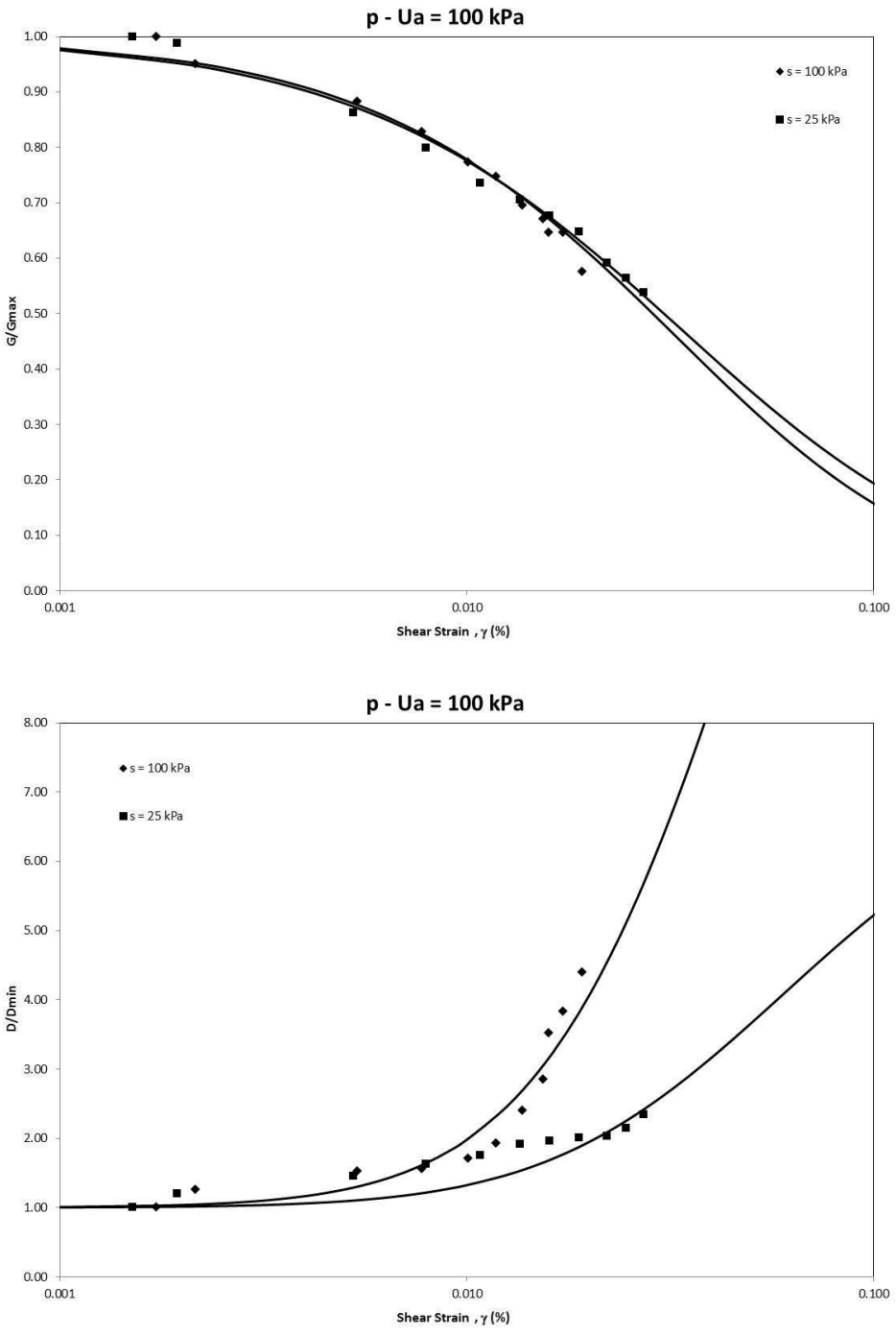

Figure 5-27 Suction-dependent variation of G/G_{max} and D/D_{min} with □, $p - u_a$ = 100 kPa

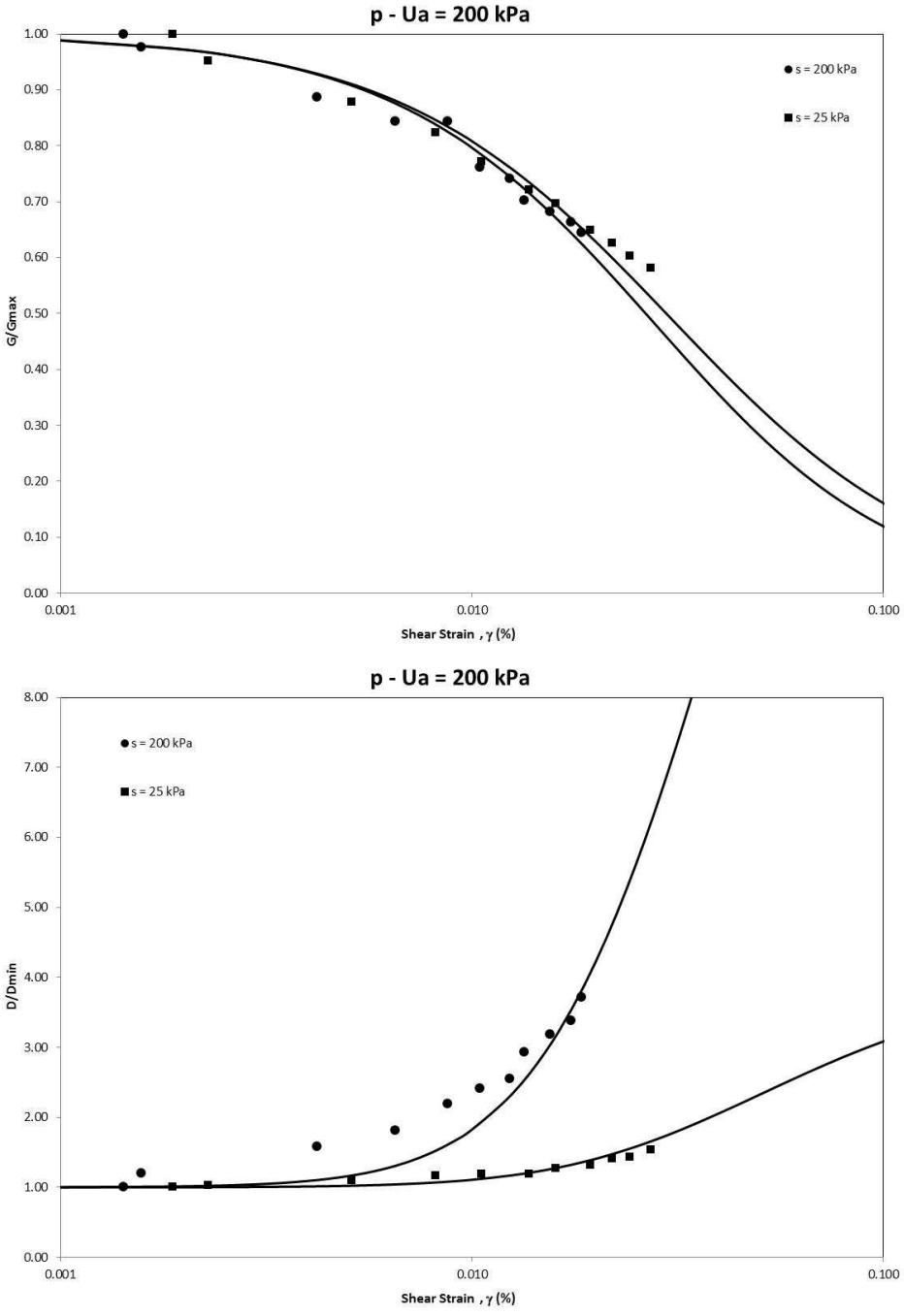

Figure 5-28 Suction-dependent variation of G/G_{max} and D/D_{min} with □, $p - u_a$ = 200 kPa

Next chapter contains the summary and conclusions from this research study, and also provides some recommendations for future research work.

Chapter 6

Conclusions and Recommendations

The engineering performance of earth structures subjected to static and non-static loading under unsaturated conditions requires a thorough assessment of key soil properties such as shear wave velocity, shear modulus, and material damping. Traditional soil mechanics, however, has generally focused on soil extreme conditions, that is, completely dry or saturated states of the soil.

In the last few decades, sustained efforts have been made to gain a better understanding of partially saturated soil behavior by using field and laboratory based measurements of soil suction, the analysis of swell-collapse behavior, and the assessment of soil-water retention properties. However, very limited efforts have been devoted to a thorough characterization of stiffness properties of unsaturated soils at small- to mid-strain levels, particularly shear modulus and material damping. The lack of experimental evidence of this type has been the chief motivation for the present work.

The main objective of this work was to study the dynamic response of intermediate unsaturated soils when subjected to small- to mid-shear strain levels under controlled matric suction and net mean stress states. The experimental program involved a comprehensive series of servo/suction-controlled resonant column tests performed on statically compacted specimens of poorly graded sand with silt, including constant net confining pressures ranging between 25 kPa and 200 kPa, and at constant matric suction states also ranging between 25 kPa and 200 kPa. The experimental results have further substantiated the relevant role played by matric suction in the small- to mid-strain response of compacted intermediate soils in terms of stiffness and damping.

6.1 Conclusions

The following specific and concise conclusions can be drawn from the experimental findings and modeling accomplished in the present research work:

1. A fully servo/suction-controlled, proximitor-based resonant column apparatus (RC) was used to perform a comprehensive series of RC tests on statically compacted specimens of SP-SM soil. According to the observed results, the device was found suitable to yield repeatable results of shear modulus and material damping.

2. As expected, the shear modulus, Gmax, of the test soil shows a general tendency to increase with increasing matric suction. This can be directly attributed to the fact that an increase in matric suction causes an increase in the effective stress acting on the soil skeleton; therefore, an improvement in soil stiffness is expected.

3. Likewise, and also as expected, the shear modulus, Gmax, of the test soil shows a general tendency to increase with increasing net mean stress, which can be attributed to the same phenomenon as described above.

4. In general, the normalized shear modulus G/Gmax decreases with increasing shear strain after a relatively well-defined “threshold” limit. This ratio, however, undergoes a significant decrease when the matric suction applied to the soil specimen is less than the soil air-entry value.

5. In general, the normalized damping ratio D/Dmin increases with increasing shear strain after a relatively well-defined “threshold” limit. This ratio undergoes a significant decrease when the net mean stress applied to the soil specimen is increased; this decrement seems to be independent of the matric suction state applied to the specimen.

6. The threshold strain and peak strain tendencies tend to decrease when the suction states were increased, thus this response corroborated the increase in soil stiffness at higher suction values.

7. At high confinement pressures, it appears that the dynamic response of partially saturated soils is not significantly affected by changes in the matric suction.

6.2 Recommendations for Future Work

The following recommendations can be made to further the study of the dynamic properties of the investigated soil at small- to mid-strain amplitudes using the same servo/suction-controlled resonant column apparatus used in this work:

1. The influence of higher levels of matric suction (greater than 200 kPa)should be investigated in order to assess the stiffness response of compacted SP-SM soil far beyond the soil's air-entry value.

2. A thorough attempt should be made to correlate some of the key parameters used for modeling the soil-water characteristic curve (SWCC) with distinct features of both the normalized shear modulus, G/Gmax, and the normalized damping ratio, D/Dmin, degradation curves.

References

[1] Alonso, E.E., A. Gens & Josa (1990). “A constitutive model for partially saturated soils.” Geotechnique 40(3), 405-430.

[2] ASTM (1993) “Test methods for modulus and damping of soils by the resonant column method,” Standard D 4015-92, ASTM, Philadelphia, PA, pp. 581-593.

[3] Borden, R.H., Shao, L. and Gupta, A. (1996).”Dynamic properties of piedemont residual soils”. J. of Geotechnical Engineering, ASCE, 122(10): 813-821.

[4] Brull, A. (1980). Caracteristiques mécaniques des sols de fondation de chaussées en fonction de leur état d□humidité et de compacité. Proc., International Conf. on Soil Compaction, Paris, vol. 1: 113-118.

[5] Cabarkapa, Z., T. Cuccovillo & M Gunn (1999). “Some aspects of the pre-failure behaviour of unsaturated soil.” II International Conference on pre-failure behaviour of geomaterials, Turin 1, 159-165.

[6] Cho, G., and Santamarina, J.C. (2001). Unsaturated particulate materials: Particle-level studies. J. of Geotechnical and Geoenvironmental Engineering, ASCE, 127(1): 84-96.

[7] Douglas, William Allan, (2013). “Effect of stress and suction histories on dynamic properties of statically compacted silty sand”. M.S. Thesis, The University of Texas at Arlington, Arlington, Texas.

[8] Fredlund, D. G. and Rahardjo, H. (1993). "Soil mechanics for unsaturated soils," John Wiley and Sons, Inc., New York.

[9] Fredlund, D. G., Xing, A., Huang, S., (1994). “Predicting the permeability functions for unsaturated soils using the soil-water characteristic curve.” Can. Geotech. J. 31, 533-546.

[10] Fredlund, M. D., Wilson, G. W., and Fredlund, D. G., (1997). “Prediction of the soil-water characteristic curve from the grain-size distribution curve.” Proceedings of the 3rd Symposium on Unsaturated Soil, Rio de Janeiro, Brazil, 13-23.

[11] Fredlund D. G. (1998). “Bringing unsaturated soil mechanics into engineering practice.” II International Conference on Unsaturated Soils, UNSAT 98, Beijing 2, 1-36.

[12] Fredlund, M. D., Fredlund, D. G., and Wilson, G. W. (2000). “An equation to represent grain-size distribution.” Can. Geotech. J., 37(4), 817-827.

[13] Geotechnical Consulting and Testing System (2009). CATS Resonant column and torsional shear test mode 1.8: User guide and reference. GCTS, Tempe, AZ.

[14] Greening, P.D. and Nash, D.F. (2004). “Frequency domain determination of Go using bender elements.” Geotechnical Testing Journal, 27(3), 1-7.

[15] Hoyos, L. R., Puppala A., and Chainuwat, P. (2004). “Dynamic Properties of Chemically Stabilized Sulfate Rich Clay.” J. of Geotechnical Engineering, ASCE, 2004.130:153-162.

[16] Hoyos, L. R., Suescun, E.A., Pineda, J. and Puppala A. (2010). “Small-strain stiffness of compacted silty sand using a proximitor-based suction-controlled resonant column device.” Fifth International Conference Unsaturated Soils, Barcelona, Spain.

[17] Huoo-Ni, S. (1987). Dynamic properties of sand under true triaxial stress states from resonant column/torsional shear tests. Ph.D. Dissertation, Univ. of Texas, Austin, TX.

[18] Kramer, Steven L. (1996), “Geotechnical earthquake engineering,” Prentice Hall, First Edition.

[19] Leong, E.C., Cahyadi, J. and Rahardjo, H. (2006). “Stiffness of a compacted residual soil”. Unsaturated Soils 2006, 1169-1180..

[20] Mancuso, C., Vassallo R., and d□Onofrio A. (2002). Small strain behavior of a silty sand in controlled-suction resonant column–torsional shear tests. Canadian Geotechnical Journal, 39: 22-31.

[21] Mitchell, J. K. (1993). “Fundamental of soil behavior,” John Wiley & Sons, New York.

[22] Picornell, M., and Nazarian, S. (1998). Effects of soil suction on low-strain shear modulus of soils. Proc., 2nd International Conf. on Unsaturated Soils, Beijing, vol. 2: 102-107.

[23] Qian, X., Gray, D.H., and Woods, R.D. (1991). Resonant column tests on partially saturated sands. Geotechnical Testing Journal, ASTM, 14(3): 266-275.

[24] Stokoe, K. H. II, Anderson, A. M., Hoar, R. J., and Isenhower, W. M. (1978). “Insitu and laboratory shear velocity and modulus,” Proceedings from Earthquake Engineering and Soil Dynamics Conference, ASCE, III, The University of Texas, Austin, TX, pp. 1498-1502.

[25] Stoke, K. H. and Huoo-Ni, S. (1985). “Effects of stress state and strain amplitude on shear modulus of dry sand,” Proceedings of the Second Symposium on the Interaction of Non-Nuclear Munitions with Structures, Panama City, FL, pp. 407-412.

[26] Suescun, Eduardo Alfonso, (2010). “Development of a suction controlled resonant column apparatus with self-contained bender elements”. M.S. Thesis, The University of Texas at Arlington, Arlington, Texas

[27] Vassallo, R., Mancuso, C., and Vinale, F. (2006). Effects of net stress and suction history on small strain stiffness of a compacted clayey silt. Canadian Geotechnical Journal, 44(4): 447-462.

[28] Vinale, F., A. d□Onofrio, C. Mancuso, F. Santucci De Magistris & F. Tatsuoka (1999). “The prefailure behaviour of soils as construction materials.” II International Conference on pre-failure behaviour of geomaterials, Turin.

[29] Takkabutr, P. (2006). “Experimental investigations on small-strain stiffness properties of partially saturated soils via resonant column and bender element testing”. Ph. D. Dissertation, The University of Texas at Arlington, Arlington, Texas.

[30] Wu, S., Gray, D.H., and Richart, Jr., F.E. (1984). Capillary effects on dynamic modulus of sands and silts. Journal of Geotechnical Engineering, ASCE, 110(9): 1188-1203.

[31] Zhang, J., Andrus, R. and Juang H. (2005). “Normalized shear modulus and material damping ratio relationships”. Journal of Geotechnical and Environmental Engineering, ASCE, 131(4): 453-464

Biographical Information

Alejandro Hernán Pino Bravo was born on January 14, 1978 in the City of Popayán, Colombia. He received his bachelor degree in Civil Engineering from Universidad del Cauca, Popayán, Colombia in October 2001. After graduating, he worked as a civil engineer for consulting companies in Colombia, and obtained the degree of specialist on geotechnical engineering from the Universidad Nacional de Colombia in 2007. Thereafter, he had been offering consulting services for public and private sectors. In 2012, he decided to pursue graduate studies majoring in geotechnical engineering at The University of Texas at Arlington, Arlington, Texas, USA. Mr. Alejandro Hernán Pino Bravo received his Master of Science degree in Civil Engineering from The University of Texas at Arlington in August 2013.